INSTRUMENTAL ANALYSIS OF THE FATTY ACID AND OXYLIPIN PATTERN WITH A FOCUS ON THE PRODUCT FORMATION OF LIPOXYGENASES

Dissertation

to obtain the academic degree

Doctor rerum naturalium

(Dr. rer. nat.)

Faculty of Mathematics and Natural Sciences

of the

Bergische Universität Wuppertal

by

Laura Kutzner

Cottbus

- 2020 -

The PhD thesis can be quoted as follows:

urn:nbn:de:hbz:468-20210113-094942-3
[http://nbn-resolving.de/urn/resolver.pl?urn=urn%3Anbn%3Ade%3Ahbz%3A468-20210113-094942-3]

DOI: 10.25926/fy6x-m726
[https://doi.org/10.25926/fy6x-m726]

Erster Gutachter: ..... Prof. Dr. Nils Helge Schebb

Zweiter Gutachter: .....Prof. Dr. Hartmut Kühn

Tag der mündlichen Prüfung: ..... _____. _____. 2020

Tag der Promotion: ..... _____. _____. 2020

Für meine Familie

Table of Contents

Chapter 1

Introduction and scope

Polyunsaturated fatty acids (PUFA) of the omega-6 and omega-3 (n6, n3) class are essential nutrients to humans and most mammals that are unable to *de novo* synthesize these fatty acids [1]. Especially long-chain PUFA such as arachidonic acid (ARA), eicosapentaenoic acid (EPA) and docosahexaenoic acid (DHA) are physiologically important as constituents maintaining the structural integrity of cell membranes, to warrant normal neural development, for signal transduction and as precursors of eicosanoids and other oxylipins [2]. Essential fatty acids are provided by the diet, e.g. by PUFA-rich plant seeds and oils that contain large amounts of linoleic acid (LA) [3] or meat and animal products that are a direct source of ARA [4]. Supply of n3-PUFA is achieved by the intake of alpha-linolenic acid (ALA), which is contained in plant seeds, such as chia or linseed, or directly as long chain n3-PUFA by the consumption of e.g. fatty cold-water fish or fish oil supplements [5, 6]. Long-chain n6- and n3-PUFA can be synthesized from their C18-precursor fatty acids LA and ALA by a cascade of enzymatic desaturation and elongation steps [7]. However, due to competition for the same enzymes the desaturation of ALA is inhibited by the presence of LA [8]. Therefore, an increased consumption of LA during the last century [3] and the subsequently increased dietary n6/n3-PUFA ratio render the conversion of ALA into EPA and particularly DHA rather inefficient [9]. A direct intake of EPA and DHA leads to a pronounced elevation of blood EPA+DHA levels, which increase in a dose-response manner [10]. An efficient uptake and incorporation of these n3-PUFA have important implications for human health, since EPA and DHA are associated with beneficial effects. DHA is a major fatty acid in the cell membrane lipids of the retina and brain gray matter [11] and contributes to normal brain function and

vision [12]. For example, a diet deprived of n3-PUFA (ALA) during pre- and postnatal development of rhesus monkeys led to reduced plasma DHA levels and visual acuity [13]. Moreover, n3-PUFA can inhibit key enzymes involved in triglyceride synthesis in the liver, thereby reducing very low density lipoprotein (VLDL) assembly and secretion. Therefore, n3-PUFA contribute to the maintenance of normal blood concentrations of triglycerides and can be used to treat hypertriglyceridemia [14]. A relationship between EPA and DHA consumption and the reduction of blood pressure has been established [12] and the most likely mechanism is a shift in the production of lipid mediators from n6-PUFA to n3-PUFA derived oxylipins, which act vasodilatory and anti-hypertensive [15].

These bioactive lipid mediators are formed in the ARA cascade by three major enzymatic pathways and autoxidation. Cyclooxygenase (COX) enzymes including the consecutively expressed COX-1 and the inducible COX-2, are prostaglandin endoperoxide H synthases and as such involved in the formation of prostanoids. PUFA, e.g. ARA, are thereby oxygenated to prostaglandin G_2 (PGG_2), which is reduced to PGH_2 in a peroxidase reaction of the COX enzyme. This compound is further converted to biologically active prostaglandins (e.g. PGE_2, PGD_2, $PGF_{2\alpha}$) and thromboxanes (e.g. TXA_2) by the action of specific synthases [16-18] or by spontaneous, non-enzymatic rearrangement [19]. Arachidonate lipoxygenases (ALOX/LOX) are dioxygenase enzymes that catalyze the insertion of molecular oxygen into fatty acid substrates containing at least one bisallylic methylene [20]. Their main products are stereo- and regio-specific hydroperoxy fatty acids, which can be reduced to the corresponding hydroxy derivatives by e.g. glutathione peroxidases [21]. Based on their product specificity with ARA as substrate, different ALOX isoforms have been characterized and their genes were named accordingly, e.g. *ALOX5*, *ALOX15*, *ALOX12*. While all ALOX isoforms possess the dioxygenase activity, several isoforms also exhibit other catalytic functions. For example, ALOX5 is capable of epoxide formation via its leukotriene A_4 synthase activity [22]. Moreover, primary ALOX products (hydro(pero)xy fatty acids) can serve as substrate for further

oxygenation by the same or another ALOX isoform [23]. Both properties are physiologically relevant as they are the prerequisite for the formation of bioactive leukotrienes [24] as well as multiple hydroxylated fatty acids, e.g. lipoxins [25]. The family of cytochrome P450 monooxygenases (CYP) that have an established role in the transformation of xenobiotics constitute another physiologically important branch of the ARA cascade. Free fatty acids are subject to *bis*-allylic oxidation, ω/ω-1 hydroxylation or olefin epoxidation to form mid-chain as well as terminal hydroxy fatty acids and *cis*-epoxy fatty acids [26]. Depending on the number of *cis*-double bonds of the fatty acid substrate, CYPs catalyze the formation of various regio-isomeric epoxy fatty acids, which are enzymatically hydrolyzed to the – usually less bioactive – vicinal dihydroxy fatty acids by the soluble epoxide hydrolase (sEH) [27]. While the regio- and stereochemistry of enzymatic oxygenation of PUFA is usually tightly controlled, a multitude of oxylipins can be formed autoxidatively including prostaglandin-like structures (isoprostanes) [28], hydro(pero)xy fatty acids [29] and both *cis*- and *trans*-epoxy fatty acids [30]. While there is a vast number of ARA derived bioactive oxylipins formed in the ARA cascade, n3-PUFA such as EPA and DHA can be utilized as substrate by the COX, ALOX and CYP enzymes leading to the formation of oxylipins with distinct biological activities. For example, EPA is converted to PGE_3 by the COX enzyme. Thereby the formation of vasodilatory acting PGE_2 is attenuated and PGE_3 exhibits lower activity with several of the PGE receptors [31]. Similarly, the ALOX5 product LTB_4 is a potent chemoattractant, while its EPA-derived analog LTB_5 is less active [32]. In addition to this reduction of pro-inflammatory activities, ALOX catalyzed oxygenation of n3-PUFA gives rise to a group of anti-inflammatory, pro-resolving multiple hydroxylated fatty acids that were termed specialized pro-resolving mediators (SPMs) [33].

Since n6- and n3-PUFA compete for the same enzymes the endogenous n3-PUFA status governs their oxylipin formation. In fact, an increase in blood EPA and DHA levels by dietary intervention leads to a concomitant elevation of their oxylipins including the SPM pathway markers 18-HEPE and 17-HDHA [34]. However, for an efficient uptake of dietary n3-PUFA also the background diet,

especially the n6-PUFA intake, should be considered. In *chapter 2*, changes in the tissue n3-PUFA levels and their oxylipins upon n3-PUFA feeding were investigated in a murine model with consideration of the dietary n6-PUFA background. On the one hand, the effects of a high LA diet representing a Western diet and a high oleic acid (OA) diet, representing a more Mediterranean diet are compared regarding the fatty acid and oxylipin profile as well as fatty acid metabolizing enzymes. On the other hand, the effects of EPA or DHA feeding in combination with each of the n6-PUFA background diets were evaluated in order to determine if lower dietary n6-PUFA increase the bioavailability of n3-PUFA and/or favor the production of potentially anti-inflammatory n3-PUFA derived oxylipins. Studies in rodents are commonly applied e.g. to investigate how the dietary fat composition influences the tissue n3-PUFA status and the production of oxylipins [35] or the effect in various disease models such as DSS-induced colitis [36], ischemic reperfusion injury [37], sepsis [38] or zymosan-induced peritonitis, which is often used to study the *in vivo* role of SPMs [39]. However, in order to translate from e.g. mice to humans, species differences regarding enzyme expression and product formation have to be kept in mind. In *chapter 3*, the reaction specificity and resulting product profiles of different mammalian ALOX15 orthologs are characterized for the major long-chain n6- and n3-PUFA ARA, EPA and DHA. An evolutionary concept was hypothesized for ALOX15 specificity aiming to optimize the biosynthesis of anti-inflammatory mediators in higher primates [40]. During the course of inflammation, it is believed that a switch from predominantly pro-inflammatory mediators (e.g. ALOX5 derived leukotrienes) to anti-inflammatory lipoxins and resolvins (ALOX5/ALOX15 derived mediators) takes place [41]. ALOX15 is therefore a key enzyme in inflammation resolution and the biosynthesis of SPMs, which are formed via consecutive lipoxygenations by one or different enzymes or isoforms within a single cell or during cell-cell interactions [33]. Due to this formation pathway involving more than one enzymatic conversion step and their high biological potency, SPM levels in blood and tissue are generally low and detection in biological samples is challenging [42]. Therefore, sensitive and selective analytical tools are required for the detection of SPMs in order to allow

reproducible quantification of their *in vivo* levels. In *chapter 4,* SPMs including lipoxins derived from ARA and EPA, E- and D-series resolvins as well as DHA derived maresins and protectins were integrated in a multi-analyte LC-MS/MS method to allow their quantification in parallel to their mono-hydroxy precursors, the pro-inflammatory leukotrienes and prostaglandins as well as oxylipins formed via other enzymatic and autoxidation pathways. Instrumental and methodological parameters influencing the sensitivity were evaluated and detection of SPMs was carefully optimized for the analysis of biological samples.

In order to get a deeper insight into the formation of SPMs and the role of lipoxygenases in the formation of bioactive lipid mediators, their product profiles were thoroughly analyzed in *chapter 5*. Here, human ALOX isoforms were incubated with EPA and SPM pathway marker 18-HEPE and the LC-MS/MS method developed in *chapter 4* was applied to analyze the resulting product patterns with particular emphasis to double and triple oxygenated compounds. In order to simulate e.g. trans-cellular synthesis, 12- and 15-lipoxygenating enzymes were combined with ALOX5, which is involved in the production of SPMs by dioxygenation of the mono-hydroxylated precursors. Alongside well-established SPMs, incubation mixtures were screened for additional double and triple oxygenated products to appreciate the whole catalytic activities of the ALOX isoforms. For example, ALOX15 is known for its dual reaction specificity (as investigated in *chapter 3*) and its catalytic multiplicity [43] and therefore capable of synthesizing a more complex product pattern. Structures of the secondary products of ALOX isoforms acting alone or in combination with ALOX5 were suggested based on their collision induced dissociation product ion spectra. The formation of double or triple oxygenated secondary ALOX products likely involves various formation routes such as the leukotriene synthase activity or inverse substrate alignment at the active site of the enzyme giving rise to multiple hydroxylated compounds that might exert bioactivities similar to established SPMs.

Overall, this thesis contributes to a better understanding of the formation of n3-PUFA derived oxylipins with special emphasis on the role of lipoxygenases in the synthesis of (multiple) hydroxylated fatty acids. The distinct catalytic activities and resulting product profiles of lipoxygenases have important implications on their functional role in the biosynthesis of potent bioactive lipid mediators.

1.1 References

1. Zhang JY, Kothapalli KS, Brenna JT (2016) Desaturase and elongase-limiting endogenous long-chain polyunsaturated fatty acid biosynthesis. *Curr Opin Clin Nutr Metab Care*, 19(2), 103-110; doi: 10.1097/MCO.0000000000000254.
2. Spector AA (1999) Essentiality of fatty acids. *Lipids*, 34 Suppl, S1-3; doi: 10.1007/BF02562220.
3. Blasbalg TL, Hibbeln JR, Ramsden CE, Majchrzak SF, Rawlings RR (2011) Changes in consumption of omega-3 and omega-6 fatty acids in the United States during the 20th century. *Am J Clin Nutr*, 93(5), 950-962; doi: 10.3945/ajcn.110.006643.
4. Taber L, Chiu CH, Whelan J (1998) Assessment of the arachidonic acid content in foods commonly consumed in the American diet. *Lipids*, 33(12), 1151-1157; doi: 10.1007/s11745-998-0317-4.
5. Kris-Etherton PM, Taylor DS, Yu-Poth S, Huth P, Moriarty K, Fishell V, Hargrove RL, Zhao G, Etherton TD (2000) Polyunsaturated fatty acids in the food chain in the United States. *Am J Clin Nutr*, 71(1 Suppl), 179S-188S; doi: 10.1093/ajcn/71.1.179S.
6. Strobel C, Jahreis G, Kuhnt K (2012) Survey of n-3 and n-6 polyunsaturated fatty acids in fish and fish products. *Lipids Health Dis*, 11, 144; doi: 10.1186/1476-511X-11-144.
7. Guillou H, Zadravec D, Martin PG, Jacobsson A (2010) The key roles of elongases and desaturases in mammalian fatty acid metabolism: Insights from transgenic mice. *Prog Lipid Res*, 49(2), 186-199; doi: 10.1016/j.plipres.2009.12.002.
8. Brenner RR, Peluffo RO (1966) Effect of saturated and unsaturated fatty acids on the desaturation in vitro of palmitic, stearic, oleic, linoleic, and linolenic acids. *J Biol Chem*, 241(22), 5213-5219.
9. Brenna JT, Salem N, Jr., Sinclair AJ, Cunnane SC; International Society for the Study of Fatty Acids and Lipids, ISSFAL (2009) alpha-Linolenic acid supplementation and conversion to n-3 long-chain polyunsaturated fatty acids in humans. *Prostaglandins Leukot Essent Fatty Acids*, 80(2-3), 85-91; doi: 10.1016/j.plefa.2009.01.004
10. Browning LM, Walker CG, Mander AP, West AL, Madden J, Gambell JM, Young S, Wang L, Jebb SA, Calder PC (2012) Incorporation of eicosapentaenoic and docosahexaenoic acids into lipid pools when given as supplements providing doses equivalent to typical intakes of oily fish. *Am J Clin Nutr*, 96(4), 748-758; doi: 10.3945/ajcn.112.041343.
11. Institute of Medicine (2005) Dietary fats: Total fat and fatty acids. in: Dietary reference intakes for energy, carbohydrate, fiber, fat, fatty acids, cholesterol, protein, and amino acids, The National Academies Press, Washington, DC, 443-447; doi: 10.17226/10490.
12. EFSA Panel on Dietetic Products Nutrition and Allergies (2010) Scientific opinion on the substantiation of health claims related to docosahexaenoic acid (DHA) and maintenance of normal (fasting) blood concentrations of triglycerides (ID 533, 691, 3150), protection of blood lipids from oxidative damage (ID 630), contribution to the maintenance or achievement of a normal body weight (ID 629), brain, eye and nerve development (ID 627, 689, 704, 742, 3148, 3151), maintenance of normal brain function (ID 565, 626, 631, 689, 690, 704, 742, 3148, 3151), maintenance of normal vision (ID 627, 632, 743, 3149) and maintenance of normal spermatozoa motility (ID 628) pursuant to Article 13(1) of Regulation (EC) No 1924/2006. *EFSA Journal*, 8(10), 1734; doi: 10.2903/j.efsa.2010.1734.
13. Neuringer M, Connor WE, Van Petten C, Barstad L (1984) Dietary omega-3 fatty acid deficiency and visual loss in infant rhesus monkeys. *J Clin Invest*, 73(1), 272-276; doi: 10.1172/JCI111202.

14. Jacobson TA (2008) Role of n-3 fatty acids in the treatment of hypertriglyceridemia and cardiovascular disease. *Am J Clin Nutr*, 87(6), 1981S-1990S; doi: 10.1093/ajcn/87.6.1981S.
15. Howe PRC (1997) Dietary fats and hypertension - Focus on fish oil. *Ann Ny Acad Sci*, 827, 339-352; doi: 10.1111/j.1749-6632.1997.tb51846.x.
16. Buczynski MW, Dumlao DS, Dennis EA (2009) Thematic Review Series: Proteomics. An integrated omics analysis of eicosanoid biology. *J Lipid Res*, 50(6), 1015-1038; doi: 10.1194/jlr.R900004-JLR200.
17. Smith WL, DeWitt DL, Garavito RM (2000) Cyclooxygenases: Structural, cellular, and molecular biology. *Annu Rev Biochem*, 69, 145-182; doi: 10.1146/annurev.biochem.69.1.145.
18. Smith WL, Urade Y, Jakobsson PJ (2011) Enzymes of the cyclooxygenase pathways of prostanoid biosynthesis. *Chem Rev*, 111(10), 5821-5865; doi: 10.1021/cr2002992.
19. Yu R, Xiao L, Zhao G, Christman JW, van Breemen RB (2011) Competitive enzymatic interactions determine the relative amounts of prostaglandins E2 and D2. *J Pharmacol Exp Ther*, 339(2), 716-725; doi: 10.1124/jpet.111.185405.
20. Kuhn H, Banthiya S, van Leyen K (2015) Mammalian lipoxygenases and their biological relevance. *Biochim Biophys Acta*, 1851(4), 308-330; doi: 10.1016/j.bbalip.2014.10.002.
21. Christophersen BO (1968) Formation of monohydroxy-polyenic fatty acids from lipid peroxides by a glutathione peroxidase. *Biochim Biophys Acta*, 164(1), 35-46; doi: 10.1016/0005-2760(68)90068-4.
22. Shimizu T, Radmark O, Samuelsson B (1984) Enzyme with dual lipoxygenase activities catalyzes leukotriene A4 synthesis from arachidonic acid. *Proc Natl Acad Sci U S A*, 81(3), 689-693; doi: 10.1073/pnas.81.3.689.
23. Van Os CP, Rijke-Schilder GP, Van Halbeek H, Verhagen J, Vliegenthart JF (1981) Double dioxygenation of arachidonic acid by soybean lipoxygenase-1. Kinetics and regio-stereo specificities of the reaction steps. *Biochim Biophys Acta*, 663(1), 177-193; doi: 10.1016/0005-2760(81)90204-6.
24. Ford-Hutchinson AW, Bray MA, Doig MV, Shipley ME, Smith MJ (1980) Leukotriene B, a potent chemokinetic and aggregating substance released from polymorphonuclear leukocytes. *Nature*, 286(5770), 264-265; doi: 10.1038/286264a0.
25. Serhan CN, Hamberg M, Samuelsson B (1984) Lipoxins: novel series of biologically active compounds formed from arachidonic acid in human leukocytes. *Proc Natl Acad Sci U S A*, 81(17), 5335-5339; doi: 10.1073/pnas.81.17.5335.
26. Capdevila JH, Falck JR, Harris RC (2000) Cytochrome P450 and arachidonic acid bioactivation. Molecular and functional properties of the arachidonate monooxygenase. *J Lipid Res*, 41(2), 163-181.
27. Morisseau C, Hammock BD (2005) Epoxide hydrolases: mechanisms, inhibitor designs, and biological roles. *Annu Rev Pharmacol Toxicol*, 45, 311-333; doi: 10.1146/annurev.pharmtox.45.120403.095920.
28. Morrow JD, Awad JA, Boss HJ, Blair IA, Roberts LJ 2nd (1992) Non-cyclooxygenase-derived prostanoids (F2-isoprostanes) are formed in situ on phospholipids. *Proc Natl Acad Sci U S A*, 89(22), 10721-10725; doi: 10.1073/pnas.89.22.10721.
29. Yin H, Xu L, Porter NA (2011) Free radical lipid peroxidation: mechanisms and analysis. *Chem Rev*, 111(10), 5944-5972; doi: 10.1021/cr200084z.
30. Rund KM, Heylmann D, Seiwert N, Wecklein S, Oger C, Galano JM, Durand T, Chen R, Gueler F, Fahrer J, Bornhorst J, Schebb NH (2019) Formation of trans-epoxy fatty acids correlates with formation of isoprostanes and could serve as biomarker of oxidative stress. *Prostaglandins Other Lipid Mediat*, 144, 106334; doi: 10.1016/j.prostaglandins.2019.04.004.

31. Wada M, DeLong CJ, Hong YH, Rieke CJ, Song I, Sidhu RS, Yuan C, Warnock M, Schmaier AH, Yokoyama C, Smyth EM, Wilson SJ, FitzGerald GA, Garavito RM, Sui DX, Regan JW, Smith WL (2007) Enzymes and receptors of prostaglandin pathways with arachidonic acid-derived versus eicosapentaenoic acid-derived substrates and products. *J Biol Chem*, 282(31), 22254-22266; doi: 10.1074/jbc.M703169200.
32. Terano T, Salmon JA, Moncada S (1984) Biosynthesis and biological activity of leukotriene B5. *Prostaglandins*, 27(2), 217-232; doi: 10.1016/0090-6980(84)90075-3.
33. Serhan CN, Petasis NA (2011) Resolvins and protectins in inflammation resolution. *Chem Rev*, 111(10), 5922-5943; doi: 10.1021/cr100396c.
34. Ostermann AI, West AL, Schoenfeld K, Browning LM, Walker CG, Jebb SA, Calder PC, Schebb NH (2019) Plasma oxylipins respond in a linear dose-response manner with increased intake of EPA and DHA: results from a randomized controlled trial in healthy humans. *Am J Clin Nutr*, 109(5), 1251-1263; doi: 10.1093/ajcn/nqz016.
35. Ostermann AI, Waindok P, Schmidt MJ, Chiu CY, Smyl C, Rohwer N, Weylandt KH, Schebb NH (2017) Modulation of the endogenous omega-3 fatty acid and oxylipin profile in vivo-A comparison of the fat-1 transgenic mouse with C57BL/6 wildtype mice on an omega-3 fatty acid enriched diet. *PLoS One*, 12(9), e0184470; doi: 10.1371/journal.pone.0184470.
36. Camuesco D, Galvez J, Nieto A, Comalada M, Rodriguez-Cabezas ME, Concha A, Xaus J, Zarzuelo A (2005) Dietary olive oil supplemented with fish oil, rich in EPA and DHA (n-3) polyunsaturated fatty acids, attenuates colonic inflammation in rats with DSS-induced colitis. *J Nutr*, 135(4), 687-694; doi: 10.1093/jn/135.4.687.
37. Rund KM, Peng S, Greite R, Claassen C, Nolte F, Oger C, Galano JM, Balas L, Durand T, Chen R, Gueler F, Schebb NH (2020) Dietary omega-3 PUFA improved tubular function after ischemia induced acute kidney injury in mice but did not attenuate impairment of renal function. *Prostaglandins Other Lipid Mediat*, 146, 106386; doi: 10.1016/j.prostaglandins.2019.106386.
38. Willenberg I, Rund K, Rong S, Shushakova N, Gueler F, Schebb NH (2016) Characterization of changes in plasma and tissue oxylipin levels in LPS and CLP induced murine sepsis. *Inflamm Res*, 65(2), 133-142; doi: 10.1007/s00011-015-0897-7.
39. Bannenberg GL, Chiang N, Ariel A, Arita M, Tjonahen E, Gotlinger KH, Hong S, Serhan CN (2005) Molecular circuits of resolution: formation and actions of resolvins and protectins. *J Immunol*, 174(7), 4345-4355; doi: 10.4049/jimmunol.174.7.4345.
40. Adel S, Karst F, Gonzalez-Lafont A, Pekarova M, Saura P, Masgrau L, Lluch JM, Stehling S, Horn T, Kuhn H, Heydeck D (2016) Evolutionary alteration of ALOX15 specificity optimizes the biosynthesis of antiinflammatory and proresolving lipoxins. *P Natl Acad Sci USA*, 113(30), E4266-E4275; doi: 10.1073/pnas.1604029113.
41. Levy BD, Clish CB, Schmidt B, Gronert K, Serhan CN (2001) Lipid mediator class switching during acute inflammation: signals in resolution. *Nat Immunol*, 2(7), 612-619; doi: 10.1038/89759.
42. Murphy RC (2015) Specialized pro-resolving mediators: do they circulate in plasma? *J Lipid Res*, 56(9), 1641-1642; doi: 10.1194/jlr.C062356.
43. Ivanov I, Kuhn H, Heydeck D (2015) Structural and functional biology of arachidonic acid 15-lipoxygenase-1 (ALOX15). *Gene*, 573(1), 1-32; doi: 10.1016/j.gene.2015.07.073.

Chapter 2

Effect of dietary EPA and DHA on murine blood and liver fatty acid profile and liver oxylipin pattern depending on high and low dietary n6-PUFA

The intake of long-chain n3-polyunsaturated fatty acids (PUFA), which are associated with beneficial health effects, is low in the Western diet, while the portion of dietary n6-PUFA and hence the n6/n3-PUFA ratio is high. Strategies to improve the n3-PUFA status are n3-PUFA supplementation and/or lowering n6-PUFA intake. In the present study, mice were fed with two different sunflower oil-based control diets rich in linoleic (n6-high) or oleic acid (n6-low), either with low n3-PUFA content (~0.02%) as control or with ~0.6% eicosapentaenoic acid (EPA) or docosahexaenoic acid (DHA). The n6-low diet had only little or no effect on levels of arachidonic acid (ARA) and its free oxylipins in liver tissue. Supplementation with EPA or DHA lowered ARA levels with an effect size of n6-high < n6-low. Blood cell %EPA+DHA reached > 8% and > 11% in n6-high and n6-low groups, respectively. Elevation of EPA levels and EPA derived oxylipins was most pronounced in n6-low groups in liver tissue, while levels of DHA and DHA derived oxylipins were generally unaffected by the background diet. While the n6-low diet alone had no effect on blood and liver tissue ARA levels or n3-PUFA status, a supplementation of EPA or DHA was more effective in combination with an n6-low diet. Thus, supplementation of long-chain n3-PUFA combined with a reduction of dietary n6-PUFA is the most effective way to improve the endogenous n3-PUFA status.

Adapted from *Food & Function*, Kutzner L, Esselun C, Franke N, Schoenfeld K, Eckert GP, Schebb NH, Effect of dietary EPA and DHA on murine blood and liver fatty acid profile and liver oxylipin pattern depending on high and low dietary n6-PUFA, doi: 10.1039/D0FO01462A – Published by the Royal Society of Chemistry.

Author contributions: LK designed research, performed experiments and wrote the manuscript; CE performed experiments and wrote the manuscript; NF performed experiments; KS performed experiments as part of her master thesis under the supervision of LK; GPE, NHS designed research and wrote the manuscript.

2.1 Introduction

Polyunsaturated fatty acids (PUFA) of the n3- and n6-family are essential nutrients because humans and most mammals do not possess the Δ12- and Δ15-desaturases. [1] Therefore, FA linoleic acid (LA, C18:2n6) and alpha-linolenic acid (ALA, C18:3n3) that are contained in e.g. plant seeds and nuts must be supplied by the diet and can be elongated/desaturated to long-chain PUFA of the n6- and n3-family, which are crucial as constituents of cell membranes and precursors for bioactive lipid mediators. [2] Attention has been paid to the positive effects of long-chain n3-PUFA eicosapentaenoic acid (EPA, C20:5n3) and docosahexaenoic acid (DHA, C22:6n3) and their health implications, e.g. in cardiovascular disease [3] and inflammatory processes [4], while effects exerted by ALA are usually less pronounced [5]. At least a part of the beneficial health effects of EPA and DHA are mediated by their eicosanoids and other oxylipins or shifts in the overall oxylipin profile. These bioactive lipid mediators are formed within the arachidonic acid (ARA, C20:4n6) cascade via three major enzymatic pathways and autoxidation. PUFA are converted by cyclooxygenases (COX) to prostanoids, i.e. prostaglandins and thromboxanes, however, also hydro(pero)xy PUFA formation can be catalyzed by COX enzymes. Lipoxygenases (LOX) are dioxygenases that lead to the formation of regio- and stereo-specific hydro(pero)xy fatty acids depending on the LOX isoform as well as leukotrienes and other multiple hydroxylated PUFA derivatives. Cytochrome P450 monooxygenases (CYP) are involved in the formation of terminal and mid-chain hydroxy PUFA as well as *cis*-epoxy PUFA, which can be enzymatically hydrolyzed by the soluble epoxide hydrolases (sEH) to the corresponding vicinal dihydroxy PUFA [6, 7]. Moreover, oxylipins can be formed by autoxidative processes leading to the formation of a vast number of prostaglandin-like isoprostanes and isofuranes, hydro(pero)xy fatty acids as well as *cis*- and *trans*-epoxy PUFA [8, 9].

Due to low EPA+DHA intake and relatively inefficient conversion of ALA to EPA and DHA in humans on a Western diet, blood and tissue levels of EPA+DHA are low [5, 10]. At the same time, there is an increased ingestion of n6-PUFA, e.g.

due to consumption of plant oils rich in LA such as corn, sunflower or soybean oil leading to a high n6/n3-PUFA ratio in industrialized countries [10]. Although PUFA consumption is associated with beneficial effects such as lowering serum cholesterol [11], high levels of n6-PUFA might favor the incorporation of ARA into blood/tissue phospholipids resulting in a high capacity for the formation of ARA derived, predominantly pro-inflammatory lipid mediators [12, 13]. Similarly, supplementation with long-chain n3-PUFA EPA and DHA increases both the endogenous levels of these PUFA as well as their oxylipins in a dose-response manner [14, 15]. Moreover, due to competition for enzymatic conversion, n3-PUFA interventions may reduce the formation of ARA and other n6-PUFA derived oxylipins [15]. For example, in mice and rats dietary EPA and DHA induced a shift in the overall tissue oxylipin profile by decreasing ARA derived oxylipins and increasing n3-PUFA derived oxylipins [16, 17]. Several oxylipins synthesized from EPA or DHA exert less inflammatory activity compared to those from ARA, e.g. EPA derived LTB_5 vs. ARA derived LTB_4 [18] or are directly involved in the resolution of inflammation, e.g. EPA and DHA derived specialized pro-resolving mediators (SPMs) [19].

Balancing dietary n6- and n3-PUFA and thereby endogenous n6- and n3-PUFA levels as well as their oxylipins may have positive implications for human health, e.g. in the context of cardiovascular disease [10]. Modulation of the dietary n6/n3-PUFA ratio can be achieved by different LA/ALA ratios in order to increase the EPA+DHA status [20]. However, elevation of long-chain n3-PUFA levels is more effective, when EPA and/or DHA are supplemented directly [21] and low intake of (competing) n6-PUFA could augment n3-PUFA uptake in blood and tissue lipid pools. In fact, increased n3-PUFA levels were observed in human erythrocytes and plasma when dietary LA was low and further elevated when combined with n3-PUFA supplementation [22, 23]. A combination of EPA+DHA supplementation with saturated fat resulted in a similar decrease of ARA and a more pronounced increase of EPA erythrocyte levels compared to a combination with an n6-PUFA-rich diet [24]. Instead of increasing the intake of saturated fatty acids (SFA), dietary n6-PUFA can also be replaced by monounsaturated fatty

acids (MUFA), such as oleic acid (OA, C18:1n9), which is contained in large amounts in e.g. olive oil. For example, lower ARA phospholipid levels when comparing dietary n6-PUFA-rich diets with olive oil-rich diets have been observed in mice [25] and rats [26]. Hence, a combination of MUFA and n3-PUFA is a promising approach in order to diminish excessive n6-PUFA intake, to reach a more balanced n6/n3-PUFA ratio and thereby increasing n3-PUFA bioavailability.

In order to get a deeper and more mechanistic understanding in how a combination of dietary MUFA (OA) supplemented with EPA or DHA affects tissue levels of n3- and n6-PUFA as well as the free oxylipins derived from those FA, we fed mice two different sunflower oil-based background diets (rich in LA or rich in OA) and supplemented either EPA or DHA. This background diet was chosen in order to keep influences from dietary n3-PUFA (e.g. ALA) minimal, maintain tissue SFA relatively constant and accept little influence related to the fat origin and other ingredients (e.g. antioxidants and polyphenols from olive oil). However, results using animal models may not be (completely) transferable to humans. Mice differ from humans regarding their FA and oxylipin metabolism. For example, mice can elongate and desaturate ALA more efficiently to EPA and DHA than humans [27]. Thus, in the present study we used diets, which were low in ALA in order to assign observed effects to EPA/DHA administration rather than an efficient elongation/desaturation of ALA. It should be noted that this leads to a very low n3-PUFA content in the control groups. Analysis of a comprehensive set of both FA and free oxylipins allows to draw profound conclusions on how a background diet rich in LA or OA affects FA metabolism, how the tissue FA and oxylipin pattern can be further modified by a moderate dose of EPA or DHA and if the lowering n6-PUFA intake, n3-PUFA supplementation or a combination of both is most effective in improving the blood and tissue n3-PUFA status.

2.2 Experimental

2.2.1 Chemicals

HPLC-grade methanol (MeOH) and methyl *tert*-butyl ether (MTBE, Acros Organics) as well as LC-MS grade MeOH, acetonitrile (ACN) and acetic acid (HOAc) were purchased from Fisher Scientific (Schwerte, Germany). Ammonium acetate was purchased from Merck (Darmstadt, Germany), potassium carbonate, ethyl acetate and acetyl chloride were obtained from Sigma Aldrich (Schnelldorf, Germany). Disodium hydrogen phosphate and *n*-hexane were obtained from Carl Roth (Karlsruhe, Germany). Oxylipin standard substances and deuterated internal oxylipin standards were purchased from Cayman Chemicals via local distributor Biomol (Hamburg, Germany), E-series resolvins RvE2, 18(*S*)-RvE3 and 18(*R*)-RvE3 were a kind gift of the lab of Makoto Arita (RIKEN Center for Integrative Medical Sciences, Japan), methyl pentacosanoate (FAME C25:0) was obtained from Santa Cruz Biotechnology (Heidelberg, Germany). PCR primers were purchased from Cayman Chemicals via local distributor Biomol (Hamburg, Germany).

2.2.2 Animal experiments

Three weeks old female NMRI (Navar Medical Research Institute) mice were purchased from Charles River (Sulzbach, Germany). For this study we only used female mice, because male mice would probably attack each other after being placed in different cages one after the other following randomization into the groups. Therefore, part of the variability regarding lipid metabolism could be based on the estrous cycle, which is generally 4–5 days in length. As experimentation was conducted in a continuous period, results should encompass all estrous states and not be biased by a specific state. Furthermore, studies have shown that phenotypic differences between female and male mice are rather small [28]. Animals were housed according to the German guidelines

for animal care and had, at all times, access to water and food *ad libitum*. Mice were maintained on a 12 h light/dark cycle. Mice were randomized into 6 groups with 8 mice each: control (c)/n6-high, EPA/n6-high, DHA/n6-high, c/n6-low, EPA/n6-low and DHA/n6-low. Feeding started after one week of acclimatization, when mice were 4 weeks old. Animals were fed a total of 28 days, left-over feed was collected and weighed and new feed was distributed on a daily basis during the first week and bi-weekly during the following 3 weeks. Mice received a standard diet (product number: E15051, ssniff Spezialitäten GmbH, Soest, Germany) with 10.1% total fat consisting of different oil mixtures: for n6-PUFA-high feed commercial refined sunflower oil (Thomy, Nestlé, Frankfurt, Germany) rich in LA was used and for n6-PUFA-low feed refined sunflower oil (Henry Lamotte Oils GmbH, Bremen, Germany) rich in OA was used. For EPA/n6-high and EPA/n6-low feed EPA was added in form of EPA-ethyl ester (EE) to LA-rich and OA-rich sunflower oil, respectively, resulting in a final EPA content of 5.5–5.7% of total FA (0.55–0.57% in feed). For DHA/n6-high and DHA/n6-low feed DHA was added in form of DHA-EE to LA-rich and OA-rich sunflower oil, respectively, resulting in a final DHA content of 5.4–5.7% of total FA (0.54–0.57% in feed). All six oil mixtures contained 0.2% mixed tocopherol concentrate as antioxidant. The full composition of the diets and the FA profile of oils used as dietary fat are summarized in the appendix (Tab. 8.1). Following the feeding period, mice were killed by cervical dislocation and decapitation. Whole blood was collected in EDTA tubes and centrifuged (10 min, 1500 × g, 4 °C). Plasma was collected, blood cells were resuspended in the respective volume of PBS buffer and stored at –80 °C until analysis. Liver and other organs were quickly removed and frozen in liquid nitrogen before they were stored for longer periods of time at –80 °C.

All experiments were carried out by individuals with appropriate training and experience according to the requirements of the Federation of European Laboratory Animal Science Associations and the European Communities Council Directive (Directive 2010/63/EU).

2.2.3 Fatty acid analysis, GC-FID

The method for FA analysis based on gas chromatography with flame ionization detection (GC-FID) as described [29, 30] was slightly modified. In brief, 20 µL plasma (diluted with 30 µL H_2O) or 100 µL resuspended blood cells (BC) were mixed with 10 µL methyl pentacosanoate (FAME C25:0, 750 µM) as internal standard (IS) as well as 10 µL 0.02 mg/mL BHT and EDTA in MeOH/H_2O (50/50, *v/v*) as antioxidant and extracted with MTBE/MeOH. To 15 ± 2 mg liver tissue 10 µL IS, 50 µL H_2O and 300 µL MeOH were added and tissue was homogenized in a ball mill using pre-cooled sample holders (25 Hz, 5 min) before MTBE/MeOH extraction. Dry lipid extracts were trans-esterified with methanolic hydrogen (90–95°C, 60 min) and the resulting FAMEs were injected into the GC system. Quantification was based on theoretical response factors (tRF) utilizing C25:0 as IS and FA profile was determined by relative peak areas (taking into account the tRF). The method covers a total of 39 FAMEs (excluding C25:0).

2.2.4 Gene expression analysis by quantitative real-time PCR (qPCR)

RNA was isolated using the RNAeasy Mini Kit (Qiagen, Hilden, Germany) following the manufacturer's instructions. Previously frozen liver tissue stored at –80 °C, was thawed carefully before isolation. Following isolation, RNA concentration was determined via NanoDrop™ One/Onec (Thermo Fisher Scientific, Waltham, MA, USA) measuring the absorbance at 260 and 280 nm. Ratios of absorbance 260/280 nm and 260/230 nm were used as a marker for RNA purity. To increase purity and remove residual genomic DNA, samples were treated with TURBO DNA-free™ Kit according to the manufacturer's instructions (Thermo Fisher Scientific, Waltham, MA, USA). Following purification, 1 µg of total RNA was used for complementary cDNA synthesis using the iScript cDNA Synthesis Kit (BioRad, Munich, Germany) according to the manufacturer's instructions and BioRad Thermo Cycler T100 (BioRad, Munich, Germany). Until qPCR experiments, samples were stored at –80 °C. Quantitative real-time PCR was conducted using a CFX Connect™ system (BioRad, Munich, Germany). A

list of all used oligonucleotide primer sequences, primer concentrations, product sizes and the applied PCR protocol can be found in the appendix (Tab. 8.2). For all experiments, the initial denaturation step was conducted at 95 °C for 3 min, followed by a varying number of cycles each consisting of a short denaturation phase (95 °C, 10 s), an annealing phase with differing temperatures (53 °C to 62.8 °C) and durations (30 s to 45 s) depending on the primer used and a final elongation step (72 °C, 30 s). Gene expression was analyzed with BioRad CFX Manager 3.1 software using the 2ΔΔCq method. Results were normalized to expression levels of housekeeping genes beta-2-microglobuline (B2M) and phosphoglycerate kinase 1 (PGK1) and expressed in % relative to the c/n6-high group.

2.2.5 Oxylipin analysis, LC-MS/MS

Oxylipin extraction and measurement was performed as described [31, 32]. In brief, to 50 ± 5 mg liver tissue 10 µL antioxidant mixture, 10 µL deuterated IS and 300 µL ice-cold MeOH were added and tissue samples were homogenized using a ball mill as described above. After centrifugation of tissue homogenates (10 min, 20000 × g, 4 °C), supernatants were diluted with 2.7 mL 0.1 M disodium hydrogen phosphate buffer (pH 6) and loaded onto the pre-conditioned solid phase extraction cartridges (SPE; Bond Elut Certify II, 200 mg, 3 mL; Agilent, Waldbronn, Germany). After washing the SPE cartridges with water and MeOH/water (50/50, *v/v*) and drying (30 s, –200 mbar), oxylipins were eluted with ethyl acetate/*n*-hexane (75/25, *v/v*) with 1% HOAc and evaporated to dryness in a vacuum concentrator. Reconstituted sample extracts were injected into the LC-MS/MS system (Agilent 1290 binary pump coupled to AB Sciex 6500 QTRAP MS) and separated on a Zorbax Eclipse Plus C18 reversed phase column (Agilent, Waldbronn, Germany) with a binary gradient using 0.1% HOAc with 5% solvent B as solvent A and ACN/MeOH/HOAc (800/150/1, *v/v/v*) as solvent B. Measurement was carried out in scheduled selected reaction monitoring (SRM) mode and quantification was carried out by external calibration (analyte/IS area ratio). A total of 137 oxylipins was analyzed in the liver samples.

2.2.6 Data analysis and statistical analysis

For concentrations and relative levels of FA and oxylipins as well as relative gene expression mean values and standard error of the mean (SEM) were calculated using Microsoft Office Excel 2016 software (Redmond, WA, USA). Concentrations of FA and oxylipins were only quantified when exceeding the lower limit of quantification (LLOQ). If ≥ 50% of the concentrations within a group were > LLOQ, concentrations < LLOQ were set to ½ LLOQ and mean ± SEM were calculated. If the mean did not exceed LLOQ or < 50% of the samples within a group were > LLOQ, "< LLOQ" is displayed for the whole group. For relative FA profile (% of total FA) FA < LLOQ were set to zero and mean ± SEM were only calculated if ≥ 50% of the values within a group were > LLOQ.

Enzyme activity estimates were calculated based on product/precursor ratios as follows: D6D-index = C18:3n6/C18:2n6, D5D-index = C20:4n6/C20:3n6 [33], Elovl-index = C22:4n6/C20:4n6 [34]. Calculation of %n3 in highly unsaturated fatty acids (HUFA) and %n6 in HUFA was based on Lands *et al*. (2018) [35].

Statistical analysis was carried out using GraphPad Prism 6.01 software (GraphPad Software, San Diego, CA, USA). Statistically significant differences were determined by two-way ANOVA analysis (factor 1: background diet n6-high/n6-low; factor 2: n3-PUFA supplementation c/EPA/DHA) with Tukey's post-test for multiple comparisons (each mean with every other mean): ns ($p > 0.05$), * ($p < 0.05$), ** ($p < 0.01$), *** ($p < 0.001$), **** ($p < 0.0001$) and are summarized in the appendix (Tab. 8.8). If a whole group was < LLOQ, a modified two-way ANOVA (fewer groups) and/or a one-way ANOVA (comparison of groups with the same background diet) or a t-Test was performed. For relative gene expression data outliers were removed based on ROUT outlier test (Q = 1%).

2.3 Results

2.3.1 Animal food consumption and effect on body weight

All experimental diets contained 10.1% fat and the total FA compositions of the oils used for the preparation of the feed were analyzed by GC-FID (appendix, Tab. 8.1). Initial change of diets resulted in an increased consumption of food on the first day of the feeding period across all groups vs. food consumption for the rest of the feeding period (34.0 ± 0.9 g vs. 26.4 ± 0.5 g; $p < 0.0001$). Neither the high/low n6-PUFA content of the diet nor the added EPA or DHA had an effect on food consumption (appendix, Tab. 8.3). Weight of mice increased during the feeding period (appendix, Tab. 8.4). Changes in weight were similar across all groups and independent from the different fats used in the diets.

2.3.2 Relative fatty acid profile and n3-PUFA status

Four weeks of feeding a diet with high or low content of n6-PUFA and very low n3-PUFA content (~0.2% in feeding oils; appendix Tab. 8.1) led to a strikingly different FA profile in murine liver tissue. This affected all FA classes (SFA, MUFA, PUFA) except %n3-PUFA, which were similarly low (2.6 ± 0.3% (c/n6-high) and 2.0 ± 0.3% (c/n6-low); Fig. 2.1, appendix Tab. 8.5 A-2). Noteworthy, lower %SFA were attributable to higher total liver FA and accumulating OA in the c/n6-low compared to the c/n6-high group. Consistent with the major dietary FA class (high LA vs. high OA), extreme differences were observed for %MUFA and %n6-PUFA: MUFA were the dominant FA class in the c/n6-low group (59 ± 3%) and 2.0-fold higher compared to the c/n6-high group (29 ± 3%), while n6-PUFA were the dominant FA class in the c/n6-high group (37 ± 2%) and 2.7-fold higher compared to the c/n6-low group (14 ± 2%). Feeding the EPA-rich diet resulted in an increase of %n3-PUFA in liver tissue regardless of the n6-PUFA content (8.3 ± 0.5% and 8.1 ± 1.1% in EPA/n6-high and EPA/n6-low, respectively). A similar increase of %n3-PUFA was observed in the

DHA-supplemented groups (9.6 ± 0.8% and 9.9 ± 0.7% in DHA/n6-high and DHA/n6-low, respectively; Fig. 2.1). In animals on an n6-PUFA-high diet neither EPA nor DHA supplementation significantly affected %MUFA or %n6-PUFA. In animals fed an n6-PUFA-low diet %MUFA (c/n6-low 59 ± 3%) were decreased by supplementation with EPA to 48 ± 3% and DHA to 45 ± 2%.

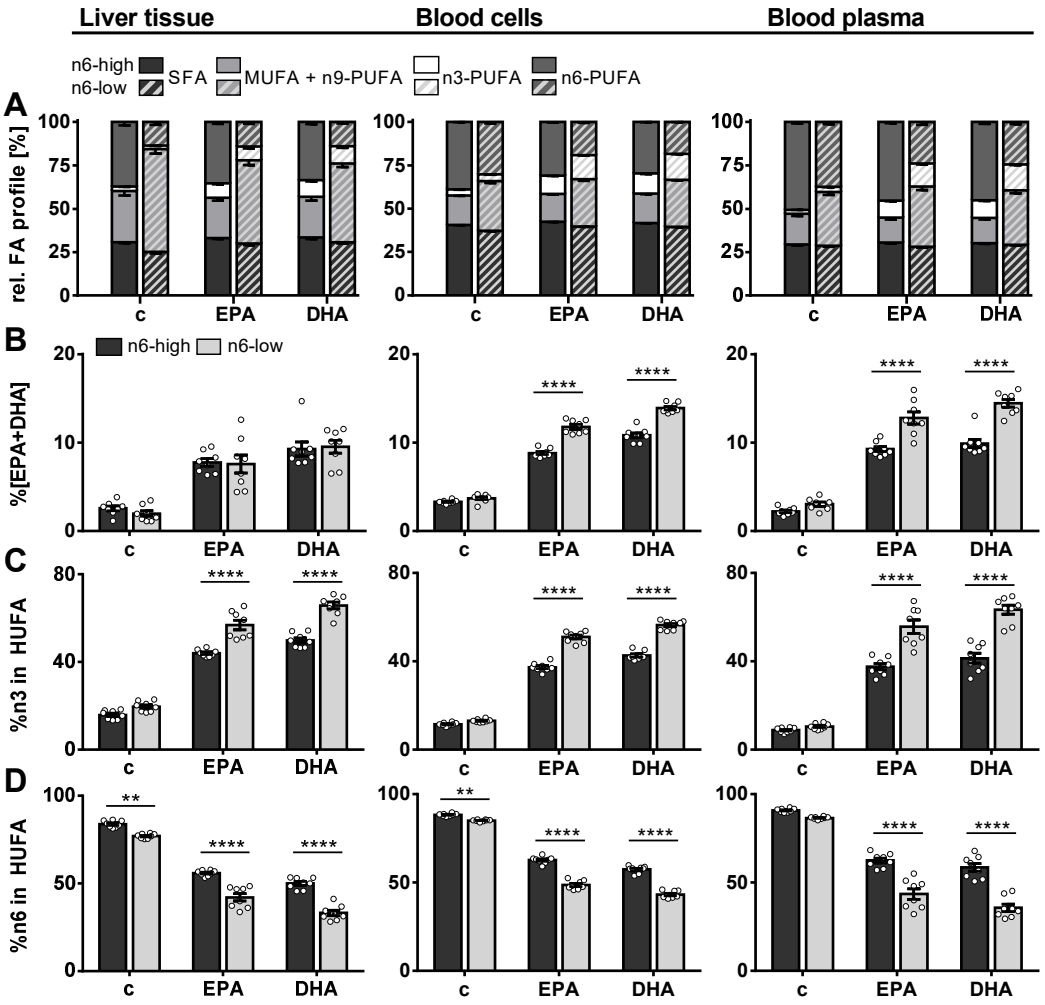

Fig. 2.1: Relative fatty acid profile in mouse liver, blood cells and blood plasma. (**A**) Relative levels of saturated (SFA), monounsaturated (MUFA), n3- and n6-polyunsaturated fatty acids (PUFA) as well as (**B**) %EPA+DHA, (**C**) %n3 in highly unsaturated fatty acids (HUFA) and (**D**) %n6 in HUFA in liver tissue, blood cells and blood plasma of NMRI mice after 28 days of feeding an n6-PUFA-rich diet (dark grey) or an n6-PUFA-low diet (light grey) without (c) or with n3-PUFA supplementation (EPA, DHA). Sum of MUFA includes one n9-PUFA (C20:3n9). Shown are mean ± SEM as well as individual values for B–D (n = 8). Statistically significant differences (* $p < 0.05$; ** $p < 0.01$; *** $p < 0.001$; **** $p < 0.0001$) were determined by two-way ANOVA with Tukey's post-test and are indicated for n6-high vs. n6-low groups (results for comparisons of all groups are summarized in the appendix, Tab. 8.8).

Regarding the n3-PUFA status, liver %EPA+DHA was not different between the groups fed an n6-PUFA-high or n6-PUFA-low based diet (Fig. 2.1). In contrast, in BC increase of %EPA+DHA relative to the control group was in the order of EPA/n6-high < EPA/n6-low < DHA/n6-high < DHA/n6-low with a 2.7–3.2-fold increase for EPA-fed groups and a 3.3–3.8-fold increase for DHA-fed groups. Thus, for both the n6-high and n6-low background diet DHA supplementation increased BC %EPA+DHA more efficiently than EPA supplementation. Importantly, while %EPA+DHA was not different between the control groups c/n6-high and c/n6-low, elevation of BC %EPA+DHA upon n3-PUFA feeding was clearly more pronounced when combined with an n6-PUFA-low background diet. This was also the case in blood plasma. Levels of %n3 in HUFA were consistently higher in the n6-low compared to n6-high-based groups in liver, BC and plasma and more effectively raised by DHA feeding in liver and BC. %n6 in HUFA showed the reversed trend (Fig. 2.1). Complete relative FA profiles in liver, BC and plasma are summarized in the appendix (Fig. 8.1, Tab. 8.5).

2.3.3 Fatty acid concentrations in liver tissue

Dominant FA in liver tissue was OA in both control groups, however, 3.3-fold lower in the c/n6-high compared to c/n6-low group (16 ± 4 g/kg vs. 53 ± 10 g/kg). Higher dietary LA resulted in 2.6-fold higher LA in the c/n6-high compared to c/n6-low group (13.4 ± 1.1 g/kg vs. 5.2 ± 0.6 g/kg). Despite this pronounced difference in liver LA concentrations (Fig. 2.2), tissue ARA concentrations were not different between the two background diets (6.5 ± 0.2 g/kg vs. 5.6 ± 0.3 g/kg).

Fig. 2.2 (right, page 23): Fatty acid concentrations in mouse liver tissue. Concentrations [g/kg wet tissue] of n9-MUFA and -PUFA as well as n3- and n6-PUFA in liver tissue of NMRI mice after 28 days of feeding an n6-PUFA-rich diet (dark grey) or an n6-PUFA-low diet (light grey) without (c) or with n3-PUFA supplementation (EPA, DHA). Shown are mean ± SEM as well as individual values (n = 8). If > 50% of the samples within one group were < LLOQ (lower limit of quantification), no mean was calculated and the LLOQ is indicated as dotted line. Statistically significant differences (* $p < 0.05$; ** $p < 0.01$; *** $p < 0.001$; **** $p < 0.0001$) were determined by two-way ANOVA with Tukey's post-test and are indicated for n6-high vs. n6-low groups (results for comparisons of all groups are summarized in the appendix, Tab. 8.8). Arrows and gene names indicate enzymes involved in FA desaturation and elongation and proposed formation routes adapted from Guillou *et al*. (2010) [50].

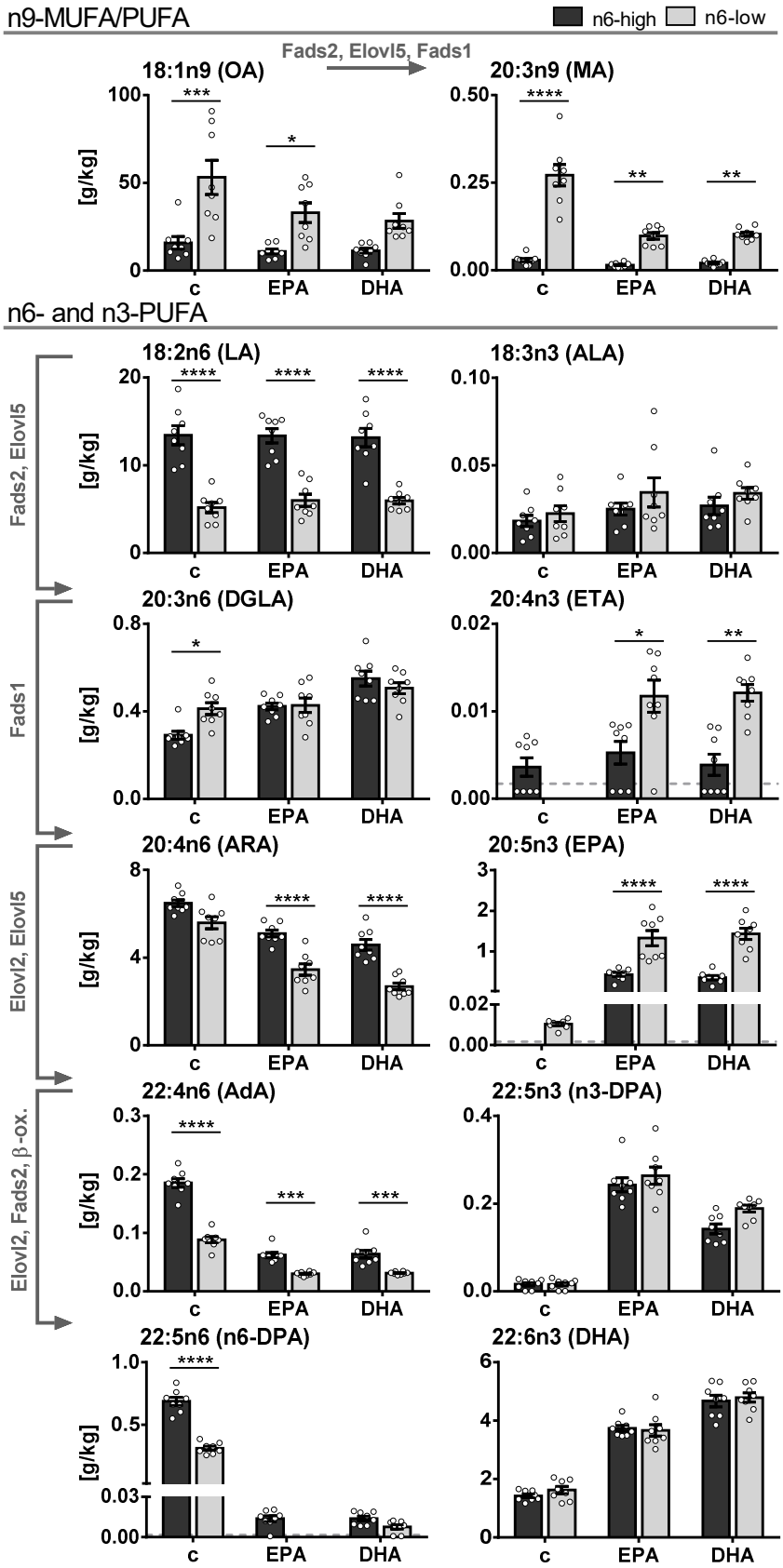
n9-MUFA/PUFA
n6-high
n6-low
Fads2, Elovl5, Fads1
18:1n9 (OA)
20:3n9 (MA)
[g/kg]
c
EPA
DHA
n6- and n3-PUFA
Fads2, Elovl5
Fads1
Elovl2, Elovl5
Elovl2, Fads2, β-ox.
18:2n6 (LA)
18:3n3 (ALA)
20:3n6 (DGLA)
20:4n3 (ETA)
20:4n6 (ARA)
20:5n3 (EPA)
22:4n6 (AdA)
22:5n3 (n3-DPA)
22:5n6 (n6-DPA)
22:6n3 (DHA)

In contrast to ARA, its downstream elongation/desaturation products, i.e. adrenic acid (AdA, C22:4n6) and n6-docosapentaenoic acid (n6-DPA, C22:5n6), were lower in the c/n6-low group. Long-chain n3-PUFA EPA, n3-DPA and DHA were similar in both control groups.

Upon n3-PUFA feeding, ARA concentrations were reduced in all feeding groups, while dihomo-gamma linolenic acid (DGLA, C20:3n6) levels were elevated in n6-high groups and LA levels were unaffected. Notably, ARA concentrations were lower in EPA/n6-low and DHA/n6-low groups compared to EPA/n6-high and DHA/n6-high groups (Fig. 2.2). EPA, which did not exceed the LLOQ in c/n6-high, was increased to 0.43 ± 0.05 g/kg in the EPA/n6-high group. In the EPA/n6-low group, EPA increased from 0.010 ± 0.001 g/kg (c/n6-low) to 1.3 ± 0.2 g/kg corresponding to a 130-fold increase and 3.1-fold higher concentration compared to the n6-PUFA-high based diet. Interestingly, DHA supplementation had a similar effect on EPA concentrations in liver tissue (DHA/n6-high: 0.36 ± 0.05 g/kg, DHA/n6-low: 1.4 ± 0.1 g/kg). The elongation product of EPA, n3-DPA, was effectively elevated by both EPA and DHA supplementation, however, more pronounced in EPA-fed groups. The n6-PUFA background diet had no effect on n3-DPA levels (Fig. 2.2). Liver tissue DHA concentrations increased upon EPA feeding and were more efficiently elevated in DHA-fed groups. In contrast to EPA levels, DHA concentrations did not differ between the groups fed the n6-high or n6-low background diets (Fig. 2.2). All liver FA concentrations and statistical analyses are summarized in the appendix (Tab. 8.5 A-1, Tab. 8.8 A-1).

2.3.4 Fatty acid metabolizing enzyme expression in liver

Gene expression of several markers of β-oxidation as well as FA elongation and desaturation were assessed via transcription analysis in qPCR experiments (Fig. 2.3; appendix Tab. 8.6).

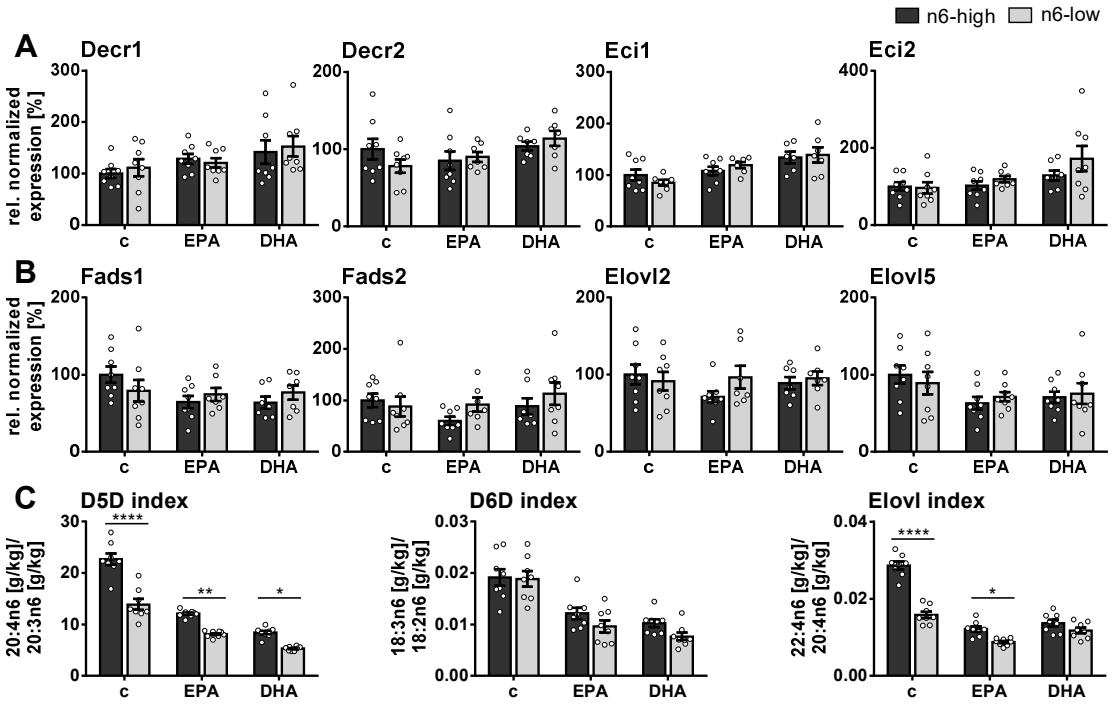

Fig. 2.3: Gene expression of enzymes and enzyme activity indices in mouse liver. Normalized gene expression relative to the c/n6-high group of enzymes involved in fatty acid β-oxidation, desaturation and elongation in liver tissue of NMRI mice after 28 days of feeding an n6-PUFA-rich diet (dark grey) or an n6-PUFA-low diet (light grey) without (c) or with n3-PUFA supplementation (EPA, DHA). Shown are mean ± SEM (n = 6–8) as well as individual values for (**A**) 2,4-dienoyl-CoA reductase 1 and 2 (Decr1, Decr2), *cis*-Δ^3-enoyl-CoA isomerase 1 and 2 (Eci1, Eci2), (**B**) Δ5- and Δ6-fatty acid desaturase (Fads1, Fads2), elongase 2 and 5 (Elovl2, Elovl5) and (**C**) product/precursor ratio of C20:4n6/C20:3n6, C18:3n6/C18:2n6 and C22:4n6/C20:4n6 as estimates for enzyme activity of Δ5- and Δ6-fatty acid desaturase (D5D, D6D) and elongase, respectively. For relative gene expression data outliers were removed based on ROUT outlier test (Q = 1%). Statistically significant differences (* $p < 0.05$; ** $p < 0.01$; *** $p < 0.001$; **** $p < 0.0001$) were determined by two-way ANOVA with Tukey's post-test and are indicated for n6-high vs. n6-low groups (results for comparisons of all groups are summarized in the appendix, Tab. 8.8).

Both n3-PUFA supplementation and the n6-low/n6-high background diet had only little or no effect on the gene expression of the key players of β-oxidation (appendix, Fig. 8.2). Hadha and Hadhb, which are involved in the mitochondrial β-oxidation were statistically not different among all groups. This was also the case for the peroxisomal equivalents Ehhadh and Hsd17b4 as well as carnitine palmitoyltransferase 1a and 2 (Cpt1a/Cpt2). Enzymes which act as "auxiliary enzymes" in β-oxidation of long-chain PUFA, i.e. 2,4-dienoyl-CoA reductase 1 (Decr1) and 2 (Decr2) as well as *cis*-Δ^3-enoyl-CoA isomerase 1 (Eci1) and 2 (Eci2), were unaffected by the n6-high and n6-low background diets (Fig. 2.3 A). However, Eci1 and Eci2 mRNA levels in DHA/n6-low compared to the c/n6-low

group were increased. Enzymes involved in FA desaturation and elongation, i.e. Δ5-desaturase (D5D; Fads1), Δ6-desaturase (D6D; Fads2), elongases 2 (Elovl2) and 5 (Elovl5), were not significantly affected by the diet (Fig. 2.3 B). Estimates for enzyme activity based on FA product/precursor ratios were consistently lower for n3-PUFA supplementation (D5D-, D6D-, Elovl-index). The n6-PUFA background diet affected the D5D- and Elovl-indices, which were always lower in the n6-low groups, except for the Elovl-index in DHA-fed groups (Fig. 2.3 C).

2.3.5 Oxylipin concentrations in liver tissue

In liver tissue, the trends of concentrations and the diet induced changes of ARA, EPA and DHA derived oxylipins were overall similar to their precursor PUFA, as shown for a set of representative oxylipins covering all branches of enzymatic oxylipin formation within the ARA cascade (Fig. 2.4; all quantified oxylipins are summarized in the appendix, Tab. 8.7). Levels of ARA derived oxylipins did not differ significantly between c/n6-high and c/n6-low groups (Fig. 2.4), which is consistent with ARA concentrations in liver tissue (Fig. 2.2). Prostanoids, i.e. PGE_2, PGD_2, TXB_2, were very low in control groups and mostly undetectable in n3-PUFA-fed groups (Fig. 2.4). ARA derived 15-LOX product (15-HETE) was reduced upon DHA feeding combined with an n6-PUFA-low background diet. The 5-LOX and 12-LOX products 5-HETE and 12-HETE showed a consistent trend towards lower levels, which was not significant due to high inter-individual variation. CYP derived 14(15)-EpETrE and its sEH product 14,15-DiHETrE were reduced by both EPA and DHA feeding, (Fig. 2.4; appendix Tab. 8.7–8.8).

Fig. 2.4 (right, page 27): Oxylipin concentrations in mouse liver tissue. Concentrations [nmol/kg] of selected oxylipins derived from ARA, EPA and DHA including COX derived prostanoids, 5-, 12- and 15-LOX products, SPMs and SPM precursors, CYP derived epoxy- and ω-hydroxy-FA as well as CYP/sEH derived dihydroxy-FA in liver tissue of NMRI mice after 28 days of feeding an n6-PUFA-rich diet (dark grey) or an n6-PUFA-low diet (light grey) without (c) or with n3-PUFA supplementation (EPA, DHA). Shown are mean ± SEM as well as individual values (n = 8). If > 50% of the samples within one group were < LLOQ (lower limit of quantification), no mean was calculated and the LLOQ is indicated as dotted line. Statistically significant differences (* $p < 0.05$; ** $p < 0.01$; *** $p < 0.001$; **** $p < 0.0001$) were determined by two-way ANOVA with Tukey's post-test and are indicated for n6-high vs. n6-low groups (results for comparisons of all groups are summarized in the appendix, Tab. 8.8).

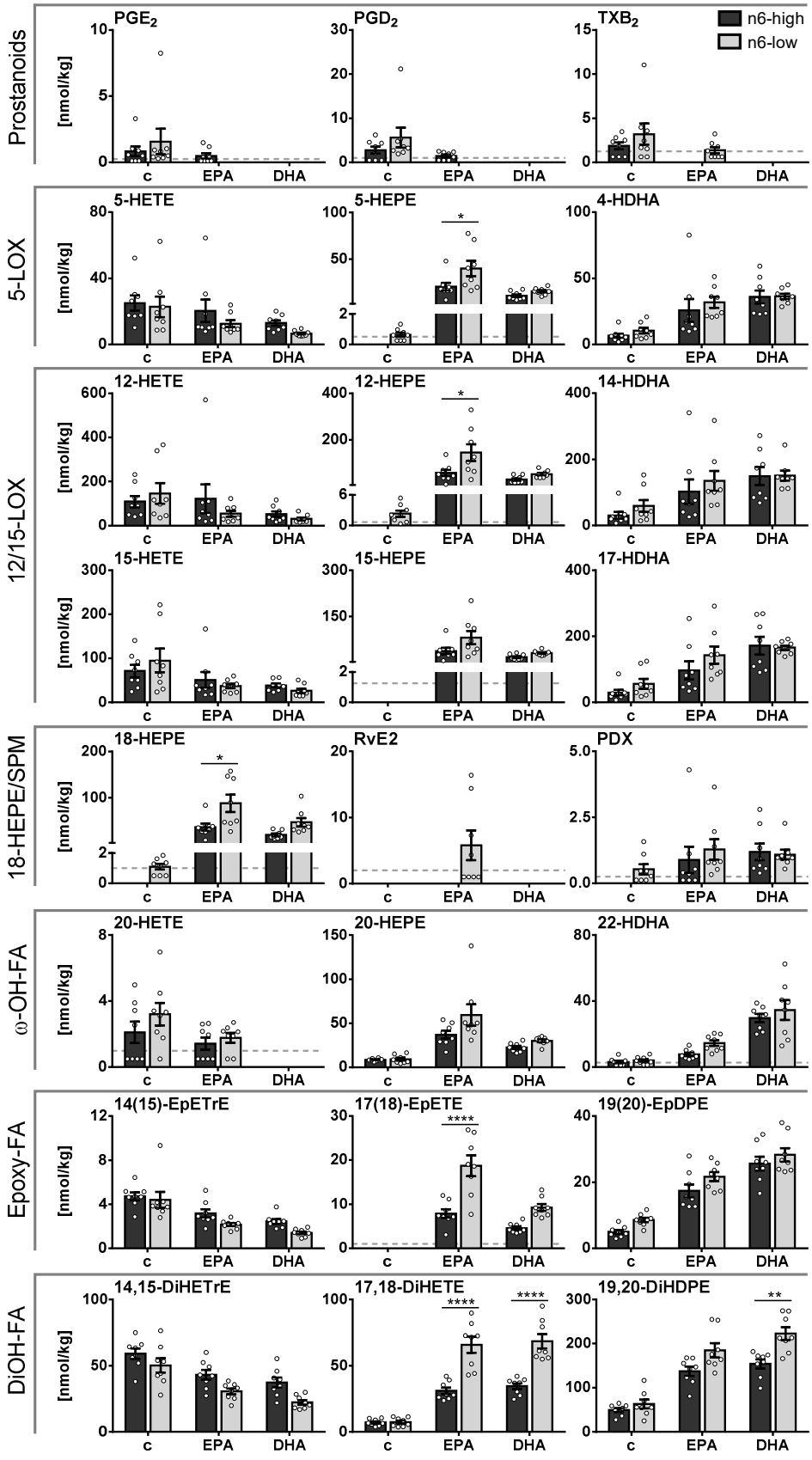
Prostanoids
5-LOX
12/15-LOX
18-HEPE/SPM
ω-OH-FA
Epoxy-FA
DiOH-FA
n6-high
n6-low
[nmol/kg]
PGE2
PGD2
TXB2
5-HETE
5-HEPE
4-HDHA
12-HETE
12-HEPE
14-HDHA
15-HETE
15-HEPE
17-HDHA
18-HEPE
RvE2
PDX
20-HETE
20-HEPE
22-HDHA
14(15)-EpETrE
17(18)-EpETE
19(20)-EpDPE
14,15-DiHETrE
17,18-DiHETE
19,20-DiHDPE
c
EPA
DHA

EPA derived oxylipins were very low or < LLOQ in both control groups (c/n6-high and c/n6-low) and were elevated by n3-PUFA supplementation. Particularly EPA feeding resulted in higher HEPE concentrations in liver tissue, which was more pronounced for the n6-low basal diet for 5-, 12- and 18-HEPE. In contrast to EPA tissue levels, EPA supplementation resulted in higher levels of EPA derived LOX products compared to DHA in n6-low groups. The effect of highest EPA derived oxylipin levels in the EPA/n6-low group was also observed for SPM precursor 18-HEPE. Consistently, SPM RvE2 exceeded the LLOQ in 50% of the animals within this group (Fig. 2.4) and consistent SRM transitions support its identity (Fig. 2.5). EPA derived CYP/sEH products 17(18)-EpETE and 17,18-DiHETE were stronger elevated in EPA/n6-low compared to EPA/n6-high groups. Consistent with DHA liver concentrations, DHA derived LOX products (HDHAs) were not different between the n6-high and n6-low groups and increased upon both EPA and DHA feeding, though this was not significant for EPA/n6-high group or 14-HDHA. CYP products of DHA were similarly modulated upon n3-PUFA feeding and only the sEH product 19,20-DiHDPE was higher in the DHA/n6-low compared to DHA/n6-high group (Fig. 2.4).

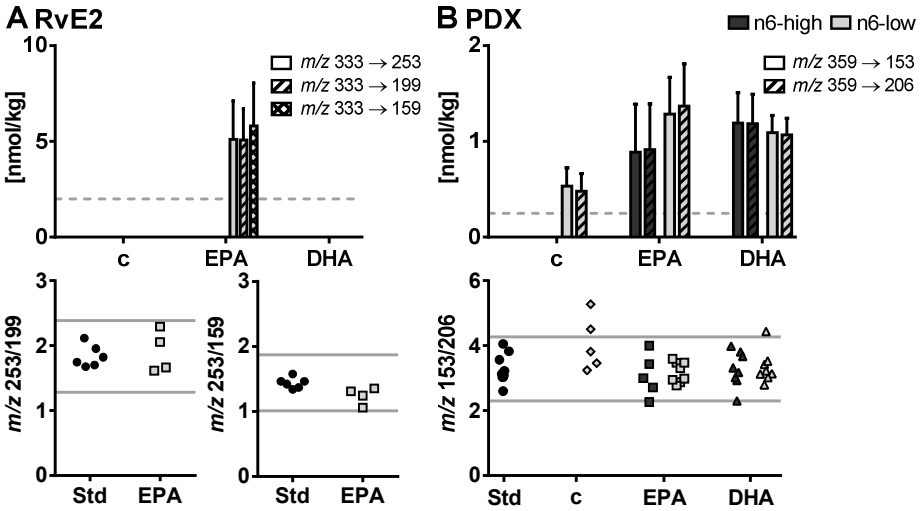

Fig. 2.5: Levels of SPMs (**A**) RvE2 and (**B**) PDX (10(*S*),17(*S*)-DiHDHA) derived from EPA and DHA, respectively, in liver tissue of NMRI mice after 28 days of feeding an n6-PUFA-rich diet (dark grey) or an n6-PUFA-low diet (light grey) without (c) or with n3-PUFA supplementation (EPA, DHA). **Top:** Shown are concentrations (mean ± SEM) quantified using 2–3 SRM transitions for each compound. If > 50% of the samples within one group were < LLOQ (lower limit of quantification), no mean was calculated and the LLOQ is indicated as dotted line. **Bottom:** Shown are area ratios of 2–3 SRM transitions for every sample > LLOQ in comparison to area ratios of calibration standards (RvE2: 1–100 nM, PDX: 0.25–500 nM). Deviation of ± 30% from mean area ratio of calibration standards are indicated as grey line.

2.4 Discussion

In the present study, we addressed the following questions: i) does a replacement of dietary LA with OA lead to a reduction of tissue ARA concentrations, ii) how are tissue levels of supplemented EPA and DHA affected by a low n6-PUFA background diet, iii) are the changes attributable to hepatic expression of lipid-metabolizing enzymes and iv) how does an n6-PUFA-low background diet affect the modulation of the tissue free oxylipin profile.

Low dietary LA and high OA has no effect on tissue ARA concentration

The n3-PUFA status is associated with a lower risk for cardiovascular and inflammatory diseases [3, 4]. This might be in part linked to a reduced formation of pro-inflammatory n6-PUFA derived lipid mediators, such as 2-series prostaglandins or 4-series leukotrienes, due to competition of n3- and n6-PUFA for enzymatic conversion. Besides increasing n3-PUFA intake, lower levels of ARA and ARA derived lipid mediators might be achieved by decreasing the intake of n6-PUFA via the diet. Despite a strong reduction of LA concentrations in liver tissue of the c/n6-low group, tissue ARA concentrations were not affected. The D6D enzyme, which catalyzes the first step in LA-to-ARA conversion, i.e. desaturation of LA to GLA, is discussed as the rate-limiting enzyme in this conversion [1]. It seems likely that the LA content (~10%) in the n6-low dietary oil is sufficient for an effective supply with LA and further increase of LA does not enhance ARA production due to saturation of the D6D. Similarly, in a systematic review, no correlation was found between LA intake and ARA levels in humans on a Western diet, while intake of GLA (D6D product of LA) was found to increase ARA [36]. Lower concentrations of ARA elongation/desaturation products, AdA and n6-DPA, in the c/n6-low group also indicate an intent of maintaining liver ARA levels by slower ARA conversion. Moreover, higher liver OA, which presumably accumulated in the neutral lipid fraction as shown for mouse and rat liver [37, 38], might not be able to replace ARA from hepatic phospholipids. It should be noted that, while the liver tissue was not macroscopically different from the n6-high groups, the OA-rich diet led to an increase of total liver FA in NMRI mice. Total

FA levels in the c/n6-low group were comparable to total fat in liver of C57BL/6J mice fed with a high fat diet (60% fat) [39, 40]. However, increase in liver FA by OA feeding might be a mouse-specific effect and may not be transferable to humans.

Elevation of blood and tissue EPA upon n3-PUFA feeding is more efficient when dietary LA is low

Regarding n3-PUFA supplementation, an effective uptake and elevation of blood and tissue n3-PUFA levels as well as subsequent metabolization to bioactive lipid mediators might be influenced by the ratio of (competing) n6- and n3-PUFA in the diet. Supplementation of the n6-low, OA-rich diet with n3-PUFA resulted in a trend towards lower total FA in liver tissue and levels of n3-PUFA were elevated at the expense of MUFA indicating an efficient uptake. In C57BL/6J mice on a high-fat/high-sucrose diet, elevated OA content in total liver lipids was decreased by administration of EPA-EE, which also resulted in a reduction of the hepatic TG content [41].

The more effective elevation of EPA with an n6-low background diet was evident in both the EPA- and DHA-fed groups. The levels of n3-DPA, which were also elevated by n3-PUFA feeding, however, without further elevation by the n6-low diet, indicate a slower enzymatic elongation of EPA to n3-DPA and thereby causing an accumulation of EPA. In human erythrocytes, increased EPA+DHA levels were observed when dietary LA was low and might be attributed to a more effective ALA-to-SDA or C24:5n3-to-C24:6n3 conversion or competition for esterification into membrane phospholipids [23]. An increased ALA-to-EPA conversion on an n6-low background may be excluded here, as ALA and eicosatetraenoic acid (ETA, C20:4n3) levels were overall low in liver tissue (< 0.05%).

A similar increase of EPA levels regardless of supplementation with EPA or DHA was unexpected, even though the DHA diet contained a small amount of EPA. This effect was specifically observed in the liver. Elevation of tissue EPA when DHA is supplemented is in line with previous studies e.g. in rat liver phospholipids

[17] and in rat liver total fat dietary DHA led to a comparable increase of EPA levels as dietary EPA [42]. DHA may be retro-converted to EPA in the mouse liver tissue as observed in human HepG2 cells [43]. Elevated mRNA levels of genes encoding for auxiliary enzymes for β-oxidation of PUFA, Eci1 and Eci2, in DHA/n6-low group compared to control group could indicate an increased β-oxidation of unsaturated FA and/or retro-conversion in liver of DHA-fed mice. Also, the elevation of EPA could result from a modulation of the ALA-EPA-DHA turn-over, e.g. a slower elongation, desaturation or β-oxidation of EPA in DHA supplemented groups [44, 45] and lower n3-DPA levels in DHA-fed vs. EPA-fed groups despite similar EPA concentrations could give a hint to a slower EPA elongation.

In contrast to EPA, DHA levels were not influenced by lowering the n6-PUFA content of the diet. Both DHA and EPA feeding resulted in an elevation of DHA for the two background diets. DHA could be formed from EPA either via a pathway involving elongation, desaturation and peroxisomal β-oxidation as reviewed by Sprecher (2000) [46] or a delta-4 desaturation by D6D as shown for human cells [47]. Although, it is believed that this conversion is relatively inefficient, it might occur with higher rates in rats and mice [27]. Taken together, in the used model the n6-PUFA content of the diet had a clear influence on EPA levels, while DHA was unaffected.

Hepatic elongase and desaturase mRNA levels are not significantly affected by a diet high in LA or OA

The observed reduction of tissue and blood ARA levels upon n3-PUFA feeding is consistent with studies in mice and rats, in which both EPA+DHA are administered (2–3% n3-PUFA oil and 4–10% fat in the diet) [16, 48, 49]. Interestingly, while there was little or no influence of the n6-PUFA background diet alone on ARA levels, the ARA-lowering effect of EPA and DHA supplementation was more pronounced in combination with reduced dietary LA. This might be a consequence of a competition between ARA and elevated EPA on the n6-low background or the combination of dietary n3-PUFA, low dietary LA

and consequently high OA might affect the enzymatic conversion of LA-to-ARA (and ARA-to-n6-DPA). In order to determine if these effects are a result of substrate availability and/or enzyme saturation or if the diets influence the enzyme expression, we analyzed the gene expression (qPCR) of the involved elongases and desaturases in liver. These enzymes are required for the synthesis of C20 and C22 n3- and n6-PUFA from the essential FA LA and ALA in mammals and several steps are catalyzed by D5D (Fads1) and D6D (Fads2) as well as elongase 2 and 5 (Elovl2, Elovl5) [50]. Moreover, expression of these enzymes may be regulated by the dietary n3-PUFA intake. For example, a diet deprived in n3-PUFA resulted in upregulated desaturase (D5D, D6D) and elongase (Elovl2, Elovl5) activity and expression in rat liver [51]. The product/precursor ratio of GLA/LA or the D6D-index indicates a low but similarly efficient desaturation of both high and low LA levels, which decreases with n3-PUFA feeding. However, the D6D-index showed no correlation with the Fads2 gene expression in the present study. It should be noted that enzyme activity estimates based on product/precursor FA ratios also depend on the PUFA intake [34]. In rat liver, no modulation of hepatic elongase and desaturase gene expression by different dietary ALA levels was observed by Tu *et al*. (2010) and it was concluded that substrate availability and competition are more likely regulating n3-PUFA synthesis than different enzyme expression [52]. In contrast, a replacement of dietary PUFA by MUFA increased Fads2 and Elovl2 significantly in rat liver [52], which we did not observe in mouse liver. Despite differences between FA metabolism in rats and mice, one possible explanation is that 10% PUFA (of total FA) in the c/n6-low diet in our study was high enough and therefore did not result in increased Fads2 expression.

The ARA/DGLA ratio or D5D-index was decreased by both n6-PUFA lowering and n3-PUFA elevation, resulting in an accumulation of DGLA rather than ARA. Similar to Fads2, no significant modulation of Fads1 mRNA levels was observed. The ratio of C22:4n6/C20:4n6 which can be used as estimate for elongase activity [34] is – like the D5D-index – reduced by both the n6-low diet and n3-PUFA supplementation indicating a slower elongation of ARA.

Taken together, we observed that a drastic shift from dietary (n6-) PUFA to (n9-) MUFA had no effect on transcription of desaturases and elongases involved in PUFA metabolism in liver tissue. This indicates that in the used experimental model, tissue FA composition is likely governed by substrate availability and competition.

Modulation of tissue PUFA is reflected in the tissue oxylipin pattern

Both n3- and n6-PUFA compete for the enzymatic oxidation and distinct substrate preferences or different potencies of n3- and n6-PUFA derived lipid mediators have been described. For example, COX reacts slower with EPA [53], while CYP epoxygenases [54] and ALOX12/15 orthologs [55] are more efficient with EPA and DHA as substrate compared to ARA. Therefore, we investigated if the modulation of the tissue oxylipin profile was consistent with the FA pattern and if the low n6-PUFA background reduces the formation of predominantly pro-inflammatory lipid mediators derived from ARA [13]. In general, oxylipins derived from ARA, EPA and DHA displayed similar trends as the respective precursor PUFA indicating that the total tissue FA composition governs oxylipin formation.

Levels of ARA derived COX metabolites in liver tissue were overall low and therefore it is not possible to conclude on a significant effect by the dietary intervention in these healthy, non-inflamed mice. Particularly, ARA derived lipid mediators of the CYP pathway were consistent with ARA tissue levels not influenced by the background diet alone, however, reduced by n3-PUFA feeding. In mouse liver, fish oil feeding resulted in a reduction of liver ARA derived oxylipins [48] and in rat liver ARA derived oxylipins were reduced with higher efficacy by DHA feeding compared to EPA feeding [17], which was not significant in our study.

Furthermore, some pathways indicate a preferred enzymatic oxidation of n3-PUFA over n6-PUFA. For example, despite tissue ARA levels (control groups) and DHA levels (after n3-PUFA feeding) were in the same concentration range, clearly higher levels of DHA derived CYP product 19(20)-EpDPE was formed, which is consistent with a preference for the n3- over the n6-double bond by CYP

epoxygenases as mechanistically described for human CYPs [49, 56]. Moreover, despite similar DHA and 19(20)-EpDPE concentrations in DHA/n6-high and DHA/n6-low groups, higher levels of its sEH product 19,20-DiHDPE may indicate a more efficient formation of DHA derived CYP products with an n6-low background diet. For 19(20)-EpDPE, which was the most abundant EpDPE in mouse liver, inhibitory effects on angiogenesis, tumor growth and metastasis [57], protection against LPS induced cytotoxicity [58] and reduction of renal fibrosis [59] were observed. In our study, a relatively low dose of n3-PUFA led to an elevation of 19(20)-EpDPE tissue levels (2.8–3.5-fold) indicating that both EPA and DHA feeding might exert protective effects via this bioactive lipid mediator.

In contrast to hepatic EPA levels, which were similar in EPA- and DHA-fed groups, increase in hepatic EPA derived oxylipin levels was more pronounced in EPA/n6-low fed groups. The divergence between tissue EPA and EPA derived oxylipins may result from their distribution in hepatic lipid pools. The phospholipid pool is believed to provide substrate FA for the formation of free oxylipins after release by phospholipases [6]. However, as we analyzed total hepatic FA it is possible that elevated EPA in DHA-fed groups is directed to different lipid classes, e.g. hepatic TG and therefore not readily available for oxylipin formation. Moreover, oxylipins can be re-esterified to lipids or conjugated with glucuronic acid [60] and free oxylipins represent only a small fraction of the total oxylipin profile [61]. Other explanations could be an increased degradation/metabolization of EPA derived oxylipins in DHA-fed groups or a limited hepatic formation of EPA oxylipins when DHA is supplemented.

Highest levels of HEPEs and EpETEs were achieved by combining dietary EPA and low n6-PUFA. For example, 18-HEPE, a common pathway marker for E-series resolvin formation, is 80-fold elevated in the EPA/n6-low group compared to levels of the n6-low control group. For 18-HEPE itself an anti-inflammatory activity is described, such as the suppression of LPS-triggered TNF-α formation in murine macrophages [62] or lowering of IL-6 formation in murine cardiac fibroblasts stimulated with macrophage conditioned media [63]. Moreover, EPA feeding especially in combination with low dietary n6-PUFA might

be able to increase E-series resolvins, e.g. RvE2 that correlated with 18-HEPE formation and might exert anti-inflammatory properties such as reduction of neutrophil chemotactic velocity or enhancement of macrophage phagocytosis [64]. Similarly, highest levels of CYP derived 17(18)-EpETE were observed in the EPA/n6-low group resulting in an > 18-fold increase compared to the control groups, which were < LLOQ (< 1 nmol/kg) in liver tissue. This oxylipin was also found to be an abundant epoxy-FA in rat liver, heart and other tissues after n3-PUFA feeding and reduced spontaneous beating rate of neonatal cardiomyocytes more effectively than EPA regarding delay time and concentration [49]. Our results indicate that elevation of 17(18)-EpETE, which is investigated for its anti-arrhythmic effects [65], can be increased by combining EPA supplementation with low n6-PUFA intake. Interestingly, while 17(18)-EpETE levels were lower in the DHA/n6-low group, its sEH product 17,18-DiHETE was similarly elevated. Thus, also DHA feeding may efficiently raise 17(18)-EpETE, which however, was more rapidly hydrolyzed in mouse liver.

In summary, both the n3-PUFA feeding and the n6-PUFA background diet had a similar effect on the tissue oxylipin pattern compared to their precursor PUFA, except bioactive EPA derived lipid mediators, which were clearly elevated most efficiently by EPA/n6-low feeding.

Combining low dietary LA and n3-PUFA supplementation efficiently lowers %n6 in HUFA and increases blood cell %EPA+DHA

The n3-PUFA status or more precisely the n3-index (%EPA+DHA in red blood cells) has been associated with cardioprotection [66]. The %n6 in HUFA was proposed as another biomarker for health risk assessment taking into account not only the n3-PUFA status but also the n3/n6-PUFA balance (as summarized in [67]). In the present study, we observed an elevation of %EPA+DHA and %n3 in HUFA as well as a decrease of %n6 in HUFA when supplementing n3-PUFA, which was more pronounced for n6-low groups (except %EPA+DHA in liver).

%EPA+DHA in blood cells of the control groups was < 4% regardless of the background diet, which – translated to humans – has been associated with low

cardioprotection, i.e. with higher risk for primary cardiac arrest, sudden cardiac death or ischemic heart disease, while an n3-index of ≥ 8% is associated with cardioprotection [66]. Supplementation with EPA or DHA resulted in an elevation of %EPA+DHA in blood cells to > 8% and > 11% in n6-high and n6-low groups, respectively. Hence, when dietary n6-PUFA are reduced even a low supplementation with n3-PUFA (< 0.6% EPA or DHA) could be sufficient to increase %EPA+DHA to levels ≥ 8%.

The %n6 in HUFA for North Americans ranges from 75–80% and a reduction towards 60% may have a positive effect on human health as summarized by Lands *et al*. (2018) [35]. In mice receiving either of the control diets the %n6 in HUFA ranged between 77–91% (tissue and blood) and could be reduced towards 60% for mice on the n6-high diet (50–63%) and towards 40% for mice on the n6-low diet (33–49%). From this it can be concluded that despite little changes of ARA levels when dietary LA is reduced, a combination with long-chain n3-PUFA is more effective in modifying biomarkers related to the n3-PUFA status and associated with beneficial health effects.

In conclusion, in a murine model, a shift in dietary FA from mainly n6-PUFA (LA) to MUFA (OA) affected the overall FA composition of liver tissue and blood. No effect on ARA and n3-PUFA concentrations or mRNA levels of hepatic elongases/desaturases was observed. Supplementation with ~0.6% n3-PUFA (either EPA or DHA) lowered blood and tissue levels of ARA and its elongation product to a greater extend when dietary LA was low. Particularly EPA and EPA oxylipins but not DHA and DHA oxylipins were affected by the background diet and their increase was 2–3-fold more pronounced. This resulted in higher %EPA+DHA in blood cells and lower %n6 in HUFA in blood and liver for the n6-low background diet. Thus, lower doses of long-chain n3-PUFA supplementation – especially for EPA – are equally effective when the n6-PUFA background is low.

2.5 Limitations

Results obtained from experimental animal models cannot simply be extrapolated to humans, which also limits the conclusions drawn from the present study. Mice have a different FA and oxylipin metabolism than humans, for example regarding the efficiency of ALA elongation or enzyme product specificity (e.g. ALOX15). Therefore, obtained FA and oxylipin patterns cannot reflect tissue levels in humans. In order to account for that, the dietary FA composition used in this study contained a very low concentration of ALA and thus is compared to human nutrition artificial. Particularly the unsupplemented control groups received consequently a diet with an extremely high n6/n3-PUFA ratio, which may have induced an n3-PUFA deficiency in these groups. It should be noted that there are also differences in lipid, FA and oxylipin metabolism in males and females and the results described in the present study may not be (completely) transferable to male mice.

2.6 References

1. Zhang JY, Kothapalli KS, Brenna JT (2016) Desaturase and elongase-limiting endogenous long-chain polyunsaturated fatty acid biosynthesis. *Curr Opin Clin Nutr Metab Care*, 19(2), 103-110; doi: 10.1097/MCO.0000000000000254.
2. Calder PC (2012) Mechanisms of action of (n-3) fatty acids. *J Nutr*, 142(3), 592S-599S; doi: 10.3945/jn.111.155259.
3. Mozaffarian D, Wu JH (2011) Omega-3 fatty acids and cardiovascular disease: effects on risk factors, molecular pathways, and clinical events. *J Am Coll Cardiol*, 58(20), 2047-2067; doi: 10.1016/j.jacc.2011.06.063.
4. Calder PC (2015) Marine omega-3 fatty acids and inflammatory processes: Effects, mechanisms and clinical relevance. *Biochim Biophys Acta*, 1851(4), 469-484; doi: 10.1016/j.bbalip.2014.08.010.
5. Burdge GC, Calder PC (2006) Dietary alpha-linolenic acid and health-related outcomes: a metabolic perspective. *Nutr Res Rev*, 19(1), 26-52; doi: 10.1079/NRR2005113.
6. Buczynski MW, Dumlao DS, Dennis EA (2009) Thematic Review Series: Proteomics. An integrated omics analysis of eicosanoid biology. *J Lipid Res*, 50(6), 1015-1038; doi: 10.1194/jlr.R900004-JLR200.
7. Gladine C, Ostermann AI, Newman JW, Schebb NH (2019) MS-based targeted metabolomics of eicosanoids and other oxylipins: Analytical and inter-individual variabilities. *Free Radic Biol Med*, 144, 72-89; doi: 10.1016/j.freeradbiomed.2019.05.012.
8. Morrow JD, Awad JA, Boss HJ, Blair IA, Roberts LJ 2nd (1992) Non-cyclooxygenase-derived prostanoids (F2-isoprostanes) are formed in situ on phospholipids. *Proc Natl Acad Sci U S A*, 89(22), 10721-10725; doi: 10.1073/pnas.89.22.10721.
9. Rund KM, Heylmann D, Seiwert N, Wecklein S, Oger C, Galano JM, Durand T, Chen R, Gueler F, Fahrer J, Bornhorst J, Schebb NH (2019) Formation of trans-epoxy fatty acids correlates with formation of isoprostanes and could serve as biomarker of oxidative stress. *Prostaglandins Other Lipid Mediat*, 144, 106334; doi: 10.1016/j.prostaglandins.2019.04.004.
10. Simopoulos AP (2002) The importance of the ratio of omega-6/omega-3 essential fatty acids: health implications. *Biomed Pharmacother*, 56(8), 365-379; doi: 10.1016/s0753-3322(02)00253-6.
11. Beynen AC, Katan MB (1985) Why do polyunsaturated fatty acids lower serum cholesterol? *Am J Clin Nutr*, 42(3), 560-563; doi: 10.1093/ajcn/42.3.560.
12. Lands B (2014) Historical perspectives on the impact of n-3 and n-6 nutrients on health. *Prog Lipid Res*, 55, 17-29; doi: 10.1016/j.plipres.2014.04.002.
13. Lands B (2015) Omega-3 PUFAs lower the propensity for arachidonic acid cascade overreactions. *Biomed Res Int*, 2015, 285135; doi: 10.1155/2015/285135.
14. Browning LM, Walker CG, Mander AP, West AL, Madden J, Gambell JM, Young S, Wang L, Jebb SA, Calder PC (2012) Incorporation of eicosapentaenoic and docosahexaenoic acids into lipid pools when given as supplements providing doses equivalent to typical intakes of oily fish. *Am J Clin Nutr*, 96(4), 748-758; doi: 10.3945/ajcn.112.041343.
15. Ostermann AI, West AL, Schoenfeld K, Browning LM, Walker CG, Jebb SA, Calder PC, Schebb NH (2019) Plasma oxylipins respond in a linear dose-response manner with increased intake of EPA and DHA: results from a randomized controlled trial in healthy humans. *Am J Clin Nutr*, 109(5), 1251-1263; doi: 10.1093/ajcn/nqz016.

16. Ostermann AI, Waindok P, Schmidt MJ, Chiu CY, Smyl C, Rohwer N, Weylandt KH, Schebb NH (2017) Modulation of the endogenous omega-3 fatty acid and oxylipin profile in vivo – A comparison of the fat-1 transgenic mouse with C57BL/6 wildtype mice on an omega-3 fatty acid enriched diet. *PLoS One*, 12(9), e0184470; doi: 10.1371/journal.pone.0184470.
17. Leng S, Winter T, Aukema HM (2018) Dietary ALA, EPA and DHA have distinct effects on oxylipin profiles in female and male rat kidney, liver and serum. *J Nutr Biochem*, 57, 228-237; doi: 10.1016/j.jnutbio.2018.04.002.
18. Terano T, Salmon JA, Moncada S (1984) Biosynthesis and biological activity of leukotriene B5. *Prostaglandins*, 27(2), 217-232; doi: 10.1016/0090-6980(84)90075-3.
19. Serhan CN, Petasis NA (2011) Resolvins and protectins in inflammation resolution. *Chem Rev*, 111(10), 5922-5943; doi: 10.1021/cr100396c.
20. Wood KE, Mantzioris E, Gibson RA, Ramsden CE, Muhlhausler BS (2015) The effect of modifying dietary LA and ALA intakes on omega-3 long chain polyunsaturated fatty acid (n-3 LCPUFA) status in human adults: a systematic review and commentary. *Prostaglandins Leukot Essent Fatty Acids*, 95, 47-55; doi: 10.1016/j.plefa.2015.01.001.
21. Brenna JT, Salem N, Jr., Sinclair AJ, Cunnane SC; International Society for the Study of Fatty Acids and Lipids, ISSFAL (2009) alpha-Linolenic acid supplementation and conversion to n-3 long-chain polyunsaturated fatty acids in humans. *Prostaglandins Leukot Essent Fatty Acids*, 80(2-3), 85-91; doi: 10.1016/j.plefa.2009.01.004.
22. Taha AY, Cheon Y, Faurot KF, Macintosh B, Majchrzak-Hong SF, Mann JD, Hibbeln JR, Ringel A, Ramsden CE (2014) Dietary omega-6 fatty acid lowering increases bioavailability of omega-3 polyunsaturated fatty acids in human plasma lipid pools. *Prostaglandins Leukot Essent Fatty Acids*, 90(5), 151-157; doi: 10.1016/j.plefa.2014.02.003.
23. MacIntosh BA, Ramsden CE, Faurot KR, Zamora D, Mangan M, Hibbeln JR, Mann JD (2013) Low-n-6 and low-n-6 plus high-n-3 diets for use in clinical research. *Br J Nutr*, 110(3), 559-568; doi: 10.1017/S0007114512005181.
24. Dias CB, Wood LG, Garg ML (2016) Effects of dietary saturated and n-6 polyunsaturated fatty acids on the incorporation of long-chain n-3 polyunsaturated fatty acids into blood lipids. *Eur J Clin Nutr*, 70(7), 812-818; doi: 10.1038/ejcn.2015.213.
25. Giacometti J, Milin C, Tota M, Cuk M, Radosevic-Stasic B (2005) Incorporation of fatty acids into tissue phospholipids in mice fed diets rich in n-9 and n-6 fatty acids. *Croat Chem Acta*, 78(3), 397-404.
26. Hwang J, Jun HS, Shim E (2010) Rates of change in tissue fatty acid composition when dietary soybean oil is switched to olive oil. *J Health Sci*, 56(3), 275-286; doi: 10.1248/jhs.56.275.
27. Anderson BM, Ma DW (2009) Are all n-3 polyunsaturated fatty acids created equal? *Lipids Health Dis*, 8, 33; doi: 10.1186/1476-511X-8-33.
28. Prendergast BJ, Onishi KG, Zucker I (2014) Female mice liberated for inclusion in neuroscience and biomedical research. *Neurosci Biobehav Rev*, 40, 1-5; doi: 10.1016/j.neubiorev.2014.01.001.
29. Ostermann AI, Muller M, Willenberg I, Schebb NH (2014) Determining the fatty acid composition in plasma and tissues as fatty acid methyl esters using gas chromatography - a comparison of different derivatization and extraction procedures. *Prostaglandins Leukot Essent Fatty Acids*, 91(6), 235-241; doi: 10.1016/j.plefa.2014.10.002.
30. Ostermann AI, Reutzel M, Hartung N, Franke N, Kutzner L, Schoenfeld K, Weylandt KH, Eckert GP, Schebb NH (2017) A diet rich in omega-3 fatty acids enhances expression of soluble epoxide hydrolase in murine brain. *Prostaglandins Other Lipid Mediat*, 133, 79-87; doi: 10.1016/j.prostaglandins.2017.06.001.

31. Rund KM, Ostermann AI, Kutzner L, Galano JM, Oger C, Vigor C, Wecklein S, Seiwert N, Durand T, Schebb NH (2018) Development of an LC-ESI(-)-MS/MS method for the simultaneous quantification of 35 isoprostanes and isofurans derived from the major n3- and n6-PUFAs. *Anal Chim Acta*, 1037, 63-74; doi: 10.1016/j.aca.2017.11.002.
32. Kutzner L, Rund KM, Ostermann AI, Hartung NM, Galano JM, Balas L, Durand T, Balzer MS, David S, Schebb NH (2019) Development of an optimized LC-MS method for the detection of specialized pro-resolving mediators in biological samples. *Front Pharmacol*, 10, 169; doi: 10.3389/fphar.2019.00169.
33. Lankinen M, Uusitupa M, Schwab U (2018) Genes and dietary fatty acids in regulation of fatty acid composition of plasma and erythrocyte membranes. *Nutrients*, 10(11), 1785; doi: 10.3390/nu10111785.
34. Cormier H, Rudkowska I, Lemieux S, Couture P, Julien P, Vohl MC (2014) Effects of FADS and ELOVL polymorphisms on indexes of desaturase and elongase activities: results from a pre-post fish oil supplementation. *Genes Nutr*, 9(6), 437; doi: 10.1007/s12263-014-0437-z.
35. Lands B, Bibus D, Stark KD (2018) Dynamic interactions of n-3 and n-6 fatty acid nutrients. *Prostaglandins Leukot Essent Fatty Acids*, 136, 15-21; doi: 10.1016/j.plefa.2017.01.012.
36. Rett BS, Whelan J (2011) Increasing dietary linoleic acid does not increase tissue arachidonic acid content in adults consuming Western-type diets: a systematic review. *Nutr Metab (Lond)*, 8, 36; doi: 10.1186/1743-7075-8-36.
37. Picklo MJ, Sr., Idso J, Seeger DR, Aukema HM, Murphy EJ (2017) Comparative effects of high oleic acid vs high mixed saturated fatty acid obesogenic diets upon PUFA metabolism in mice. *Prostaglandins Leukot Essent Fatty Acids*, 119, 25-37; doi: 10.1016/j.plefa.2017.03.001.
38. Artmann A, Petersen G, Hellgren LI, Boberg J, Skonberg C, Nellemann C, Hansen SH, Hansen HS (2008) Influence of dietary fatty acids on endocannabinoid and N-acylethanolamine levels in rat brain, liver and small intestine. *Biochim Biophys Acta*, 1781(4), 200-212; doi: 10.1016/j.bbalip.2008.01.006.
39. Valenzuela R, Barrera C, Espinosa A, Llanos P, Orellana P, Videla LA (2015) Reduction in the desaturation capacity of the liver in mice subjected to high fat diet: Relation to LCPUFA depletion in liver and extrahepatic tissues. *Prostaglandins Leukot Essent Fatty Acids*, 98, 7-14; doi: 10.1016/j.plefa.2015.04.002.
40. Rincon-Cervera MA, Valenzuela R, Hernandez-Rodas MC, Marambio M, Espinosa A, Mayer S, Romero N, Barrera MSC, Valenzuela A, Videla LA (2016) Supplementation with antioxidant-rich extra virgin olive oil prevents hepatic oxidative stress and reduction of desaturation capacity in mice fed a high-fat diet: Effects on fatty acid composition in liver and extrahepatic tissues. *Nutrition*, 32(11-12), 1254-1267; doi: 10.1016/j.nut.2016.04.006.
41. Kajikawa S, Harada T, Kawashima A, Imada K, Mizuguchi K (2009) Highly purified eicosapentaenoic acid prevents the progression of hepatic steatosis by repressing monounsaturated fatty acid synthesis in high-fat/high-sucrose diet-fed mice. *Prostaglandins Leukot Essent Fatty Acids*, 80(4), 229-238; doi: 10.1016/j.plefa.2009.02.004.
42. Poudyal H, Panchal SK, Ward LC, Brown L (2013) Effects of ALA, EPA and DHA in high-carbohydrate, high-fat diet-induced metabolic syndrome in rats. *J Nutr Biochem*, 24(6), 1041-1052; doi: 10.1016/j.jnutbio.2012.07.014.
43. Park HG, Lawrence P, Engel MG, Kothapalli K, Brenna JT (2016) Metabolic fate of docosahexaenoic acid (DHA; 22:6n-3) in human cells: direct retroconversion of DHA to eicosapentaenoic acid (20:5n-3) dominates over elongation to tetracosahexaenoic acid (24:6n-3). *Febs Lett*, 590(18), 3188-3194; doi: 10.1002/1873-3468.12368.

44. Metherel AH, Chouinard-Watkins R, Trepanier MO, Lacombe RJS, Bazinet RP (2017) Retroconversion is a minor contributor to increases in eicosapentaenoic acid following docosahexaenoic acid feeding as determined by compound specific isotope analysis in rat liver. *Nutr Metab (Lond)*, 14, 75; doi: 10.1186/s12986-017-0230-2.
45. Metherel AH, Irfan M, Klingel SL, Mutch DM, Bazinet RP (2019) Compound-specific isotope analysis reveals no retroconversion of DHA to EPA but substantial conversion of EPA to DHA following supplementation: a randomized control trial. *Am J Clin Nutr*, 110(4), 823-831; doi: 10.1093/ajcn/nqz097.
46. Sprecher H (2000) Metabolism of highly unsaturated n-3 and n-6 fatty acids. *Biochim Biophys Acta*, 1486(2-3), 219-231; doi: 10.1016/s1388-1981(00)00077-9.
47. Park HG, Park WJ, Kothapalli KS, Brenna JT (2015) The fatty acid desaturase 2 (FADS2) gene product catalyzes Delta4 desaturation to yield n-3 docosahexaenoic acid and n-6 docosapentaenoic acid in human cells. *Faseb J*, 29(9), 3911-3919; doi: 10.1096/fj.15-271783.
48. Balvers MG, Verhoeckx KC, Bijlsma S, Rubingh CM, Meijerink J, Wortelboer HM, Witkamp RF (2012) Fish oil and inflammatory status alter the n-3 to n-6 balance of the endocannabinoid and oxylipin metabolomes in mouse plasma and tissues. *Metabolomics*, 8(6), 1130-1147; doi: 10.1007/s11306-012-0421-9.
49. Arnold C, Markovic M, Blossey K, Wallukat G, Fischer R, Dechend R, Konkel A, von Schacky C, Luft FC, Muller DN, Rothe M, Schunck WH (2010) Arachidonic acid-metabolizing cytochrome P450 enzymes are targets of omega-3 fatty acids. *J Biol Chem*, 285(43), 32720-32733; doi: 10.1074/jbc.M110.118406.
50. Guillou H, Zadravec D, Martin PG, Jacobsson A (2010) The key roles of elongases and desaturases in mammalian fatty acid metabolism: Insights from transgenic mice. *Prog Lipid Res*, 49(2), 186-199; doi: 10.1016/j.plipres.2009.12.002.
51. Igarashi M, Ma K, Chang L, Bell JM, Rapoport SI (2007) Dietary n-3 PUFA deprivation for 15 weeks upregulates elongase and desaturase expression in rat liver but not brain. *J Lipid Res*, 48(11), 2463-2470; doi: 10.1194/jlr.M700315-JLR200.
52. Tu WC, Cook-Johnson RJ, James MJ, Muhlhausler BS, Gibson RA (2010) Omega-3 long chain fatty acid synthesis is regulated more by substrate levels than gene expression. *Prostaglandins Leukot Essent Fatty Acids*, 83(2), 61-68; doi: 10.1016/j.plefa.2010.04.001.
53. Wada M, DeLong CJ, Hong YH, Rieke CJ, Song I, Sidhu RS, Yuan C, Warnock M, Schmaier AH, Yokoyama C, Smyth EM, Wilson SJ, FitzGerald GA, Garavito RM, Sui DX, Regan JW, Smith WL (2007) Enzymes and receptors of prostaglandin pathways with arachidonic acid-derived versus eicosapentaenoic acid-derived substrates and products. *J Biol Chem*, 282(31), 22254-22266; doi: 10.1074/jbc.M703169200.
54. Fischer R, Konkel A, Mehling H, Blossey K, Gapelyuk A, Wessel N, von Schacky C, Dechend R, Muller DN, Rothe M, Luft FC, Weylandt K, Schunck WH (2014) Dietary omega-3 fatty acids modulate the eicosanoid profile in man primarily via the CYP-epoxygenase pathway. *J Lipid Res*, 55(6), 1150-1164; doi: 10.1194/jlr.M047357.
55. Kutzner L, Goloshchapova K, Heydeck D, Stehling S, Kuhn H, Schebb NH (2017) Mammalian ALOX15 orthologs exhibit pronounced dual positional specificity with docosahexaenoic acid. *Biochim Biophys Acta*, 1862(7), 666-675; doi: 10.1016/j.bbalip.2017.04.001.
56. Schuchardt JP, Schmidt S, Kressel G, Willenberg I, Hammock BD, Hahn A, Schebb NH (2014) Modulation of blood oxylipin levels by long-chain omega-3 fatty acid supplementation in hyper- and normolipidemic men. *Prostaglandins Leukot Essent Fatty Acids*, 90(2-3), 27-37; doi: 10.1016/j.plefa.2013.12.008.
57. Zhang GD, Panigrahy D, Mahakian LM, Yang J, Liu JY, Lee KSS, Wettersten HI, Ulu A, Hu XW, Tam S, Hwang SH, Ingham ES, Kieran MW, Weiss RH, Ferrara KW, Hammock

BD (2013) Epoxy metabolites of docosahexaenoic acid (DHA) inhibit angiogenesis, tumor growth, and metastasis. *P Natl Acad Sci USA*, 110(16), 6530-6535; doi: 10.1073/pnas.1304321110.

58. Samokhvalov V, Jamieson KL, Vriend J, Quan S, Seubert JM (2015) CYP-epoxygenase metabolites of docosahexaenoic acid protect HL-1 cardiac cells against LPS-induced cytotoxicity Through SIRT1. *Cell Death Discov*, 1, 15054; doi: 10.1038/cddiscovery.2015.54.
59. Sharma A, Hye Khan MA, Levick SP, Lee KS, Hammock BD, Imig JD (2016) Novel omega-3 fatty acid epoxygenase metabolite reduces kidney fibrosis. *Int J Mol Sci*, 17(5), 751; doi: 10.3390/ijms17050751.
60. Turgeon D, Chouinard S, Belanger P, Picard S, Labbe JF, Borgeat P, Belanger A (2003) Glucuronidation of arachidonic and linoleic acid metabolites by human UDP-glucuronosyltransferases. *J Lipid Res*, 44(6), 1182-1191; doi: 10.1194/jlr.M300010-JLR200.
61. Ostermann AI, Koch E, Rund KM, Kutzner L, Mainka M, Schebb NH (2020) Targeting esterified oxylipins by LC-MS – Effect of sample preparation on oxylipin pattern. *Prostaglandins Other Lipid Mediat*, 146, 106384; doi: 10.1016/j.prostaglandins.2019.106384.
62. Weylandt KH, Krause LF, Gomolka B, Chiu CY, Bilal S, Nadolny A, Waechter SF, Fischer A, Rothe M, Kang JX (2011) Suppressed liver tumorigenesis in fat-1 mice with elevated omega-3 fatty acids is associated with increased omega-3 derived lipid mediators and reduced TNF-alpha. *Carcinogenesis*, 32(6), 897-903; doi: 10.1093/carcin/bgr049.
63. Endo J, Sano M, Isobe Y, Fukuda K, Kang JX, Arai H, Arita M (2014) 18-HEPE, an n-3 fatty acid metabolite released by macrophages, prevents pressure overload-induced maladaptive cardiac remodeling. *J Exp Med*, 211(8), 1673-1687; doi: 10.1084/jem.20132011.
64. Oh SF, Dona M, Fredman G, Krishnamoorthy S, Irimia D, Serhan CN (2012) Resolvin E2 formation and impact in inflammation resolution. *J Immunol*, 188(9), 4527-4534; doi: 10.4049/jimmunol.1103652.
65. Adebesin AM, Wesser T, Vijaykumar J, Konkel A, Paudyal MP, Lossie J, Zhu C, Westphal C, Puli N, Fischer R, Schunck WH, Falck JR (2019) Development of robust 17(R),18(S)-epoxyeicosatetraenoic acid (17,18-EEQ) analogues as potential clinical antiarrhythmic agents. *J Med Chem*, 62(22), 10124-10143; doi: 10.1021/acs.jmedchem.9b00952.
66. Harris WS, Von Schacky C (2004) The Omega-3 Index: a new risk factor for death from coronary heart disease? *Prev Med*, 39(1), 212-220; doi: 10.1016/j.ypmed.2004.02.030.
67. Bibus D, Lands B (2015) Balancing proportions of competing omega-3 and omega-6 highly unsaturated fatty acids (HUFA) in tissue lipids. *Prostaglandins Leukot Essent Fatty Acids*, 99, 19-23; doi: 10.1016/j.plefa.2015.04.005.

Chapter 3

Mammalian ALOX15 orthologs exhibit pronounced dual positional specificity with docosahexaenoic acid

Mammalian lipoxygenases (LOX) have been implicated in cell differentiation and in the pathogenesis of inflammatory, hyperproliferative and neurological diseases. Although the reaction specificity of mammalian LOX with n6-fatty acids (linoleic acid, arachidonic acid) has been explored in detail little information is currently available on the product patterns formed from n3-polyenoic fatty acids, which are of particular nutritional importance and serve as substrate for the biosynthesis of pro-resolving inflammatory mediators such as resolvins and maresins. Here, we expressed the ALOX15 orthologs of eight different mammalian species as well as human ALOX12 and ALOX15B as recombinant his-tag fusion proteins and characterized their reaction specificity with the most abundantly occurring polyunsaturated fatty acids (PUFA) including 5,8,11,14,17-eicosapentaenoic acid (EPA) and 4,7,10,13,16,19-docosahexaenoic acid (DHA). We found that the LOX isoforms tested accept these fatty acids as suitable substrates and oxygenate them with variable positional specificity to the corresponding n6- and n9-hydroperoxy derivatives. Surprisingly, human ALOX15 as well as the corresponding orthologs of chimpanzee and orangutan, which oxygenate arachidonic acid mainly to 15(S)-H(p)ETE, exhibit a pronounced dual reaction specificity with DHA forming similar amounts of 14- and 17-H(p)DHA. Moreover, ALOX15 orthologs prefer DHA and EPA over ARA when equimolar concentrations of n3- and n6-PUFA were supplied simultaneously. Taken together, these data indicate that the reaction specificity of mammalian LOX isoforms is variable and strongly depends on the chemistry of fatty acid substrates. Most mammalian ALOX15 orthologs exhibit dual positional specificity with n3-polyunsaturated fatty acids.

Reprinted from *Biochimica et Biophysica Acta*, 1862(7), Kutzner L, Goloshchapova K, Heydeck D, Stehling S, Kühn H, Schebb NH, Mammalian ALOX15 orthologs exhibit pronounced dual positional specificity with docosahexaenoic acid, 666-675, doi: 10.1016/j.bbalip.2017.04.001; Copyright (2017), with permission from Elsevier.

Author contributions: LK designed research, performed experiments and wrote the manuscript; KG performed experiments; DH designed research, performed experiments and wrote the manuscript; SS performed experiments; HK designed research, performed experiments and wrote the manuscript; NHS designed research and wrote the manuscript.

3.1 Introduction

Lipoxygenases (LOX) are fatty acid dioxygenases, which oxygenate polyenoic fatty acids (polyunsaturated fatty acids, PUFA) to specific hydroperoxy derivatives [1, 2]. These enzymes are found in two of the three domains of terrestrial life (bacteria, eucarya) but have not been identified in archaea [3]. Mammalian LOX have been implicated in the biosynthesis of pro- and anti-inflammatory lipid mediators [4-6] but they also play a role in cell differentiation [7-9], apoptosis [10] and in the pathogenesis of hyperproliferative [11] and neurological [12] disorders. The human genome involves six functional LOX genes, which encode for six different LOX isoforms. Five human LOX genes (*ALOX15*, *ALOX15B*, *ALOX12*, *ALOX12B*, *ALOXE3*) have been mapped to a joint LOX gene cluster located on the short arm of chromosome 17. Only the gene encoding for human ALOX5 is located on the long arm of chromosome 10 [13]. The mouse genome involves single orthologs for all human ALOX isoforms but in addition it contains an *Aloxe12* gene, which is present as corrupted pseudogene in the human genome [13]. Among mammalian LOX the ALOX15 orthologs are somewhat special because of two reasons: i) In contrast to other LOX isoforms (ALOX5, ALOX12, ALOX12B, ALOX15B) ALOX15 orthologs accept complex ester lipids (phospholipids, cholesterol esters) as substrates even if these lipids are incorporated in complex lipid-protein assemblies [14, 15]. ii) ALOX15 orthologs exhibit dual reaction specificity with arachidonic acid (ARA, C20:4n6) as substrate since 12(*S*)- and 15(*S*)-H(p)ETE have been identified as oxygenation products [16, 17]. Interestingly, in mammals there are two types of ALOX15 orthologs. Highly developed primates (humans, chimpanzee, orangutan) express ARA 15-lipoxygenating ALOX15 orthologs, whereas lower primates and other mammals (rhesus monkeys, rats, mice, pigs) express ARA 12-lipoxygenating enzymes [18]. The ALOX15 ortholog of gibbons constitutes a transition enzyme, which converts ARA to an almost 1:1 mixture of 12(*S*)- and 15(*S*)-H(p)ETE [18]. Although there are exceptions (rabbit ALOX15) from this evolutionary concept of ALOX15 specificity, it was suggested that this change

from ARA 12- to ARA 15-lipoxygenation improves the biosynthetic capacity for pro-resolving lipoxins, which optimizes inflammatory resolution [18].

Lipoxins [19] are ARA-derived eicosanoids, which are biosynthesized via transcellular mechanisms involving several LOX isoforms (ALOX5, ALOX15, ALOX15B, ALOX12) as well as the 5-lipoxygenase activating protein [20]. More recently, additional pro-resolving fatty acid derivatives derived from eicosapentaenoic acid (EPA, C20:5n3) and docosahexaenoic acid (DHA, C22:6n3) such as resolvins [21], protectins and maresins [22] have been identified and the biosynthesis of these mediators may also involve the catalytic activity of ARA 12- and 15-lipoxygenating LOX. To predict the biosynthetic capacity of mammalian LOX isoforms for lipoxin, resolvin and protectin biosynthesis it is important to characterize the reaction specificity of these enzymes with EPA and DHA. Unfortunately, for the time being only scattered information is available about the reaction specificity of mammalian ALOX15 orthologs with these fatty acids as substrate. To fill this gap, we expressed 12- and 15-lipoxygenating ALOX15 orthologs from eight different mammalian species as well as human ALOX12 and ALOX15B as his-tag fusion proteins in *E. coli*. The recombinant enzyme preparations were used to characterize the reaction specificity with n6-PUFA [linoleic acid (LA, C18:2n6), gamma-linolenic acid (GLA, C18:3n6), arachidonic acid (ARA, C20:4n6)] and n3-PUFA [eicosapentaenoic acid (EPA, C20:5n3) and docosahexaenoic acid (DHA, C22:6n3)]. We found that the reaction specificity of ALOX15 orthologs with n3-PUFA is variable and cannot be predicted from the product pattern of ARA oxygenation. For instance, human ALOX15, which oxygenates ARA to a 1:10 mixture of 12- (n9-oxygenation) and 15-H(p)ETE (n6-oxygenation) converts DHA with pronounced dual positional specificity to 17-H(p)DHA (n6-oxygenation) and 14-H(p)DHA (n9-oxygenation) in very similar amounts. In contrast, human ALOX12 and human ALOX15B oxygenate most fatty acids tested with singular positional specificity.

3.2 Experimental

3.2.1 Chemicals

The chemicals used were obtained from the following sources: 5,8,11,14-all-*cis*-eicosatetraenoic acid (arachidonic acid, ARA), 5,8,11,14,17-all-*cis*-eicosapentaenoic acid (EPA), 4,7,10,13,16,19-all-*cis*-docosahexaenoic acid (DHA), 9,12-all-*cis*-octadecadienoic acid (linoleic acid, LA), 9,12,15-all-*cis*-octadecatrienoic acid (gamma-linolenic acid, GLA) as well as HPLC standards of 5-HETE, 12-HETE, 15-HETE, 13-HODE, 13-HOTrE, 15-HEPE, 14-HDHA and 17-HDHA from Cayman Chem. (distributed by Biomol, Hamburg, Germany); LC/MS oxylipin standards and deuterated internal standards from Cayman Chemicals (distributed by Biomol, Hamburg, Germany); HPLC solvents from Baker (Deventer, The Netherlands); LC/MS grade acetonitrile, acetic acid and methanol from Fisher Scientific (Nidderau, Germany); the *E. coli* strain BL21 (DE3) pLysS from Invitrogen (Carlsbad, USA); the *E. coli* strain Rosetta2(DE3)pLysS from Novagen (Darmstadt, Germany).

3.2.2 Bacterial expression of LOX isoforms

ALOX15 orthologs from different mammalian species were cloned and expressed as described in [18]. In brief, the cDNA of these enzymes was inserted into the multicloning site of the bacterial expression plasmid pET28b and competent bacteria [BL21(DE3)pLysS] or [Rosetta2(DE3)pLysS] were transformed with the recombinant pET28b expression plasmids. The enzymes were then expressed as N-terminal his-tag fusion proteins in 50 mL liquid cultures using the optimized EnPresso-Expression system (BioSilta Oy, Oulu, Finland) following the instruction of the vendor. After the induction period the bacteria were pelleted, washed and resuspended in 4 mL PBS. Cells were disrupted by sonication (tip sonifier), debris was spun down and routinely the clear lysis supernatant was used as enzyme source for direct activity assays. In some cases, the enzymes

were enriched by affinity chromatography on Ni-NTA agarose. Mammalian ALOX15 orthologs from humans (humALOX15), chimpanzees (chiALOX15), orangutans (ponALOX15), gibbons (gibALOX15), rhesus monkeys (macALOX15), rabbits (rabALOX15), pig (pigALOX15), rat (ratALOX15) and mouse (mouALOX15) as well as human LOX isoforms ALOX15B (humALOX15B) and platelet-type ALOX12 (humALOX12) were expressed as described [19].

3.2.3 Fatty acid oxygenase activity

For routine activity assay, aliquots of the enzyme preparations (5–100 µL) were incubated in 0.2–0.5 mL of PBS containing the different fatty acids at a final concentration of 160 µM. When an equimolar mixture of several fatty acids was present in the activity assay each fatty acid contributed 58 µM to the final substrate concentration. The mixture was incubated for 3–5 min at room temperature and the hydroperoxy compounds formed were reduced with 10 µL of a methanolic $SnCl_2$ solution (10 mg/mL). For HPLC/MS analysis of the hydroxy fatty acids, the incubation mixture was acidified to pH 3 with 20 µL of concentrated acetic acid and the samples were lipid extracted twice with 0.5 mL ethyl acetate. The extracts were combined, the solvent was evaporated and the remaining lipids were reconstituted in a small volume (50–100 µL) of methanol. For HPLC/UV analysis of the reaction products, 0.5 mL of ice-cold methanol was directly added to the incubation mixture after reduction of the oxygenation products. Then, the samples were incubated on ice for 15 min and precipitated proteins were removed by centrifugation. Aliquots of the supernatant were then injected to RP-HPLC/UV for preparation of the conjugated dienes formed during the LOX reaction.

3.2.4 HPLC/MS analysis

The lipid extracts of the LOX incubations were mixed with deuterated internal standards (IS) ($^2H_4$-9-HODE, $^2H_8$-5-HETE, $^2H_8$-12-HETE, $^2H_6$-20-HETE).

Quantification of LOX products was carried out by HPLC/MS as reported in [23] with modifications described in [24]. In brief, chromatographic separation of the reaction products was achieved on an Agilent 1290 instrument (Agilent, Waldbronn, Germany) equipped with an Agilent Zorbax Eclipse Plus C18 reversed phase column (2.1 × 150 mm, particle size 1.8 µm). A binary solvent gradient with 0.1% aqueous acetic acid as solvent A and acetonitrile/methanol/acetic acid (800/150/1, *v/v/v*) as solvent B at a flow rate of 0.3 mL/min was used. Injection volume was 5 µL utilizing a HTS xt-PAL autosampler (Axel Semrau, Sprockhoevel, Germany). Mass spectrometric detection was performed on an AB Sciex 6500 QTRAP instrument (SCIEX, Darmstadt, Germany) in scheduled selected reaction monitoring mode following negative ion electrospray ionization. Data analysis was carried out with Multiquant 2.1.1. (AB Sciex). Hydroxy fatty acids were quantified by external calibration (0.25–500 nM) with standards obtained from Cayman using peak area ratios of analyte to deuterated IS. Hydroxy fatty acids present in an incubation mixture without enzyme preparation were subtracted from the concentration formed in enzymatic incubations. Fragmentation analysis was carried out in enhanced product ion mode operating the third quadrupole as linear ion trap.

3.2.5 HPLC/UV analysis

HPLC/UV analysis of the LOX products was carried out on a Shimadzu instrument equipped with a Hewlett-Packard diode array detector 1040 A recording the absorbance at 235 nm. The LOX products were separated on a Nucleosil C18 column (Marcherey-Nagel, Düren, Germany; KS-system, 250 × 4 mm, 5 µm particle size) coupled with a guard column (30 × 4 mm, 5 µm particle size). A solvent system of methanol/water/acetic acid (85/15/0.1,*v/v/v;* isocratic elution) was used at a flow rate of 1 mL/min. Normal phase HPLC/UV (NP-HPLC-UV) was performed on a Zorbax-SIL column (Agilent, 250 × 4 mm, 5 µm particle size) with a solvent system consisting of *n*-hexane/2-propanol/acetic acid (100/2/0.1, *v/v/v*; isocratic elution) and a flow rate of 1 mL/min.

3.2.6 Assay repetitions and statistical evaluation

To explore the reaction specificity of the different enzyme preparations different sets of experiments were carried out: i) The different substrate fatty acids (ARA, EPA, DHA) were separately added to the incubation mixture and the patterns of the oxygenation products were analyzed for each sample. These activity assays were carried out in quadruplicate using two different enzyme preparations. For gibbon ALOX15 the experiments were only performed in triplicate using two different enzyme preparations. ii) An equimolar mixture of ARA, EPA and DHA was prepared and the reaction was initiated by the addition of enzyme. These activity assays were carried out in duplicate using a single enzyme preparation. iii) An equimolar mixture of LA and GLA was prepared and the reaction was initiated by the addition of enzyme. These activity assays were carried out as a single experimental series. Statistical evaluation of the activity data was carried out using Students t-test (Microsoft Excel 12.8, 2008).

3.3 Results

3.3.1 Reaction specificity of human ALOX15 with n3- and n6-PUFA

Mammalian ALOX15 orthologs exhibit variable reaction specificities of ARA oxygenation. According to the evolutionary concept of ALOX15 specificity lower primates and other mammals express ARA 12-lipoxygenating orthologs. In contrast, higher primates express ARA 15-lipoxygenating enzymes [18]. If n3-PUFA such as EPA and DHA are oxygenated with a similar reaction specificity 15-H(p)EPE and 17-H(p)DHA are expected as major oxygenation products of EPA and DHA, respectively. When we analyzed the product pattern of ARA oxygenation by human ALOX15 (humALOX15) we confirmed the dual reaction specificity [17]. Under our experimental conditions 15-H(p)ETE and 12-H(p)ETE were formed in a ratio of 93:7 (Fig. 3.1 A). When EPA was used (Fig. 3.1 B) as substrate a similar dual reaction specificity was observed but here the share of

12-H(p)EPE (n9-oxygenation) was significantly higher (16%). Interestingly, DHA (Fig. 3.1 C) was oxygenated to an almost 1:1 mixture of 14-H(p)DHA (n9-oxygenation) and 17-H(p)DHA (n6-oxygenation). These data indicate that the reaction specificity of humALOX15 is variable and depends on the chemistry of the fatty acid substrate. With increasing number of double bonds the relative share of the n9-oxygenation product was increased and reached similar values as the major oxygenation product for DHA oxygenation.

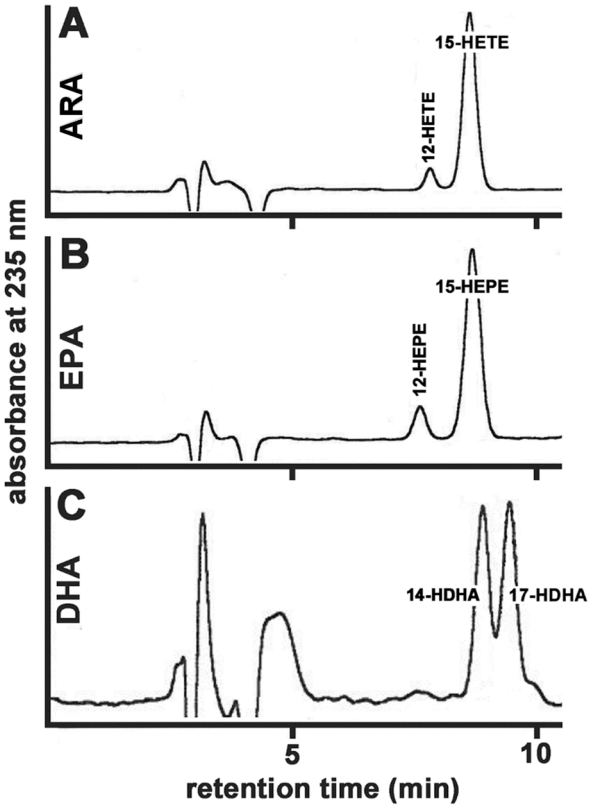

Fig. 3.1: Reaction specificity of human ALOX15 with different polyenoic fatty acids. Recombinant human ALOX15 was expressed in *E. coli* as N-terminal his-tag fusion protein. Aliquots of the bacterial lysis supernatant were incubated in PBS with different polyenoic fatty acids (160 µM final substrate concentration) for 5 min. After reduction with $SnCl_2$ the products were prepared and analyzed by NP-HPLC/UV as described in the experimental section. (**A**) Arachidonic acid as substrate (**B**) Eicosapentaenoic acid as substrate. (**C**) Docosahexaenoic acid as substrate.

3.3.2 Reaction specificity of other mammalian LOX isoforms

When we determined the reaction specificity of ARA, EPA and DHA oxygenation catalyzed by other 15-lipoxygenating ALOX15 orthologs (chimpanzee, orangutan, rabbit) we observed a similar behavior as for the humALOX15

(Tab. 3.1). With ARA dual reaction specificities were observed and the extent of 12-H(p)ETE formation varied between 5–8% of the overall product mixture. Similarly, the share of the minor oxygenation products (15-H(p)ETE) formed by the 12-lipoxygenating ALOX15 orthologs varied between 0.4–11%. Human ALOX15B (humALOX15B) and human ALOX12 (humALOX12) exhibited a singular positional specificity since the relative shares of the minor oxygenation product (12-H(p)ETE in case of humALOX15B and 15-H(p)ETE in case of humALOX12) did not exceed 1%.

Tab. 3.1: Reaction specificity of mammalian ALOX isoforms with 5,8,11,14-eicosatetraenoic acid (ARA) as substrate. Recombinant enzymes were expressed in *E. coli* as N-terminal his-tag fusion proteins. Aliquots of the bacterial lysis supernatant were incubated in PBS with arachidonic acid (160 µM final substrate concentration) for 5 min. After reduction with $SnCl_2$ the products were prepared and analyzed by LC-MS. Results are shown as mean ± SD.

Enzyme	Major product	Relative share [%]	Minor product	Relative share [%]	n6/n9-ratio
Arachidonic acid 15-lipoxygenating enzymes					
humALOX15	15-HETE	92.6 ± 0.6	12-HETE	7.4 ± 0.6	12.5
chiALOX15	15-HETE	92.5 ± 0.6	12-HETE	7.5 ± 0.6	12.3
ponALOX15	15-HETE	92.3 ± 0.5	12-HETE	7.7 ± 0.5	12.1
rabALOX15	15-HETE	95.1 ± 0.2	12-HETE	4.9 ± 0.2	19.4
humALOX15B	15-HETE	100 ± 0	12-HETE	0 ± 0	> 100
Arachidonic acid 12-lipoxygenating enzymes					
macALOX15	12-HETE	99.6 ± 0.3	15-HETE	0.4 ± 0.3	< 0.01
ratALOX15	12-HETE	96.7 ± 2.6	15-HETE	3.3 ± 2.6	0.03
mouALOX15	12-HETE	89.4 ± 1.0	15-HETE	10.6 ± 1.0	0.12
pigALOX15	12-HETE	92.2 ± 4.4	15-HETE	7.8 ± 4.4	0.09
humALOX12	12-HETE	100 ± 0	15-HETE	0 ± 0	< 0.01

When EPA was employed as substrate the dual positional specificity of the ARA 15-lipoxygenating ALOX15 orthologs was more pronounced (Tab. 3.2). Except for the rabbit enzyme (relative share of 12-H(p)EPE 3.4%) the relative share of the minor oxygenation product 12-H(p)EPE varied between 13–16%. For ARA oxygenation this value did not exceed 8%. The ARA 12-lipoxygenating ALOX15 orthologs also exhibited a dual positional specificity with EPA and as expected from the ARA oxygenation pattern 12-H(p)EPE was identified as major product of EPA oxygenation. Surprisingly, for rat and mouse ALOX15 [ratALOX15

(66.6%), mouALOX15 (75.7%)] 15-H(p)EPE was identified as major reaction product. As it was the case with ARA humALOX15B and humALOX12 oxygenated EPA with singular positional specificity to 15-H(p)EPE and 12-H(p)EPE, respectively.

Tab. 3.2: Reaction specificity of mammalian ALOX isoforms with 5,8,11,14,17-eicosapentaenoic acid (EPA) as substrate. Recombinant enzymes were expressed in *E. coli* as N-terminal his-tag fusion proteins. Aliquots of the bacterial lysis supernatant were incubated in PBS with eicosapentaenoic acid (160 µM final substrate concentration) for 5 min. After reduction with $SnCl_2$ the products were prepared and analyzed by LC-MS. Results are shown as mean ± SD.

Enzyme	Major product	Relative share [%]	Minor product	Relative share [%]	n6/n9-ratio
Arachidonic acid 15-lipoxygenating enzymes					
humALOX15	15-HEPE	84.4 ± 1.3	12-HEPE	15.6 ± 1.3	5.4
chiALOX15	15-HEPE	84.6 ± 0.6	12-HEPE	15.4 ± 0.6	5.5
ponALOX15	15-HEPE	86.6 ± 0.9	12-HEPE	13.4 ± 0.9	6.5
rabALOX15	15-HEPE	96.6 ± 0.7	12-HEPE	3.4 ± 0.7	29.8
humALOX15B	15-HEPE	99.0 ± 0.7	12-HEPE	1.0 ± 0.7	> 100
Arachidonic acid 12-lipoxygenating enzymes					
macALOX15	12-HEPE	83.4 ± 0.9	15-HEPE	16.6 ± 0.9	0.20
ratALOX15	15-HEPE	66.6 ± 0.7	12-HEPE	33.4 ± 0.7	**2.0**
mouALOX15	15-HEPE	75.7 ± 0.9	12-HEPE	24.3 ± 0.9	**3.1**
pigALOX15	12-HEPE	65.3 ± 1.3	15-HEPE	34.7 ± 1.3	0.53
humALOX12	12-HEPE	100 ± 0	15-HEPE	0 ± 0	< 0.01

As indicated by NP-HPLC/UV (Fig. 3.1 C) humALOX15 oxygenated DHA with pronounced dual specificity and almost equal amounts of 14-H(p)DHA and 17-H(p)DHA were formed. This finding was confirmed by HPLC-MS (Tab. 3.3) and the ALOX15 orthologs of chimpanzee (chiALOX15) and orangutan (ponALOX15) exhibited similar reaction specificities. However, the share of the minor oxygenation product 14-H(p)DHA was considerably lower for the rabbit ortholog (rabALOX15). For the ARA 12-lipoxygenating ALOX15 orthologs 14-H(p)DHA was the major oxygenation product (n9-oxygenation) and the relative share of the minor oxygenation product 17-H(p)DHA (n6-oxygenation) varied between 0% (macALOX15, mouALOX15) and 46% (ratALOX15). If one compares the reaction specificities of mouALOX15 and ratALOX15 with EPA and DHA it can be concluded that the rat enzyme exhibits a pronounced dual

specificity with both fatty acids. Similarly, mouALOX15 oxygenates EPA with pronounced dual specificity, whereas the n9-oxygenation product 14-H(p)DHA was dominant with DHA. In fact, under our experimental conditions we did not find significant amounts of 17-H(p)DHA with this enzyme (singular n9-oxygenase activity).

Tab. 3.3: Reaction specificity of mammalian ALOX isoforms with 4,7,10,13,16,19-docosahexaenoic acid (DHA) as substrate. Recombinant enzymes were expressed in *E. coli* as N-terminal his-tag fusion proteins. Aliquots of the bacterial lysis supernatant were incubated in PBS with docosahexaenoic acid (160 µM final substrate concentration) for 5 min. After reduction with $SnCl_2$ the products were prepared and analyzed by LC-MS. Results are shown as mean ± SD.

Enzyme	Major product	Relative share [%]	Minor product	Relative share [%]	n6/n9-ratio
Arachidonic acid 15-lipoxygenating enzymes					
humALOX15	17-HDHA	58.9 ± 5.5	14-HDHA	41.1 ± 5.5	1.5
chiALOX15	17-HDHA	56.6 ± 4.3	14-HDHA	43.4 ± 4.3	1.3
ponALOX15	17-HDHA	61.0 ± 9.0	14-HDHA	39.0 ± 9.0	1.7
rabALOX15	17-HDHA	92.0 ± 0.8	14-HDHA	8.0 ± 0.8	11.5
humALOX15B	17-HDHA	97.5 ± 1.5	14-HDHA	2.5 ± 1.5	48.3
Arachidonic acid 12-lipoxygenating enzymes					
macALOX15	14-HDHA	100 ± 0	17-HDHA	0 ± 0	< 0.01
ratALOX15	14-HDHA	53.8 ± 7.3	17-HDHA	46.2 ± 7.3	0.89
mouALOX15	14-HDHA	100 ± 0	17-HDHA	0 ± 0	< 0.01
pigALOX15	14-HDHA	76.4 ± 5.3	17-HDHA	23.6 ± 5.3	0.31
humALOX12	14-HDHA	100 ± 0	17-HDHA	0 ± 0	< 0.01

In an additional set of experiments, we compared the reaction specificity of mammalian ALOX15 orthologs with two different C18-PUFA (LA and GLA). When GLA (Fig. 3.2 A+B), which carries both n11- and n8-bisallylic methylenes, was used as substrate for ARA 15-lipoxygenating enzymes (humALOX15, humALOX15B) 13-H(p)OTrE (n6-oxygenation product) was dominant. Only small amounts of a second conjugated diene were detected, which was assumed to be the corresponding n9-oxygenation product of GLA [10-H(p)OTrE]**.** This late eluting compound was dominant, when the ARA 12-lipoxygenating ratALOX15 was used as catalyst (Fig. 3.2 C). The structure of this product was characterized as 10-hydroxy-6,8,12-octadecatrienoic acid [10-H(p)OTrE] by means of MS/MS. The fragment ions at *m/z* 153.0 and *m/z* 181.1 represent α-cleavage fragments

on either side of the OH-group. Moreover, intense secondary fragmentation ions can be explained by the loss of water (–18) and carbon dioxide (–44) from different primary fragments (Fig. 3.2 F). Since n9-oxygenation is not possible with LA (lacking n11-bisallylic methylene) dominant formation of 13-H(p)ODE was observed for human ALOX15 and human ALOX15B (Fig. 3.2 D+E). Since human [25] and mouse ALOX12 [26] have previously been suggested not to react with LA we did not consider these enzymes for activity assays. However, when other ARA 15-lipoxygenating ALOX15 orthologs (chimpanzee, orangutan, rabbit) reacted with GLA 13-H(p)OTrE was identified as major oxygenation product. In contrast, 10-H(p)OTrE prevailed for ARA 12-lipoxygenating ALOX15 orthologs (Tab. 3.4).

Tab. 3.4: Reaction specificity of mammalian ALOX isoforms with gamma-linolenic acid (6,9,12-octadecatrienoic acid, GLA) as substrate. Recombinant enzymes were expressed in *E. coli* as N-terminal his-tag fusion proteins. Aliquots of the bacterial lysis supernatant were incubated in PBS with GLA (57 µM final substrate concentration) for 4 min. After reduction with $SnCl_2$ the products were prepared and analyzed by HPLC/UV. Mean ± SD were calculated with the Microsoft Excel software package (version 12.1.0.).

Enzyme	Major product	Relative share [%]	Minor product	Relative share [%]	n6/n9 ratio
Arachidonic acid 15-lipoxygenating enzymes					
humALOX15	13-HOTrE	90.9	10-HOTrE	9.1	10.0
chiALOX15	13-HOTrE	89.8	10-HOTrE	10.2	7.6
ponALOX15	13-HOTrE	85.9	10-HOTrE	14.1	6.0
rabALOX15	13-HOTrE	87.7	10-HOTrE	12.3	7.1
humALOX15B	13-HOTrE	88.4	10-HOTrE	11.6	8.8
mean ± SD	**13-HOTrE**	**88.4 ± 1.8**	**10-HOTrE**	**11.5 ± 2.0**	**7.9 ± 1.5**
Arachidonic acid 12-lipoxygenating enzymes					
macALOX15	10-HOTrE	80.6	13-HOTrE	19.4	0.24
ratALOX15	10-HOTrE	70.2	13-HOTrE	29.8	0.42
mouALOX15	10-HOTrE	71.7	13-HOTrE	28.3	0.39
pigALOX15	10-HOTrE	80.1	13-HOTrE	19.9	0.25
mean ± SD	**10-HOTrE**	**75.7 ± 5.5**	**13-HOTrE**	**19.9 ± 5.5**	**0.33 ± 0.09**

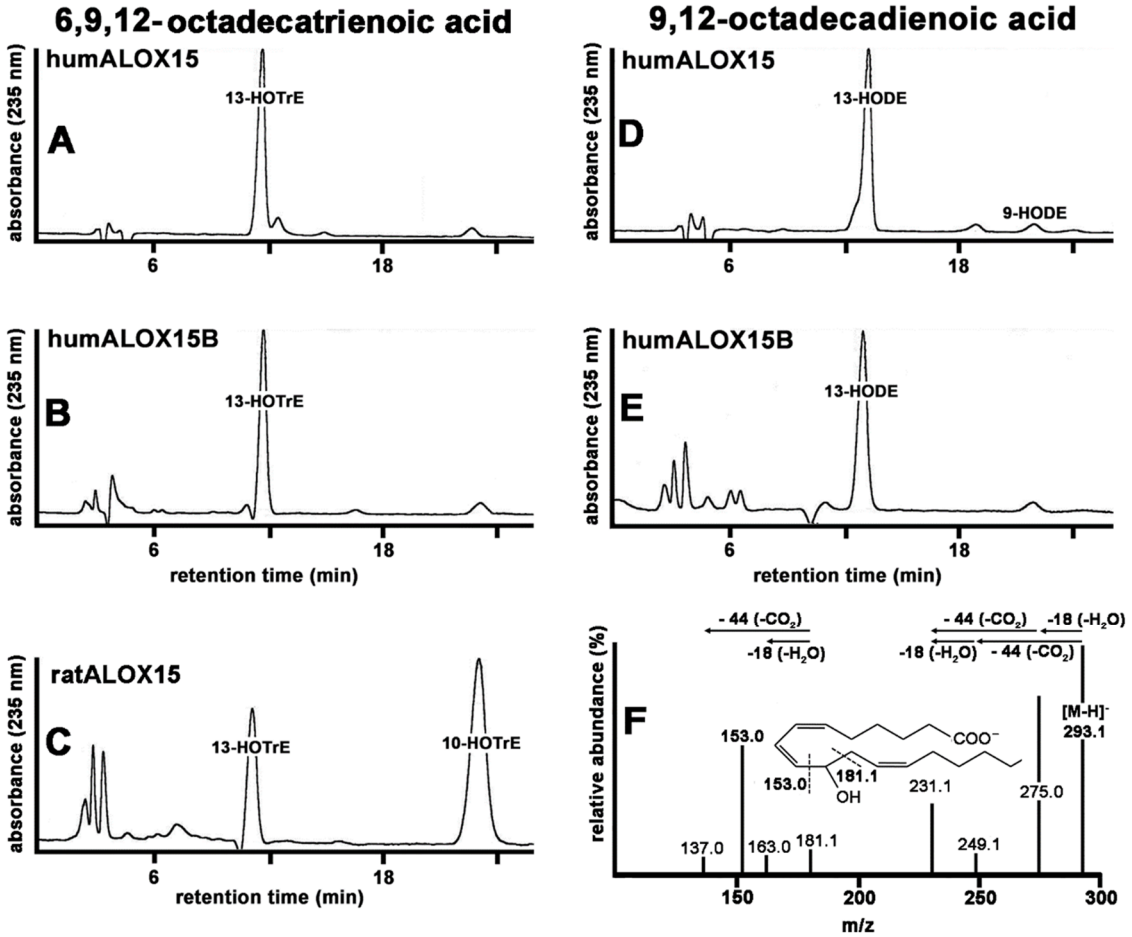

Fig. 3.2: Reaction specificity of selected human ALOX isoforms with 6,9,12-octadecatrienoic acid (GLA) and 9,12-octadecadienoic acid (LA). Recombinant ALOX isoforms were expressed in *E. coli* as N-terminal his-tag fusion proteins. Aliquots of the bacterial lysis supernatant were incubated in PBS for 5 min with LA (60 µM) and GLA (60 µM). After reduction with $SnCl_2$ the products were extracted, the conjugated dienes were prepared by RP-HPLC and further analyzed by NP-HPLC/UV as described in the experimental section. (**A**) humALOX15 with GLA, (**B**) humALOX15B with GLA, (**C**) ratALOX15 with GLA, (**D**) humALOX15 with LA, (**E**) humALOX15B with LA. The UV-spectra of the dominant products (conjugated diene chromophore) taken during the chromatographic run (data not shown) are consistent with the chemical structure of the products. (**F**) Fragment ion spectrum of the major GLA oxygenation product formed by ratALOX15 (panel **C**). The fragmentation pattern supports that the reaction product is 10-hydroxy-6,8,12-octadecatrienoic acid (10-HOTrE).

3.3.3 Reaction specificity of gibbon ALOX15

According to the evolutionary concept of ALOX15 specificity gibbon ALOX15 (gibALOX15) constitutes a transition enzyme, which exhibits pronounced dual reaction specificity with ARA [18]. We incubated recombinant gibALOX15 with ARA, EPA and DHA and analyzed the product pattern by HPLC/MS. Here we confirmed the pronounced dual reaction specificity with ARA (Tab. 3.5). Under

our experimental conditions a ratio of 15-H(p)ETE/12-H(p)ETE (n6/n9-oxygenation) of 2.0 was calculated, when ARA was the only oxygenation substrate in the incubation mixture. In contrast, 12-H(p)EPE (n9-oxygenation) was the major oxygenation product of EPA oxygenation and here a n6/n9-oxygenation ratio of 0.98 was calculated (Tab. 3.5). Similarly, for DHA oxygenation (Tab. 3.5) 14-H(p)DHA (n9-oxygenation) was identified as major oxygenation product and 17-H(p)DHA was formed in lower amounts (n6/n9-oxygenation ratio of 0.54). Comparing the n6/n9-oxygenation ratios for ARA (n6/n9 = 2.0), EPA (n6/n9 = 0.98), and DHA (n6/n9 = 0.54) one can conclude that with an increasing number of double bonds in the fatty acid substrates the relative share of the n9-oxygenation product increased.

Tab. 3.5: Reaction specificity of gibbon ALOX15 with different polyenoic fatty acids. Recombinant gibbon LOX (bacterial lysate supernatant) was incubated either with a single PUFA substrate (160 µM ARA, or 160 µM EPA, or 160 µM DHA) in PBS for 5 min or with an equimolar mixture (58 µM each) of ARA, EPA and DHA. After the incubation period the reaction products were reduced with $SnCl_2$, extracted with ethyl acetate and analyzed by HPLC/MS. Results are shown as mean ± SD.

Substrate		n6-oxygenation	Relative share [%]	n9-oxygenation	Relative share [%]	n6/n9-ratio
Individual substrates	ARA	15-HETE	66.8 ± 0.6	12-HETE	33.2 ± 0.6	2.0
	EPA	15-HEPE	49.0 ± 5.8	12-HEPE	51.0 ± 5.8	0.98
	DHA	17-HDHA	35.0 ± 1.5	14-HDHA	65.0 ± 1.5	0.54
Substrate mixture	ARA	15-HETE	58.3 ± 1.9	12-HETE	41.7 ± 1.9	1.4
	EPA	15-HEPE	44.3 ± 1.3	12-HEPE	55.7 ± 1.3	0.79
	DHA	17-HDHA	24.4 ± 3.6	14-HDHA	75.6 ± 3.6	0.33

3.3.4 PUFA selectivity of 12- and 15-lipoxygenating mammalian LOX isoforms

After we have identified the reaction specificity of mammalian LOX isoforms with separately supplied PUFA, we next explored whether simultaneous conversion of different PUFA might alter the enzyme characteristics. For this purpose, the enzyme preparations were incubated with an equimolar mixture of ARA, EPA and DHA (58 µM each) and this series of experiments more adequately mirrors the *in vivo* situation. Employing this methodological approach, we aimed at obtaining

the following information: i) Is there a preferential oxygenation of a certain PUFA from the equimolar PUFA mixture? ii) Is the reaction specificity of the enzymes for a given PUFA altered by the simultaneous presence of another PUFA?

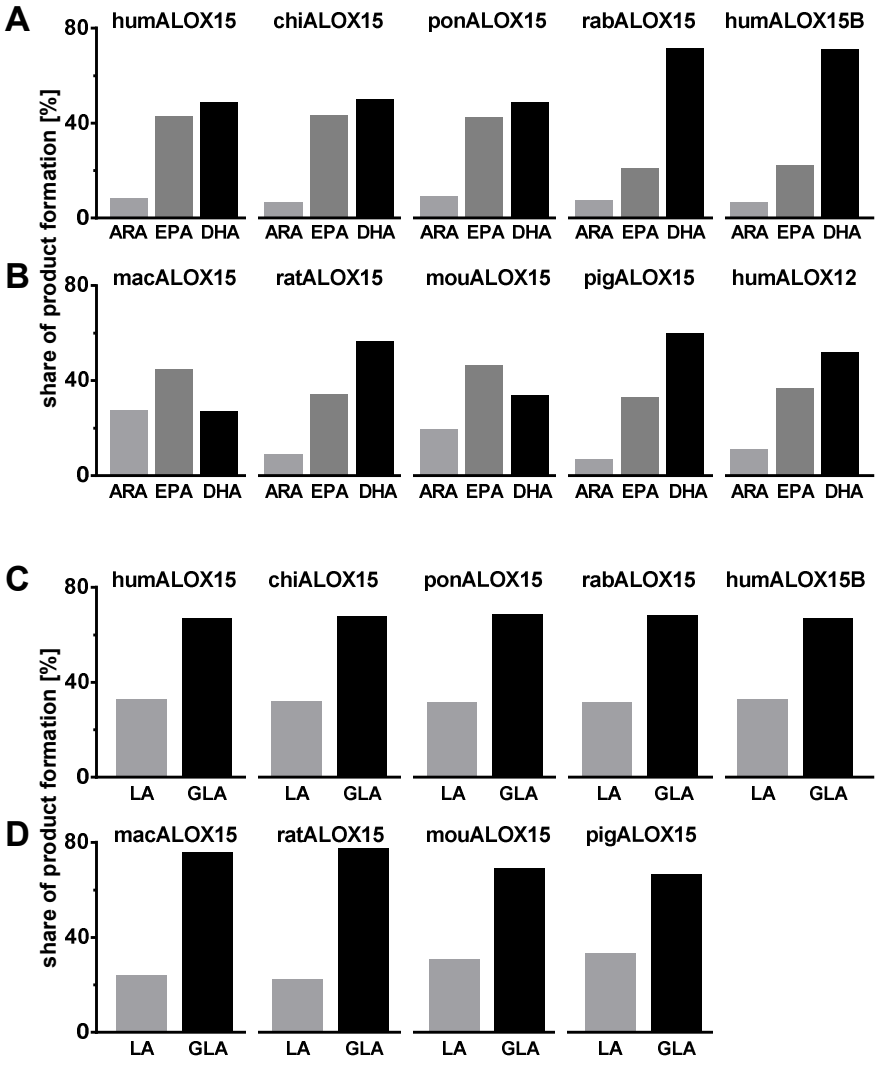

Fig. 3.3: Substrate preference of mammalian LOX isoforms. Aliquots of the bacterial lysis supernatant were incubated in PBS for 5 min with an equimolar mixture of different polyenoic fatty acids (58 µM each). After reduction with $SnCl_2$ the products were extracted. The products of ARA, EPA and DHA oxygenation (panels **A**+**B**) were analyzed by HPLC/MS. For analysis of the LA and GLA oxygenation products (panels **C**+**D**) the conjugated dienes were prepared by RP-HPLC/UV and further analyzed by NP-HPLC/UV. The relative shares of the major oxygenation products were calculated based on determined concentrations (12-HETE+15-HETE for ARA, 12-HEPE+15-HEPE for EPA, 14-HDHA+17-HDHA for DHA), or peak area ratio on RP-HPLC/UV (13-HODE for LA, 13-HOTrE+10-HOTrE for GLA). Two independent experiments yielding similar results were carried out with each fatty acid mixture and one of them was used for data presentation. (**A**) Products formed from an equimolar mixture of ARA+EPA+DHA by ARA 15-lipoxygenating enzymes, (**B**) Products formed from an equimolar mixture of ARA+EPA+DHA by ARA 12-lipoxygenating enzymes, (**C**) Products formed from an equimolar mixture of LA and GLA by ARA 15-lipoxygenating enzymes, (**D**) Products formed from an equimolar mixture of LA and GLA by ARA 12-lipoxygenating enzymes.

i) To answer the first question we quantified the relative shares of the major DHA oxygenation products (sum of 14- and 17-HDHA) formed during the incubation by the different enzymes. Here we found that the relative share of the DHA oxygenation products varied between 49% (ponALOX15) and 72% (rabALOX15). No significant ($p = 0.401$) differences were found when the relative shares of DHA oxygenation products of the ARA 15-lipoxygenating enzymes (58.1 ± 12.1%) were compared with the corresponding values obtained for the ARA 12-lipoxygenating enzymes (46.0 ± 14.4%). These data indicate that the majority of the reaction products formed during the incubation period originate from DHA (Fig. 3.3 A+B). The relative shares of EPA oxygenation products (34.4 ± 11.6% for ARA 15-lipoxygenating enzymes vs. 39.1 ± 6.1% for 12-lipoxygenating enzymes, $p=0.871$) varied between 21% (rabALOX15) and 43% (chiALOX15), and the means were lower than those of the DHA derived products. The relative shares of ARA oxygenation products (7.5 ± 1.1% for ARA 15-lipoxygenating enzymes vs. 14.9 ± 8.6% for 12-lipoxygenating enzymes, $p = 0.128$) varied between 7% (humALOX15B) and 11% (humALOX12). The means were even lower than those calculated for the EPA-derived oxygenation products. Taken together these results indicate that under our experimental conditions DHA is the preferred substrate for almost all LOX isoforms tested. Moreover, our results suggest that the relative shares of the oxygenation products are increased depending on the number of double bonds in the fatty acid substrate. The only exceptions from this rule are macALOX15 and mouALOX15 (Fig. 3.3). For these enzymes the relative share of the ARA oxygenation products was rather high (27.7% for macALOX15, 19.4% for mouALOX15%) and the EPA oxygenation products contributed even more (44.9% for macALOX15, 46.5% for mouALOX15) to the product mixture. The percentage of DHA oxygenation products was 27.4% for macALOX15 and 34.1% for mouALOX15, which was equal or a little higher than that of ARA oxygenation products but clearly lower than the percentage of EPA-derived oxygenation products. A similar experiment was carried out with an equimolar mixture of LA and GLA (Fig. 3.3 C+D). Here we found that GLA was preferentially oxygenated by all LOX isoenzymes (67.8 ± 0.7% for ARA 15-lipoxygenating enzymes vs. 72.3 ± 5.3% for ARA

12-lipoxygenating enzymes) and there was no significant difference between ARA 12- and 15-lipoxygenating LOX isoforms ($p = 0.101$). These data confirm our previous conclusion (see above) that PUFA with a higher number of double bonds are preferred LOX substrates when PUFA are simultaneously offered and this does not depend on the reaction specificity of the enzymes.

ii) To answer the second question we determined the reaction specificity of the different enzymes in this experimental setup. For direct comparison we calculated for each enzyme the ratio of n6/n9-products as specificity coefficients: 15-H(p)ETE/12-H(p)ETE ratio for ARA oxygenation, 15-H(p)EPE/12-H(p)EPE ratio for EPA oxygenation, 17-H(p)DHA/14-H(p)DHA ratio for DHA oxygenation. Then we compared these values for the incubation samples, in which a single substrate was provided, with the corresponding samples, in which ARA, EPA and DHA were simultaneously present. The results are summarized in Tab. 3.6. Analyzing the product patterns of ARA oxygenation by 15-lipoxygenating mammalian ALOX15 orthologs (humALOX15, chiALOX15, ponALOX15, rabALOX15) we found that in the absence of other fatty acids the 15-H(p)ETE/12-H(p)ETE ratio varied between 12 and 19 and these data confirm our previous conclusion that 15-H(p)ETE was the major ARA oxygenation product (Tab. 3.1). When other PUFA substrates were present the specificity coefficients were somewhat lower but there was no statistically significant difference ($p = 0.675$). These data suggest that the presence of other fatty acid substrates in the incubation mixture does hardly impact the reaction specificity of ARA oxygenation. The specificity of ARA oxygenation by humALOX15B was not altered at all by the presence of other fatty acid substrates. For this enzyme 15-H(p)ETE was the only ARA oxygenation product (specificity coefficient > 100) regardless whether pure ARA or an equimolar mixture of ARA+EPA+DHA was used. Similar results were obtained when the product patterns of EPA and DHA were compared between the two experimental setups. From Tab. 3.6 it can be seen that the specificity coefficients calculated for EPA and DHA oxygenation were rather similar when oxygenation of a single fatty acid was compared with the oxygenation of the fatty acid mixtures.

Tab. 3.6: Reaction specificity of mammalian LOX isoforms with a single substrate and with an equimolar mixture of three different PUFA substrates. Recombinant mammalian LOX isoforms (bacterial lysate supernatants) were incubated either with a single PUFA substrate (160 µM ARA, or 160 µM EPA, or 160 µM DHA) in PBS for 5 min or with an equimolar mixture (58 µM each) of ARA, EPA and DHA. After the incubation period the reaction products were reduced with $SnCl_2$, extracted with ethyl acetate and analyzed by HPLC/MS. From the experimental raw data the specificity coefficients (15-HETE/12-HETE-ratio for ARA, 15-HEPE/12-HEPE-ratio for EPA, 17-HDHA/14-HDHA-ratio for DHA), which characterize the reaction specificity of the different LOX isoforms with the different substrates, were calculated.

Products	**ARA oxygenation products**		**EPA oxygenation products**		**DHA oxygenation products**	
Specificity	15-HETE/12-HETE ratio		15-HEPE/12-HEPE ratio		17-HDHA/14-HDHA ratio	
Substrates	ARA+EPA +DHA	ARA only	ARA+EPA +DHA	EPA only	ARA+EPA +DHA	DHA only
Arachidonic acid 15-lipoxygenating enzymes						
humALOX15	5.8	12.5	6.0	5.4	1.4	1.5
chiALOX15	6.0	12.3	5.6	5.5	1.5	1.3
ponALOX15	5.4	12.1	6.2	6.5	1.3	1.7
rabALOX15	28.5	19.4	47.4	29.8	10.8	11.5
humALOX15B	> 100	> 100	> 100	> 100	> 100	48.3
Arachidonic acid 12-lipoxygenating enzymes						
macALOX15	< 0.01	< 0.01	0.01	0.20	0.01	< 0.01
ratALOX15	0.21	0.03	1.9	2.0	0.45	0.89
mouALOX15	0.03	0.12	2.5	3.1	0.03	< 0.01
pigALOX15	0.14	0.09	0.55	0.53	0.07	0.31
humALOX12	< 0.01	< 0.01	< 0.01	< 0.01	< 0.01	< 0.01

Analyzing the product patterns of ARA oxygenation by ARA 12-lipoxygenating mammalian ALOX15 orthologs (macALOX15, ratALOX15, mouALOX15, pigALOX15) we calculated specificity coefficients [15-H(p)ETE/12-H(p)ETE-ratio] < 1 confirming the previous finding (Tab. 3.1) that 12-H(p)ETE was the major ARA oxygenation product for these enzymes. Similar data were obtained when a mixture of ARA+EPA+DHA was used. Interestingly, for EPA and DHA oxygenation the situation is somewhat more complex. As indicated in Tab. 3.2, macALOX15 converts EPA with high specificity (specificity coefficient of 0.2) to 12-H(p)EPE and this result was confirmed in this experiment. Simultaneous presence of other PUFA substrates did even augment the reaction specificity of EPA oxygenation by this enzyme ortholog (specificity coefficient of 0.01). For ratALOX15 (specificity coefficient of 2.0) and mouALOX15 (specificity coefficient

of 3.1) the preferred formation of 15-H(p)EPE (n6-oxygenation) was also observed with an equimolar mixture of ARA+EPA+DHA as substrate (specificity coefficient of 1.9 for ratALOX15 and 2.5 for mouALOX15). These results indicate that the unusual reaction specificity of EPA oxygenation by these two enzymes is hardly impacted by the simultaneous presence of other fatty acids. With DHA (Tab. 3.6) ratALOX15 exhibits a pronounced dual reaction specificity (specificity coefficient of 0.89) and this was also the case when different fatty acids were present in the reaction mixture (specificity coefficient of 0.45). The mouALOX15 converts DHA mainly to 14-H(p)DHA (specificity coefficient < 0.01) and a similar product pattern was also observed when other fatty acids were present (specificity coefficient of 0.03). The pigALOX15 exhibits dual reaction specificity (specificity coefficient of 0.53) for EPA oxygenation and a similar value (specificity coefficient 0.55) was obtained when ARA+EPA+DHA were simultaneously present. With DHA this enzyme predominantly forms 14-H(p)DHA (specificity coefficient of 0.31) and a similar product pattern was formed when other fatty acids were included in the incubation mixture (specificity coefficient of 0.07). The humALOX12 exhibited singular reaction specificity with all fatty acids (exclusive formation of 12-H(p)ETE, 12-H(p)EPE, 14-H(p)DHA) and this product pattern does not depend on the absence or presence of other fatty acids in the incubation mixture.

Since ARA and LA are the most abundant PUFA in many human cells [27, 28] we tested the impact of LA on ARA oxygenation and *vice versa*. For this purpose, we incubated selected ALOX isoforms with an equimolar mixture of ARA and LA and quantified the reaction products by NP-HPLC. Here we found (Fig. 3.4) that ARA is the preferred substrate for most ALOX isoforms tested and that the reaction specificity of ARA oxygenation (12-H(p)ETE/15-H(p)ETE ratio) was hardly impacted by the presence of LA. ARA 15-lipoxygenating enzymes produce 15-H(p)ETE as major oxygenation product in the absence (Tab. 3.1) and in the presence of LA (Fig. 3.4). Similarly, ARA 12-lipoxygenating enzymes form 12-H(p)ETE as major oxygenation product regardless whether LA is present or not. There are some minor differences in the 12-H(p)ETE/15-H(p)ETE ratio but

we never observed inversion of the reaction specificity. These data are consistent with our results obtained with the mixtures of ARA + EPA + DHA on the one hand and with LA + GLA on the other (Fig. 3.3).

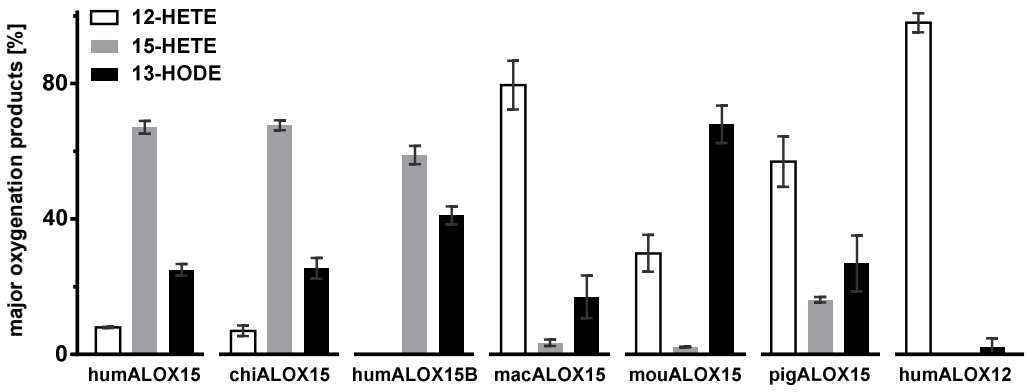

Fig. 3.4: Formation of oxygenation products from an equimolar mixture of LA and ARA by selected mammalian LOX isoforms. Aliquots of the bacterial lysis supernatant were incubated in PBS for 5 min with an equimolar mixture of LA and ARA (75 µM each). After reduction, the products were prepared by RP-HPLC and further analyzed by NP-HPLC. A single experiment was carried out and each sample was analyzed in duplicate.

3.4 Discussion

The reaction specificity of LOX isoforms is of biological relevance

The reaction specificity of LOX isoforms is an important enzyme property since the biological activities of these enzymes depend on this enzyme characteristic. ARA 5-lipoxygenating enzymes (ALOX5 orthologs) have been implicated in the biosynthesis of 5,6-leukotrienes, which function as pro-inflammatory mediators [1, 29]. ARA 12- and 15-lipoxygenating ALOX isoforms cannot produce 5,6-leukotriene precursors but they have been implicated in the biosynthesis of pro-resolving mediators [30, 31]. On the other hand, corresponding reactions cannot be catalyzed by ALOX5 orthologs. Moreover, the different PUFA oxygenation products, such as 5-H(p)ETE, 12-H(p)ETE, 15-H(p)ETE and 13-H(p)ODE exhibit differential bioactivities [32-34] and thus, the reaction specificity of LOX isoforms is of biological relevance. Although dual reaction specificities have been reported for several LOX isoforms [16, 17, 35] most enzymes prefer (> 90%) the formation

of a single product isomer from naturally occurring PUFA. Recently, it was reported that gibbon ALOX15 exhibits pronounced dual reaction specificity of ARA oxygenation [18] but this is a rare exception among mammalian LOX. However, with artificial PUFA dual reaction specificity has been reported for rabbit ALOX15 and soybean LOX [36]. The results of those experiments suggested that it might be important for the reaction specificity of LOX, how the fatty acid substrates are aligned at the active site of the enzyme [36]. This conclusion allows the possibility that ARA, EPA and DHA are differently aligned at the active site of a particular LOX isoform, which consequently may lead to the formation of a different product pattern.

Human, chimpanzee and orangutan ALOX15 orthologs exhibit pronounced dual reaction specificity with DHA

We demonstrate here that the ALOX15 orthologs of higher primates (man, chimpanzee, orangutan) oxygenated DHA with pronounced dual reaction specificity forming similar amounts of n6- (17-HDHA) and n9- (14-HDHA) oxygenation products. In contrast, rabbit ALOX15 mainly forms the n6-oxygenated derivative (17-HDHA, 92%). Among the ARA 12-lipoxygenating ALOX15 orthologs only rat ALOX15 exhibits pronounced dual reaction specificity (n6/n9-ratio of 0.89). The other ALOX15 orthologs strongly favor 14-HDHA formation. Reaction specificity of PUFA oxygenation by mammalian ALOX15 orthologs is thus variable, species-dependent and strongly impacted by the chemical structure of the substrate. Interestingly, this is not the case for human ALOX15B and human ALOX12. For humALOX15B the n6-oxygenation product is dominant regardless whether n6 (LA, GLA, ARA) or n3-polyenoic fatty acids (EPA, DHA) were used. Similarly, for humALOX12 the n9-oxygenation products (12-HETE, 12-HEPE, 14-HDHA) were identified as major oxygenation products. The differences in the reaction specificity of DHA oxygenation by humALOX15 (dual specificity) on the one hand and by humALOX15B (singular specificity) on the other may be of practical importance for investigations of eicosanoid metabolism of cells and tissues. For instance, IL4-treated human

monocytes/macrophages express both ALOX15 [37] and ALOX15B [38]. These cells convert exogenous and endogenous ARA predominantly to 15-HETE but for the time being it remains unclear whether this product formation is related to the catalytic activity of ALOX15 or ALOX15B. Our results on the different reaction specificities of recombinant ALOX15 and ALOX15B with DHA suggest that experiments with DHA should answer this question. If 17HDHA is formed as major oxygenation product by IL4-treated monocytes ALOX15B is likely to be the metabolic source. In contrast, when similar amounts of 14- and 17-HDHA can be detected ALOX15 should be involved. To the best of our knowledge such experiments have not been carried out so far.

The demonstrated capability of human ALOX15 to catalyze hydrogen abstraction from both, the n8- and the n11-bisallylic methylene of DHA, could be of biological relevance leading to the formation of pro-resolving mediators, such as 7,16,17-trihydroxy-DHA (resolvin D2). Biosynthesis of this metabolite involves hydrogen abstraction from C9 (catalyzed by ALOX5), from C12 (n11-bisallylic methylene, catalyzed by ALOX12 or by 12-lipoxygenating ALOX15 orthologs) and from C15 (n8-bisallylic methylene, catalyzed by 15-lipoxygenating ALOX15 orthologs). Since human ALOX15 can catalyze hydrogen abstraction from both, C15 (formation of 17-HDHA) and C12 (formation of 14-HDHA) of DHA, ALOX12 may not be required for resolvin D2 biosynthesis. In contrast, according to our data ALOX12 or humALOX15B should not be capable of catalyzing resolvin D2 formation alone. Although this theoretical discussion must be substantiated by direct experimental data on resolvin D2 biosynthesis the reaction specificity data presented here suggest that humALOX15 appears to be optimized during evolution for resolvin D2 biosynthesis.

The presence of additional polyenoic fatty acids does not modify the reaction specificity with a given substrate

In biological systems liberation of polyenoic fatty acids from the cellular phospholipids is not PUFA specific because of the broad substrate specificity of the ester lipid hydrolyzing enzymes [39, 40]**.** This lack of specificity leads to the

liberation of several PUFA following cell stimulation and thus, different polyenoic fatty acids are usually liberated for further metabolism. However, for characterization of the reaction specificity of ALOX isoforms the assay systems usually involve a single substrate. The results of such experiments might thus be misleading if the presence of additional polyenoic fatty acids in the assay system would impact the reaction specificity of a given enzyme. Here we found that simultaneous incubations of ARA, EPA and DHA did only lead to minor alterations in the product patterns. These data indicate that the presence of additional polyenoic fatty acids in the substrate mixture does not substantially alter the reaction specificity for a given enzyme-substrate combination. Translating these findings to the *in vivo* situation our data suggest that it is possible to predict the *in vivo* reaction specificity of a LOX isoform from *in vitro* assays carried out with a single PUFA substrate.

Substrate selectivity and preference of ALOX isoforms

The reaction specificity of mammalian LOX isoforms with ARA as substrate has frequently been studied. However, there is little information on the reactivity of these enzymes with other biologically relevant PUFA. Rabbit ALOX15 exhibits a broad substrate specificity reacting with all abundantly occurring PUFA [41]. Native bovine [42] and porcine [35] ALOX15 orthologs also react with C18-, C20- and C22-PUFA and thus, our results on the reaction specificity of other mammalian ALOX15 orthologs are consistent with the literature. Human ALOX15B was first described in human skin [43] but has subsequently also been detected in other cells and tissues [44]. Although this enzyme prefers ARA as substrate it also oxygenates LA [43]. Here we confirmed the capability of humALOX15B to oxygenate LA but also showed that GLA was oxidized with singular positional specificity to the corresponding n6-hydro(pero)xy derivative [13-H(p)OTrE]. When LA and GLA were simultaneously present in the incubation mixture humALOX15B preferred GLA as substrate (GLA *vs.* LA oxygenation ratio of about 9:1, Tab. 3.4). This observation can be extended to all long-chain PUFA. Almost all ALOX15 orthologs preferentially convert fatty acids with a higher

degree of unsaturation. In simultaneous incubations of ARA, EPA and DHA this substrate preference leads to dominant conversion of DHA and EPA compared to ARA (ratio 8:43:49 for ARA:EPA:DHA derived products for humALOX15). This finding might be important for the *in vivo* situation. Although the n6- (LA + ARA) vs. n3- (EPA + DHA) ratio in most mammalian cells depends on a number of factors such as diet [45, 46], age [47] and sex [46] n6-fatty acids are usually more abundant in most cells and tissues than DHA and EPA [27, 28]. Because of the preferred conversion of DHA and EPA by human ALOX15 the low tissue levels of these fatty acids might still lead to a substantial formation of the corresponding H(p)EPE and H(p)DHA *in vivo*. Several studies demonstrate that supplementation of DHA and EPA leads to increased levels of these fatty acids in cells and tissues and in the blood [48, 49]. In this case, the substrate preference would lead to a higher relative increase in H(p)EPE and H(p)DHA compared to their precursor PUFA. Indeed, intervention studies with n3-PUFA indicate a higher increase of EPA/DHA-derived oxylipins compared to their precursor fatty acids, e.g. 15-fold increase of 12-HEPE compared to 4-fold increase of EPA [48]. The molecular basis for these observations remained elusive but in the light of our findings the previous results become plausible. Considering that the beneficial health effects of n3-PUFA are still not fully understood the substrate preference of ALOX15 described here suggests that these enzymes and their products might play a key role in n3-PUFA biology.

3.5 References

1. Haeggstrom JZ, Funk CD (2011) Lipoxygenase and leukotriene pathways: biochemistry, biology, and roles in disease. *Chem Rev*, 111(10), 5866-5898; doi: 10.1021/cr200246d.
2. Ivanov I, Heydeck D, Hofheinz K, Roffeis J, O'Donnell VB, Kuhn H, Walther M (2010) Molecular enzymology of lipoxygenases. *Arch Biochem Biophys*, 503(2), 161-174; doi: 10.1016/j.abb.2010.08.016.
3. Horn T, Adel S, Schumann R, Sur S, Kakularam KR, Polamarasetty A, Redanna P, Kuhn H, Heydeck D (2015) Evolutionary aspects of lipoxygenases and genetic diversity of human leukotriene signaling. *Prog Lipid Res*, 57, 13-39; doi: 10.1016/j.plipres.2014.11.001.
4. Di Gennaro A, Haeggstrom JZ (2012) The leukotrienes: immune-modulating lipid mediators of disease. *Adv Immunol*, 116, 51-92; doi: 10.1016/B978-0-12-394300-2.00002-8.
5. Janakiram NB, Mohammed A, Rao CV (2011) Role of lipoxins, resolvins, and other bioactive lipids in colon and pancreatic cancer. *Cancer Metastasis Rev*, 30(3-4), 507-523; doi: 10.1007/s10555-011-9311-2.
6. Pace-Asciak CR (2015) Pathophysiology of the hepoxilins. *Biochim Biophys Acta*, 1851(4), 383-396; doi: 10.1016/j.bbalip.2014.09.007.
7. Rapoport SM, Schewe T (1986) The maturational breakdown of mitochondria in reticulocytes. *Biochim Biophys Acta*, 864(3-4), 471-495; doi: 10.1016/0304-4157(86)90006-7.
8. van Leyen K, Duvoisin RM, Engelhardt H, Wiedmann M (1998) A function for lipoxygenase in programmed organelle degradation. *Nature*, 395(6700), 392-395; doi: 10.1038/26500.
9. Cole BK, Kuhn NS, Green-Mitchell SM, Leone KA, Raab RM, Nadler JL, Chakrabarti SK (2012) 12/15-Lipoxygenase signaling in the endoplasmic reticulum stress response. *Am J Physiol Endocrinol Metab*, 302(6), E654-665; doi: 10.1152/ajpendo.00373.2011.
10. Claria J (2006) Regulation of cell proliferation and apoptosis by bioactive lipid mediators. *Recent Pat Anticancer Drug Discov*, 1(3), 369-382; doi: 10.2174/157489206778776961.
11. Schneider C, Pozzi A (2011) Cyclooxygenases and lipoxygenases in cancer. *Cancer Metastasis Rev*, 30(3-4), 277-294; doi: 10.1007/s10555-011-9310-3.
12. Palacios-Pelaez R, Lukiw WJ, Bazan NG (2010) Omega-3 essential fatty acids modulate initiation and progression of neurodegenerative disease. *Mol Neurobiol*, 41(2-3), 367-374; doi: 10.1007/s12035-010-8139-z.
13. Funk CD, Chen XS, Johnson EN, Zhao L (2002) Lipoxygenase genes and their targeted disruption. *Prostaglandins Other Lipid Mediat*, 68-69, 303-312; doi: 10.1016/s0090-6980(02)00036-9.
14. Kuhn H, Belkner J, Wiesner R, Brash AR (1990) Oxygenation of biological membranes by the pure reticulocyte lipoxygenase. *J Biol Chem*, 265(30), 18351-18361.
15. Belkner J, Stender H, Kuhn H (1998) The rabbit 15-lipoxygenase preferentially oxygenates LDL cholesterol esters, and this reaction does not require vitamin E. *J Biol Chem*, 273(36), 23225-23232; doi: 10.1074/jbc.273.36.23225.
16. Bryant RW, Bailey JM, Schewe T, Rapoport SM (1982) Positional specificity of a reticulocyte lipoxygenase. Conversion of arachidonic acid to 15-S-hydroperoxy-eicosatetraenoic acid. *J Biol Chem*, 257(11), 6050-6055.
17. Kuhn H, Barnett J, Grunberger D, Baecker P, Chow J, Nguyen B, Bursztyn-Pettegrew H, Chan H, Sigal E (1993) Overexpression, purification and characterization of human

recombinant 15-lipoxygenase. *Biochim Biophys Acta*, 1169(1), 80-89; doi: 10.1016/0005-2760(93)90085-n.

18. Adel S, Karst F, Gonzalez-Lafont A, Pekarova M, Saura P, Masgrau L, Lluch JM, Stehling S, Horn T, Kuhn H, Heydeck D (2016) Evolutionary alteration of ALOX15 specificity optimizes the biosynthesis of antiinflammatory and proresolving lipoxins. *Proc Natl Acad Sci U S A*, 113(30), E4266-4275; doi: 10.1073/pnas.1604029113.
19. Machado FS, Aliberti J (2008) Role of lipoxin in the modulation of immune response during infection. *Int Immunopharmacol*, 8(10), 1316-1319; doi: 10.1016/j.intimp.2008.01.001.
20. Lehmann C, Homann J, Ball AK, Blocher R, Kleinschmidt TK, Basavarajappa D, Angioni C, Ferreiros N, Hafner AK, Radmark O, Proschak E, Haeggstrom JZ, Geisslinger G, Parnham MJ, Steinhilber D, Kahnt AS (2015) Lipoxin and resolvin biosynthesis is dependent on 5-lipoxygenase activating protein. *Faseb J*, 29(12), 5029-5043; doi: 10.1096/fj.15-275487.
21. Gyurko R, Van Dyke TE (2014) The role of polyunsaturated omega-3 fatty acid eicosapentaenoic acid-derived resolvin E1 (RvE1) in bone preservation. *Crit Rev Immunol*, 34(4), 347-357; doi: 10.1615/critrevimmunol.2014009982.
22. Serhan CN, Dalli J, Colas RA, Winkler JW, Chiang N (2015) Protectins and maresins: New pro-resolving families of mediators in acute inflammation and resolution bioactive metabolome. *Biochim Biophys Acta*, 1851(4), 397-413; doi: 10.1016/j.bbalip.2014.08.006.
23. Ostermann AI, Willenberg I, Schebb NH (2015) Comparison of sample preparation methods for the quantitative analysis of eicosanoids and other oxylipins in plasma by means of LC-MS/MS. *Anal Bioanal Chem*, 407(5), 1403-1414; doi: 10.1007/s00216-014-8377-4.
24. Willenberg I, Meschede AK, Gueler F, Jang MS, Shushakova N, Schebb NH (2015) Food polyphenols fail to cause a biologically relevant reduction of COX-2 activity. *PLoS One*, 10(10), e0139147; doi: 10.1371/journal.pone.0139147.
25. Chen XS, Brash AR, Funk CD (1993) Purification and characterization of recombinant histidine-tagged human platelet 12-lipoxygenase expressed in a baculovirus/insect cell system. *Eur J Biochem*, 214(3), 845-852; doi: 10.1111/j.1432-1033.1993.tb17988.x.
26. Chen XS, Kurre U, Jenkins NA, Copeland NG, Funk CD (1994) cDNA cloning, expression, mutagenesis of C-terminal isoleucine, genomic structure, and chromosomal localizations of murine 12-lipoxygenases. *J Biol Chem*, 269(19), 13979-13987.
27. Hodson L, Skeaff CM, Fielding BA (2008) Fatty acid composition of adipose tissue and blood in humans and its use as a biomarker of dietary intake. *Prog Lipid Res*, 47(5), 348-380; doi: 10.1016/j.plipres.2008.03.003.
28. Manzoni Jacintho T, Gotho H, Gidlund M, Garcia Marques C, Torrinhas R, Mirtes Sales M, Linetzky Waitzberg D (2009) Anti-inflammatory effect of parenteral fish oil lipid emulsion on human activated mononuclear leukocytes. *Nutr Hosp*, 24(3), 288-296.
29. Sanak M (2016) Eicosanoid mediators in the airway inflammation of asthmatic patients: What is new? *Allergy Asthma Immunol Res*, 8(6), 481-490; doi: 10.4168/aair.2016.8.6.481.
30. Serhan CN, Petasis NA (2011) Resolvins and protectins in inflammation resolution. *Chem Rev*, 111(10), 5922-5943; doi: 10.1021/cr100396c.
31. Dalli J, Colas RA, Serhan CN (2013) Novel n-3 immunoresolvents: structures and actions. *Sci Rep*, 3, 1940; doi: 10.1038/srep01940.
32. Kuhn H (1996) Biosynthesis, metabolization and biological importance of the primary 15-lipoxygenase metabolites 15-hydro(pero)XY-5Z,8Z,11Z,13E-eicosatetraenoic acid

and 13-hydro(pero)XY-9Z,11E-octadecadienoic acid. *Prog Lipid Res*, 35(3), 203-226; doi: 10.1016/s0163-7827(96)00008-2.

33. Kuhn H, Banthiya S, van Leyen K (2015) Mammalian lipoxygenases and their biological relevance. *Biochim Biophys Acta*, 1851(4), 308-330; doi: 10.1016/j.bbalip.2014.10.002.
34. Kuhn H, O'Donnell VB (2006) Inflammation and immune regulation by 12/15-lipoxygenases. *Prog Lipid Res*, 45(4), 334-356; doi: 10.1016/j.plipres.2006.02.003.
35. Reddy RG, Yoshimoto T, Yamamoto S, Funk CD, Marnett LJ (1994) Expression of porcine leukocyte 12-lipoxygenase in a baculovirus/insect cell system and its characterization. *Arch Biochem Biophys*, 312(1), 219-226; doi: 10.1006/abbi.1994.1302.
36. Kuhn H, Sprecher H, Brash AR (1990) On singular or dual positional specificity of lipoxygenases. The number of chiral products varies with alignment of methylene groups at the active site of the enzyme. *J Biol Chem*, 265(27), 16300-16305.
37. Conrad DJ, Kuhn H, Mulkins M, Highland E, Sigal E (1992) Specific inflammatory cytokines regulate the expression of human monocyte 15-lipoxygenase. *Proc Natl Acad Sci U S A*, 89(1), 217-221; doi: 10.1073/pnas.89.1.217.
38. Wuest SJ, Crucet M, Gemperle C, Loretz C, Hersberger M (2012) Expression and regulation of 12/15-lipoxygenases in human primary macrophages. *Atherosclerosis*, 225(1), 121-127; doi: 10.1016/j.atherosclerosis.2012.07.022.
39. Dennis EA, Cao J, Hsu YH, Magrioti V, Kokotos G (2011) Phospholipase A2 enzymes: physical structure, biological function, disease implication, chemical inhibition, and therapeutic intervention. *Chem Rev*, 111(10), 6130-6185; doi: 10.1021/cr200085w.
40. Adlercreutz P (2013) Immobilisation and application of lipases in organic media. *Chem Soc Rev*, 42(15), 6406-6436; doi: 10.1039/c3cs35446f.
41. Schewe T, Rapoport SM, Kuhn H (1986) Enzymology and physiology of reticulocyte lipoxygenase: comparison with other lipoxygenases. *Adv Enzymol Relat Areas Mol Biol*, 58, 191-272; doi: 10.1002/9780470123041.ch6.
42. Takahashi Y, Ueda N, Yamamoto S (1988) Two immunologically and catalytically distinct arachidonate 12-lipoxygenases of bovine platelets and leukocytes. *Arch Biochem Biophys*, 266(2), 613-621; doi: 10.1016/0003-9861(88)90294-9.
43. Brash AR, Boeglin WE, Chang MS (1997) Discovery of a second 15S-lipoxygenase in humans. *Proc Natl Acad Sci U S A*, 94(12), 6148-6152; doi: 10.1073/pnas.94.12.6148.
44. Shappell SB, Boeglin WE, Olson SJ, Kasper S, Brash AR (1999) 15-lipoxygenase-2 (15-LOX-2) is expressed in benign prostatic epithelium and reduced in prostate adenocarcinoma. *Am J Pathol*, 155(1), 235-245; doi: 10.1016/S0002-9440(10)65117-6.
45. Abbott SK, Else PL, Atkins TA, Hulbert AJ (2012) Fatty acid composition of membrane bilayers: importance of diet polyunsaturated fat balance. *Biochim Biophys Acta*, 1818(5), 1309-1317; doi: 10.1016/j.bbamem.2012.01.011.
46. Slater-Jefferies JL, Hoile SP, Lillycrop KA, Townsend PA, Hanson MA, Burdge GC (2010) Effect of sex and dietary fat intake on the fatty acid composition of phospholipids and triacylglycerol in rat heart. *Prostaglandins Leukot Essent Fatty Acids*, 83(4-6), 219-223; doi: 10.1016/j.plefa.2010.07.006.
47. Delion S, Chalon S, Guilloteau D, Lejeune B, Besnard JC, Durand G (1997) Age-related changes in phospholipid fatty acid composition and monoaminergic neurotransmission in the hippocampus of rats fed a balanced or an n-3 polyunsaturated fatty acid-deficient diet. *J Lipid Res*, 38(4), 680-689.
48. Schuchardt JP, Schneider I, Willenberg I, Yang J, Hammock BD, Hahn A, Schebb NH (2014) Increase of EPA-derived hydroxy, epoxy and dihydroxy fatty acid levels in human plasma after a single dose of long-chain omega-3 PUFA. *Prostaglandins Other Lipid Mediat*, 109-111, 23-31; doi: 10.1016/j.prostaglandins.2014.03.001.

49. Schuchardt JP, Ostermann AI, Stork L, Kutzner L, Kohrs H, Greupner T, Hahn A, Schebb NH (2016) Effects of docosahexaenoic acid supplementation on PUFA levels in red blood cells and plasma. *Prostaglandins Leukot Essent Fatty Acids*, 115, 12-23; doi: 10.1016/j.plefa.2016.10.005.

Chapter 4

Development of an optimized LC-MS method for the detection of specialized pro-resolving mediators in biological samples

The cardioprotective and anti-inflammatory effects of long-chain omega-3 polyunsaturated fatty acids (n3-PUFA) are believed to be partly mediated by their oxygenated metabolites (oxylipins). In the last two decades, interest in a novel group of autacoids termed specialized pro-resolving mediators (SPMs) increased. These are actively involved in the resolution of inflammation. SPMs are multiple hydroxylated fatty acids including resolvins, maresins and protectins derived from the n3-PUFA eicosapentaenoic acid (EPA) and docosahexaenoic acid (DHA) as well as lipoxins derived from arachidonic acid (ARA). In the present paper, we developed an LC-MS/MS method for a comprehensive set of 18 SPMs derived from ARA, EPA and DHA and integrated it into our targeted metabolomics platform. Quantification was based on external calibration utilizing five deuterated internal standards in combination with a second internal standard for quality assessment of sample preparation in each sample. The tandem mass spectrometric parameters were carefully optimized for sensitive and specific detection. The influence of source parameters of the used AB Sciex 6500 QTRAP instrument as well as electronic parameters and the selection of transitions are discussed. The method was validated/characterized based on the criteria listed in the European Medicines Agency (EMA) guideline on bioanalytical method validation and method performance is demonstrated regarding recovery of internal standards (between 78 ± 4% and 87 ± 3% from 500 µL of human serum) as well as extraction efficacy of SPMs in spiked plasma (intra-day accuracy within ± 20% and ± 15% at 0.1 nM and 0.3 nM in plasma, respectively). Based on the lower limits of quantification of 0.02–0.2 nM, corresponding to 0.44–3.6 pg on column, SPMs were generally not detectable/quantifiable in plasma and serum supporting that circulating levels of SPMs are very low, i.e. < 0.1 nM in healthy subjects. Following septic shock or peritonitis, SPMs could be quantified in the samples of several patients. However, in these studies with a small number of patients no clear correlation with severity of inflammation could be observed.

Adapted from *Frontiers in Pharmacology*, 10, Kutzner L, Rund KM, Ostermann AI, Hartung NM, Galano JM, Balas L, Durand T, Balzer MS, David S, Schebb NH, Development of an optimized LC-MS method for the detection of specialized pro-resolving mediators in biological samples, 169, doi: 10.3389/fphar.2019.00169 – Published by Frontiers.

Author contributions: LK designed research, performed experiments and wrote the manuscript; KMR, AIO, NMH performed experiments; JMG, LB, TD synthesized standard compounds; MSB, SD designed clinical study and provided clinical samples; NHS designed research and wrote the manuscript.

4.1 Introduction

Inflammation is a defensive mechanism of the organism to respond to invading microorganisms or tissue injury. In an attempt to destroy pathogens and restore normal tissue function, inflammatory mediators, such as vasoactive amines and peptides, cytokines, chemokines and lipid mediators are produced [1]. For example, lipid mediators derived from arachidonic acid (ARA), e.g. prostaglandin E_2 (PGE_2) and leukotriene B_4 (LTB_4) are released that act vasodilative [2] and trigger the recruitment of neutrophils to the site of inflammation [3]. This process results in a state of acute inflammation, which ideally leads to the elimination of the infectious agent and is self-limited [4]. In the past decades it was shown that the resolution of inflammation is an active process based on the production of pro-resolving mediators that inhibit neutrophil influx and stimulate monocytes and macrophages in order to remove apoptotic neutrophils and cell debris [1, 5].

Host defense and inflammation may be harmful to the organism if it fails to resolve the inflammation and return to homeostasis, and the resulting chronic inflammation is a leading cause of diseases [5, 6]. Resolution of inflammation is introduced by a lipid mediator class switching characterized by a shift from the predominantly pro-inflammatory mediators such as leukotrienes that amplify acute inflammation to the mostly anti-inflammatory pro-resolving lipoxins (LX) [7]. Moreover, multiple hydroxylated fatty acids derived from the long-chain omega-3 polyunsaturated fatty acids (n3-PUFA) eicosapenatenoic acid (EPA) and docosahexaenoic acid (DHA) including resolvins (E- and D-series Rv), protectins and maresins (MaR) have been described that exert inflammation resolving properties (Fig. 4.1–4.2) [8, 9]. These classes of bioactive molecules are enzymatically formed involving lipoxygenase (LOX), cyclooxygenase (COX) and may include cytochrome P450 (CYP) pathways and were termed specialized pro-resolving mediators (SPMs). As SPM production requires several conversion steps by enzymes, which may not be expressed in a single cell type, it thus requires the interplay of different cell types during the resolution of inflammation [10]. The anti-inflammatory activity of SPMs was demonstrated in *in vitro* and *in*

vivo models of different inflammatory diseases and the widely appreciated health benefits associated with the intake of long-chain n3-PUFA might partly be based on the enhanced production of SPMs [6]. For the formation of SPMs the time course has to be considered, as highest levels of SPMs are not observed during the initiation of inflammation but in the resolution phase [5, 11].

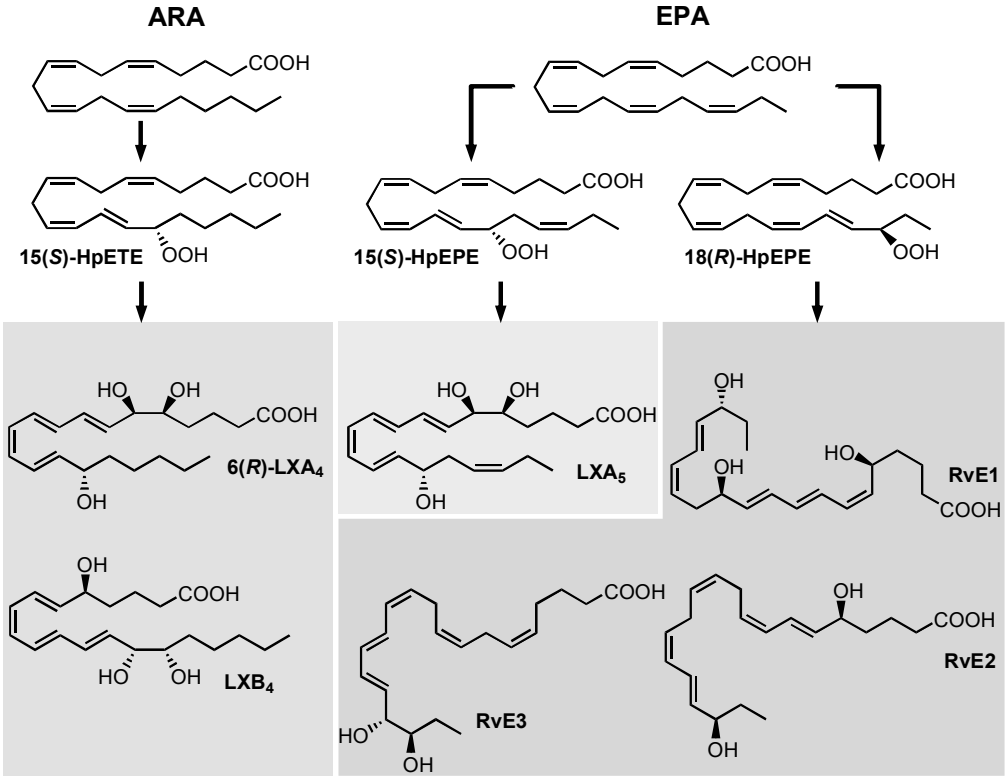

Fig. 4.1: Simplified overview of structures and formation routes of SPMs including ARA-derived 4-series lipoxins as well as EPA-derived 5-series lipoxin and E-series resolvins.

Among the firstly recognized lipid mediators involved in the resolution of inflammation are ARA derived trihydroxy eicosatetraenoic acids that are formed in sequential lipoxygenations catalyzed by different LOX enzymes during cell-cell interactions and therefore referred to as lipoxins (LX) [12, 13]. Different routes of LX biosynthesis have been described: A double lipoxygenation of ARA catalyzed by 15-LOX and leukocyte 5-LOX leads to the formation of an epoxy-intermediate, which is enzymatically hydrolyzed to form both, 5(*S*),6(*R*),15(*S*)-trihydroxy eicosatetraenoic acid (6(*R*)-LXA_4) or 5(*S*),14(*R*),15(*S*)-trihydroxy eicosatetraenoic acid (LXB_4) (Fig. 4.1) [12]. The other route of formation involves

the 5-LOX initiated synthesis of LTA_4 in human neutrophils and its subsequent lipoxygenation by platelet-type 12-LOX during neutrophil-platelet interactions [12]. While LOX catalyzed LX formation leads to 15(*S*)-LX, 15(*R*)-LX are formed by aspirin acetylated COX-2 [12, 14]. Resolvins (Rv) are formed during the resolution phase of acute inflammation partly by cell-cell interactions from the n3-PUFA EPA and DHA and are therefore categorized into E-series and D-series Rv, respectively [15]. E-series Rv are formed from 18(*R*)-hydro(pero)xy eicosapentaenoic acid (18(*R*)-H(p)EPE), a hydroxylation product of EPA (Fig. 4.1). The route of formation of 18(*R*)-H(p)ETE is unclear and it may be catalyzed by acetylated COX-2 in the presence of aspirin [16], by microbial CYP [17] or autoxidation [18]. Subsequent 5-lipoxygenation of 18(*R*)-H(p)EPE leads to the formation of both, 5(*S*),12(*R*),18(*R*)-trihydroxy eicosapentaenoic acid (RvE1) via enzymatic hydrolysis of an epoxide-containing intermediate or to 5(*S*),18(*R*)-dihydroxy eicosapentaenoic acid (RvE2) [5, 19]. However, also the formation of 18(*S*)-H(p)EPE by acetylated COX-2 and subsequent conversion to 18(*S*)-RvE1 and 18(*S*)-RvE2 was observed [20]. Another pathway involves the action of 12/15-LOX on 18(*R*)- or 18(*S*)-H(p)EPE, leading to the formation of pro-resolving 17(*R*),18(*R*)-dihydroxy eicosapenatenoic acid (18(*R*)-RvE3) and 17(*R*),18(*S*)-dihydroxy eicosapenatenoic acid (18(*S*)-RvE3), respectively [21, 22].

D-series Rv are formed in two iterative lipoxygenation steps (Fig. 4.2): 17(*S*)-hydro(pero)xy-docosahexaenoic acid (17(*S*)-H(p)DHA) is formed by 15-lipoxygenation from DHA and serves as substrate for 5-LOX in a second lipoxygenation step at the C-7 or C-4. Thereby, dihydroxylated RvD5 and trihydroxylated RvD1 and RvD2 are formed (C-7) as well as dihydroxylated RvD6 and trihydroxylated RvD3 and RvD4 (C-4) [5, 15]. A second class of pro-resolving mediators derived from DHA are dihydroxylated (neuro)protectins ((N)PD), e.g. 10(*R*),17(*S*)-dihydroxy docosahexaenoic acid ((N)PD1) formed from 17(*S*)-H(p)DHA via an epoxide intermediate and subsequent enzymatic hydrolysis [15, 23, 24]. The 12-lipoxygenation product 14(*S*)-H(p)DHA serves as precursor for a third class of DHA derived SPMs that are synthesized by

macrophages and involved in resolution of inflammation and therefore termed maresins (MaR) [25]. The proposed formation scheme includes – similar to (N)PD1 – a single lipoxygenation step and formation of 7(*R*),14(*S*)-dihydroxy docosahexaenoic acid (MaR1) via an epoxide containing intermediate [25].

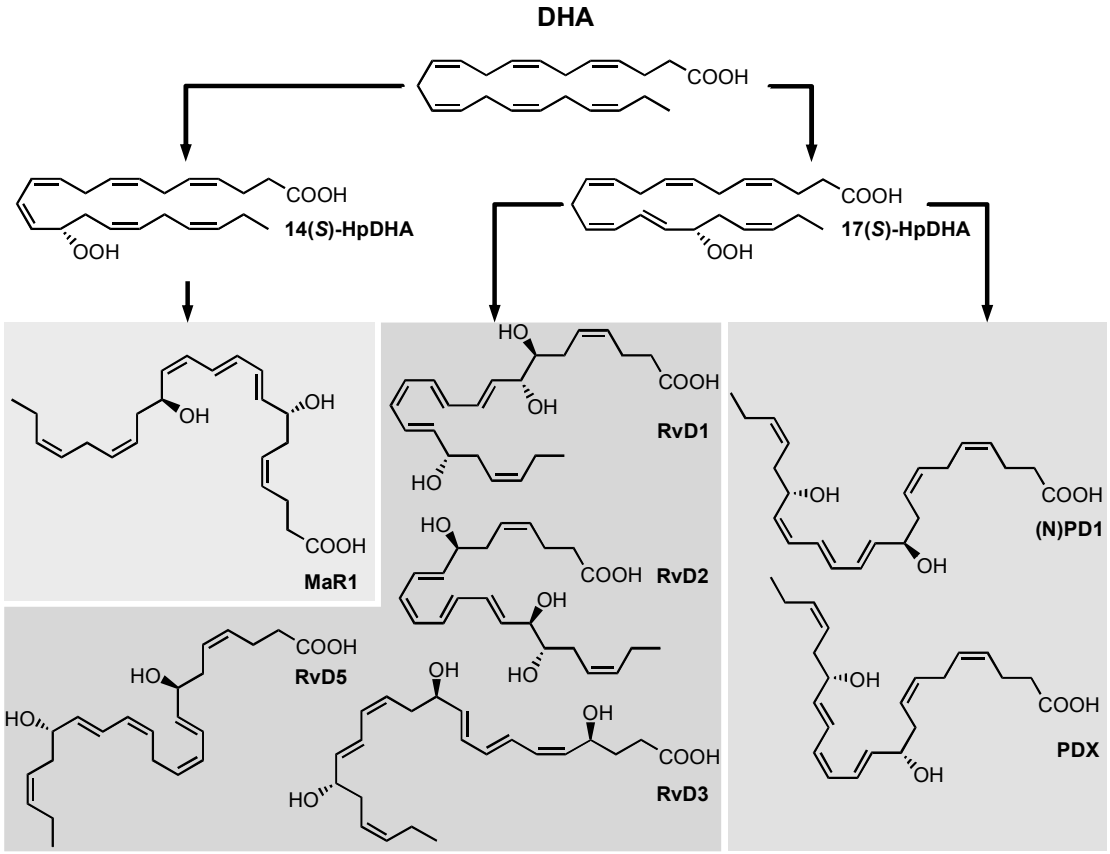

Fig. 4.2: Simplified overview of structures and formation routes of SPMs including DHA-derived maresins, D-series resolvins and protectins.

Because SPM formation involves multiple enzymatic transformations and likely cell-cell interactions, concentrations of SPMs compared to their mono-hydroxylated precursors are low [26] and bioactivity of these potent mediators is reported for the picomolar to lower nanomolar range [27]. Hence, analysis of SPMs requires powerful selective and sensitive methodologies. Methodological approaches used for SPM detection include gas chromatography, which was applied e.g. for the characterization of LX [28]. Enzyme linked immunoassays can be used for the detection of single compounds [29, 30], though their specificity might be limited with respect to a large number of possible regio- and

stereoisomers formed. Nowadays, methods used for identification and quantification of SPMs and other oxylipins are mostly based on reversed phase liquid chromatography (RP-LC) [26, 31-35], chiral LC [20, 36, 37] or both [38, 39] hyphenated via electrospray ionization (ESI) to tandem mass spectrometric (MS/MS) detection. However, despite application of state-of-the-art LC-MS/MS based methodology, SPM detection in biological samples remains challenging. For example, results regarding the detection of SPMs in plasma from healthy individuals and correlation between n3-PUFA supplementation and plasma SPM levels are conflicting and the presence of SPMs in this matrix has been questioned [40]. Whereas the biosynthesis of SPMs in healthy individuals might be limited, increased SPM formation is expected in inflammatory diseases or in response to inflammatory stimuli. However, this could not be supported by Skarke *et al.* (2015) and no alteration of plasma SPM levels in response to bacterial lipopolysaccharide (LPS) during the inflammatory or resolution phase could be observed in healthy individuals [34]. In contrast, SPMs were detected in plasma from patients suffering severe sepsis at levels from ~1–500 pM [41]. Overall, it remains to be elucidated whether SPMs circulate in blood of healthy individuals and which endogenously formed SPMs are relevant in inflammation [34, 40].

In order to enable these studies, the most sensitive and accurate quantification in biological samples is required. Therefore, in the present paper we developed an LC-MS/MS method using one of the most sensitive MS instruments commercially available. A focus was set on the optimization of instrumental parameters, internal standard (IS) recovery, precision and accuracy for a comprehensive set of ARA, EPA and DHA derived SPMs. Our LC-MS/MS method allows the simultaneous quantification of SPMs with other enzymatically and autoxidatively formed oxylipins. Method validation was performed oriented at the guideline by the European Medicines Agency (EMA) on bioanalytical method validation. Finally, the method was applied on clinically relevant human samples from patients with and without septic shock or peritonitis.

4.2 Experimental

4.2.1 Chemicals

Authentic standard substances of SPMs were purchased from Cayman Chemicals (local distributor: Biomol, Hamburg, Germany), i.e. resolvins (Rv) RvE1, RvD1, 17(*R*)-RvD1, RvD2, RvD3, RvD5, maresins (MaR) MaR1 and 7(*S*)-MaR1, protectin PDX as well as lipoxins (LX) LXA_5, 6(*R*)-LXA_4, 15(*R*)-LXA_4, 6(*S*)-LXA_4 and LXB_4 as well as deuterated IS including $^2H_5$-RvD1, $^2H_5$-RvD2, $^2H_5$-LXA_4, $^2H_4$-LTB_4 and $^2H_4$-9,10-DiHOME. Additionally, Rv 18(*R*)-RvE2, 18(*R*)-RvE3 and 18(*S*)-RvE3, which were a kind gift of the lab of Makoto Arita (RIKEN Center for Integrative Medical Sciences, Japan) were synthesized as described [21, 22, 42]. (Neuro)protectin (N)PD1 was synthesized as follows: The (N)PD1-methyl ester was synthesized for its C10-epimer as described [43] replacing the (*S*)-1,2,4-butanetriol by its (*R*)-enantiomer as starting material for the introduction of the *E,E*-iododiene. Methyl ester-(N)PD1 was than hydrolyzed with 1 M LiOH in MeOH/H_2O (1/1) followed by acidification with McIlvains buffer (pH 5) producing (N)PD1 as a colorless oil in 97% yield. Acetonitrile (ACN), LC-MS grade methanol (MeOH) and acetic acid were obtained from Fisher Scientific (Schwerte, Germany). HPLC grade *n*-hexane and disodium hydrogen phosphate dihydrate were purchased from Carl Roth (Karlsruhe, Germany). All other chemicals were purchased from Sigma Aldrich (Schnelldorf, Germany). Pure water was generated by a GenPure UF/UV Ultrapure water system from TKA Wasseraufbereitungssysteme GmbH (Niederelbert, Germany). For human plasma generation human whole blood was collected into EDTA monovettes (S-Monovette K3E, 02.1066.001, Sarstedt, Nümbrecht, Germany), centrifuged (15 min, 4 °C, 1200 × g) and plasma was pooled (five healthy volunteers, aged 25–38 years). For human serum generation human whole blood was collected into monovettes (S-Monovette with clotting activator, 02.10063, Sarstedt, Nümbrecht, Germany), incubated for 30 min at room temperature, centrifuged (10 min, 4 °C, 2500 × g) and serum was pooled (three healthy female subjects,

aged 26–27 years). Plasma and serum were immediately stored at –80 °C until analysis.

4.2.2 Mass spectrometric optimization

Mass spectrometric detection was performed on a 6500 QTRAP instrument (AB Sciex, Darmstadt, Germany) coupled to a 1290 Infinity LC System (Agilent, Waldbronn, Germany). Analyses were carried out in negative electrospray ionization (ESI(-)) mode. The influence of source parameters [electrode protrusion, probe x- and y-axis position, source temperature, nebulizer gas (GS1) and auxiliary (drying) gas (GS2)] was assessed in flow injection analysis (FIA) mode injecting 5 µL of a standard solution (100 nM) at a flow rate of 300 µL min^{-1} (ca. 50% Solvent B, see below). For the Ion Drive Turbo V source (AB Sciex, Darmstadt, Germany) the ESI probe can be arranged along the y-axis (0 to 13 mm, with 13 mm representing the closest position relative to the orifice) and optimization ranges were chosen from 0.0 to 5.0 mm in steps of 0.5 mm. Along the x-axis (0 to 10 mm, with 5 mm as center position relative to the orifice) the ESI probe was adjusted from 2.5 to 7.5 mm in steps of 0.5 mm. Additionally, the protrusion of the electrode was adjusted with typical values ranging from < 0.5 to approx. 2 mm. The source temperature was ranged between 300 and 550 °C (with constant GS2 of 60 psi), the pressure of the auxiliary (drying) gas (GS2) was ranged from 40 to 70 psi (with constant temperature 475 °C) and the nebulizer gas (GS1) between 30 and 70 psi.

For MS detection collision induced dissociation (CID) fragment ion spectra were monitored (100 nM standard solution) applying a CE range between –16 and –30 V depending on the substance. Two to three of the most intense and specific fragments were selected and individually optimized regarding the adjustment of electronic parameters including declustering potential (DP), collision energy (CE), collision cell exit potential (CXP) as well as collision activated dissociation (CAD) gas pressure. Optimization ranges for these parameters were chosen as follows: DP from –20 to –100 V in steps of 10 V, CE from –13 to –31 V (to –39 V for RvD2

m/z 175.0) in steps of 2 V and re-optimized in steps of 1 V, CXP from –4 to –18 V in steps of 2 V. Influence of CAD gas was assessed for representative compounds in low (6 psi), medium (9 psi) and high (15 psi) mode for different CEs.

4.2.3 LC-MS/MS method

Chromatographic separation was performed on a Zorbax Eclipse Plus C18 reversed phase column (2.1 × 150 mm, particle size 1.8 µm, pore size 9.5 nm; Agilent, Waldbronn, Germany) using a binary solvent gradient. Solvent A was 0.1% acetic acid mixed with 5% solvent B and solvent B was ACN/MeOH/acetic acid (800/150/1, *v/v/v*). The flow rate was set to 0.3 mL min^{-1} and the linear gradient was as follows: 21% B at 0 min, 21% B at 1.0 min, 26% B at 1.5 min, 51% B at 10 min, 66% B at 19 min, 98% B at 25.1 min, 98% B at 27.6 min, 21% B at 27.7 min and 21% B at 31.5 min. For MS detection the 6500 QTRAP mass spectrometer (AB Sciex, Darmstadt, Germany) was operated in negative electrospray ionization (ESI(-)) mode. Nitrogen was used as curtain gas and CAD gas (nitrogen generator IMT-PN1450 PAN, INMATEC, Herrsching, Germany). Zero air was used as nebulizer (GS1) and drying gas (GS2) generated with an air compressor (SL-S 5.5, Renner, Güglingen, Germany) and zero air generator (UHP-300-ZA-S-E, Parker, Kaarst, Germany). In the optimized method, the probe position was 0.250 cm along the vertical (y-) axis and 0.550 cm along the horizontal (x-) axis, electrode protrusion was 1–1.5 mm, the ion spray voltage was –4500 V, curtain gas (N_2) was kept at 35 psi, nebulizer gas (GS1) and drying gas (GS2) were adjusted to 60 psi each and source temperature was 475 °C. Detection was carried out in scheduled selected reaction monitoring (SRM) mode (detection window 90 s, cycle time 0.4 s) with the CAD gas set to 15 psi and individually optimized electronic parameters for each SPM (Tab. 4.1). Including the SPMs described here, the method covered the quantitative detection of 175 enzymatically and chemically formed oxylipins as described [44].

4.2.4 Method characterization

Method characterization and validation was carried out in terms of sensitivity, linearity, intraday precision and accuracy, oriented at the guideline of the European Medicine Agency (EMA) for bioanalytical method development [45]. Calibration standards covering a concentration range from LLOQ up to 500 nM (100 nM for RvE2, 18(*R*)- and 18(*S*)-RvE3) of SPMs were measured and linearity was assessed by plotting the peak area ratio (analyte/IS) against the analyte concentration (linear least square regression, weighting $1/x^2$). Accuracy was within ± 15% of the nominal concentration (except ± 20% for LLOQ). Intraday accuracy and precision were assessed in plasma spiked with a subset of SPMs at four different concentration levels (0.1, 0.3, 1 and 3 nM in plasma) and additionally in serum at one concentration level (3 nM in serum). SPMs were spiked into plasma/serum samples directly at the beginning of sample preparation and unspiked plasma and serum was prepared alongside. Accuracy was determined by comparison of the determined concentration to the concentration in the spiking standard solution. Precision was calculated as relative standard deviation (n = 4).

Extraction efficacy of the deuterated IS was determined by calculation of the recovery rates utilizing an IS 2 added at the end of sample preparation. For evaluation of ion suppression effects by the matrix, IS was spiked into serum at the beginning of sample preparation (pre SPE) and into the serum extract at the end of sample preparation (post SPE).

4.2.5 Sample preparation

SPMs were extracted from plasma or serum samples and effluents from peritoneal dialysis (PD) using solid phase extraction (SPE) [44]. In the first step a mixture of 20 deuterated IS (final concentration of 20 nM each, including $^2H_5$-RvD1, $^2H_5$-RvD2, $^2H_5$-LXA$_4$, $^2H_4$-LTB$_4$ and $^2H_4$-9,10-DiHOME), antioxidant mixture (0.2 mg/mL BHT, 100 µM indomethacin, 100 µM soluble epoxide

hydrolase inhibitor *trans*-4-[4-(3-adamantan-1-yl-ureido)-cyclohexyloxy]-benzoic acid (*t*-AUCB) in MeOH) were added to 500 µL of plasma/serum or 1200 µL of PD exudates. Then 1400 µL ice-cold MeOH (3360 µL for PD exudates) were added for protein precipitation (at least 30 min at –80 °C). Following centrifugation, the supernatant was evaporated under a gentle nitrogen stream to < 50% MeOH, diluted with 0.1 M disodium hydrogen phosphate buffer (pH 5.5) and loaded onto the preconditioned SPE column (Bond Elut Certify II, 200 mg, 3 mL; Agilent, Waldbronn, Germany). Oxylipins were eluted with ethyl acetate/*n*-hexane (75/25, *v/v*) containing 1% acetic acid. After evaporation to dryness in a vacuum concentrator (30 °C, 1 mbar, ca. 60 min; Christ, Osterode, Germany) sample extracts were reconstituted in 50 µL MeOH containing 40 nM 1-(1-(ethylsulfonyl)piperidin-4-yl)-3-(4-(trifluoromethoxy)phenyl)urea as IS 2. Injection volume was 5 µL; for samples with low SPM content a second (10 µL) injection was used for SPM quantification.

4.2.6 Clinical samples

Peritoneal dialysis patient samples

Serum and peritoneal dialysate effluent samples from peritoneal dialysis (PD) patients from the Hannover Medical School PD outpatient clinic were obtained after written informed consent according to the declaration of Helsinki, and local ethics board approval (MHH 2014/6617). Patients were treated exclusively with biocompatible PD fluids. Dialysate samples (1–2 L) with an intra-abdominal presence ≥ 2 h were drained via PD catheter from the abdomen of patients with peritonitis (n = 4–5) and from clinically stable control patients (n = 4–5), respectively, and immediately frozen at –80 °C until further analysis. After coagulation in the fridge, serum was centrifuged within 4 hours after sampling (10 min, 2300 × g) and frozen at –80 °C until further analysis. In accordance with the current International Society for Peritoneal Dialysis recommendations on prevention and treatment of PD-related peritonitis [46] a diagnosis of peritonitis was made when at least two of the following were present: 1) clinical features

consistent with peritonitis, i.e. abdominal pain and/or cloudy dialysis effluent; 2) dialysis effluent white cell count > 100/µL (after a dwell time of at least 2 h), with > 50% polymorphonuclear; and 3) positive dialysis effluent culture.

Septic shock patient samples

Plasma samples were obtained from patients with septic shock per SEPSIS-3 definition [47] at the Hannover Medical School ICU or healthy controls after written informed consent according to the declaration of Helsinki and approved by the Hannover Medical School ethical committee (2786-2015). Included were 18 patients with early septic shock (< 12 h) and high need for high doses of norepinephrine (> 0.4 µg/kg/min) that were neither pregnant, aged < 18 years nor had an end-stage chronic disease. All patients were part of the recently published EXCHANGE trial [48]. Blood was drawn within 12 h after diagnosis, plasma was centrifuged within < 6 h after sampling (10 min, 3500 × g) and frozen at –80 °C until further analysis.

4.3 Results and Discussion

In order to enable sensitive and selective detection of SPMs electronic MS parameter were carefully optimized for each compound and the impact of source parameters on sensitivity was thoroughly assessed.

4.3.1 Optimization of mass spectrometric detection

The influence of source parameters (probe position, source gases, source temperature) on sensitivity was assessed. Three SPMs, i.e. RvE1, RvD2 and RvD5 were chosen representing the structure of di- and trihydroxy fatty acids and a broad elution window and thus different compositions of the mobile phase during elution and evaporation with retention times of 6.19 min (RvE1, 40% solvent B), 9.52 min (RvD2, 50% solvent B) and 13.80 min (RvD5, 57% solvent B). The protrusion of the electrode was adjusted from < 0.5 mm to 2 mm and

showed only a little effect on the sensitivity of SPM detection (Fig. 4.3 A). Even though signal intensity was higher (ca. 10%) with small protrusion, the signal was more unstable and noisier compared to a higher protrusion. Therefore 1–1.5 mm was found to be optimal, consistent with the manufacturer's recommendation. Moving the ESI probe closer towards the orifice along the y-axis (from 0 to 5 mm), which is the closest recommended position for typical LC flow rates of 200–1000 µL min^{-1}, yielded a 36% higher signal for RvE1 (40% solvent B) and only 17% for the later eluting RvD5 (57% solvent B). The probe position along the y-axis was set to 2.5 mm resulting in 9–20% lower signal compared to the position at 5 mm (Fig. 4.3 B). However, during the analysis of biological specimen a position of the probe close to the orifice leads to a transfer of neutral compounds and thus a rapid contamination of the MS. Unexpectedly, moving the ESI probe farther right along the x-axis (5–7.5 mm) gave higher signal intensity of 7–10% compared to directly before the orifice (5 mm), whereas movement to the left side (5–2.5 mm) resulted in 17–27% lower signal intensity. Hence, an off-center x-position of the ESI probe of 5.5 mm was chosen (Fig. 4.3 C). Overall it can be concluded that the signal intensity can be further improved by maximal 15% (protrusion), 20% (y-axis) and 10% (x-axis) compared to the chosen values and has therefore only little influence on the performance of the MS for the detection of SPMs. This can be explained by the wide heating region and a large spray cone compared to a relatively small orifice in the ion source. Thus it can be concluded that using a medium value of the recommended ranges for the probe position seems to be sufficient as default position for the detection of SPMs and other oxylipins.

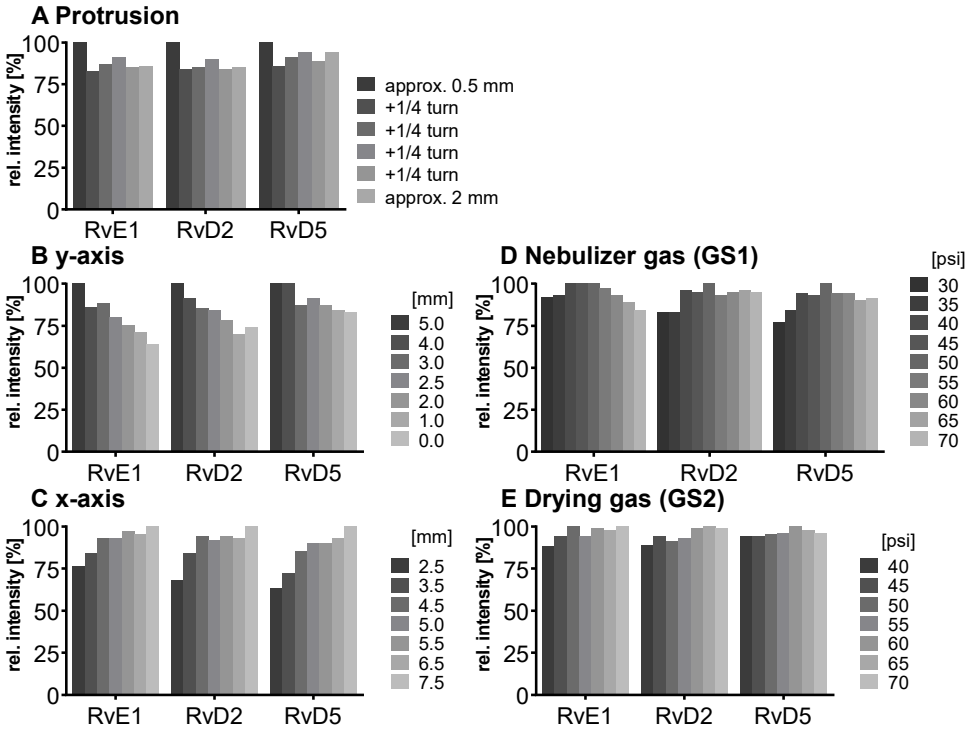

Fig. 4.3: Optimization of source parameters in SRM mode for compounds RvE1, RvD2 and RvD5. (**A**) Electrode protrusion was adjusted between approx. 0.5 mm and 2 mm, (**B**) probe position along the y-axis was optimized between 0 mm (farthest position relative to orifice) and 5 mm, (**C**) probe position along the x-axis was optimized between 2.5 mm and 7.5 mm (5 mm = center position relative to orifice), (**D**) nebulizer gas (GS1) was optimized between 30 psi and 70 psi, (**E**) auxiliary (heater) gas (GS2) was optimized between 40 psi and 70 psi at constant source temperature of 475 °C. Optimization was carried out in FIA mode with pure standards (100 nM).

In the next step, the influence on signal intensity of nebulizer gas (GS1) as well as auxiliary gas (GS2) from the two heated jets and its temperature was assessed. With optimized source gases a signal gain of 16–23% (GS1) and 6–12% (GS2) can be achieved (Fig. 4.3 D+E) and 60 psi was selected for both gases. The temperature was found to be a critical parameter and was optimized in a range from 300 to 550 °C. Higher GS2 temperature led to higher intensities for RvE1 and RvD2 (36% and 45% signal gain with 550 °C compared to 300 °C). In contrast, for later eluting RvD5 maximal intensity was observed at TEM 450 °C (Fig. 4.4 A) indicating a thermal degradation at higher temperatures. This is not only a solvent evaporation effect, because for PGE_2 (RT 8.99 min) a decreasing signal intensity was also found above 400 °C. Thus, the temperature has to be carefully optimized, since higher temperature improves desolvatization of stable compounds but is disadvantageous for thermo-labile compounds, particularly

those eluting with high percentage of organic solvent leading to higher thermal stress due to faster solvent evaporation. We selected a source temperature of 475 °C as compromise allowing the detection of all SPMs as well as other oxylipins. This is consistent with other methods using 400 to 580 °C for the detection of SPMs on the same instrument type [33, 49].

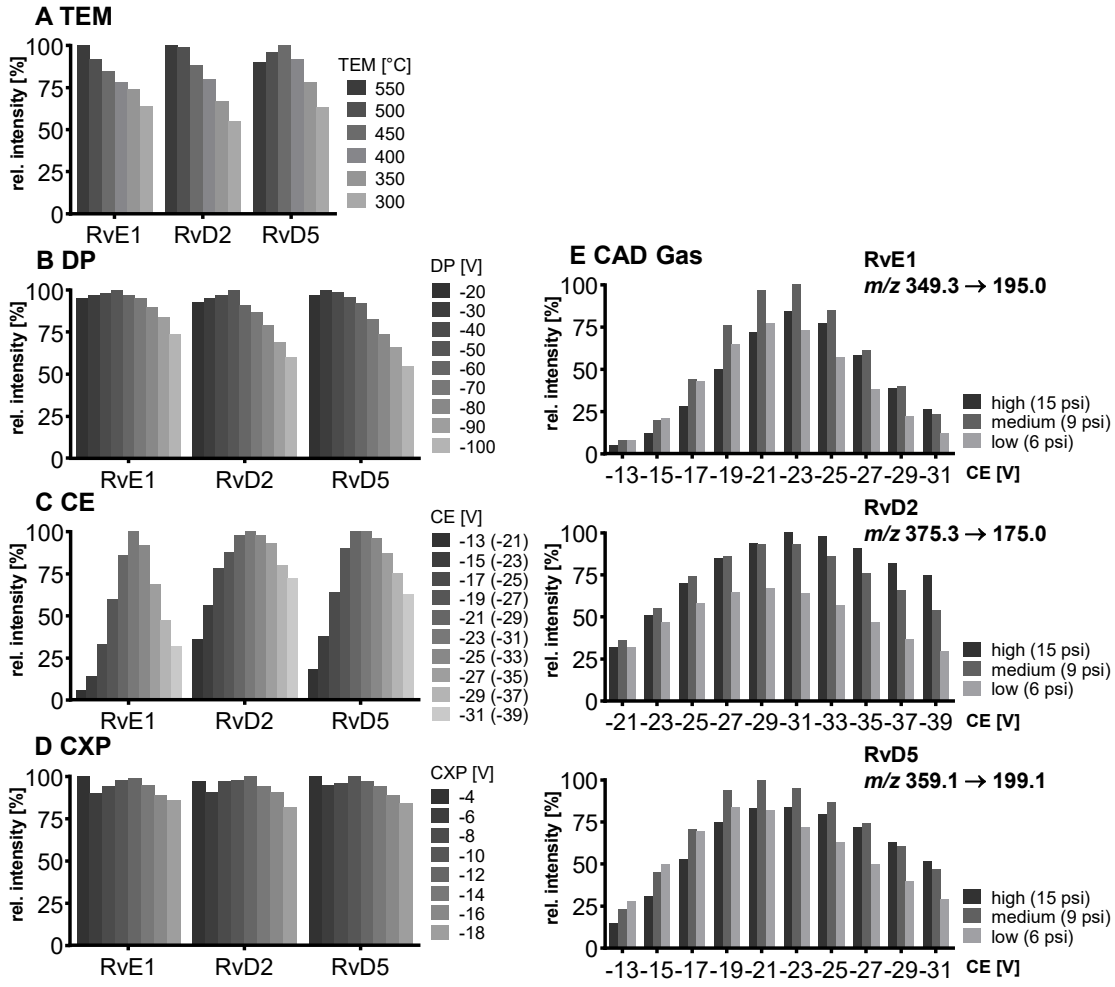

Fig. 4.4: Mass spectrometric optimization of electronic parameters as well as collision gas and source temperature in SRM mode for compounds RvE1, RvD2 and RvD5. Shown is the influence of parameters on signal intensity within a range around the optimum value. (**A**) Source temperature (TEM) between 300 °C and 550 °C, (**B**) declustering potential (DP) between –20 and –100 V (**C**) collision energy (CE) in steps of 2 V from –13 to –31 V for RvE1 (*m/z* 349.3 → 195.0) and RvD5 (*m/z* 359.1 → 199.1), CE from –21 to –39 V for RvD2 (*m/z* 375.3 → 175.0) with collision activated dissociation (CAD) gas set to high (15 psi), (**D**) collision cell exit potential (CXP) in steps of 2 V from –4 to –18 V, (**E**) collision energy (CE) in steps of 2 V from –13 to –31 V for RvE1 (*m/z* 349.3 → 195.0) and RvD5 (*m/z* 359.1 → 199.1), CE from –21 to –39 for RvD2 (*m/z* 375.3 → 175.0) with collision activated dissociation (CAD) gas set to high (15 psi), medium (9 psi) and low (6 psi).

Careful optimization of the electronic parameters declustering potential (DP), collision energy (CE) and collision cell exit potential (CXP) was carried out for each individual compound and the influence of the collision activated dissociation (CAD) gas pressure was determined: For DP the impact on signal intensity was minimal (< 10%) within a range of –20 to –60 V, while higher DP led to a declining signal (Fig. 4.4 B). The DP (similar to the potential termed nozzle-skimmer voltage, cone voltage in instruments from other companies) which is applied to the orifice plate allows the dissociation of ion clusters. High DP leads to in-source fragmentation due to collision with gas molecules taking place at the relatively low vacuum in the transfer region [50]. Because of the large orifice of the instrument, which is a major difference compared to older models of the type of instrument, only little influence on the signal results for oxylipins within a DP between –40 and –60 V. Therefore, a standard DP of –60 V could be selected for all oxylipins, even though we used the optimal parameters for the SPMs (Tab. 4.1).

As expected, CE led to massive differences in signal intensities of 64–94% from highest to lowest within the tested range (–13 to –31 V; –21 to –39 V for RvD2) emphasizing the significant impact of CE on occurrence and extent of collision induced fragmentation (CID) and thus sensitivity in SRM mode (Fig. 4.4 C). Fine tuning was performed for each of the CEs in steps of 1 V and variation of CEs ± 1 V around the optimum caused a signal decline of maximal 5% indicating that – though a critical parameter – CE optimization in smaller steps than 2 V is not required for our instrument. For most SPMs CEs from –19 to –23 V were optimal for all fragments, in some cases such as for RvD2 (*m/z* 375.3 → 175.0) higher CEs (–25 to –31 V) were required to provide sufficient energy for fragmentation in order to ensure sensitive detection. For different adjustments of CAD gas pressure the trend of CEs and optimal CE were mostly similar (high, 15 psi; medium, 9 psi; low, 6 psi). CAD gas set to “low” gave overall lowest intensities at optimal CE, while highest intensities were observed for CAD gas set to “medium” or “high” depending on the fragment ion (Fig. 4.4 E). This may be caused by increasing probability for ions to undergo CID with higher CAD gas pressure [51].

On the other hand, higher potential at lower gas pressure might lead to more intense collisions because of higher kinetic energy of the ions. Optimal CAD gas pressure gives 16–33% higher signal intensities compared to the lowest pressure. In our method, CAD gas is set to high resulting in lower intensities for e.g. RvE1 (*m/z* 349.3 → 195.0) or RvD5 (*m/z* 359.1 → 199.1) and better sensitivity for RvD2 (*m/z* 375.3 → 175.0). Optimal collision cell exit potential (CXP) was between –8 and –14 V for all compounds and ± 2 V around the optimum caused a signal decline of maximal 6% (Fig. 4.4 D). Therefore, despite an optimal CXP was chosen, a standard default value of –10 V seems to be suitable for SPMs and other oxylipins.

For each compound two or three specific transitions were chosen, as exemplarily shown in Fig. 4.5 A–D, to ensure both selective and sensitive detection and thus quantification alongside with identification of SPMs in biological sample material. For most of the compounds the mass transition with highest sensitivity, i.e. best signal-to-noise ratio was selected as primary transition, whereas alternative transitions were comparable (e.g. RvD2, PDX) or less sensitive (e.g. RvD3, 6(*R*)-LXA$_4$) (Tab. 4.1). For method characterization, quantification was carried out on all transitions and concentrations determined with different transitions were compared e.g. in order to evaluate matrix interferences and support compound identity. For all compounds α-cleavage ions referring to a cleavage of the carbon chain in α-position of the hydroxy group with a double bond in β- or γ-position (α-hydroxy-β/γ-ene fragmentation mechanism) with or without an additional loss of H_2O/CO_2 were used for quantification. Their formation has been described for SPMs and other oxylipins earlier [52-54]. For example, the most sensitive transition selected for RvE1 (*m/z* 349.3 → 195.0) is based on α-hydroxy-β-ene rearrangement, the alternative transitions (*m/z* 349.3 → 205.0, *m/z* 349.3 → 161.0) are formed in an α-hydroxy-γ-ene rearrangement with elimination of H_2O (*m/z* 205.0) and of H_2O/CO_2 (*m/z* 161.0) (Fig. 4.5 B) [54]. For RvD2 the most sensitive fragment (*m/z* 375.3 → 175.0) is unlikely to be formed by an α-cleavage and may be formed by a γ-cleavage towards the hydroxy group or another mechanism (Fig. 4.5 C). However, as this fragment is the most

sensitive with our instrument and is also used by other groups for RvD2 [36, 37, 55], it was chosen as primary transition. These backbone fragments ("chain-cut ions" [52]) are specific allowing to discriminate between regioisomers, whereas fragments referred to as "peripheral-cut ions" [52] that result from the unspecific loss of water (hydroxy group) and/or carbon dioxide (carboxylic group) are not selective and do not allow to draw conclusions on the position of the hydroxy groups being essential for the selective detection of e.g. RvD5, PD1 and MaR1 (DHA-derived dihydroxy-FA, Q1 mass: *m/z* 359.1) and other isobaric enzymatic or autoxidation products which could be formed from PUFA. Similar fragments were observed for the other SPMs and specific transitions chosen are consistent with literature [26, 32-36, 38, 49, 56]. Overall, the selection of appropriate transitions is a crucial step for the detection of SPMs and other oxylipins. Due to multiple hydroxy groups most SPMs give rise to intense ions originating from a cleavage within the molecular backbone allowing specific detection.

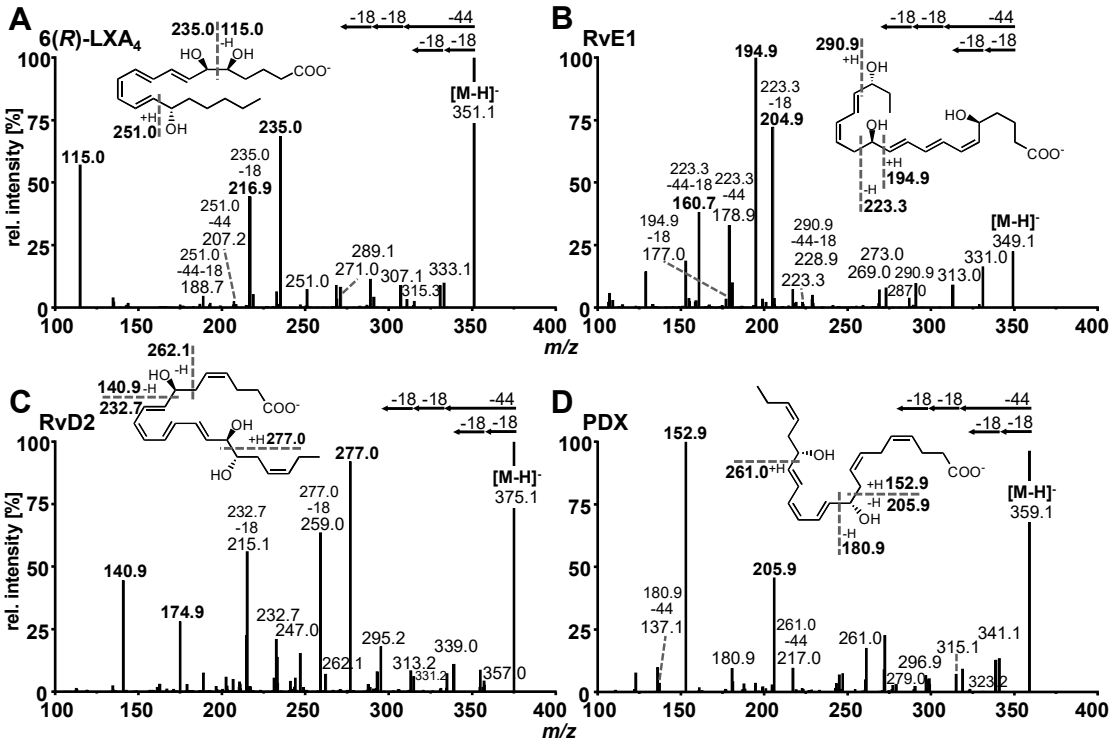

Fig. 4.5: Collision induced dissociation (CID) product ion spectra of representative SPMs comprising (**A**) ARA derived lipoxin 5(*S*),6(*R*),15(*S*)-LXA$_4$, (**B**) EPA derived E-series resolvin RvE1, (**C**) DHA derived D-series resolvin RvD2, (**D**) DHA derived protectin PDX. The dashed lines in the structures depict suggested sites of fragmentation leading to specific transitions.

4.3.2 Chromatographic separation

The chromatographic separation was carried out on a state-of-the-art C18 reversed phase column filled with sub-2 µm particles and optimized gradient. In addition to the optimized detection described here the chromatographic separation enables the simultaneous analysis of 175 enzymatically and autoxidatively formed lipid mediators within 31.5 min [44]. The method covers a total of 18 SPMs that elute in the first part of the chromatogram within 10 min and allows the chromatographic resolution of most of the SPMs yielding narrow peaks with a peak width at half maximum (FWHM) of 3–4 s (Fig. 4.6, Tab. 4.1).

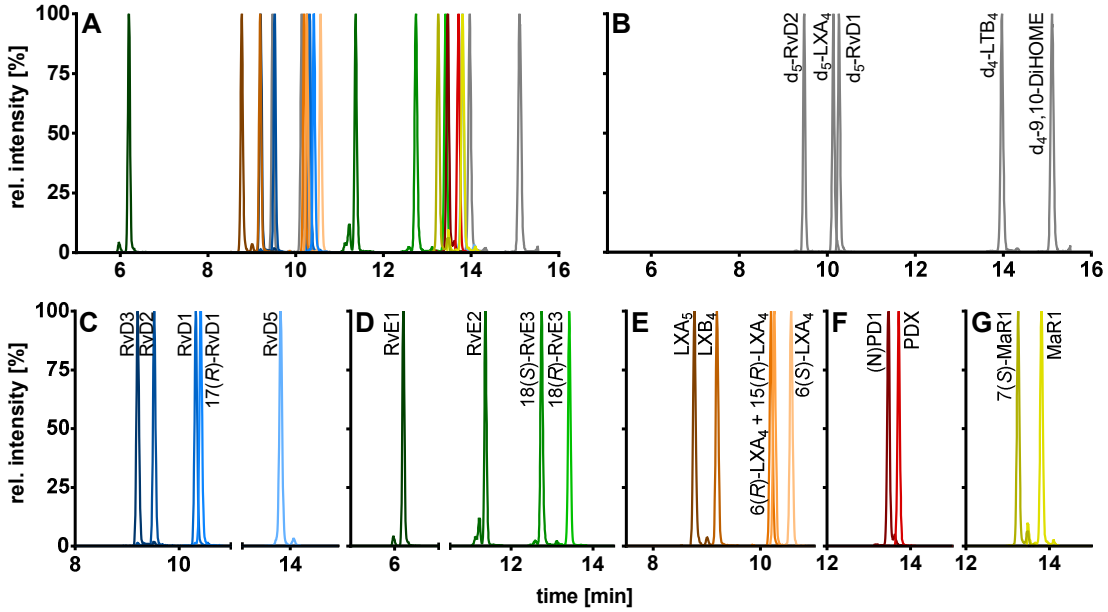

Fig. 4.6: Chromatographic separation of (**A**) 18 SPMs (100 nM each) and (**B**) 5 deuterated internal standards (20 nM) covered by the method including (**C**) DHA derived D-series resolvins, (**D**) EPA derived E-series resolvins, (**E**) EPA and ARA derived lipoxins, DHA derived (**F**) protectins and (**G**) maresins. Separation was carried out on an RP-18 column (2.1 × 150 mm, particle size 1.8 µm, pore size 9.5 nm) with an H_2O/MeOH/ACN/HOAc gradient.

The chromatographic separation of SPMs is crucial due to the large number of stereo- and regioisomers regarding position and configuration of the hydroxy group (*R*, *S*) bearing carbons and the conjugated double bonds (*E*, *Z*) that exhibit identical fragmentation patterns and similar chromatographic behavior [57]. Our method allows for sufficient chromatographic resolution (R) of the critical separation pairs, namely stereoisomers MaR1 and 7(*S*)-MaR1 (R = 4.7) and the

protectins (N)PD1 and PDX (R = 2.0) (Fig. 4.6 F–G). The two aspirin-triggered isomers 17(*R*)-RvD1 and 15(*R*)-LXA_4 are not baseline separated from 17(*S*)-RvD1 (R = 0.9) and 6(*R*)-LXA_4 (R = 0.6), respectively (Fig. 4.6 C,E). With this performance the method is better or comparable to that reported by other groups [26, 58], while baseline separation can be achieved by using chiral stationary phases [36, 38, 59]. Based on the incomplete separation, 17(*R*)-RvD1 and 15(*R*)-LXA_4 were not included in the calibration mixture and quantification was based on calibration curves of 17(*S*)-RvD1 and 6(*R*)-LXA_4, respectively. For RvD5 (RT 13.80 min), MaR1 (RT 13.81 min) and PDX (RT 13.71 min) with an $[M-H]^-$ of *m/z* 359.1 the choice of specific (and alternative) transitions is crucial to differentiate between these compounds and to allow the specific quantification. The fragments *m/z* 359.1 → 250.2 (MaR1(1)) and *m/z* 359.1 → 153.1 (PDX(1)) are the most intense and specific fragments for MaR1 and PDX, respectively. However, for RvD5 (*m/z* 359.1 → 199.1) both MaR1 (0.6%) and PDX (3%) show a signal on this transition. To ensure a reliable quantification of RvD5 in presence of high PDX concentrations a second transition (*m/z* 359.1 → 141.0, RvD5(2)) was therefore included as alternative fragment.

4.3.3 Sensitivity

The limit of detection (LOD) and lower limit of quantification (LLOQ) were determined according to the EMA guideline for bioanalytical methods [45]. The LOD was set to the lowest (calibration) standard injected yielding a signal-to-noise-ratio (S/N) ≥ 3; the LLOQ was set to the lowest calibration standard yielding an S/N ≥ 5 and an accuracy within ± 20% of the nominal concentration. The S/N (peak-to-peak) was determined manually as exemplarily shown for RvD2 (Fig. 4.7, for LOD and LLOQ of exemplary SPMs see appendix Fig. 8.4). As listed in Tab. 4.1, for our method the LOD was between 0.1 and 1.5 nM (0.18–2.7 pg on column) for the most sensitive transition, whereas for alternative transitions similarly low or higher LODs were determined. Despite different instrumentation, comparable or slightly higher detection limits are reported in literature, e.g. 3 pg on column [26], 1.3–4.9 pg on column [35], 0.10–5.2 pg on column in plasma

sample [34] of which all used an S/N of at least 3 as criterion. It should be noted that LODs of as low as 0.02 pg are reported for the same instrument as used in our lab [32]. However, the use of different criteria for LOD determination might explain this huge difference of 1–2 orders of magnitude. The LLOQ ranged from 0.25–2.0 nM (corresponding to 0.025–0.2 nM in plasma/serum) for the quantifier.

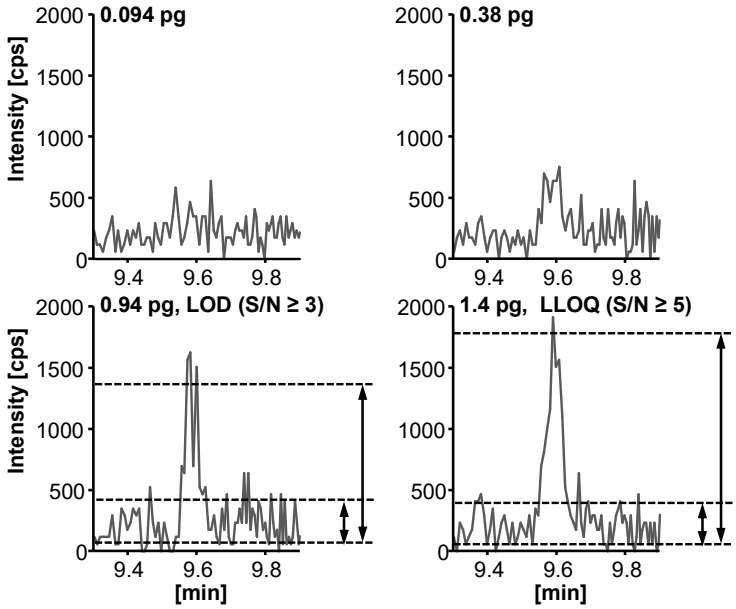

Fig. 4.7: Determination of the limit of detection (LOD) and the lower limit of quantification (LLOQ) exemplarily shown for resolvin D2 (RvD2, *m/z* 375.3 → 175.0) with an injection volume of 10 µL. LOD is defined as peak-to-peak signal-to-noise-ratio (S/N) ≥ 3 and LLOQ as S/N ≥ 5 and an accuracy within ± 20% of the nominal concentration.

Slightly better i.e. lower LLOQs can be achieved with higher injection volume (10 µL: LLOQ of 0.18–1.0 nM (0.018–0.1 nM in plasma/serum); Tab. 4.1, Fig. 4.8). Further increasing the injection volume resulted in an inacceptable peak shape due to reconstitution of the sample extract in pure organic solvent [44]. Reconstitution of the sample extract in a 1:1 methanol/water mixture allows for higher injection volumes (up to 20 µL) with acceptable peak shape for the analytes. However, less polar oxylipins were not sufficiently dissolved leading to unacceptable low recoveries of e.g. epoxy-FA but also monohydroxy-FA (Fig. 4.9). Therefore, it would not be possible to accurately quantify SPM precursors such as 17-HDHA or CYP-derived oxylipins, which may be used as indicators for n3-PUFA supplementation [40], parallel to SPMs. Overall, it can be summarized that in our hands under optimized conditions the lowest

concentration which can be quantified for SPMs and other oxylipins is about 1 nM in the injected solvent corresponding to about 1 pg on column.

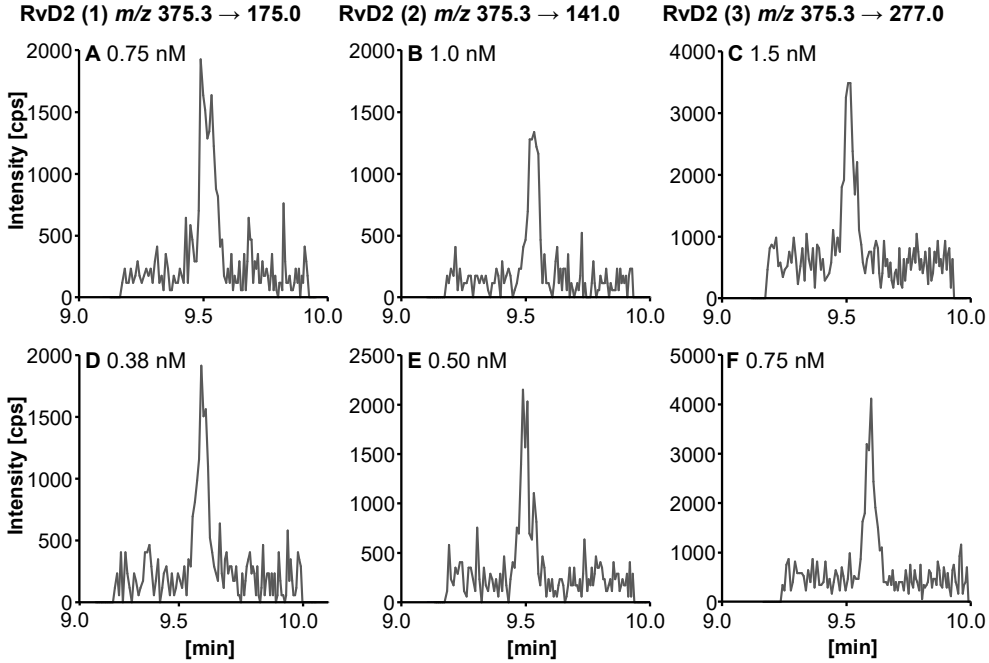

Fig. 4.8: Lower limits of quantification (LLOQ) for resolvin D2 on all three transitions (*m/z* 175.0, *m/z* 141.0, *m/z* 277.0). With an injection volume of 10 µL (**D**–**F**) lower LLOQs can be achieved compared to injection volumes of 5 µL (**A**–**C**).

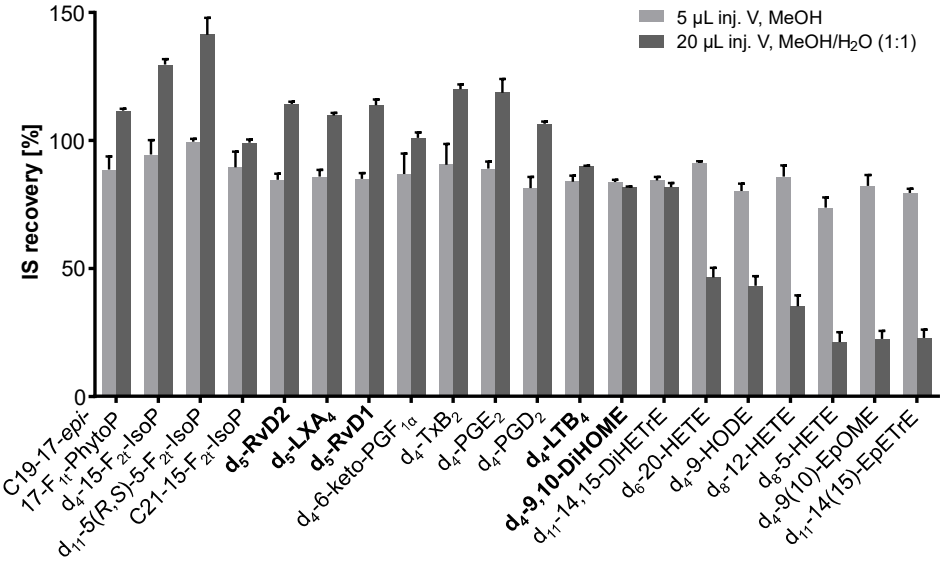

Fig. 4.9: Recovery of 20 deuterated internal standards (IS) used for quantification of SPMs (**bold**) and other oxylipins in plasma. Insufficient recovery rates for less polar IS when sample extract was reconstituted in 50:50 MeOH:H_2O and 20 µL were injected; good recovery rates when sample extract was reconstituted in 100% MeOH and 5 µL were injected. Recovery of IS 1 (added directly at the beginning of sample preparation) was determined utilizing 1-(1-(ethylsulfonyl)piperidin-4-yl)-3-(4-(trifluoromethoxy)phenyl)urea as IS 2 (added after sample preparation directly before measurement).

4.3.4 IS recovery and ion suppression

Recovery of IS used for SPM quantification was between 78 ± 4% ($^2H_4$-LTB$_4$) and 87 ± 3% ($^2H_5$-RvD2) from 500 µL of human serum (n = 3, Fig. 4.10). If the IS was added after the solid phase extraction step recovery rates were between 90 ± 2% ($^2H_4$-LTB$_4$) and 105 ± 5% ($^2H_5$-RvD2) (Fig. 4.10). From this it can be concluded that with the SPE procedure as established in our laboratory [44] IS are sufficiently well extracted from matrix (> 75%) and matrix effects are efficiently reduced (maximal ± 10%). It should be noted, that IS for quantification of all other oxylipins covered by our method show good recoveries from matrix between 72 ± 3% ($^2H_8$-5-HETE) and 105 ± 6% ($^2H_{11}$-5(*R*,*S*)-5-F$_{2t}$-IsoP) (Fig. 4.10). Thus, it can be assumed that a method allowing a good recovery rate of both polar oxylipins such as prostanoides (e.g. PGE$_2$) and less polar hydroxy-PUFA (e.g. 5-HETE) is also appropriate for the extraction of SPMs.

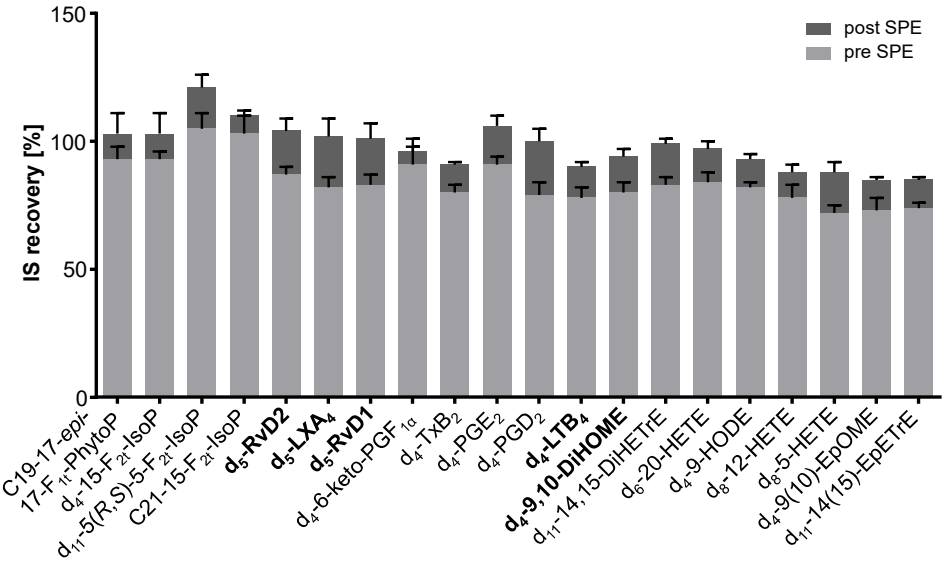

Fig. 4.10: Recovery and evaluation of matrix effects for 20 deuterated internal standards (IS) used for quantification of SPMs (**bold**) and other oxylipins in 500 µL serum. Recovery of IS 1 (added directly at the beginning of sample preparation, pre SPE) was determined utilizing 1-(1-(ethylsulfonyl)piperidin-4-yl)-3-(4-(trifluoromethoxy)phenyl)urea as IS 2 (added after sample preparation, directly before measurement). Evaluation of ion suppression was based on IS recovery when IS was added directly before reconstitution of sample extract after SPE (post SPE).

Tab. 4.1: Optimized parameters of the LC-ESI(-)-MS/MS method for the quantification of SPMs. Shown are mass transitions for quantification in scheduled SRM mode, electronical MS parameters (DP, EP, CE, CXP), the assigned IS, RT, FWHM, LOD and the calibration range (LLOQ/ULOQ).

Analyte		Mass transition		MS parameters				IS	RT [1]	FWHM [2]	LOD [3]		Calibration range [4]		
		Q1	Q3	DP	EP	CE	CXP		[min]	[sec]	[nM]	[pg on column]	LLOQ (5 µL) [5] [nM]	LLOQ (10 µL) [5] [nM]	ULOQ [6] [nM]
5(*S*),6(*R*),15(*S*)-LXA$_4$	(1)	351.2	115.2	-40	-10	-20	-8	$^2H_5$-LXA$_4$	10.19	3.5	0.18	0.31	0.25	0.18	500
	(2)	351.2	235.0	-40	-10	-20	-12				0.75	1.3	1.0	0.50	500
	(3)	351.2	217.1	-40	-10	-27	-12				2.0	3.5	5.0	2.0	500
5(*S*),6(*R*),15(*R*)-LXA$_4$ [8]	(1)	351.2	115.0	-40	-10	-20	-8	$^2H_5$-LXA$_4$	10.26	3.7	0.18	0.31	0.25	0.18	500
	(2)	351.2	235.1	-40	-10	-20	-12				0.75	1.3	1.0	0.50	500
	(3)	351.2	217.1	-40	-10	-27	-12				2.0	3.5	5.0	2.0	500
5(*S*),6(*S*),15(*S*)-LXA$_4$	(1)	351.2	115.1	-40	-10	-20	-8	$^2H_5$-LXA$_4$	10.57	3.5	0.18	0.31	0.25	0.18	500
	(2)	351.2	235.2	-40	-10	-20	-12				0.50	0.88	1.0	0.50	500
	(3)	351.2	217.1	-40	-10	-27	-12				2.0	3.5	5.0	2.0	500
LXB$_4$	(1)	351.2	221.0	-40	-10	-22	-13	$^2H_5$-LXA$_4$	9.19	3.5	0.50	0.88	1.0	0.50	500
	(2)	351.2	233.1	-40	-10	-22	-13				0.50	0.88	1.0	0.50	500
	(3)	351.2	251.0	-40	-10	-19	-13				1.5	2.6	5.0	2.0	500
LXA$_5$	(1)	349.1	114.9	-40	-10	-19	-5	$^2H_5$-LXA$_4$	8.77	3.2	0.10	0.18	0.25	0.18	500
	(2)	349.1	215.0	-40	-10	-25	-13				0.50	0.88	1.0	0.50	500
	(3)	349.1	233.1	-40	-10	-19	-11				0.75	1.3	1.0	0.75	500
RvE1	(1)	349.3	195.0	-50	-10	-23	-10	$^2H_5$-RvD2	6.19	3.5	0.38	0.66	0.50	0.25	500
	(2)	349.3	161.0	-50	-10	-25	-8				0.75	1.3	1.0	0.75	500
	(3)	349.3	205.0	-50	-10	-22	-10				1.0	1.8	2.0	1.0	500
RvE2	(1)	333.2	253.3	-60	-10	-20	-9	$^2H_4$-9,10-	11.37	3.8	1.0	1.7	2.0	1.0	100
	(2)	333.2	159.2	-60	-10	-25	-10	DiHOME			1.0	1.7	2.0	1.0	100
	(3)	333.2	199.1	-60	-10	-23	-10				1.0	1.7	2.0	1.0	100
18(*S*)-RvE3	(1)	333.2	201.3	-60	-10	-20	-9	$^2H_4$-9,10-	12.75	3.8	0.50	0.84	1.0	0.50	100
	(2)	333.2	245.3	-60	-10	-18	-9	DiHOME			0.50	0.84	1.0	0.50	100
18(*R*)-RvE3	(1)	333.2	201.3	-60	-10	-20	-9	$^2H_4$-9,10-	13.42	4.0	0.25	0.42	0.50	0.25	100
	(2)	333.2	245.3	-60	-10	-18	-9	DiHOME			0.25	0.42	0.50	0.25	100
RvD1 [7]	(1)	375.3	141.0	-40	-10	-20	-8	$^2H_5$-RvD1	10.32	3.6	-	-	0.25	0.18	500
	(2)	375.3	215.0	-40	-10	-27	-13				-	-	0.25	0.18	500
	(3)	375.3	233.3	-40	-10	-20	-12				-	-	0.50	0.25	500
17(*R*)-RvD1 [8]	(1)	375.3	140.9	-40	-10	-20	-8	$^2H_5$-RvD1	10.41	3.6	0.38	0.71	0.75	0.38	500
	(2)	375.3	215.1	-40	-10	-27	-13				0.50	0.94	0.75	0.38	500
	(3)	375.3	233.0	-40	-10	-20	-12				0.75	1.4	1.5	0.75	500
RvD2	(1)	375.3	175.0	-50	-10	-31	-12	$^2H_5$-RvD2	9.52	3.8	0.38	0.71	0.75	0.38	500
	(2)	375.3	141.0	-50	-10	-23	-8				0.75	1.4	1.0	0.50	500
	(3)	375.3	277.0	-50	-10	-19	-14				0.75	1.4	1.5	0.75	500

Tab. 4.1: Continued. Optimized parameters of the LC-ESI(-)-MS/MS method for the quantification of SPMs.

Analyte	Mass transition			MS parameters				IS	RT [1]	FWHM [2]	LOD [3]		Calibration range [4]		
		Q1	Q3	DP	EP	CE	CXP		[min]	[sec]	[nM]	[pg on column]	LLOQ (5 µL) [5] [nM]	LLOQ (10 µL) [5] [nM]	ULOQ [6] [nM]
RvD3	(1)	375.3	147.0	-60	-10	-27	-10	$^2H_5$-RvD2	9.20	3.6	0.18	0.33	0.38	0.18	500
	(2)	375.3	137.0	-60	-10	-27	-8				1.0	1.9	2.0	1.0	500
	(3)	375.3	181.0	-60	-10	-23	-10				1.5	2.8	5.0	2.0	500
RvD5	(1)	359.1	199.1	-40	-10	-23	-10	$^2H_4$-LTB$_4$	13.80	4.4	0.38	0.68	0.75	0.38	500
	(2)	359.1	141.0	-40	-10	-20	-8				1.0	1.8	2.0	1.0	500
	(3)	359.1	261.0	-40	-10	-19	-14				2.0	3.6	5.0	2.0	500
MaR1	(1)	359.1	250.2	-50	-10	-21	-12	$^2H_4$-LTB$_4$	13.81	4.2	1.5	2.7	2.0	1.0	500
	(2)	359.1	177.0	-50	-10	-23	-10				2.0	3.6	5.0	2.0	500
	(3)	359.1	221.0	-50	-10	-20	-8				2.0	3.6	5.0	2.0	500
7(*S*)-MaR1	(1)	359.1	250.1	-50	-10	-21	-12	$^2H_4$-LTB$_4$	13.25	4.2	0.25	0.45	0.50	0.25	500
	(2)	359.1	177.0	-50	-10	-23	-10				1.5	2.7	2.0	1.0	500
	(3)	359.1	221.0	-50	-10	-20	-8				1.5	2.7	5.0	2.0	500
(N)PD1	(1)	359.0	153.0	-50	-10	-21	-8	$^2H_4$-9,10-	13.48	4.1	0.25	0.45	0.50	0.25	500
	(2)	359.0	206.0	-50	-10	-21	-12	DiHOME			0.18	0.32	0.38	0.18	500
PDX	(1)	359.1	153.1	-50	-10	-22	-8	$^2H_4$-9,10-	13.71	4.1	0.18	0.32	0.25	0.18	500
	(2)	359.1	206.1	-50	-10	-22	-12	DiHOME			0.10	0.18	0.25	0.18	500
$^2H_5$-RvD2	IS	380.2	175.0	-55	-10	-31	-10	–	9.47	3.5	–		–		
$^2H_5$-LXA$_4$	IS	356.3	222.2	-55	-10	-25	-13	–	10.13	3.6	–		–		
$^2H_5$-RvD1	IS	380.3	141.0	-50	-10	-19	-8	–	10.26	3.6	–		–		
$^2H_4$-LTB$_4$	IS	339.2	197.2	-65	-10	-23	-9	–	13.97	4.3	–		–		
$^2H_4$-9,10-DiHOME	IS	317.2	203.4	-80	-10	-29	-8	–	15.11	4.6	–		–		

DP, declustering potential; EP, entrance potential; CE, collision energy; CXP, collision cell exit potential; IS, internal standard; RT, retention time; FWHM, full width at half maximum; LOD, limit of detection; LLOQ/ULOQ, lower/upper limit of quantification

[1] Relative standard deviation for RT within one batch was ≤ 0.10% (± 0.01 min)
[2] Full peak width at half maximum (FWHM) was determined as mean width of standards, concentration LLOQ–500 nM
[3] LOD was set to the lowest concentration yielding a signal to noise ratio ≥ 3 (injection volume of 5 µL)
[4] Calibration was performed as weighted regression using $1/x^2$ weighting
[5] LLOQ was set to the lowest calibration standard injected yielding a signal to noise ratio ≥ 5 and an accuracy within ± 20%
[6] ULOQ concentration does not represent the end of the dynamic range, but is the highest calibration standard injected
[7] No determination of LOD due to impurity of IS $^2H_5$-RvD1; LLOQ was set to lowest concentration yielding an S/N ≥ 5 and an accuracy within ± 20%
[8] Compounds 17(*R*)-RvD1 and 15(*R*)-LXA$_4$ were not included in the calibration mixture and quantification was based on the calibration curves of their isomers RvD1 and 5(*S*),6(*R*),15(*S*)-LXA$_4$, respectively.

4.3.5 Extraction efficacy and intraday accuracy and precision

In order to evaluate the accuracy and precision of the quantification of concentrations of SPMs in biological samples, human plasma (with SPM levels < LOD) was spiked at four concentration levels (0.1, 0.3, 1 and 3 nM in plasma) with a subset of SPMs. At 0.1 nM plasma concentration and 5 µL injection volume all of the spiked compounds were detected with at least two different specific transitions (Tab. 4.2). Accuracies were within ± 20% of the nominal (added) concentration for the quantifier (except RvE1) and precisions were < 20%. For some less sensitive alternative transitions 0.1 nM was below the LLOQ leading to higher variation of the determined concentrations, as e.g. 82 ± 35% for RvD3 *m/z* 375.3 → 137.0 (Tab. 4.2). However, as lower LLOQs can be achieved with higher injection volume, better accuracies and precisions were obtained with an injection volume of 10 µL, e.g. 103 ± 15% for RvD3 *m/z* 375.3 → 137.0 (Tab. 4.2). For spiking levels from 0.3–3 nM in plasma determined concentrations using the quantifier were within ± 15% compared to the added concentration and precision < 15%. However, also quantification using alternative transitions resulted in acceptable accuracy (maximal ± 21%) and precision (< 16%) for concentrations > LLOQ. The only exception is RvE1, which was quantified with an accuracy of 68–81% for all spiking levels in plasma, most likely due to interferences by the plasma matrix, e.g. ion suppression, which was not observed in human serum (accuracy 108% for RvE1, Tab. 4.2). Matrix interference could also lead to the slightly higher determined concentrations for RvD5 (121–122%) with an injection volume of 10 µL (Tab. 4.2).

Tab. 4.2 (right, page 97): Intraday accuracy (acc.) and precision (prec.) for the extraction of a subset of SPMs from human plasma (500 µL) and human serum (500 µL). SPMs were spiked into plasma at four concentration levels of 0.1, 0.3, 1.0 and 3.0 nM and additionally into serum at the highest concentration level (3.0 nM in serum). Accuracy was calculated based on the determined concentration in sample after sample preparation utilizing SPE extraction in comparison to the concentration in the spiking standard solution. Precision was expressed as relative standard deviation of the sample set (n = 4). For concentration levels 0.1 and 0.3 nM acc. and prec. for 5 µL and 10 µL injection volume are shown. Quantification was carried out for the quantifier (most sensitive transition) as well as for the alternative transitions if concentration was > LOD. No calculation of accuracy and precision was carried out if analyte was in ≥ 50% of the samples < LOD.

Analyte	Mass transition			0.1 nM in plasma [1]				0.3 nM in plasma [1]				1.0 nM in plasma		3.0 nM in plasma		3.0 nM in serum	
				5 µL		10 µL		5 µL		10 µL		5 µL		5 µL		5 µL	
		Q1	Q3	acc. [%]	prec. [%]	acc. [%]	prec. [%]	acc. [%]	prec. [%]	acc. [%]	prec. [%]	acc. [%]	prec. [%]	acc. [%]	prec. [%]	acc. [%]	prec. [%]
6(*R*)-LXA$_4$	**(1)**	**351.2**	**115.2**	**94**	**14**	**93**	**5**	**100**	**10**	**92**	**4**	**98**	**2**	**99**	**4**	**97**	**3**
	(2)	351.2	235.0	72	11	83	9	88	9	79	6	94	2	99	4	94	4
	(3)	351.2	217.1	< LOD		75	22	76	7	94	11	99	5	98	5	98	3
6(*S*)-LXA$_4$	**(1)**	**351.2**	**115.1**	**82**	**17**	**87**	**4**	**93**	**4**	**86**	**5**	**85**	**0**	**88**	**5**	**88**	**1**
	(2)	351.2	235.2	71	22	73	8	86	5	83	4	87	2	88	2	87	5
	(3)	351.2	217.1	< LOD		102	11	95	5	87	2	85	8	87	5	87	2
LXB$_4$	**(1)**	**351.2**	**221.0**	**105**	**5**	**106**	**9**	**96**	**8**	**97**	**4**	**98**	**5**	**100**	**3**	**95**	**3**
	(2)	351.2	233.1	109	14	119	10	103	8	97	7	96	3	100	4	92	2
	(3)	351.2	251.0	< LOD		< LOD		102	9	101	15	93	2	100	5	95	6
LXA$_5$	**(1)**	**349.1**	**114.9**	**114**	**7**	**119**	**7**	**110**	**5**	**114**	**4**	**111**	**4**	**112**	**3**	**102**	**4**
	(2)	349.1	215.0	97	9	105	5	106	3	112	1	105	5	111	4	102	4
	(3)	349.1	233.1	86	9	100	7	93	4	109	7	106	5	113	4	103	6
RvE1	**(1)**	**349.3**	**195.0**	**68**	**8**	**78**	**4**	**73**	**6**	**81**	**6**	**69**	**8**	**71**	**7**	**108**	**2**
	(2)	349.3	161.0	81	17	73	15	74	11	79	6	72	11	68	5	105	6
	(3)	349.3	205.0	< LOD		72	7	62	12	79	7	73	5	69	6	108	5
RvD1	**(1)**	**375.3**	**141.0**	**94**	**9**	**96**	**4**	**98**	**3**	**91**	**3**	**96**	**7**	**100**	**1**	**97**	**1**
	(2)	375.3	215.0	94	8	93	4	91	7	93	4	93	5	98	4	98	4
	(3)	375.3	233.3	80	5	82	14	89	9	91	8	95	6	101	1	98	1
RvD2	**(1)**	**375.3**	**175.0**	**101**	**8**	**98**	**3**	**96**	**5**	**104**	**4**	**98**	**7**	**100**	**4**	**105**	**3**
	(2)	375.3	141.0	99	10	98	7	91	6	94	5	94	9	97	3	108	2
	(3)	375.3	277.0	105	13	93	5	105	2	98	5	98	9	96	2	105	3
RvD3	**(1)**	**375.3**	**147.0**	**105**	**8**	**103**	**6**	**109**	**5**	**103**	**4**	**106**	**7**	**103**	**3**	**113**	**2**
	(2)	375.3	137.0	82	35	103	15	102	9	103	11	106	10	105	4	115	4
	(3)	375.3	181.0	< LOD		128	11	101	17	105	6	112	14	106	4	116	6
RvD5	**(1)**	**359.1**	**199.1**	**109**	**3**	**122**	**11**	**111**	**4**	**121**	**4**	**109**	**10**	**107**	**4**	**106**	**3**
	(2)	359.1	141.0	111	6	110	12	107	16	116	8	102	11	104	6	107	5
	(3)	359.1	261.0	< LOD		< LOD		115	7	98	8	108	13	108	3	100	5
MaR1	**(1)**	**359.1**	**250.2**	**110**	**19**	**119**	**14**	**109**	**10**	**107**	**4**	**105**	**8**	**104**	**5**	**105**	**5**
	(2)	359.1	177.0	88	24	122	12	99	7	107	6	93	11	100	6	101	3
	(3)	359.1	221.0	< LOD		< LOD		110	11	113	5	92	11	104	2	104	7
7(*S*)-MaR1	**(1)**	**359.1**	**250.1**	**97**	**6**	**94**	**12**	**99**	**4**	**102**	**2**	**91**	**9**	**96**	**4**	**103**	**2**
	(2)	359.1	177.0	105	9	90	18	99	2	103	7	99	5	97	6	103	3
	(3)	359.1	221.0	< LOD		< LOD		110	13	108	3	95	11	97	4	104	3
(N)PD1	**(1)**	**359.0**	**153.0**	**87**	**17**	**114**	**9**	**91**	**11**	**95**	**3**	**98**	**6**	**92**	**4**	**98**	**3**
	(2)	359.0	206.0	95	8	99	15	109	8	96	6	98	7	89	3	105	5
PDX	**(1)**	**359.1**	**153.1**	**96**	**5**	**106**	**3**	**98**	**2**	**99**	**4**	**94**	**6**	**93**	**5**	**102**	**3**
	(2)	359.1	206.1	103	6	96	6	95	6	95	5	89	8	90	4	101	2

[1] concentrations < LLOQ and > LOD were quantified to calculate accuracy and precision

In summary, all three chosen transitions were suitable for quantification of SPMs in human plasma and serum; however, for routine measurement the two most sensitive transitions (one quantifier and one qualifier ion) seem to be sufficient. In the unspiked plasma/serum of healthy individuals used for the spiking experiment no SPMs could be detected, i.e. they did not exceed the LOD. It should be noted that we found good recoveries in freshly spiked human plasma and serum samples, however, the SPMs could be degraded during storage of the samples. Though most oxylipins are stable during storage at –80 °C [60] lower SPM levels have been reported in plasma which was stored for a longer period of time [32]. It would be important to investigate the stability of naturally formed SPMs as well as spiked analytes in future studies because this could lead to the high concentration differences reported in biological samples. Regarding SPM levels in human plasma and/or serum reported concentrations differ considerably. For example, in baseline human plasma concentrations of RvD1 and RvE1 that lie within the working range of our method were reported, such as 0.0454 nM (RvD1) and 0.521–1.00 nM (RvE1) [61], 0.10–0.11 nM (RvD1) and 0.11–0.14 nM (RvE1) [55]. However, also concentrations below our LLOQ were found in human plasma, e.g. 0.007 nM RvD1 [32] or were not detected at all [34]. In human serum SPM amounts were considerably higher compared to the plasma analyzed in the same study, probably due to formation during coagulation [32]. Interestingly, in another study with plasma and serum from healthy volunteers after n3-PUFA supplementation comparable SPM levels were found in plasma and serum [26]. Therefore, differences in sample generation, handling and storage may impact detectability and quantity of low levels of SPMs. In our study we could not detect SPMs in blank plasma and serum, while in spiked samples SPM levels as low as 0.1 nM could be detected. Thus, our study supports earlier reports that the circulating levels of SPMs in healthy individuals are very low, as described e.g. by Colas *et al.* (2014) [32]. In order to come to comparable results regarding the concentration of SPMs in biological samples all methods used should be validated based on internationally accepted guidelines. Moreover, direct comparison of results obtained by different, independent laboratories as e.g. performed by Norris *et al*. (2018) [62] in form of round robin trials are required.

4.3.6 SPM formation in peritonitis

SPMs and other oxylipins were quantified in peritoneal dialysate and serum samples, which were obtained from patients with end stage renal disease treated by peritoneal dialysis (PD) as renal replacement therapy [63] with (peritonitis, n = 4–5) and without (control, n = 4–5) acute inflammation.

In peritoneal effluents pro-inflammatory mediators PGE_2 and LTB_4 were elevated in the peritonitis group compared to the control group (Fig. 4.11) and similar trends were observed for the 5-, 12- and 15-LOX products. However, SPMs were detected only in a single sample and therefore not displayed in Fig. 4.11. 15-lipoxygenation products were quantified only in low concentrations (≤ 1 nM) and SPM precursor 18-HEPE was < LLOQ in > 50% of the samples.

In the serum 12 SPMs could be quantified in > 50% of the samples including di- and trihydroxylated ARA, EPA and DHA derived PUFA ranging from concentrations as low as 0.24 ± 0.07 nM (18(*R*)-RvE3) to 36 ± 15 nM (RvE2) in the peritonitis group (Fig. 4.11, appendix Fig. 8.5). Overall, SPM concentrations as well as their precursors showed no significant difference between peritonitis and control group. A trend towards higher 5- and 12-lipoxygenation and lower 15-lipoxygenation products and 18-HEPE in peritonitis could be observed with high inter-individual variation, while for SPMs no consistent trend towards an elevation or reduction in peritonitis was observed (Fig. 4.11). For SPMs that were detected in the PD patients' serum samples (e.g. RvE2, RvD2) a pro-resolving action in peritonitis was reported earlier, mainly observed as a reduction of PMN recruitment (summarized in [64, 65]). However, these effects as well as the presence of SPMs in peritoneal lavages were mostly shown in zymosan-induced murine peritonitis models and data on human clinical samples are scarce. Surprisingly, no detectable levels of SPMs were found in the dialysate of PD patients, despite being in direct contact to the inflamed tissue within a confined space. A reason could be the time point for sample collection, as SPM concentrations change during the inflammation/resolution process. In murine peritonitis models SPM formation was reduced with time after the initiation of

inflammation (highest after 2–6 h, reduced/not detectable after 9–24 h) [66-68], with induction of a more severe, non-self-resolving inflammation [68, 69] or were not detected [70, 71]. In clinical samples, the individual time-course and severity of the inflammation as well as the strong dilution of lipid mediators in the PD solution (1–2 L) or differences in sample collection and processing in the clinical daily routine can have an influence on lipid mediator levels and could explain SPM levels < LLOQ in the dialysate from peritonitis patients. The SPM pathway markers such as 17-HDHA, though not statistically significant, were elevated in the peritonitis group compared to control group and could serve as indicator for potential SPM formation during peritonitis. In contrast, the overall similar levels in the serum of control and peritonitis patients of both pro- and anti-inflammatory lipid mediators might indicate a sustained systemic inflammation of end stage renal disease patients. Due to the reduction in renal clearance, poor biocompatibility of PD fluids and oxidative stress, chronic inflammation processes are enhanced in long-term PD patients [72, 73]. Therefore, elevated levels of inflammation-associated lipid mediators, small sample size and high inter-individual variation might mask differences in SPM concentrations between control and peritonitis group.

Fig. 4.11 (right, page 101): Concentration of selected lipid mediators in (**1**) peritoneal dialysate and (**2**) serum from patients with end stage renal disease treated with peritoneal dialysis (PD) with (peritonitis, n = 4–5) or without (control, n = 4–5) acute inflammation. Shown are concentrations in nM as individual values and mean ± SEM of (**A**) ARA derived pro-inflammatory lipid mediators, 5-, 12- and 15-lipoxygenation products/SPM precursors as well as di- and tri-hydroxylated products/SPMs derived from (**B**) ARA, (**C**) EPA and (**D**) DHA. For concentrations < LLOQ, the LLOQ is given. Mean ± SEM are only calculated if ≥ 50% of the samples are > LLOQ. The LLOQ is indicated as dotted line. In dialysates of the control group one outlier was eliminated based on Grubb's test ($\alpha = 0.05$). Statistically significant differences between control and peritonitis group are indicated by $^*p < 0.05$ calculated by Mann-Whitney *U* test.

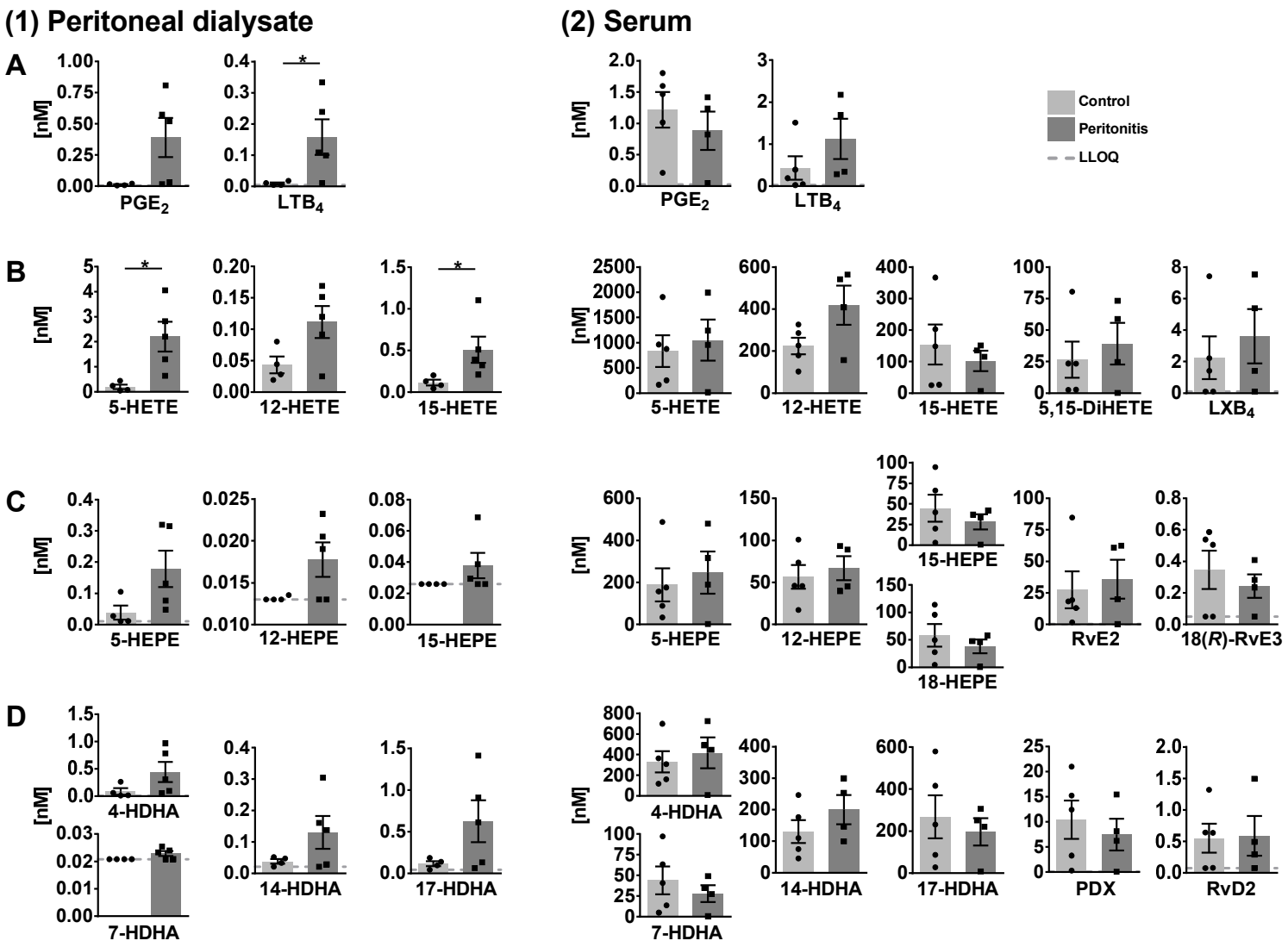
(1) Peritoneal dialysate
(2) Serum
A
B
C
D
[nM]
PGE2
LTB4
5-HETE
12-HETE
15-HETE
5,15-DiHETE
LXB4
5-HEPE
12-HEPE
15-HEPE
18-HEPE
RvE2
18(R)-RvE3
4-HDHA
7-HDHA
14-HDHA
17-HDHA
PDX
RvD2
Control
Peritonitis
LLOQ
*

4.3.7 SPM formation in septic shock

In plasma samples from patients with septic shock (n=18, APACHE II score 41.5 (22–52)), severe clinical and humoral signs of inflammation (CRP 236 mg/L (68–422 mg/L)) and multi-organ failure, SPMs and other oxylipins were quantified and compared to plasma samples of healthy individuals serving as control (n = 10). In control samples, 4 SPMs (RvE2, LXB_4, (N)PD1 and PDX) were detected and exceeded LLOQ only in 2 individuals (0.027–0.16 nM). In plasma from septic shock patients, 12 SPMs were quantified with large inter-individual variation ranging from < LLOQ (< 0.018 nM) up to > 20 nM (Fig. 4.12; appendix Fig. 8.6). Most SPMs including LX, E- and D-series Rv were quantified in less than half of the study population (1–6 individuals), whereas protectins (N)PD1 (median conc. 0.15 nM) and PDX (median conc. 0.072 nM) were quantified in 12–13 individuals (Fig. 4.12). Despite high inter-individual variation, a trend towards higher levels (median concentration) of pro-inflammatory mediators, SPM precursors and SPMs from different enzymatic pathways (COX, 5-LOX, 15-LOX) and different PUFA (ARA, EPA, DHA) in plasma from septic shock patients compared to control was observed. This is consistent with earlier reports of an elevation of metabolites formed in the ARA cascade during inflammation (e.g. in a DSS-induced colitis model [74]) and could be caused by increased phospholipase A2 (PLA_2) activity in response to the inflammatory stimuli e.g. in neutrophils [75]. A slightly more pronounced elevation of SPM pathway markers, e.g. 17-HDHA (0.42 vs. 6.2 nM) compared to pro-inflammatory markers such as PGE_2 (0.056 vs. 0.078 nM) could suggest an attempt of the body to resolve the inflammation; however, high mortality (72%) indicates failed resolution. In fact, despite the small sample size higher SPMs and their mono-hydroxylated precursors were found in non-survivors (n = 13) compared to survivors of septic shock (n = 5) (Fig. 4.12). A similar observation was reported by Dalli *et al.* (2017), where higher plasma concentrations of SPMs including RvD1, RvD5 and (N)PD1 and pathway marker 17-HDHA in sepsis non-survivors were found. It should be noted that in this study several SPMs (e.g. PDX 0.004–0.008 nM) were found in a concentration below our LLOQ making it difficult to compare absolute concentrations [41].

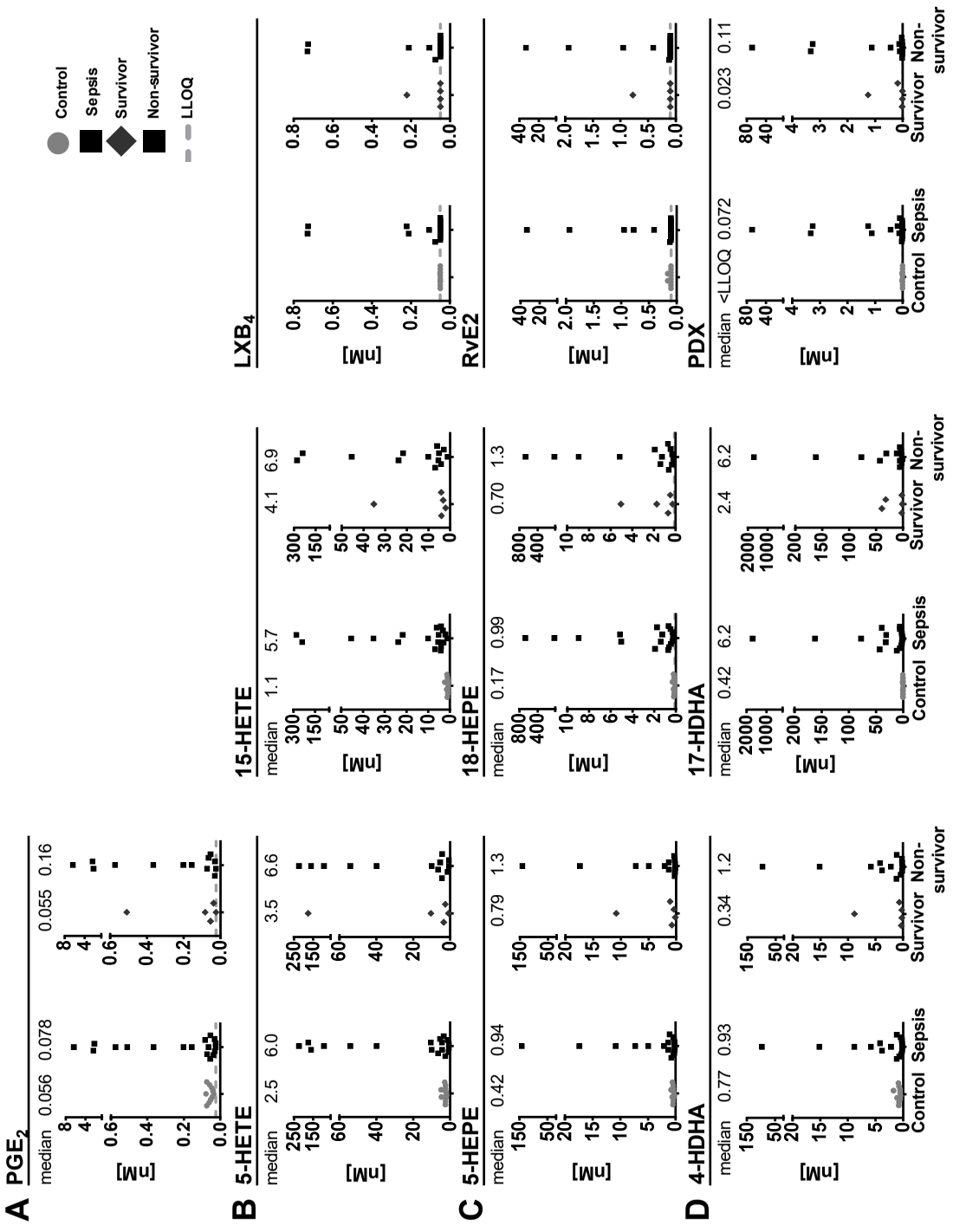

Fig. 4.12: Concentration of selected lipid mediators measured in plasma from patients with (sepsis, n = 18) and without (control, n = 10) septic shock. Patients with septic shock are divided into survivors (> 28 days, n = 5) and non-survivors (n = 13). Shown are concentrations in nM as individual values of (**A**) ARA derived PGE_2, 5-lipoxygenation products and SPM pathway marker as well as SPMs derived from (**B**) ARA, (**C**) EPA and (**D**) DHA. Median is given, if > 50% of the samples are > LLOQ. The LLOQ is indicated as dotted line.

Our study did not unveil an obvious correlation of SPM levels to clinical signs of inflammation, severity of sepsis or days of survival. However, possible correlations might be masked by the small and heterogeneous group of individuals: The patients were of different gender, age, health condition previous septic shock diagnosis and different pathogens were involved in the development of septic shock. No alteration of SPMs during inflammation or resolution phase was also observed in a human LPS induced sepsis model [34] or SPMs were not detected in plasma samples from patients with hepatic failure despite showing clinical signs of inflammation [37]. In summary, although our study demonstrated the presence of detectable SPM concentrations in an exemplary cohort of extremely sick septic shock patients, it might not support a role of SPMs as biomarkers to predict the clinical outcome in sepsis.

4.4 Conclusion

A new method for the detection of SPMs was developed by careful optimization of MS parameters in combination to an UHPLC chromatographic separation using one of the most sensitive – and commonly used for oxylipin quantification – instruments available. The resulting LOD were 0.18–2.7 pg on column corresponding to an LLOQ of 0.02–0.2 nM in biological samples such as plasma. SPMs were generally not detectable/quantifiable in plasma and serum of healthy individuals, while good recovery rates were found in spiked samples. These results strongly support findings that circulating levels of SPMs are very low, i.e. < 0.1 nM in healthy subjects. In samples from patients with end stage renal disease (and peritonitis) or septic shock SPMs and precursors were detectable; however, not directly correlated with the health status and clinical outcome.

4.5 References

1. Medzhitov R (2008) Origin and physiological roles of inflammation. *Nature*, 454(7203), 428-435; doi: 10.1038/nature07201.
2. Higgs GA (1986) The role of eicosandoids in inflammation. *Prog Lipid Res*, 25(1-4), 555-561; doi: 10.1016/0163-7827(86)90113-X.
3. Haribabu B, Verghese MW, Steeber DA, Sellars DD, Bock CB, Snyderman R (2000) Targeted disruption of the leukotriene B(4) receptor in mice reveals its role in inflammation and platelet-activating factor-induced anaphylaxis. *J Exp Med*, 192(3), 433-438; doi: 10.1084/jem.192.3.433.
4. Serhan CN, Chiang N, Dalli J (2015) The resolution code of acute inflammation: Novel pro-resolving lipid mediators in resolution. *Semin Immunol*, 27(3), 200-215; doi: 10.1016/j.smim.2015.03.004.
5. Serhan CN, Petasis NA (2011) Resolvins and protectins in inflammation resolution. *Chem Rev*, 111(10), 5922-5943; doi: 10.1021/cr100396c.
6. Calder PC (2015) Marine omega-3 fatty acids and inflammatory processes: Effects, mechanisms and clinical relevance. *Biochim Biophys Acta*, 1851(4), 469-484; doi: 10.1016/j.bbalip.2014.08.010.
7. Levy BD, Clish CB, Schmidt B, Gronert K, Serhan CN (2001) Lipid mediator class switching during acute inflammation: signals in resolution. *Nat Immunol*, 2(7), 612-619; doi: 10.1038/89759.
8. Serhan CN (2014) Pro-resolving lipid mediators are leads for resolution physiology. *Nature*, 510(7503), 92-101; doi: 10.1038/nature13479.
9. Bennett M, Gilroy DW (2016) Lipid mediators in inflammation. *Microbiol Spectr*, 4(6); doi: 10.1128/microbiolspec.MCHD-0035-2016.
10. Serhan CN, Chiang N, Dalli J, Levy BD (2014) Lipid mediators in the resolution of inflammation. *Cold Spring Harb Perspect Biol*, 7(2), a016311; doi: 10.1101/cshperspect.a016311.
11. Werz O, Gerstmeier J, Libreros S, De la Rosa X, Werner M, Norris PC, Chiang N, Serhan CN (2018) Human macrophages differentially produce specific resolvin or leukotriene signals that depend on bacterial pathogenicity. *Nat Commun*, 9(1), 59; doi: 10.1038/s41467-017-02538-5.
12. Serhan CN (2005) Lipoxins and aspirin-triggered 15-epi-lipoxins are the first lipid mediators of endogenous anti-inflammation and resolution. *Prostaglandins Leukot Essent Fatty Acids*, 73(3-4), 141-162; doi: 10.1016/j.plefa.2005.05.002.
13. Serhan CN, Hamberg M, Samuelsson B (1984) Lipoxins: novel series of biologically active compounds formed from arachidonic acid in human leukocytes. *Proc Natl Acad Sci U S A*, 81(17), 5335-5339; doi: 10.1073/pnas.81.17.5335.
14. Claria J, Serhan CN (1995) Aspirin triggers previously undescribed bioactive eicosanoids by human endothelial cell-leukocyte interactions. *Proc Natl Acad Sci U S A*, 92(21), 9475-9479; doi: 10.1073/pnas.92.21.9475.
15. Hong S, Gronert K, Devchand PR, Moussignac RL, Serhan CN (2003) Novel docosatrienes and 17S-resolvins generated from docosahexaenoic acid in murine brain, human blood, and glial cells. Autacoids in anti-inflammation. *J Biol Chem*, 278(17), 14677-14687; doi: 10.1074/jbc.M300218200.
16. Serhan CN, Clish CB, Brannon J, Colgan SP, Chiang N, Gronert K (2000) Novel functional sets of lipid-derived mediators with antiinflammatory actions generated from omega-3 fatty acids via cyclooxygenase 2-nonsteroidal antiinflammatory drugs and transcellular processing. *J Exp Med*, 192(8), 1197-1204; doi: 10.1084/jem.192.8.1197.

17. Arita M, Clish CB, Serhan CN (2005) The contributions of aspirin and microbial oxygenase to the biosynthesis of anti-inflammatory resolvins: novel oxygenase products from omega-3 polyunsaturated fatty acids. *Biochem Biophys Res Commun*, 338(1), 149-157; doi: 10.1016/j.bbrc.2005.07.181.
18. Ostermann AI, Willenberg I, Weylandt KH, Schebb NH (2015) Development of an online-SPE–LC–MS/MS method for 26 hydroxylated polyunsaturated fatty acids as rapid targeted metabolomics approach for the LOX, CYP, and autoxidation pathways of the arachidonic acid cascade. *Chromatographia*, 78(5), 415-428; doi: 10.1007/s10337-014-2768-8.
19. Tjonahen E, Oh SF, Siegelman J, Elangovan S, Percarpio KB, Hong S, Arita M, Serhan CN (2006) Resolvin E2: identification and anti-inflammatory actions: pivotal role of human 5-lipoxygenase in resolvin E series biosynthesis. *Chem Biol*, 13(11), 1193-1202; doi: 10.1016/j.chembiol.2006.09.011.
20. Oh SF, Pillai PS, Recchiuti A, Yang R, Serhan CN (2011) Pro-resolving actions and stereoselective biosynthesis of 18S E-series resolvins in human leukocytes and murine inflammation. *J Clin Invest*, 121(2), 569-581; doi: 10.1172/jci42545.
21. Isobe Y, Arita M, Matsueda S, Iwamoto R, Fujihara T, Nakanishi H, Taguchi R, Masuda K, Sasaki K, Urabe D, Inoue M, Arai H (2012) Identification and structure determination of novel anti-inflammatory mediator resolvin E3, 17,18-dihydroxyeicosapentaenoic acid. *J Biol Chem*, 287(13), 10525-10534; doi: 10.1074/jbc.M112.340612.
22. Isobe Y, Arita M, Iwamoto R, Urabe D, Todoroki H, Masuda K, Inoue M, Arai H (2013) Stereochemical assignment and anti-inflammatory properties of the omega-3 lipid mediator resolvin E3. *J Biochem*, 153(4), 355-360; doi: 10.1093/jb/mvs151.
23. Serhan CN, Gotlinger K, Hong S, Lu Y, Siegelman J, Baer T, Yang R, Colgan SP, Petasis NA (2006) Anti-inflammatory actions of neuroprotectin D1/protectin D1 and its natural stereoisomers: assignments of dihydroxy-containing docosatrienes. *J Immunol*, 176(3), 1848-1859; doi: 10.4049/jimmunol.176.3.1848.
24. Balas L, Guichardant M, Durand T, Lagarde M (2014) Confusion between protectin D1 (PD1) and its isomer protectin DX (PDX). An overview on the dihydroxy-docosatrienes described to date. *Biochimie*, 99, 1-7; doi: 10.1016/j.biochi.2013.11.006.
25. Serhan CN, Yang R, Martinod K, Kasuga K, Pillai PS, Porter TF, Oh SF, Spite M (2009) Maresins: novel macrophage mediators with potent antiinflammatory and proresolving actions. *J Exp Med*, 206(1), 15-23; doi: 10.1084/jem.20081880.
26. Mas E, Croft KD, Zahra P, Barden A, Mori TA (2012) Resolvins D1, D2, and other mediators of self-limited resolution of inflammation in human blood following n-3 fatty acid supplementation. *Clin Chem*, 58(10), 1476-1484; doi: 10.1373/clinchem.2012.190199.
27. Serhan CN (2017) Discovery of specialized pro-resolving mediators marks the dawn of resolution physiology and pharmacology. *Mol Aspects Med*, 58, 1-11; doi: 10.1016/j.mam.2017.03.001.
28. Brezinski DA, Serhan CN (1991) Characterization of lipoxins by combined gas chromatography and electron-capture negative ion chemical ionization mass spectrometry: formation of lipoxin A4 by stimulated human whole blood. *Biol Mass Spectrom*, 20(2), 45-52; doi: 10.1002/bms.1200200202.
29. Chiang N, Takano T, Clish CB, Petasis NA, Tai HH, Serhan CN (1998) Aspirin-triggered 15-epi-lipoxin A4 (ATL) generation by human leukocytes and murine peritonitis exudates: development of a specific 15-epi-LXA4 ELISA. *J Pharmacol Exp Ther*, 287(2), 779-790.
30. Kirkby NS, Chan MV, Lundberg MH, Massey KA, Edmands WM, MacKenzie LS, Holmes E, Nicolaou A, Warner TD, Mitchell JA (2013) Aspirin-triggered 15-epi-lipoxin A4 predicts

cyclooxygenase-2 in the lungs of LPS-treated mice but not in the circulation: implications for a clinical test. *Faseb J*, 27(10), 3938-3946; doi: 10.1096/fj.12-215533.

31. Masoodi M, Mir AA, Petasis NA, Serhan CN, Nicolaou A (2008) Simultaneous lipidomic analysis of three families of bioactive lipid mediators leukotrienes, resolvins, protectins and related hydroxy-fatty acids by liquid chromatography/electrospray ionisation tandem mass spectrometry. *Rapid Commun Mass Spectrom,* 22(2), 75-83; doi: 10.1002/rcm.3331.
32. Colas RA, Shinohara M, Dalli J, Chiang N, Serhan CN (2014) Identification and signature profiles for pro-resolving and inflammatory lipid mediators in human tissue. *Am J Physiol Cell Physiol*, 307(1), C39-54; doi: 10.1152/ajpcell.00024.2014.
33. Jónasdóttir HS, Ioan-Facsinay A, Kwekkeboom J, Brouwers H, Zuurmond A-M, Toes R, Deelder AM, Giera M (2015) An Advanced LC–MS/MS Platform for the Analysis of Specialized Pro-Resolving Lipid Mediators. *Chromatographia*, 78(5), 391-401; doi: 10.1007/s10337-014-2779-5.
34. Skarke C, Alamuddin N, Lawson JA, Li X, Ferguson JF, Reilly MP, FitzGerald GA (2015) Bioactive products formed in humans from fish oils. *J Lipid Res*, 56(9), 1808-1820; doi: 10.1194/jlr.M060392.
35. Le Faouder P, Baillif V, Spreadbury I, Motta JP, Rousset P, Chene G, Guigne C, Terce F, Vanner S, Vergnolle N, Bertrand-Michel J, Dubourdeau M, Cenac N (2013) LC-MS/MS method for rapid and concomitant quantification of pro-inflammatory and pro-resolving polyunsaturated fatty acid metabolites. *J Chromatogr B Analyt Technol Biomed Life Sci*, 932, 123-133; doi: 10.1016/j.jchromb.2013.06.014.
36. Homann J, Lehmann C, Kahnt AS, Steinhilber D, Parnham MJ, Geisslinger G, Ferreiros N (2014) Chiral chromatography-tandem mass spectrometry applied to the determination of pro-resolving lipid mediators. *J Chromatogr A*, 1360, 150-163; doi: 10.1016/j.chroma.2014.07.068.
37. Toewe A, Balas L, Durand T, Geisslinger G, Ferreiros N (2018) Simultaneous determination of PUFA-derived pro-resolving metabolites and pathway markers using chiral chromatography and tandem mass spectrometry. *Anal Chim Acta*, 1031, 185-194; doi: 10.1016/j.aca.2018.05.020.
38. Massey KA, Nicolaou A (2013) Lipidomics of oxidized polyunsaturated fatty acids. *Free Radic Biol Med*, 59, 45-55; doi: 10.1016/j.freeradbiomed.2012.08.565.
39. Barden AE, Mas E, Croft KD, Phillips M, Mori TA (2015) Specialized proresolving lipid mediators in humans with the metabolic syndrome after n-3 fatty acids and aspirin. *Am J Clin Nutr*, 102(6), 1357-1364; doi: 10.3945/ajcn.115.116384.
40. Murphy RC (2015) Specialized pro-resolving mediators: do they circulate in plasma? *J Lipid Res*, 56(9), 1641-1642; doi: 10.1194/jlr.C062356.
41. Dalli J, Colas RA, Quintana C, Barragan-Bradford D, Hurwitz S, Levy BD, Choi AM, Serhan CN, Baron RM (2017) Human sepsis eicosanoid and proresolving lipid mediator temporal profiles: Correlations with survival and clinical outcomes. *Crit Care Med*, 45(1), 58-68; doi: 10.1097/ccm.0000000000002014.
42. Ogawa S, Urabe D, Yokokura Y, Arai H, Arita M, Inoue M (2009) Total synthesis and bioactivity of resolvin E2. *Org Lett*, 11(16), 3602-3605; doi: 10.1021/ol901350g.
43. Dayaker G, Durand T, Balas L (2014) A versatile and stereocontrolled total synthesis of dihydroxylated docosatrienes containing a conjugated E,E,Z-triene. *Chemistry*, 20(10), 2879-2887; doi: 10.1002/chem.201304526.
44. Rund KM, Ostermann AI, Kutzner L, Galano JM, Oger C, Vigor C, Wecklein S, Seiwert N, Durand T, Schebb NH (2018) Development of an LC-ESI(-)-MS/MS method for the simultaneous quantification of 35 isoprostanes and isofurans derived from the major n3- and n6-PUFAs. *Anal Chim Acta*, 1037, 63-74; doi: 10.1016/j.aca.2017.11.002.

45. European Medicines Agency (2011) Guideline on bioanalytical method validation. EMEA/CHMP/EWP/192217/2009 Rev. 1 Corr. 2** Committee for Medicinal Products for Human Use (CHMP), July 21, 2011.
46. Li PK, Szeto CC, Piraino B, de Arteaga J, Fan S, Figueiredo AE, Fish DN, Goffin E, Kim YL, Salzer W, Struijk DG, Teitelbaum I, Johnson DW (2016) ISPD peritonitis recommendations: 2016 update on prevention and treatment. *Perit Dial Int*, 36(5), 481-508; doi: 10.3747/pdi.2016.00078.
47. Singer M, Deutschman CS, Seymour CW, Shankar-Hari M, Annane D, Bauer M, Bellomo R, Bernard GR, Chiche JD, Coopersmith CM, Hotchkiss RS, Levy MM, Marshall JC, Martin GS, Opal SM, Rubenfeld GD, van der Poll T, Vincent JL, Angus DC (2016) The third international consensus definitions for sepsis and septic shock (Sepsis-3). *JAMA*, 315(8), 801-810; doi: 10.1001/jama.2016.0287.
48. Knaup H, Stahl K, Schmidt BMW, Idowu TO, Busch M, Wiesner O, Welte T, Haller H, Kielstein JT, Hoeper MM, David S (2018) Early therapeutic plasma exchange in septic shock: a prospective open-label nonrandomized pilot study focusing on safety, hemodynamics, vascular barrier function, and biologic markers. *Crit Care*, 22(1), 285; doi: 10.1186/s13054-018-2220-9.
49. Vlasakov I, Norris P, Winkler J, Dalli J, Serhan C (2016) Lipid mediator metabololipidomics LC-MS-MS spectra book 2016. Prof. Charles N. Serhan Laboratory, Boston, MA.
50. Gabelica V, De Pauw E (2005) Internal energy and fragmentation of ions produced in electrospray sources. *Mass Spectrom Rev*, 24(4), 566-587; doi: 10.1002/mas.20027.
51. Sleno L, Volmer DA (2004) Ion activation methods for tandem mass spectrometry. *J Mass Spectrom*, 39(10), 1091-1112; doi: 10.1002/jms.703.
52. Hong S, Lu Y, Yang R, Gotlinger KH, Petasis NA, Serhan CN (2007) Resolvin D1, protectin D1, and related docosahexaenoic acid-derived products: Analysis via electrospray/low energy tandem mass spectrometry based on spectra and fragmentation mechanisms. *J Am Soc Mass Spectrom*, 18(1), 128-144; doi: 10.1016/j.jasms.2006.09.002.
53. Murphy RC, Barkley RM, Zemski Berry K, Hankin J, Harrison K, Johnson C, Krank J, McAnoy A, Uhlson C, Zarini S (2005) Electrospray ionization and tandem mass spectrometry of eicosanoids. *Anal Biochem*, 346(1), 1-42; doi: 10.1016/j.ab.2005.04.042.
54. Lu Y, Hong S, Yang R, Uddin J, Gotlinger KH, Petasis NA, Serhan CN (2007) Identification of endogenous resolvin E1 and other lipid mediators derived from eicosapentaenoic acid via electrospray low-energy tandem mass spectrometry: spectra and fragmentation mechanisms. *Rapid Commun Mass Spectrom*, 21(1), 7-22; doi: 10.1002/rcm.2798.
55. Barden A, Mas E, Croft KD, Phillips M, Mori TA (2014) Short-term n-3 fatty acid supplementation but not aspirin increases plasma proresolving mediators of inflammation. *J Lipid Res*, 55(11), 2401-2407; doi: 10.1194/jlr.M045583.
56. Hassan IR, Gronert K (2009) Acute changes in dietary omega-3 and omega-6 polyunsaturated fatty acids have a pronounced impact on survival following ischemic renal injury and formation of renoprotective docosahexaenoic acid-derived protectin D1. *J Immunol*, 182(5), 3223-3232; doi: 10.4049/jimmunol.0802064.
57. Hansen TV, Dalli J, Serhan CN (2016) Selective identification of specialized pro-resolving lipid mediators from their biosynthetic double di-oxygenation isomers. *RSC Adv*, 6(34), 28820-28829; doi: 10.1039/c6ra00414h.
58. Sun YP, Oh SF, Uddin J, Yang R, Gotlinger K, Campbell E, Colgan SP, Petasis NA, Serhan CN (2007) Resolvin D1 and its aspirin-triggered 17R epimer. Stereochemical

assignments, anti-inflammatory properties, and enzymatic inactivation. *J Biol Chem*, 282(13), 9323-9334; doi: 10.1074/jbc.M609212200.

59. Lehmann C, Homann J, Ball AK, Blocher R, Kleinschmidt TK, Basavarajappa D, Angioni C, Ferreiros N, Hafner AK, Radmark O, Proschak E, Haeggstrom JZ, Geisslinger G, Parnham MJ, Steinhilber D, Kahnt AS (2015) Lipoxin and resolvin biosynthesis is dependent on 5-lipoxygenase activating protein. *Faseb J*, 29(12), 5029-5043; doi: 10.1096/fj.15-275487.
60. Jonasdottir HS, Brouwers H, Toes REM, Ioan-Facsinay A, Giera M (2018) Effects of anticoagulants and storage conditions on clinical oxylipid levels in human plasma. *Biochim Biophys Acta*, 1863(12), 1511-1522; doi: 10.1016/j.bbalip.2018.10.003.
61. Psychogios N, Hau DD, Peng J, Guo AC, Mandal R, Bouatra S, Sinelnikov I, Krishnamurthy R, Eisner R, Gautam B, Young N, Xia J, Knox C, Dong E, Huang P, Hollander Z, Pedersen TL, Smith SR, Bamforth F, Greiner R, McManus B, Newman JW, Goodfriend T, Wishart DS (2011) The human serum metabolome. *PLoS One*, 6(2), e16957; doi: 10.1371/journal.pone.0016957.
62. Norris PC, Skulas-Ray AC, Riley I, Richter CK, Kris-Etherton PM, Jensen GL, Serhan CN, Maddipati KR (2018) Identification of specialized pro-resolving mediator clusters from healthy adults after intravenous low-dose endotoxin and omega-3 supplementation: a methodological validation. *Sci Rep*, 8(1), 18050; doi: 10.1038/s41598-018-36679-4.
63. Ellam T, Wilkie M (2015) Peritoneal dialysis. *Medicine*, 43(8), 484-488; doi: 10.1016/j.mpmed.2015.05.001.
64. Serhan CN (2010) Novel lipid mediators and resolution mechanisms in acute inflammation: to resolve or not? *Am J Pathol*, 177(4), 1576-1591; doi: 10.2353/ajpath.2010.100322.
65. Recchiuti A, Serhan CN (2012) Pro-resolving lipid mediators (SPMs) and their actions in regulating miRNA in novel resolution circuits in inflammation. *Front Immunol*, 3, 298; doi: 10.3389/fimmu.2012.00298.
66. Bannenberg GL, Chiang N, Ariel A, Arita M, Tjonahen E, Gotlinger KH, Hong S, Serhan CN (2005) Molecular circuits of resolution: formation and actions of resolvins and protectins. *J Immunol*, 174(7), 4345-4355; doi: 10.4049/jimmunol.174.7.4345.
67. Divanovic S, Dalli J, Jorge-Nebert LF, Flick LM, Galvez-Peralta M, Boespflug ND, Stankiewicz TE, Fitzgerald JM, Somarathna M, Karp CL, Serhan CN, Nebert DW (2013) Contributions of the three CYP1 monooxygenases to pro-inflammatory and inflammation-resolution lipid mediator pathways. *J Immunol*, 191(6), 3347-3357; doi: 10.4049/jimmunol.1300699.
68. Chiang N, Fredman G, Backhed F, Oh SF, Vickery T, Schmidt BA, Serhan CN (2012) Infection regulates pro-resolving mediators that lower antibiotic requirements. *Nature*, 484(7395), 524-528; doi: 10.1038/nature11042.
69. Fredman G, Li Y, Dalli J, Chiang N, Serhan CN (2012) Self-limited versus delayed resolution of acute inflammation: temporal regulation of pro-resolving mediators and microRNA. *Sci Rep*, 2, 639; doi: 10.1038/srep00639.
70. Dioszeghy V, Rosas M, Maskrey BH, Colmont C, Topley N, Chaitidis P, Kuhn H, Jones SA, Taylor PR, O'Donnell VB (2008) 12/15-Lipoxygenase regulates the inflammatory response to bacterial products in vivo. *J Immunol*, 181(9), 6514-6524; doi: 10.4049/jimmunol.181.9.6514.
71. Spite M, Summers L, Porter TF, Srivastava S, Bhatnagar A, Serhan CN (2009) Resolvin D1 controls inflammation initiated by glutathione-lipid conjugates formed during oxidative stress. *Br J Pharmacol*, 158(4), 1062-1073; doi: 10.1111/j.1476-5381.2009.00234.x.

72. Lai KN, Leung JC (2010) Inflammation in peritoneal dialysis. *Nephron Clin Pract*, 116(1), c11-18; doi: 10.1159/000314544.
73. Velloso MS, Otoni A, de Paula Sabino A, de Castro WV, Pinto SW, Marinho MA, Rios DR (2014) Peritoneal dialysis and inflammation. *Clin Chim Acta*, 430, 109-114; doi: 10.1016/j.cca.2013.12.003.
74. Willenberg I, Ostermann AI, Giovannini S, Kershaw O, von Keutz A, Steinberg P, Schebb NH (2015) Effect of acute and chronic DSS induced colitis on plasma eicosanoid and oxylipin levels in the rat. *Prostaglandins Other Lipid Mediat*, 120, 155-160; doi: 10.1016/j.prostaglandins.2015.04.002.
75. Levy R, Dana R, Hazan I, Levy I, Weber G, Smoliakov R, Pesach I, Riesenberg K, Schlaeffer F (2000) Elevated cytosolic phospholipase A(2) expression and activity in human neutrophils during sepsis. *Blood*, 95(2), 660-665; doi: 10.1182/blood.V95.2.660.

Chapter 5

Human lipoxygenase isoforms form complex patterns of double and triple oxygenated compounds from eicosapentaenoic acid

Lipoxygenases (ALOX) are lipid peroxidizing enzymes that catalyze the biosynthesis of pro- and anti-inflammatory lipid mediators and have been implicated in (patho-)physiological processes. In humans, six functional ALOX isoforms exist and their arachidonic acid oxygenation products have been characterized. Products include leukotrienes and lipoxins which are involved in the regulation of inflammation and resolution. Oxygenation of n3-polyunsaturated fatty acids gives rise to specialized pro-resolving mediators, e.g. resolvins. However, the catalytic activity of different ALOX isoforms can lead to a multitude of potentially bioactive products. Here, we characterized the patterns of oxygenation products formed by human recombinant ALOX5, ALOX15, ALOX15B and ALOX12 from eicosapentaenoic acid (EPA) and its 18-hydroxy derivative 18-HEPE with particular emphasis on double and triple oxygenation products. ALOX15 and ALOX5 formed a complex mixture of various double oxygenation products from EPA, which include 5,15-diHEPE and various 8,15-diHEPE isomers. Their biosynthetic mechanisms were explored using heavy oxygen isotopes ($H_2{}^{18}O$, ${}^{18}O_2$ gas) and three catalytic activities contributed to product formation: i) fatty acid oxygenase activity, ii) leukotriene synthase activity, iii) lipohydroperoxidase activity. For ALOX15B and ALOX12 more specific product patterns were identified, which was also the case when these enzymes reacted in concert with ALOX5. Several double oxygenated compounds were formed from 18-HEPE by ALOX5, ALOX15B and ALOX12 including previously identified resolvins (RvE2, RvE3), while formation of triple oxygenation products, e.g. 5,17,18-triHEPE, required ALOX5. Taken together our data show that EPA can be converted by human ALOX isoforms to a large number of secondary oxygenation products, which might exhibit bioactivity.

Reprinted from *Biochimica et Biophysica Acta,* 1865(12), Kutzner L, Goloshchapova K, Rund KM, Jübermann M, Blum M, Rothe M, Kirsch SF, Schunck WH, Kühn H, Schebb NH, Human lipoxygenase isoforms form complex patterns of double and triple oxygenated compounds from eicosapentaenoic acid, 158806, doi: 10.1016/j.bbalip.2020.158806; Copyright (2020), with permission from Elsevier.

Author contributions: LK designed research, performed experiments and wrote the manuscript; KG, KMR, MB, MR performed experiments; MJ, SFK synthesized 18-HEPE; WHS designed research and contributed to discussion; HK designed research, performed experiments and wrote the manuscript; NHS designed research and wrote the manuscript.

5.1 Introduction

Lipoxygenases (ALOX isoforms) are non-heme iron containing enzymes that catalyze the oxygenation of polyunsaturated fatty acids (PUFA) by a sequence of steps involving hydrogen abstraction, rearrangement of double bonds, insertion of molecular oxygen and peroxy radical reduction leading to the formation of hydroperoxy PUFA. These primary oxygenation products can either be reduced to the respective hydroxy derivatives or can be converted to more complex oxygenation products via alternative secondary reactions [1]. Structural prerequisite for a fatty acid to be oxygenized by an ALOX isoform is the presence of at least one bisallylic methylene. Therefore, PUFA such as arachidonic acid (ARA) carrying several bisallylic methylenes can be oxidized by different ALOX isoforms to several hydroperoxy products. There are six functional *ALOX* genes in the human genome (*ALOX5, ALOX12, ALOX12B, ALOX15, ALOX15B, ALOXE3*) encoding for six functionally distinct ALOX isoforms. The nomenclature of ALOX isoforms is still a matter of discussion. However, according to the gene-based nomenclature the enzymes can be named as ALOX5, ALOX12, ALOX12B, ALOX15, ALOX15B and ALOXE3 [1].

Although the major ARA lipoxygenation products formed by the different human ALOX isoforms are well characterized, the overall product pattern is more complex. Some ALOX isoforms exhibit dual reaction specificity, e.g. human ALOX15 catalyzes the synthesis of both 15- and 12-HETE in a ratio of about 10:1 [2]. Furthermore, some ALOX isoforms exhibit multiple catalytic activities, by which hydroperoxy PUFA formed during the oxygenase reaction can be converted to secondary decomposition products [3]. For instance, human ALOX5 exhibits in addition to its fatty acid dioxygenase activity a 5,6-leukotriene A_4 (LTA_4) synthase activity [4]. For rabbit ALOX15 additional lipohydroperoxidase [5] and 14,15-LTA_4 synthase [6] activities were observed. Alternative alignments of substrate fatty acids at the active site of a given ALOX isoform may also contribute to the formation of more complex product patterns [7]. Since the primary ALOX products of most PUFA such as 15-H(p)ETE and 5-H(p)ETE still

carry bisallylic methylenes they also constitute ALOX substrates. Their enzyme catalyzed dioxygenation can also contribute to the formation of a complex product mixture. The formation of double lipoxygenation products was first described for soybean LOX-1, which oxygenated its primary ARA oxygenation product 15(*S*)-HpETE to a mixture of 8(*S*),15(*S*)- and 5(*S*),15(*S*)-diHpETE at lower rates [8, 9]. Recombinant human ALOX15 also accepts hydro(pero)xy PUFA as substrate and incubation of this enzyme with the ALOX5 product 5-HpETE led to the formation of 5,15- and 5,12-diH(p)ETE isomers [10]. Moreover, rabbit and pig ALOX15 orthologs exhibit LTA_4 synthase activities leading to the formation of epoxy PUFA that spontaneously hydrolyze to form dihydroxy eicosanoids [3]. When pure native rabbit ALOX15 was incubated *in vitro* with 15-HETE derivatives large amounts of conjugated trienes such as 8,15-, 5,15- and 14,15-diHETE were formed [11]. In addition, a mixture of conjugated tetraenes was detected [12] and 5,14,15-triHETE was identified as major representative. Experiments with $^{17}O_2$ gas indicated that the oxygen atoms at C5 and C14 originated from atmospheric oxygen [11]. Such trihydroxy PUFA were also described by Serhan *et al*. [13, 14] as a result of interactions between the ALOX5 and ALOX15 pathways leading to the formation of lipoxin A_4 (5,6,15-triHETE; LXA_4) and lipoxin B_4 (5,14,15-triHETE; LXB_4). However, as opposed to the triple oxygenation pathway the epoxide hydrolysis pathway has been suggested as major biosynthetic route in these experiments. Another biosynthetic route for lipoxins involves a coordinated action of ALOX5 and ALOX12, which converts the ALOX5 product 5,6-LTA_4 to LXA_4 or LXB_4 [15].

In order to appreciate the capacity of human ALOX isoforms for the formation of bioactive multiple hydroxylated PUFA, it is crucial to understand their capability to form di- and trihydroxylated PUFA. The formation of such products from ARA was previously explored in different cellular and subcellular *in vitro* assays [16]. Apart from the early recognized chemotactic properties of LTB_4 [17], biological activities have also been described for double lipoxygenation products from ARA. For example, 8(*S*),15(*S*)-diHETE, which is formed by ALOX15, attenuated LTB_4-induced hyperalgesia [18] and 5(*S*),12(*S*)-diHETE, which is formed by the

consecutive action of ALOX5 and ALOX12, showed inhibitory effects on platelet aggregation [19]. Moreover, double and triple oxygenated products of n3-PUFA e.g. eicosapentaenoic acid (EPA), such as the E-series resolvins, exhibit anti-inflammatory, pro-resolving activities in nanogram doses [20, 21]. For ARA 12- and 15-lipoxygenating ALOX isoforms (ALOX15, ALOX15B, ALOX12) as well as for human ALOX5, EPA constitutes an effective substrate [22, 23]. Enzymatic oxygenation of this PUFA may lead to the formation of structurally similar multiple hydroxylated products, which might exhibit biological activities. When EPA was incubated *in vitro* with human PMNs the formation of multiple hydroxylated products, such as 5,6-diHEPE and various LTB_5 isomers (5,12-diHEPE) was observed [24]. Furthermore, as described for ARA, the interaction of different ALOX isoforms leads to the formation of bioactive di- or trihydroxylated fatty acids from EPA, such as the lipoxenes (EPA derived lipoxins) [25].

In order to further investigate the biosynthesis of potentially bioactive EPA derived double and triple oxygenated compounds, we analyzed the product patterns formed from EPA by the catalytic activities of four recombinant human ALOX isoforms (ALOX15, ALOX15B, ALOX12, ALOX5) under identical experimental conditions. Moreover, we compared the product patterns produced during single enzyme incubations with those formed during consecutive and simultaneous incubations of two different ALOX isoforms. Finally, synthetic 18(*R*,*S*)-HEPE was applied as substrate for the ALOX isoforms in order to investigate the formation of specialized pro-resolving mediators (SPMs) by ALOX catalyzed oxygenation of 18-HEPE.

5.2 Experimental

5.2.1 Chemicals

Fatty acids (*cis*-5,8,11,14,17-eicosapentaenoic acid, EPA), oxylipin standard substances and deuterated internal standards (IS) were purchased from Cayman

Chemicals (local distributor: Biomol, Hamburg, Germany) except $^{2}H_5$-*cis*-5,8,11,14,17-eicosapentaenoic acid, which was purchased from Sigma Aldrich (Taufkirchen, Germany). Standards for RvE2, 18(*S*)- and 18(*R*)-RvE3 were a kind gift of the lab of Makoto Arita (RIKEN Center for Integrative Medical Sciences, Japan). 18(*R*,*S*)-hydroxy-5*Z*,8*Z*,11*Z*,14*Z*,16*E*-eicosapentaenoic acid (18(*R*,*S*)-HEPE) was synthesized as described elsewhere. $H_2{}^{18}O$ (97% isotopic purity) and $^{18}O_2$ gas (99% isotopic purity) were purchased from Sigma Aldrich (Taufkirchen, Germany). LC-MS grade acetic acid (HOAc), methanol (MeOH) and acetonitrile (ACN) were obtained from Fisher Scientific (Schwerte, Germany). Disodium hydrogen phosphate dihydrate and *n*-hexane were purchased from Carl Roth (Karlsruhe, Germany). All other chemicals were obtained from Sigma Aldrich (Schnelldorf, Germany) or VWR (Darmstadt, Germany).

5.2.2 Enzyme expression

Human ALOX isoforms were expressed as N-terminal His-tag fusion proteins in *E. coli* using the protocols described previously [26]. In brief, the coding regions of human ALOX cDNAs were sub-cloned into the bacterial expression plasmid pET28b. Competent bacteria [Rosetta 2 DE3 pLysS] were transformed with 100–400 ng of the pET28b-ALOX plasmids and cells were grown on kanamycin containing agar plates. Two well-separated bacterial clones were selected for each enzyme and five 1 mL bacterial pre-cultures (LB medium with 50 µg/mL kanamycin and 35 µg/mL chloramphenicol) were grown at 37 °C for 6 h and 180 rpm agitation. When the pre-culture reached an optical density (OD) at 600 nm of 0.1–0.15 at 1:50 dilution an appropriate amount of the pre-culture was added to a 50 mL main culture to reach an OD600 of 0.15. The main culture was grown overnight at 30 °C and the culture was continuously shaken at 250 rpm in Ultra Yield flasks (Thomson Instrument Company, Oceanside, USA) covered with an air top seal (Fisher Scientific, Schwerte, Germany). The culture medium was prepared from glucose-free minimal essential medium by the addition of trace elements and was supplemented with 40 g/L dextrin, 0.24 g/L tryptone/peptone and 0.48 g/L yeast extract. Before starting the bacterial culture, antibiotics and

glucose were added. Finally, 100 µL 1:20 diluted antifoam 204 (Sigma, Deisenhofen, Germany) and 50 µL glycoamylase from Aspergillus niger (Amylase AG 300L; Novozymes, Bagsværd, Denmark) were also supplied. Expression of the recombinant enzymes was induced by the addition of 1 mM (final concentration) isopropyl-β-thiogalactopyranoside (IPTG). The cultures were incubated for 24 h at 22 °C and 230–250 rpm agitation. Bacteria were harvested by centrifugation and the resulting pellet was reconstituted in 5 mL PBS. Cells were lysed by sonication, cell debris was spun down and the lysis supernatant was used for direct activity assays without further purification.

5.2.3 Enzyme incubation

Enzyme preparations were incubated with ARA (100 µM, 3 min) and main products (monohydroxy PUFA) were quantified with LC-UV. Enzyme preparations were adjusted to equal ARA oxygenase activity and used for EPA or 18(*R*,*S*)-HEPE incubations.

To explore patterns of oxygenation products aliquots of enzyme preparations were incubated alone or in combination with ALOX5 in 250 µL PBS containing a final concentration of 10 µM EPA or 18(*R*,*S*)-HEPE. For incubations involving ALOX5 buffer contained additionally ATP (0.1 mM), $CaCl_2$ (0.4 mM), EDTA (0.1 mM) and dipalmitoylphosphatidylcholine (1.4 µg/mL). For the single enzyme incubations, the reaction mixture was incubated for 15 min at room temperature (RT). For the combined enzyme incubations, after 15 min an aliquot of the ALOX5 preparation was added to the reaction mixture and the samples were incubated for additional 15 min. Simultaneous incubations and incubations in reversed order were carried out for the combinations ALOX12/ALOX5 and ALOX15B/ALOX5. No-enzyme control incubations were performed using 250 µL PBS and 10 µM substrate. The hydroperoxides were reduced with 25 µL methanolic $SnCl_2$ (10 mg/mL), or by the addition of 1 mg of solid $NaBH_4$ and afterwards acidified with 15 µL HOAc. 250 µL of ice-cold MeOH were added,

protein precipitates were spun down and the protein free supernatants were stored at –80 °C until analysis.

In selected experiments ALOX-catalyzed fatty acid oxygenation was carried out under $^{18}O_2$ atmosphere. For this purpose, we first anaerobized an appropriate volume (5 mL) of PBS containing the substrate fatty acid by flushing the solution extensively (30 min) with argon gas. Then, we slowly bubbled $^{18}O_2$ gas through this solution so that the sample was saturated with $^{18}O_2$ gas. 250 µL of this solution were transferred to a 500 µL reaction tube, which was previously filled with argon gas. Next, $^{18}O_2$ gas was bubbled through this solution to form an $^{18}O_2$ atmosphere above the sample. Finally, the reaction was initiated by the addition of small volumes of partly anaerobized enzyme solutions (stored for 1 h under argon atmosphere). To carry out incubations in $H_2{}^{18}O$ buffer 50 µL of 20-fold concentrated PBS were added to 1 mL of $H_2{}^{18}O$. Small amounts of a methanolic stock solution of the substrate were added to 250 µL $H_2{}^{18}O$ buffer and the reaction was initiated by the addition of small volumes of enzyme preparation. Fatty acid hydroperoxides were reduced by the addition of 1 mg $NaBH_4$ and after acidification (addition of 25 µL HOAc) proteins were precipitated by the addition of 500 µL ACN. Precipitated proteins were spun down and the protein free supernatants were stored at –80 °C until analysis.

5.2.4 MS/MS experiments

For LC-MS/MS analysis, an aliquot of the sample was diluted with MeOH, 10 µL antioxidant mixture were added (containing 0.2 mg/mL BHT, 100 µM indomethacin and 100 µM *t*-AUCB in MeOH) as well as 10 µL of deuterated oxylipin internal standards (IS; 100 nM in MeOH). The sample mixture was vortexed and centrifuged (10 min, 4 °C, 20 000 × g), supernatant was diluted with 0.1 M disodium hydrogen phosphate buffer (pH 6), adjusted to pH 6 and a MeOH content of approximately 15% and applied to the preconditioned SPE cartridges (Bond Elut Certify II, Agilent, Waldbronn, Germany). Cartridges were prepared and samples applied as described and free oxylipins were eluted with ethyl

acetate/*n*-hexane (75:25) containing 1% HOAc [27, 28]. Oxylipins were quantified in scheduled selected reaction monitoring (SRM) mode on a SCIEX QTRAP instrument (5500/6500; AB Sciex, Darmstadt, Germany) using external calibration and 20 deuterated IS [27, 28]. Additionally, EPA was quantified using the same LC-MS/MS method as for oxylipin analysis (*m/z* 301.3 → 257.1, DP –80 V, CE –16 V, CXP –6 V) with $^{2}H_{5}$-EPA as IS (*m/z* 306.1 → 262.2, DP –80 V, CE –16 V, CXP –6 V). Analyst 1.6.2 (AB Sciex) was used for operating the instrument and qualitative analyses and Multiquant 2.1.1 (AB Sciex) was used for data quantification.

For semi-quantitative measurement of the sum of EPA derived ALOX products, sample extracts were measured in selected ion monitoring (SIM) mode: *m/z* 317.2 and DP –75 V for mono-, *m/z* 333.2 and DP –90 V for double, and *m/z* 349.2 and DP –80 V for triple oxygenated products in different dilutions of the sample extract. For monohydroxy fatty acids, only the abundance of major products (5-, 12-, 15-HEPE) that were identified based on retention time of authentic standards were included. For double and triple oxygenated compounds, peaks eluting between 9.0–17.0 min (di-OH) or 5.0–13.0 min (tri-OH), exceeding a height of 5×10^{5} cps and signal of no-enzyme incubation were included. Obtained peak areas of mono- as well as putative double and triple oxygenated products were summed with consideration of the dilution factor and expressed as relative share of total products detected for each sample.

For qualitative evaluation of formed products with no authentic standards commercially available to date, collision induced dissociation (CID) product ion spectra were recorded for double (*m/z* 333.2) and triple oxygenated (*m/z* 349.2) products with the following electronic parameters: CE ramp from –18 V to –26 V, DP –80 V, EP –10 V, CXP –11 V, a scan rate of 1000 Da/s and a scan range of 100–340/350 Da. In the EPA and 18(*R*,*S*)-HEPE incubations those peaks were labeled as products, which largely exceeded the no enzyme and no substrate control incubations. Molecular structures (position of OH-groups) were concluded from fragmentation patterns based on typical fragmentation mechanisms

described for eicosanoids [29]. For unexpected formation of ions with even numbered *m/z*, sites of fragmentation were suggested despite the deviation of 1 Da between expected and observed fragment ion mass. To support several of the suggested structures of the major double oxygenated ALOX5 and ALOX15 products as well as their dominant formation route product ion spectra were obtained for $^{18}O_2$- and $H_2{}^{18}O$-incubation mixtures: *m/z* 333.2 for $^{16}O/^{16}O$, *m/z* 335.2 for $^{16}O/^{18}O$ and *m/z* 337.2 for $^{18}O/^{18}O$ (CE ramp –18 V to –26 V, DP –80 V, EP –10 V, CXP –11 V, scan rate 1000 Da/s, scan range 55–340 Da).

5.2.5 Chiral LC-MS/MS analysis of 18-HEPE

Separation of 18-HEPE enantiomers in ALOX incubation mixtures was carried out as described by Blum *et al.* [30]. In brief, an Agilent ZORBAX SB-C8 column was coupled to a Lux-Amylose-1 column. 10 µL sample extract (as described above) were injected and analytes were separated with a linear gradient of ACN/MeOH/H_2O/glacial HOAc starting at 27:3:70:0.05 and ending at 63:7:30:0.05 after 30 min with a flow rate of 0.4 mL/min utilizing an Agilent 1290 infinity UHPLC system. Detection was carried out using an Agilent 6490 Triple Quad MS (Agilent, Waldbronn, Germany) operated in negative ESI-mode using selected reaction monitoring (SRM).

5.2.6 Data analysis

Incubations of enzymes were carried out as independent replicates as indicated in the figure legend. For quantitative evaluation of enzyme incubations, mean ± SD (n = 3) were calculated using Microsoft Office Excel 2016 software (Redmond, WA, USA). Figures and graphs were generated with GraphPad Prism 6.01 (GraphPad Software, San Diego, CA, USA).

5.3 Results

5.3.1 Product specificity of human ALOX isoforms with EPA alone and in combination with ALOX5

In previous studies we have identified the major oxygenation products formed from EPA by different human ALOX isoforms but we did not exactly quantify product formation [23]. To fill this gap, we first quantified the ARA oxygenase activity of our enzyme preparations (ALOX15, ALOX15B, ALOX12, ALOX5) in separate activity assays and adjusted the enzyme concentrations to similar ARA oxygenase activities. These normalized enzyme preparations were then employed for the EPA oxygenase assays and residual EPA as well as formed mono-hydro(pero)xy fatty acids were quantified. Recovered EPA varied between 1.4 and 26% (Fig. 5.1 A, left) and these data demonstrate that EPA is accepted as substrate by all tested enzymes. When we incubated ALOX15, ALOX15B and ALOX12 consecutively with ALOX5 only 1–2% of EPA were recovered (Fig. 5.1 A, right). These data indicate that the remaining EPA, which was not oxygenated during the first incubation period, was completely oxygenated by ALOX5 during the second incubation period. Next, we quantified the formation of major products 5-, 12- and 15-HpEPE, which were analyzed as their respective hydroxy derivatives (HEPEs) (Fig. 5.1 B). Here, we confirmed our previous findings [23] that the ARA 15-lipoxygenating ALOX15B forms almost exclusively 15-HEPE (n6/n9-ratio > 100) and thus, the enzyme exhibits a singular reaction specificity with this particular substrate. In contrast, ALOX15 converted EPA to a mixture of 15- and 12-HEPE (n6/n9-ratio 6.2) and this data is consistent with our previous report [23]. Dominant 12-HEPE formation was shown for ALOX12 (n6/n9-ratio < 0.01) and as expected 5-HEPE was the major ALOX5 oxygenation product. Notably, formation of HEPEs differed considerably between the ALOX isoforms and compared to ALOX12 and ALOX15B significantly lower levels of mono-oxygenation products were quantified for ALOX15 and ALOX5 (Fig. 5.1 B, left). It should be stressed at this point that minor amounts of other HEPEs, i.e.

8-, 9-, 11- and 18-HEPE, were also detected. However, the relative shares of these products varied between 0.08%–2% of total mono-oxygenation products.

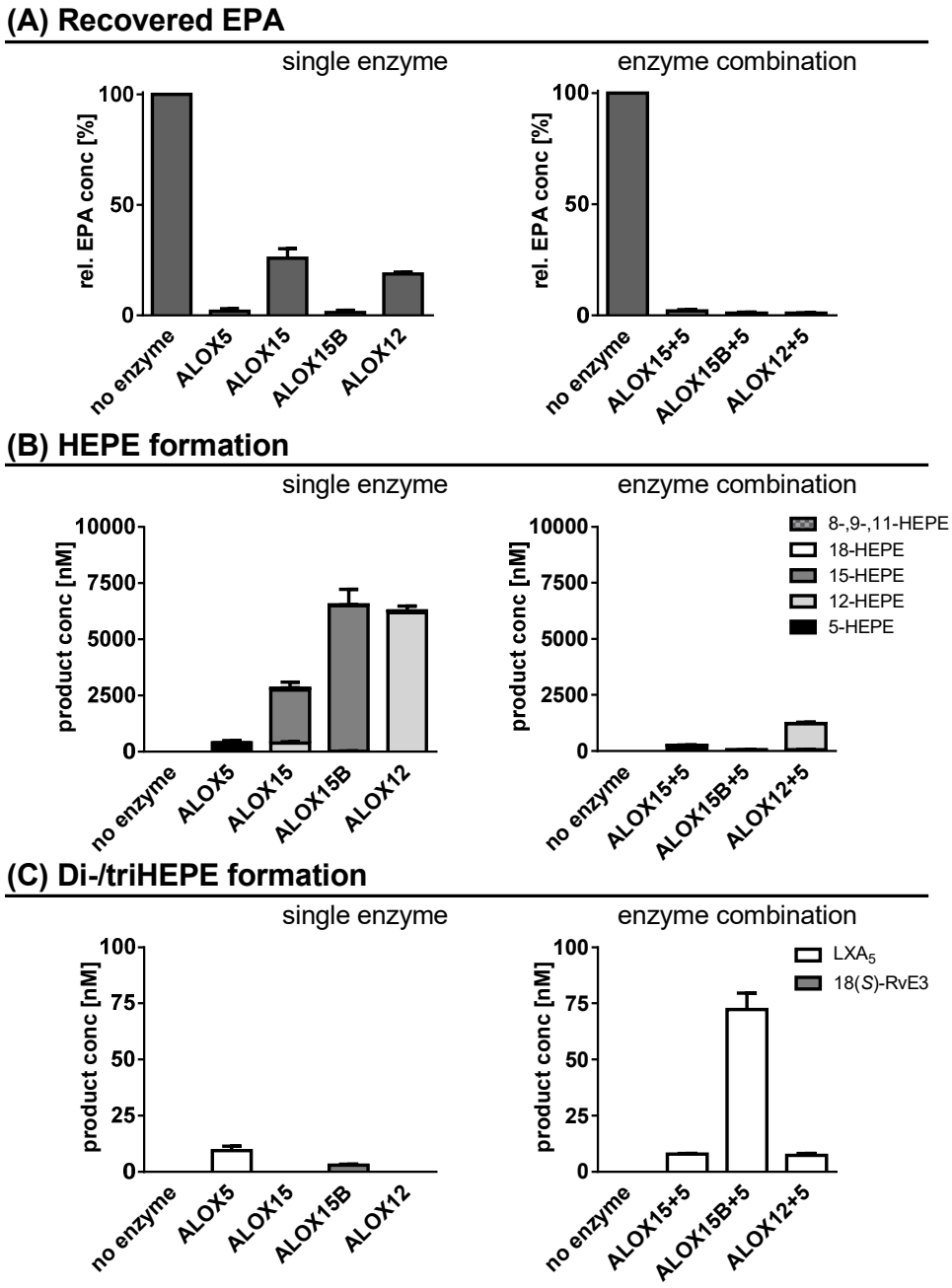

Fig. 5.1: Formation and quantification of well-established single, double and triple oxygenation products from EPA by recombinant human ALOX isoforms. Single and combined enzyme incubations were carried out as described (10 µM EPA, 15 min, RT; n = 3) and remaining substrate (EPA) as well as specific mono-, di- and tri-HEPEs that could be identified based on authentic standards were quantified by LC-MS/MS. (**A**) Recovered EPA relative to no enzyme incubation in %; (**B**) assay concentration of EPA derived hydroxy fatty acids (HEPEs); (**C**) assay concentration of EPA derived specialized pro-resolving mediators comprising di- and trihydroxy fatty acids (di-/triHEPEs).

Interestingly, HEPE formation during consecutive incubations of human ALOX15, ALOX15B and ALOX12 with human ALOX5 was clearly lower compared to single enzyme incubations (Fig. 5.1 B, right), while the recovered EPA indicated complete substrate consumption. Moreover, the ratios of 5-lipoxygenation product vs. 12/15-lipoxygenation product(s) were different for each enzyme combination. For the ALOX12+ALOX5 combination 12-HEPE levels were higher than 5-HEPE levels (5-HEPE:12-HEPE 1:18). For the ALOX15+ALOX5 combination 5-HEPE was the major mono-oxygenation product, whereas 12-HEPE and 15-HEPE were detected in lower amounts (5-HEPE>12-HEPE>15-HEPE = 32:11:1). For the ALOX15B+ALOX5 combination only small amounts of mono-HEPEs were detected with 15-HEPE being the major reaction product, while 5-HEPE was not detected (Fig. 5.1 B, right). Apparent EPA consumption and formation of monohydroxy PUFA indicate that ALOX isoforms are capable of converting EPA to further products other than HEPEs, which was particularly evident for ALOX5 single enzyme and combined incubations (Fig. 5.1 A+B).

5.3.2 Formation of secondary and tertiary oxygenation products

In order to further explore the product pattern of human ALOX isoforms, we next investigated the formation of secondary and tertiary oxygenation products in the single and combined enzyme incubations. For instance, 15-HpEPE formed during the incubation of ALOX15 and ALOX15B can further be converted by ALOX5 to 5,15-diHpEPE. The same product could also be formed when ALOX15 or ALOX15B employ their own EPA oxygenation product (15-HpEPE) as substrate for secondary oxygenation. When we quantified specific di- and triHEPE compounds, we found the formation of small amounts of lipoxin A_5 [5(*S*),6(*R*),15(*S*)-triHEPE] in the ALOX5 sample (Fig. 5.1 C, left), which was also formed when ALOX5 was combined with ALOX15, ALOX15B or ALOX12 (Fig. 5.1 C, right). Only small amounts of 18(*S*)-RvE3 [17(*R*),18(*S*)-diHEPE] were detected in the ALOX15B incubation sample (Fig. 5.1 C, left), while detected levels of RvE2 [5(*S*),18(*R*)-diHEPE] were not considered because SRM transitions were inconsistent (appendix Fig. 8.8 A).

Tab. 5.1: Relative distribution of primary and secondary oxygenation products for ALOX5, ALOX15, ALOX15B and ALOX12 incubations as well as combined incubations of these enzymes with ALOX5. Estimates for the share of mono-, double and triple oxygenated compounds were determined based on relative abundance (peak areas) at *m/z* 317.2, 333.2 and 349.2 in selected ion monitoring mode. Monohydroxy fatty acids at *m/z* 317.2 (5-HEPE, 12-HEPE, 15-HEPE) were identified by comparing their retention times with those of authentic standards. For double oxygenated compounds (*m/z* 333.2, retention time between 9.0–17 min) and triple oxygenated compounds (*m/z* 349.2, retention time between 5.0–13 min) areas of peaks exceeding a height of 5×10^5 cps and signal of no-enzyme incubation were summed (n = 3).

Enzyme(s)	*m/z* 317.2 [%]	*m/z* 333.2 [%]	*m/z* 349.2 [%]
ALOX5	29 ± 4	70 ± 4	1.1 ± 0.1
ALOX15	73 ± 3	25 ± 3	2.1 ± 0.05
ALOX15B	97 ± 0.5	3.0 ± 0.5	0.30 ± 0.04
ALOX12	98 ± 0.4	1.6 ± 0.2	0.79 ± 0.14
ALOX15+5	23 ± 4	73 ± 3	4.8 ± 0.7
ALOX15B+5	3.0 ± 0.6	89 ± 1	8.1 ± 0.4
ALOX12+5	44 ± 2	53 ± 2	2.9 ± 0.03

Due to the low formation of these specific double and triple oxygenated compounds, we next screened for EPA derivatives containing two or three oxygen atoms (*m/z* 333.2 or *m/z* 349.2, respectively). An estimation for the relative shares of mono-, double and triple oxygenated EPA derivatives in the single and combined enzyme incubation samples based on peak areas (SIM, without fragmentation) is summarized in Tab. 5.1. We found that for ALOX12 and ALOX15B the relative shares of the mono-oxygenated EPA derivatives were dominant. Only minor amounts (less than 5%) of presumed double and triple oxygenated EPA derivatives (*m/z* 333.2, *m/z* 349.2) were formed. For ALOX15 the monohydroxy derivatives contributed 73% to the product mixture. With this enzyme about 25% double oxygenated EPA derivatives were formed. Surprisingly, for ALOX5 an inverse relation was determined. Here, the mono-oxygenated EPA derivative (5-HEPE) only contributed 29% to the product mixture, whereas the relative share of double oxygenated products was 70%. In the consecutive incubations the relative shares of mono-oxygenation products were lower when compared with the single enzyme incubations. Here, double oxygenation products prevailed for most enzyme combinations. In fact, for ALOX15B+ALOX5 combination almost 90% of the reaction products were double oxygenated derivatives and with this enzyme combination we observed up to 8%

triple oxygenation products (Tab. 5.1). A similar share of triple oxygenation products was also found for ALOX15+ALOX5 combination.

5.3.3 Structural elucidation of secondary ALOX products of EPA

Suggested structures of the oxygenated EPA derivatives were tentatively identified based on their fragmentation patterns via LC-MS/MS of the most abundant double and selected triple oxygenated products (Fig. 5.2). These products were absent in the no-enzyme controls, in which PBS was added to the incubation mixture instead of the enzyme preparation (Fig. 5.2)**.** No-substrate controls, in which MeOH was added instead of EPA, were also run (appendix, Fig. 8.7). The fragmentation patterns indicate the position of the different OH-groups as shown for representative fragmentation patterns in Fig. 5.3 (MS/MS data of all indicated compounds are summarized in the appendix; Fig. 8.9–10). It should be noted that neither the configuration of the stereo-centers, i.e. of the hydroxy group bearing C-atoms (*S* or *R*) nor the configuration (*E* or *Z*) of the double bonds or their position can be deduced from fragmentation patterns.

First, we analyzed the double oxygenated EPA derivatives formed by ALOX5 (Fig. 5.2 A). Here, we found that two 5,12-diHEPE isomers (compounds 8, 9) were dominant and 5,6-diHEPE isomers (compounds 16, 19) were also present (Tab. 5.2). The most plausible explanation for the formation of these compounds is hydrolysis of a 5,6-LTA_5 intermediate. ALOX5 exhibits a leukotriene synthase activity [31] and thus is capable of converting ARA to 5,6-epoxy LTA_4. Our data indicate that a similar reaction does also proceed with EPA. Incubations of EPA with $^{18}O_2$ gas and in $H_2{}^{18}O$ buffer support the formation of 5,6- and 5,12-diHEPE via hydrolysis of an epoxide intermediate (Fig. 5.8). Surprisingly, we also detected the formation of 5,15-diHEPE (compound 11) in the single enzyme incubation sample (Fig. 5.2, Tab. 5.2). Although we did not look in detail into the biosynthetic mechanism of this product, it might be possible that 5-HpEPE, which is formed as major mono-oxygenation product of EPA, is used as substrate by the enzyme for subsequent C15 oxygenation. This mechanistic scenario is

supported by the formation of this product during incubations with $^{18}O_2$ gas and in $H_2{}^{18}O$ buffer (Fig. 5.8). For effective oxygenation of C15 the substrate should be aligned inversely at the active site of the enzyme when compared with EPA.

When we analyzed the double oxygenated products formed by human ALOX15 we observed a rather complex product mixture and compounds 3, 4, 6, 14, 17 and 20 were dominant (Fig. 5.2 A). The suggested chemical structures of these compounds, which were deduced from their fragmentation patterns (Fig. 5.3; appendix Fig. 8.9), are summarized in Tab. 5.2. It can be seen that 8,15-dihydroxy isomers (compound 3, 4, 6) were the major double oxygenated products. These compounds can either be formed via oxygenation of 15-HpEPE by the enzyme or by spontaneous hydrolysis of a 14,15-LTA_5 intermediate. The formation of a 14,15-LTA_4 intermediate from ARA has previously been shown for purified rabbit ALOX15 [6]. Incubation of EPA and ALOX15 in $H_2{}^{18}O$ buffer indicate that while compounds 3 and 4 are formed by hydrolysis of an epoxide intermediate, compound 6 is more likely an oxygenation product of 15-HpEPE (Fig. 5.9, appendix Fig. 8.12). In addition, we observed the formation of 14,15-dihydroxy EPA (compound 14) and this product can also be formed via hydrolysis of a 14,15-epoxide intermediate or via sequential double oxygenation of EPA, which seems to be the prevailing formation route under our experimental conditions (Fig. 5.9). Finally, we observed the formation of two epoxy-hydroxy isomers [13-OH-14(15)-epoxy EPA (compound 17) and 10-OH-11(12)-epoxy EPA (compound 20)]. Epoxy-hydroxy fatty acids are typical hydroperoxidase products, which are formed when ALOX isoforms decompose their primary oxygenation products. This reaction is initiated by homolytic cleavage of the hydroperoxy group and secondary rearrangement of the alkoxy radical. This formation route is supported by the incubation of ALOX15 with $^{18}O_2$ gas indicating the insertion of two ^{18}O-atoms (Fig. 5.9). A similar pattern of secondary products has previously been described when ARA was incubated with pure rabbit ALOX15 [6].

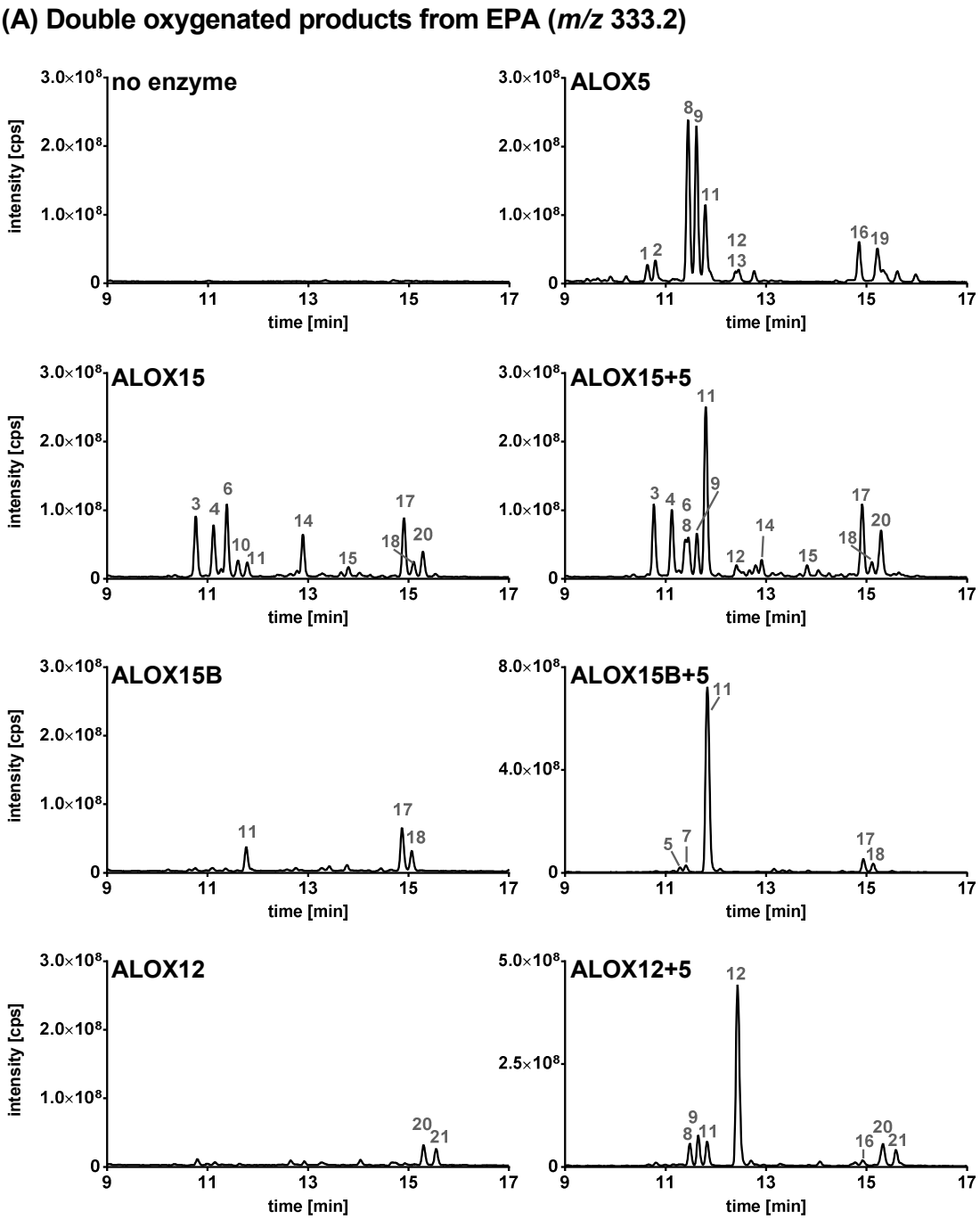

Fig. 5.2: Formation of (**A**) double and (**B**) triple oxygenation products from EPA by recombinant human ALOX isoforms. Incubations were carried out as described (10 µM EPA, 15 min, RT) and since only low levels of specific di- and triHEPEs were quantified (Fig. 5.1), single and combined enzyme incubations were screened for formation of further double and triple oxygenated compounds from EPA. Shown are total ion chromatograms (TIC) of product ion scans of *m/z* 333.2 and *m/z* 349.2 (100–350 Da, CE ramp –18 to –26 V). Major double oxygenation products are labeled as compounds 1–21 and selected triple oxygenated products are labeled as compound 22–26 and listed in Tab. 5.2.

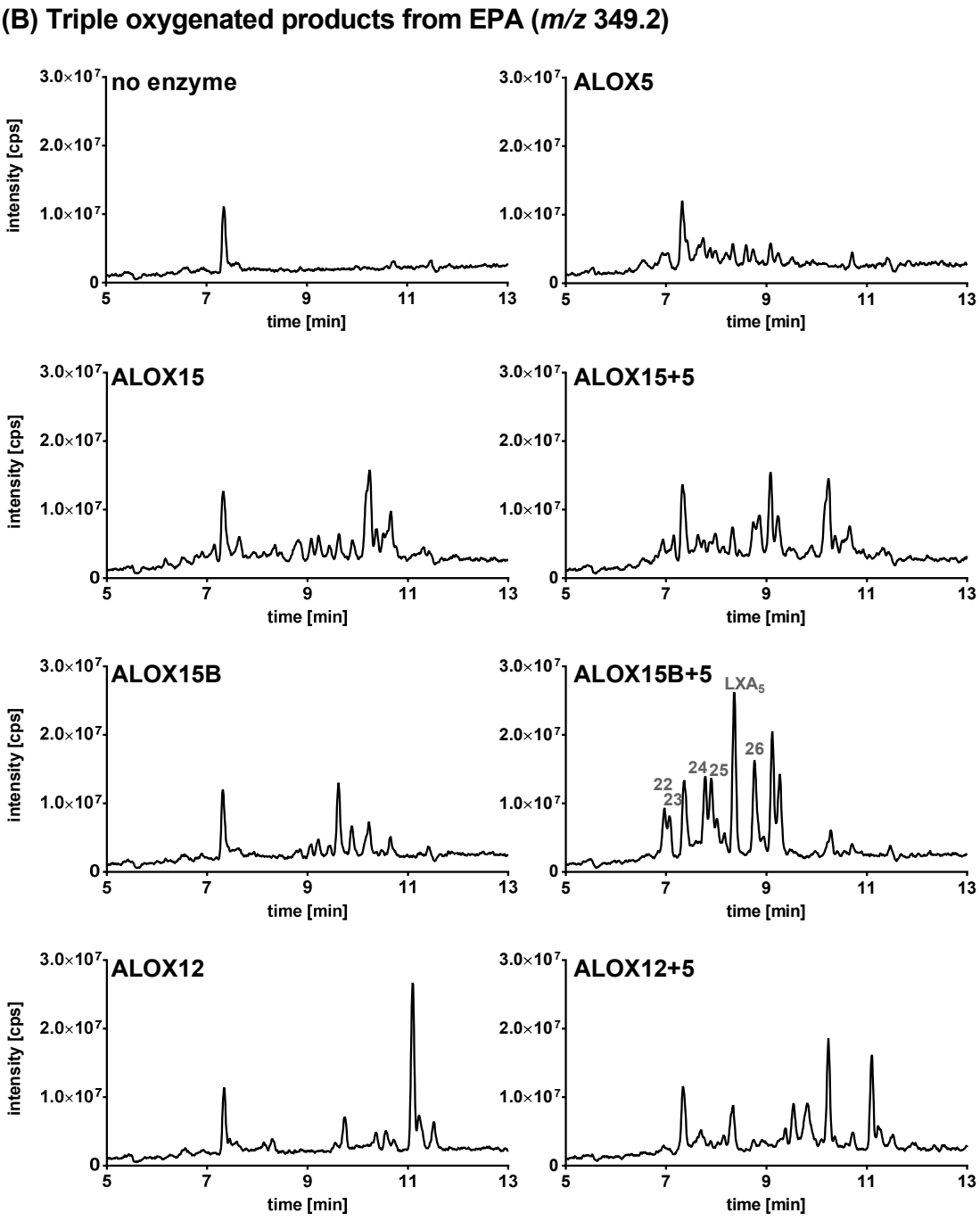

Fig. 5.2: Continued. Formation of (**A**) double and (**B**) triple oxygenation products from EPA by recombinant human ALOX isoforms.

Next, we analyzed the products formed by consecutive incubation of ALOX15 and ALOX5 and observed a similarly complex product pattern (Fig. 5.2 A). We also detected 8,15-dihydroxy (compounds 3, 4, 6) and epoxy-hydroxy (compounds 17, 20) EPA derivatives. The major difference to the single ALOX15 incubation was that in the combined incubation large amounts of 5,15-diHEPE (compound 11) were formed. This product was only present in small amounts in the ALOX15 single incubation and originated from either ALOX5-catalyzed oxygenation of 15-H(p)EPE or ALOX15-catalyzed oxygenation of 5-H(p)EPE. In both cases, this product represents a double oxygenation product of EPA, which is supported by incubations in $^{18}O_2$ atmosphere and $H_2{}^{18}O$ buffer (appendix, Fig. 8.11).

The pattern of the double oxygenated EPA derivatives formed by human ALOX15B was much less complex regardless of whether this enzyme reacted alone or in combination with ALOX5 (Fig. 5.2 A). The major products identified in the single enzyme incubation were two isomers of 13-OH-14(15)-epoxy EPA (compound 17, 18). These data indicate that ALOX15B does also exhibit a lipohydroperoxidase activity and thus, the enzyme is capable of converting its major EPA oxygenation product (15-HpEPE) to secondary decomposition products. To the best of our knowledge this has not been reported before for this enzyme. In addition, we observed the formation of 5,15-diHEPE (compound 11) and these data indicate that this enzyme is also capable of catalyzing C5 oxygenation. This result was somewhat surprising since ALOX15B exhibits a rather narrow substrate specificity [32]. The most plausible scenario for the formation of this compound is that after the enzyme has completely consumed EPA (Fig. 5.1 A) it may bind 15-HpEPE at the active site in an inverse head-to-tail like fashion and then introduces dioxygen at C5. Similar products/mechanisms have previously been suggested for ARA conversion by soybean LOX-1 [9] and rabbit ALOX15 [6]. When ALOX15B acted in concert with ALOX5 (Fig. 5.2 A) 5,15-diHEPE was identified as dominant oxygenation product and the biosynthetic pathway (sequential double oxygenation of EPA by ALOX15B and ALOX5) of this product is straightforward. Analyzing the pattern of

double oxygenated compounds formed by ALOX12 we observed small amounts of 10-OH-11(12)-epoxy EPA (compounds 20, 21; Fig. 5.2 A). These compounds constitute secondary decomposition products of 12-HpEPE and their existence indicates the lipohydroperoxidase or lipoperoxide isomerase activity of ALOX12. 10-OH-11(12)-epoxy EPA derivatives have previously been named hepoxilin B4 [33]. Acting in concert with ALOX5, 5,12-diHEPE was the dominant reaction product (compound 12; Fig. 5.2 A) and its biosynthesis involves most probably sequential oxygenation of EPA by ALOX12 and ALOX5.

Tab. 5.2: Tentative structures of EPA derived double and triple oxygenated products formed by different recombinant human ALOX isoforms. Chemical structures for EPA derived products (Fig. 5.2) were suggested based on their fragmentation patterns (Fig. 5.3, appendix Fig. 8.9–10). Compounds with similar fragmentation patterns and retention times were regarded as the same product. Marks (×) indicate enzyme incubations in which the respective compound was detected.

Compound	suggested positional isomer	ALOX						
		5	15	15+5	15B	15B+5	12	12+5
1	–	×						
2		×						
3	8,15-diHEPE		×	×				
4			×	×				
6			×	×				
10			×					
5	5,15-diHEPE					×		
7						×		
11		×	×	×	×	×		×
8	5,12-diHEPE	×		×				×
9		×		×				×
12		×		×				×
13		×						
14	14,15-diHEPE		×	×				
16	5,6-diHEPE	×						×
19		×						
15	13-OH-14(15)-EpETE		×	×				
17			×	×	×	×		
18			×	×	×	×		
20	10-OH-11(12)-EpETE		×	×			×	×
21							×	×
22	5,14,15-triHEPE					×		
23						×		
24	5,6,15-triHEPE					×		
25						×		
26						×		

A similar pattern of products was observed in combined incubations when ALOX12 and ALOX5 were incubated simultaneously (simultaneous addition of both enzymes) and in inverse-order (starting the consecutive incubation with ALOX5 prior ALOX12 addition). However, the relative abundances of the products varied. When we initiated product formation by the addition of ALOX12 and subsequently added ALOX5 compound 12 (5,12-diHEPE, Fig. 5.2) was dominant. In contrast, in simultaneous ALOX12+ALOX5 incubations higher amounts of ALOX5 derived products (compounds 8, 9, 11) were present. These products prevailed when the oxygenation reaction was initiated by the addition of ALOX5 prior to ALOX12. Similarly, ALOX5 products (compounds 8, 9) were formed in higher abundances in ALOX15B/ALOX5 assays, when the reaction was initiated by the addition of ALOX5 (appendix, Fig. 8.13).

Formation of triple oxygenated compounds from EPA was one order of magnitude lower than formation of double oxygenated products (Fig. 5.2 B). Particularly, consecutive incubation of ALOX15B and ALOX5 led to diverse triple oxygenated products including LXA_5 and various 5,6,15-triHEPE isomers as well as 5,14,15-triHEPE (LXB_5) isomers (for MS/MS spectra see appendix, Fig. 8.10). Consistent with product specificity of tested ALOX isoforms, 18-HEPE derived E-series resolvins were mostly < LLOQ.

Fig. 5.3 (right, page 131): Fragmentation patterns and suggested structures of representative double oxygenation products formed from EPA by different recombinant human ALOX isoforms. Human ALOX isoforms were incubated with EPA (10 µM, 15 min, RT) and the major double oxygenation products shown in Fig. 5.2 (no reference compound) were analyzed by mass spectrometry. Shown are collision induced dissociation product ion spectra of *m/z* 333.2 (100–350 Da, CE ramp –18 to –26 V) alongside suggested structures and fragmentation sites for representative compounds formed during incubation of ALOX15+ALOX5 (compound 11), ALOX12+ALOX5 (compound 12), ALOX5 (compound 19) as well as ALOX15 (compound 6, 14, 20). Note that only one of several possible double bond configurations is shown.

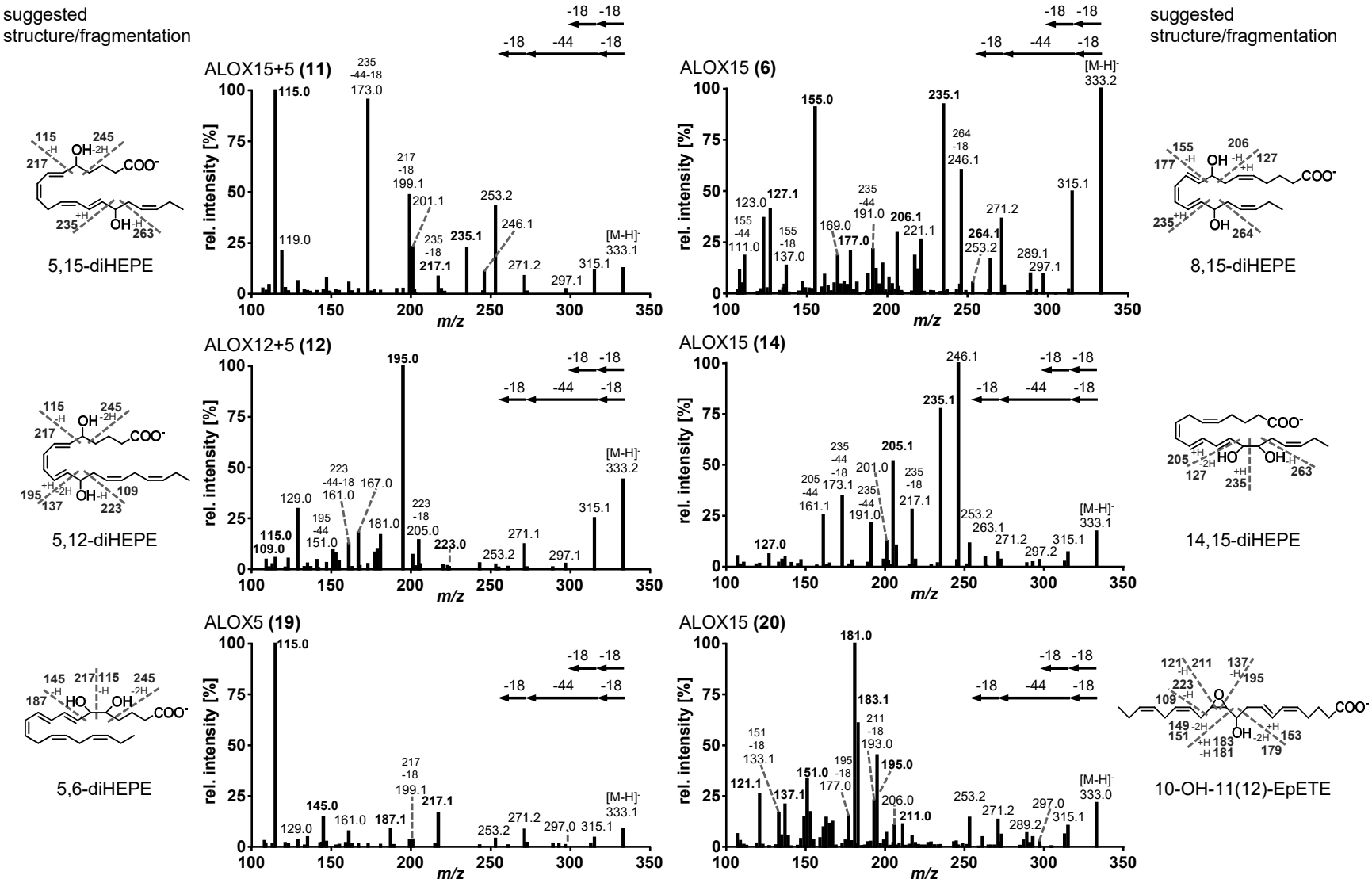
suggested structure/fragmentation
ALOX15+5 (11)
ALOX15 (6)
suggested structure/fragmentation
5,15-diHEPE
8,15-diHEPE
ALOX12+5 (12)
ALOX15 (14)
5,12-diHEPE
14,15-diHEPE
ALOX5 (19)
ALOX15 (20)
5,6-diHEPE
10-OH-11(12)-EpETE
rel. intensity [%]
m/z
[M-H]-
-18 -18
-18 -44 -18

5.3.4 18-HEPE formation and ALOX-catalyzed 18-HEPE oxygenation

First, we explored whether 18-H(p)EPE, an important pathway marker and precursor for E-series resolvins, can be formed from EPA by different ALOX isoforms. 18-HEPE was detected in the incubation mixtures of ALOX15, ALOX15B and ALOX12 exceeding the no-enzyme control 4–22-fold, while in the combined enzyme incubations 18-HEPE levels were lower (Fig. 5.4 A). To test the stereochemistry of 18-HEPE formation we analyzed the products by chiral-phase HPLC. For 18-HEPE formed by ALOX15 we observed a preponderance of the *S*-enantiomer (18(*R*)-HEPE:18(*S*)-HEPE = 1:2.5), which was less pronounced for the incubation samples of ALOX15B and ALOX12 (Fig. 5.4 B).

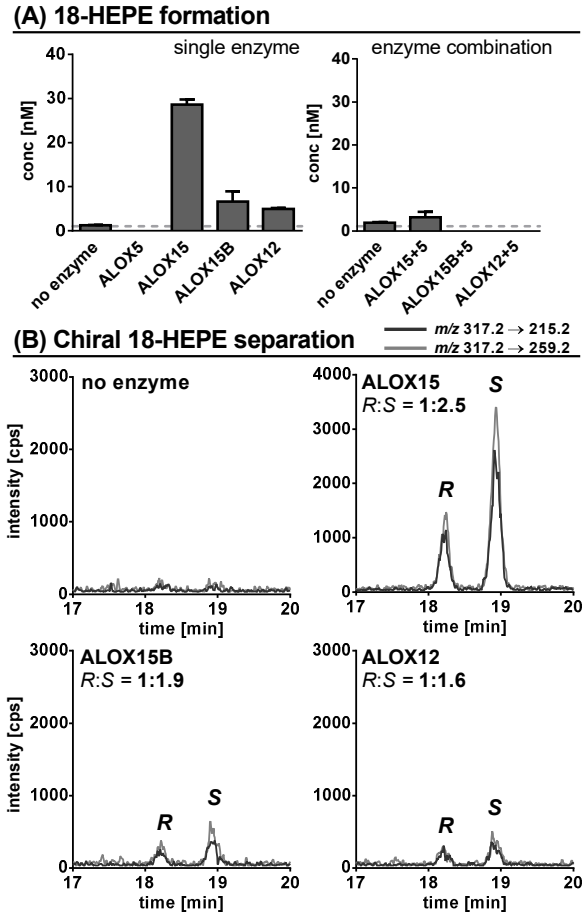

Fig. 5.4: Formation of 18-HEPE during incubations of different recombinant human ALOX isoforms with EPA. EPA was incubated with human ALOX isoforms (ALOX5, ALOX15, ALOX15B and ALOX12) alone and in combination with ALOX5 (10 µM EPA, 15 min, RT; n = 3). (**A**) Assay concentrations of 18-HEPE; (**B**) Chiral analysis of 18-HEPE formed during single enzyme incubations. Chromatographic separation was carried out with an Agilent ZORBAX SB-C8 column coupled to a Lux-Amylose-1 column (ACN/MeOH/H_2O/glacial HOAc linear gradient) and the chromatograms were recorded at two different MS/MS transitions (*m/z* 317.2 → 215.2, 259.2).

Next, we tested whether 18(*R,S*)-HEPE constitutes a suitable substrate for the different ALOX isoforms and as read-out parameters we employed i) the consumption of 18-HEPE (Fig. 5.5 A) and ii) the formation of double and triple oxygenated reaction products (Fig. 5.5 B+C). Quantifying 18-HEPE we found that ALOX5 induced major disappearance of 18-HEPE (Fig. 5.5 A, left). In fact, more than 70% of the initial substrate was consumed during the incubation period. In contrast, for ALOX15, ALOX15B and ALOX12 only minor substrate conversion was observed. When we quantified the substrate disappearance of 18-HEPE in the combined enzyme incubations we found significant substrate conversion in all samples (Fig. 5.5 A, right). This finding was not surprising since ALOX5, which effectively oxygenated 18-HEPE, was present in all samples. It was, however, surprising that the pre-incubation with ALOX15 reduced the capacity of ALOX5 for 18-HEPE oxygenation. The molecular basis for this regulatory activity has not been explored in detail. However, possible mechanisms are discussed later on in this paper (see discussion).

In principle, 18-HEPE can be converted to three different types of resolvins of the E-series: RvE1 [5(*S*),12(*R*),18(*R*)-trihydroxy EPA], RvE2 [5(*S*),18(*R*)-dihydroxy EPA], and RvE3 [17(*R*),18(*R*/*S*)-dihydroxy EPA]. When we searched our incubation samples for the formation of these products we detected significant amounts of RvE2 in the ALOX5 incubation. In the other samples RvE2 synthesis was minimal. However, significant amounts of RvE3 were present in the ALOX15B incubation (Fig. 5.5 B, left). In the combined incubation samples significant amounts of RvE2 were detected in the ALOX15B+ALOX5 incubation and in the ALOX12+ALOX5 incubation. Interestingly, in the ALOX15+ALOX5 incubation we did not observe substantial RvE2 and RvE3 formation (Fig. 5.5 B, right). Thus, here again the 18-HEPE oxygenase activity of ALOX5 was inhibited by pre-incubation with ALOX15. When we tested the formation of RvE1 in the incubation samples, we detected highest RvE1 formation in the ALOX5 sample and in the combined ALOX15B+ALOX5 and ALOX12+ALOX5 samples (Fig. 5.5 C, appendix Fig. 8.8 B+C).

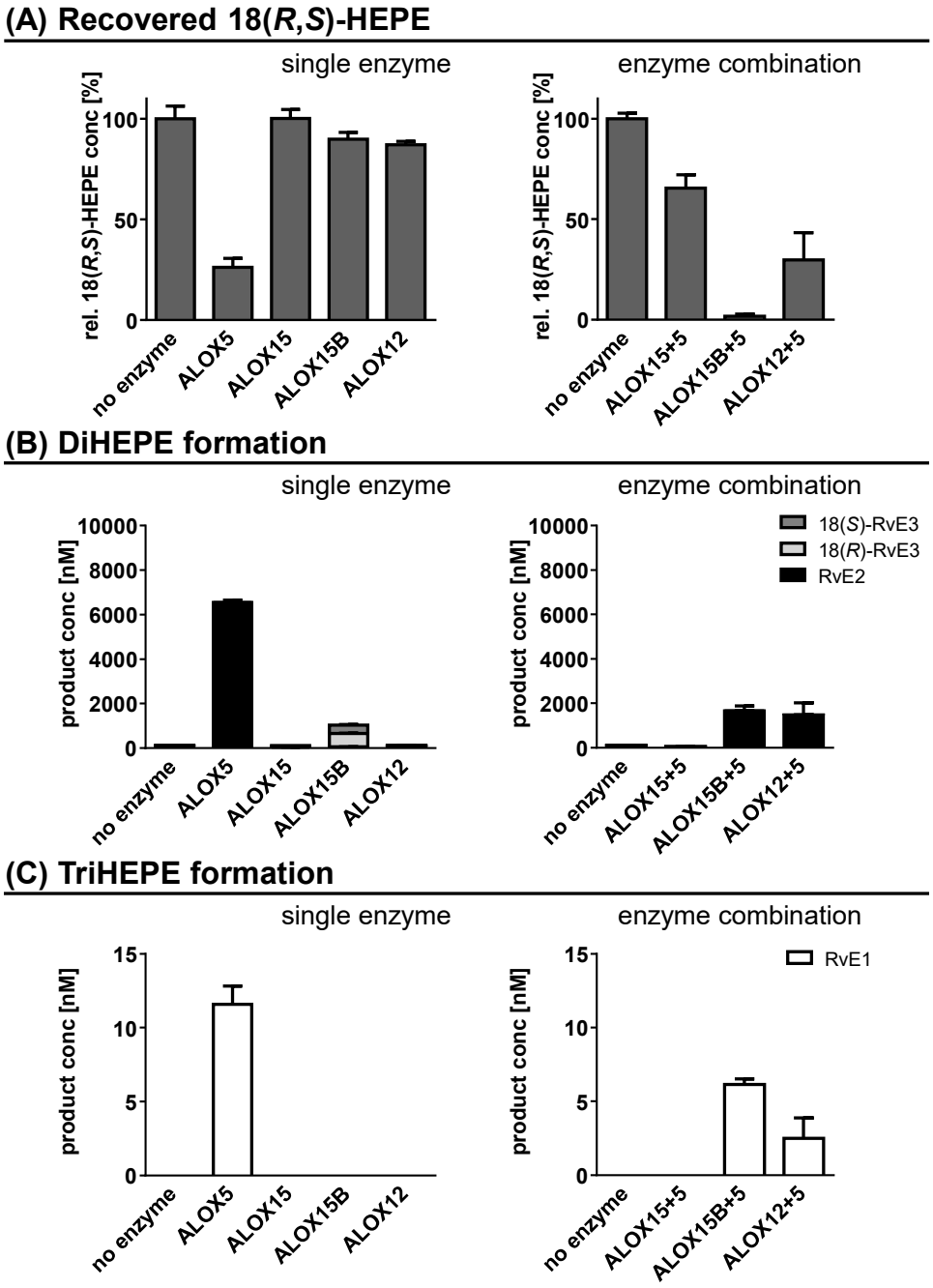

Fig. 5.5: Conversion of 18(*R*,*S*)-HEPE by recombinant human ALOX isoforms. Single and combined enzyme incubations of the different human ALOX isoforms were carried out with 18(*R*,*S*)-HEPE as described (10 µM 18(*R*,*S*)-HEPE, 15 min, RT; n = 3) and remaining substrate (18(*R*,*S*)-HEPE) as well as established di- and triHEPEs that could be identified based on authentic standards were quantified by LC-MS/MS. (**A**) Recovered 18(*R*,*S*)-HEPE after the incubation period relative to the no enzyme incubation sample in %; (**B+C**) Assay concentration of EPA derived specialized pro-resolving mediators comprising (**B**) dihydroxy eicosapentaenoic acids (diHEPEs) and (**C**) trihydroxy eicosapentaenoic acids (triHEPEs).

Finally, similar to EPA incubations, we screened 18(*R*,*S*)-HEPE incubations for other double and triple oxygenated compounds (*m/z* 333.2 and *m/z* 349.2, respectively; Fig. 5.6). We suggested different structures based on the fragmentation patterns of the formed products as shown for representative fragmentation patterns in Fig. 5.7 (MS/MS data of all indicated compounds are summarized in the appendix, Fig. 8.14–15). ALOX15 was the only enzyme for which no double or triple oxygenated compounds formed from 18-HEPE were detected, which significantly exceeded the no-enzyme incubation (Fig. 5.6). ALOX5 catalyzed the formation of another 5,18- as well as 8,18-diHEPE-isomer (compound a, b; Tab. 5.3). 18-HEPE was also accepted as substrate by ALOX12 and different 12,18-diHEPE isomers (compound c, d) were major products. Combined incubations with ALOX5 did not result in additional products. In contrast to EPA incubations, ALOX5 catalyzed the formation of relatively high levels of several triple oxygenated products and combination of ALOX5 with ALOX15B or ALOX12 showed a similar product pattern (Fig. 5.6 B). Suggested structures comprise 5,12,18-triHEPE (compound e, f; RvE1 isomers), 5,17,18-triHEPE (compound g, i) and 5,6,18-triHEPE (compound h, j) (Tab. 5.3, Fig. 5.7; appendix Fig. 8.15).

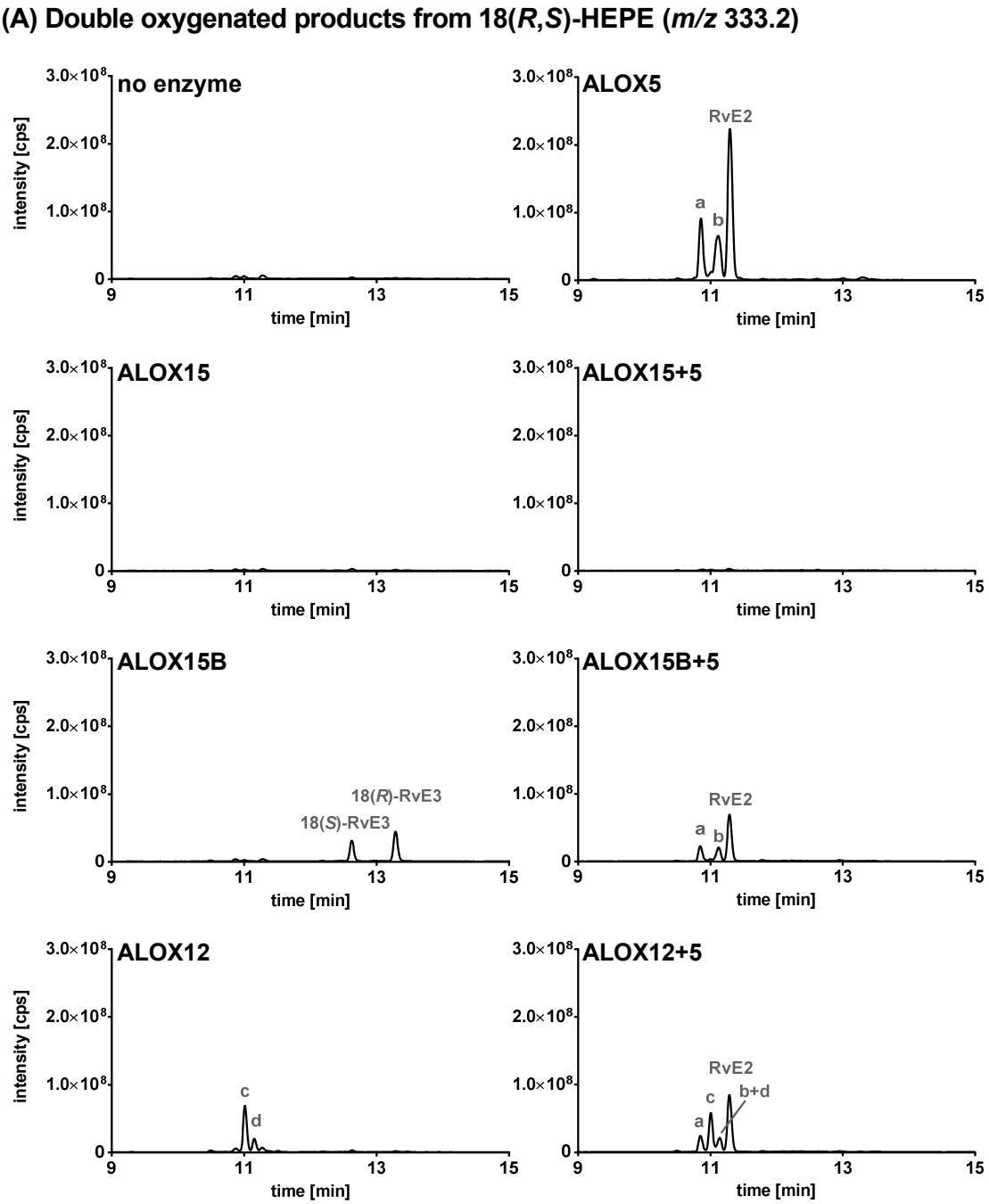

Fig. 5.6: Formation of (**A**) double and (**B**) triple oxygenation products from 18(*R*,*S*)-HEPE by recombinant human ALOX isoforms. 18(*R*,*S*)-HEPE was oxygenated by different human ALOX isoforms as described (10 µM 18(*R*,*S*)-HEPE, 15 min, RT) and single and combined enzyme incubations were screened for formation of further double and triple oxygenation products from 18(*R*,*S*)-HEPE. (**A**) Total ion chromatograms (TIC) of product ion scans of *m/z* 333.2 (100–340 Da, CE ramp –18 to –26 V) representing the double oxygenated products; (**B**) TIC traces of product ion scans of *m/z* 349.2 (100–350 Da, CE ramp –18 to –26 V) representing the triple oxygenated products. Major products are labeled as compounds a–j and listed in Tab. 5.3.

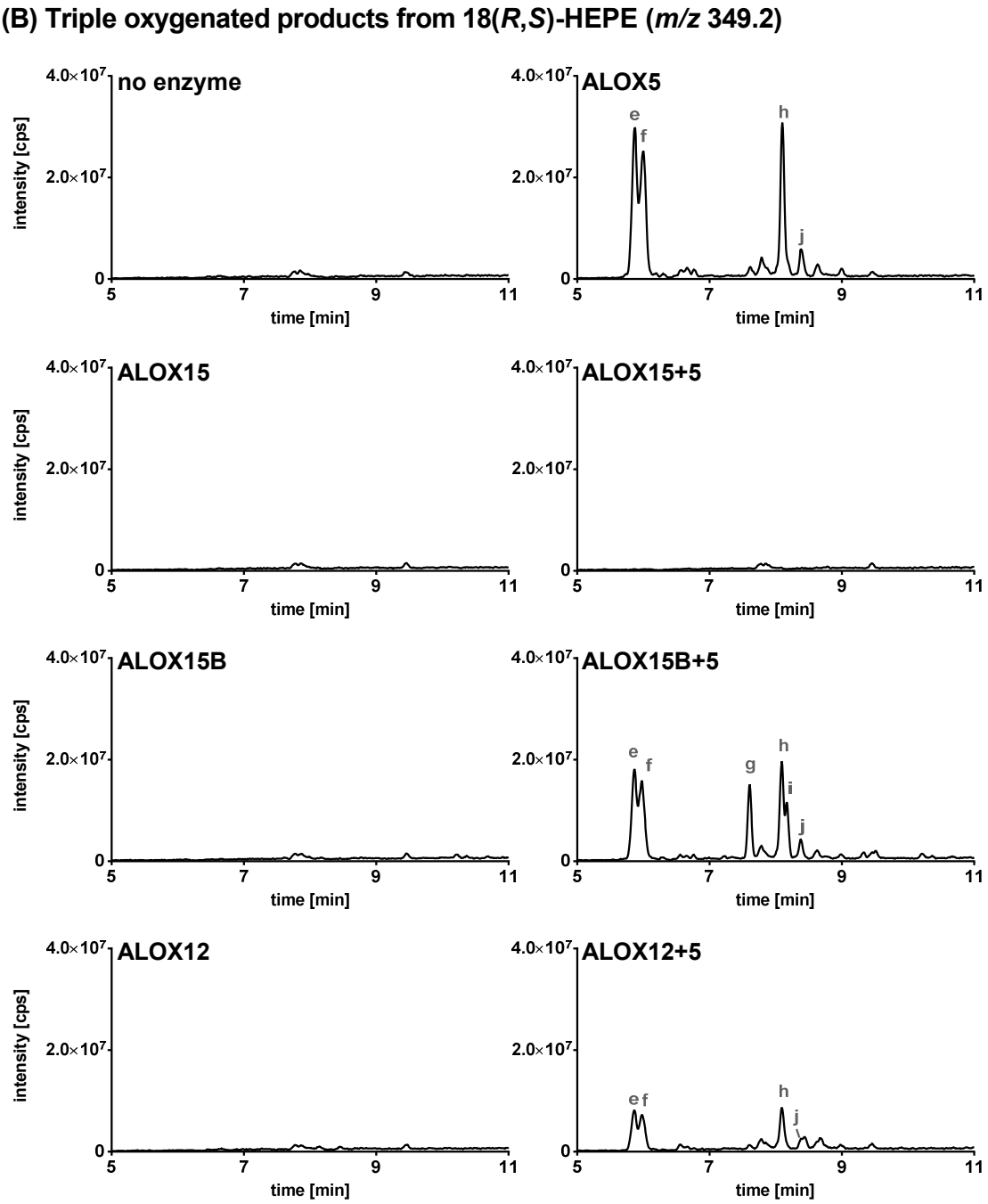

Fig. 5.6: Continued. Formation of (**A**) double and (**B**) triple oxygenation products from 18(*R*,*S*)-HEPE by recombinant human ALOX isoforms.

Tab. 5.3: Tentative structures of 18(*R*,*S*)-HEPE derived double and triple oxygenated products formed by different recombinant human ALOX isoforms. Chemical structures for 18(*R*,*S*)-HEPE derived products (Fig. 5.6) were suggested based on their fragmentation patterns (Fig. 5.7, appendix Fig. 8.14–15). Compounds with similar fragmentation patterns and retention times were regarded as the same product. Marks (×) indicate enzyme incubations in which the respective compound was detected.

Compound	suggested positional isomer	ALOX						
		5	**15**	**15+5**	**15B**	**15B+5**	**12**	**12+5**
RvE2	5(*S*),18(*R*)-diHEPE	×				×		×
18(*S*)-RvE3	17(*R*),18(*S*)-diHEPE				×			
18(*R*)-RvE3	17(*R*),18(*R*)-diHEPE				×			
a	8,18-diHEPE	×				×		×
b	5,18-diHEPE	×				×		×
c	12,18-diHEPE						×	×
d							×	×
e	5,12,18-triHEPE	×				×		×
f		×				×		×
g	5,17,18-triHEPE					×		
i						×		
h	5,6,18-triHEPE	×				×		×
j		×				×		×

Fig. 5.7 (right, page 139): Fragmentation patterns and suggested structures of representative 18(*R*,*S*)-HEPE oxygenation products formed by different recombinant human ALOX isoforms. Human ALOX isoforms were incubated with 18(*R*,*S*)-HEPE (10 µM, 15 min, RT) and the major double and triple oxygenation products shown in Fig. 5.6 (no reference compounds) were analyzed by mass spectrometry. Shown are collision induced dissociation product ion spectra of *m/z* 333.2 and *m/z* 349.2 (100–340 Da and 100–350 Da, CE ramp –18 to –26 V) alongside suggested structures and fragmentation sites for representative compounds formed during incubation of ALOX5 (compound a, b; e, h), ALOX12 (compound c) and ALOX15B+ALOX5 (compound g). Note that only one of several possible double bond configurations is shown.

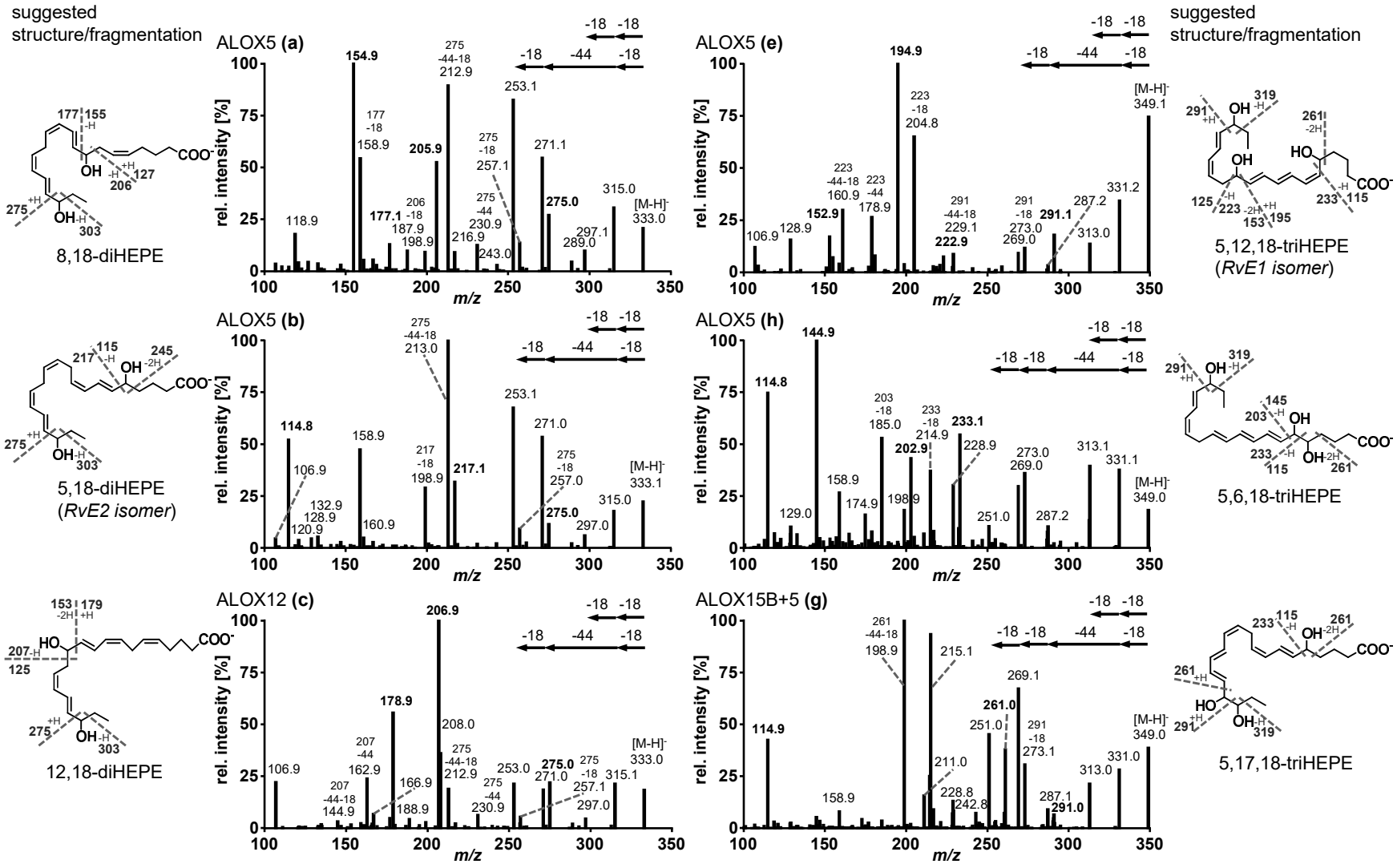
suggested structure/fragmentation
ALOX5 (a)
8,18-diHEPE
ALOX5 (b)
5,18-diHEPE (RvE2 isomer)
ALOX12 (c)
12,18-diHEPE
ALOX5 (e)
suggested structure/fragmentation
5,12,18-triHEPE (RvE1 isomer)
ALOX5 (h)
5,6,18-triHEPE
ALOX15B+5 (g)
5,17,18-triHEPE
rel. intensity [%]
m/z
[M-H]-

5.4 Discussion

ALOX5 and ALOX15 form a complex mixture of oxygenation products from EPA

Multiple hydroxylated PUFA, such as leukotrienes, lipoxins and resolvins, exhibit both pro- and anti-inflammatory bioactivities. These compounds can be formed from EPA, such as chemoattractant LTB_5 [34], lipoxins LXA_5 and LXB_5 [35] or 18-HEPE derived pro-resolving E-series resolvins [21, 36]. Since 18-HEPE is not a main product of ALOX catalyzed EPA oxygenation (Fig. 5.4), ALOX isoforms were not capable of catalyzing substantial formation of E-series resolvins on their own or in combination with ALOX5 (Fig. 5.1 C). However, structurally similar dihydroxylated compounds formed by a single or two consecutively acting ALOX isoforms might also be able to mediate physiological processes. We found that the spectrum of such products – especially for ALOX5 and ALOX15 alone or in combination – is rather complex with major products being 5,6-, 5,12-, 5,15-, 8,15-, 14,15-diHEPE isomers as well as epoxy-hydroxy-derivatives. Compared to ALOX12 and ALOX15B, ALOX5 and ALOX15 give rise to a broader product pattern: Both enzymes are capable of catalyzing hydrogen abstraction from different bisallylic methylenes of ARA (C7 and C10 for ALOX5, C13 and C10 for ALOX15) and this property is the mechanistic basis for the leukotriene synthase activities of these two enzymes [6, 31]. In other words, ALOX5 and ALOX15 are more flexible when binding their substrates at the active site and this flexibility likely contributes to the complex patterns of oxygenation products we observed in this study.

We found that ALOX5 forms at least two 5,12-diHEPE isomers (compound 8, 9; Fig. 5.2), which likely originate from hydrolysis of a 5,6-epoxy-leukotriene intermediate. This mechanistic scenario is supported by the fragmentation patterns of compounds 8 and 9 formed in the presence of heavy oxygen isotopes (as shown for compound 8; Fig. 5.8). Under $^{18}O_2$ atmosphere no products carrying two ^{18}O-atoms ($[M-H]^-$ at *m/z* 337.2) were observed (Fig. 5.8 A). In fact, products carrying one ^{18}OH- and one ^{16}OH-group ($[M-H]^-$ at *m/z* 335.2) were

formed and fragmentation spectra indicate that the ^{18}OH-group was located at C5. This oxygen atom should thus be incorporated during C5 oxygenation by ALOX5 (fragment *m/z* 335.2 → 197.0). Consistent with this data, we found that when the reaction was carried out in $H_2{}^{18}O$ buffer the fragmentation pattern (fragment *m/z* 335.2 → 195.0) indicated that the ^{18}O-atom is introduced at C12 (Fig. 5.8 B). This oxygen atom must thus originate from $H_2{}^{18}O$. A similar mechanism involving hydrolysis of a 5,6-epoxide intermediate leads to the formation of 5,6-diHEPE isomers (compounds 16, 19). In contrast to the 5,12-diHEPE isomers (compounds 8, 9), compound 11 (5,15-diHEPE) is likely formed via the double lipoxygenation pathway and three lines of experimental evidence support this conclusion: i) This product is also formed in the combined ALOX15+ALOX5 incubation showing a consistent retention time and fragmentation pattern. ii) When EPA oxygenation was carried out under $^{18}O_2$ atmosphere two ^{18}OH-groups were present ($[M-H]^-$ at *m/z* 337.2). Furthermore, the fragmentation pattern indicates an ^{18}OH-group at C5 (*m/z* 337.2 → 117.0) and at C15 (*m/z* 337.2 → 99.1; Fig. 5.8 A). iii) When the reaction was carried out in $H_2{}^{18}O$ buffer compound 11 carries two ^{16}OH-groups [*m/z* 333.2 → 115.0 (^{16}OH-group at C5) and *m/z* 333.2 → 97.1 (^{16}OH-group at C15)] and these data indicate the lack of incorporation of ^{18}O from $H_2{}^{18}O$ (Fig. 5.8 B). In contrast to the dominating dihydroxy EPA derivatives, only few fragments were observed for the two smaller but distinct compounds 1 and 2. Fragment spectra indicate the presence of an OH-group at C5 (*m/z* 333.2 → 115.0) and C18 (*m/z* 333.2 → 275.1). However, incubation with $^{18}O_2$ gas indicates incorporation of only one ^{18}O-atom at C5 and incubation in $H_2{}^{18}O$ buffer supports formation involving hydrolysis of an epoxide intermediate. Since no mechanism for such a radical rearrangement is known, these compounds might constitute structures differing from the commonly observed diHEPE derivatives. As unexpectedly the majority of the detected EPA derived compounds by ALOX5 are secondary oxygenation products, it might be possible that further oxygenation or decomposition products are formed, which were not covered by the analyzed double and triple oxygenated compounds. More detailed experiments are required to address this question.

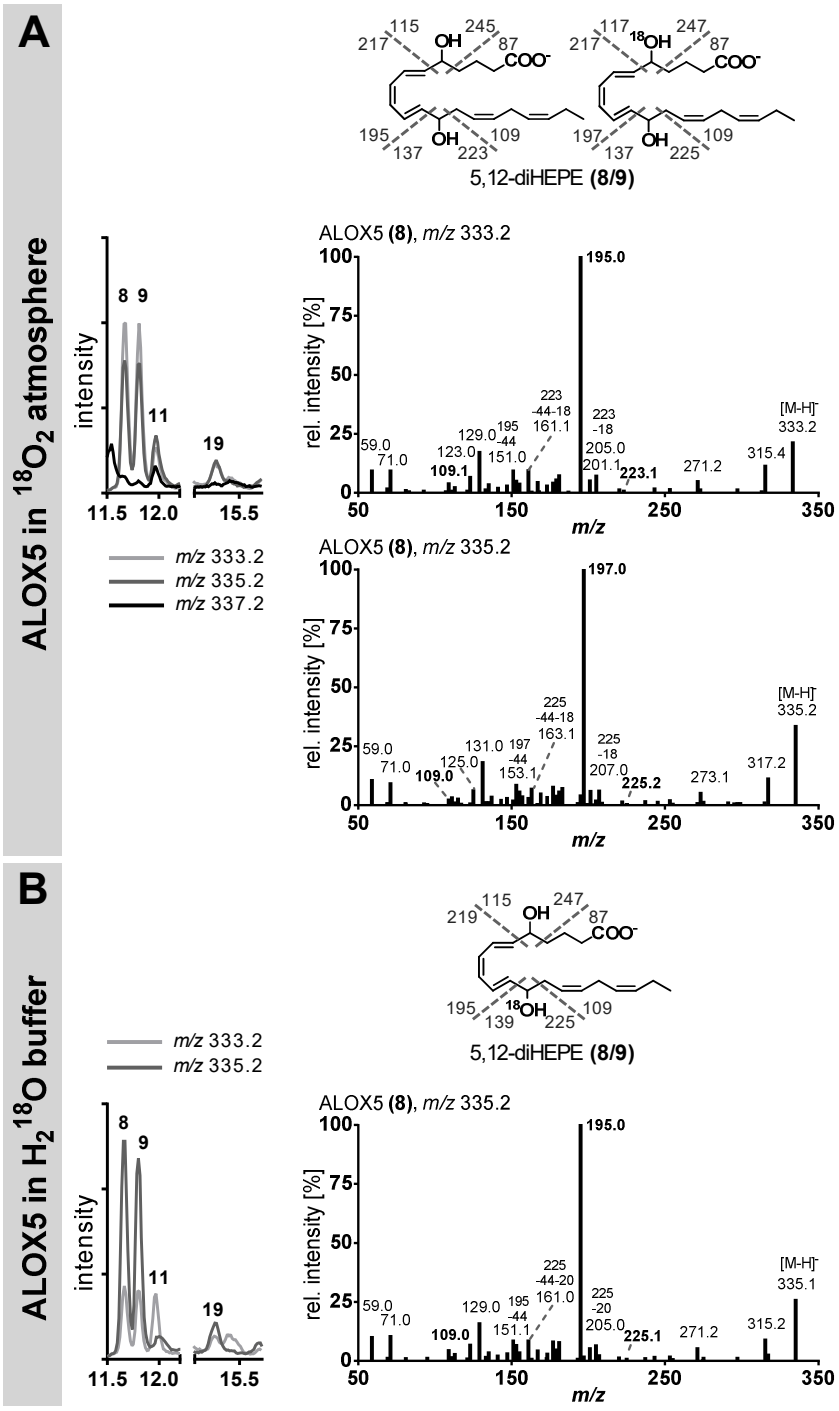

Fig. 5.8: Formation of double oxygenated products during EPA incubation with recombinant human ALOX5 (10 µM EPA, 15 min, RT) in (**A**) $^{18}O_2$ atmosphere or (**B**) in $H_2{}^{18}O$ buffer. Shown are total ion chromatograms of product ion scans (55–340 Da, *m/z* 333.2, 335.2 and 337.2; CE ramp –18 to –26 V) as well as collision induced dissociation product ion spectra of exemplary products (as indicated in Fig. 5.2). Suggested stuctures and fragmentation sites are given considering incorporation of ^{18}O- and/or ^{16}O-atoms. Note that only one of several possible double bond configurations is shown.

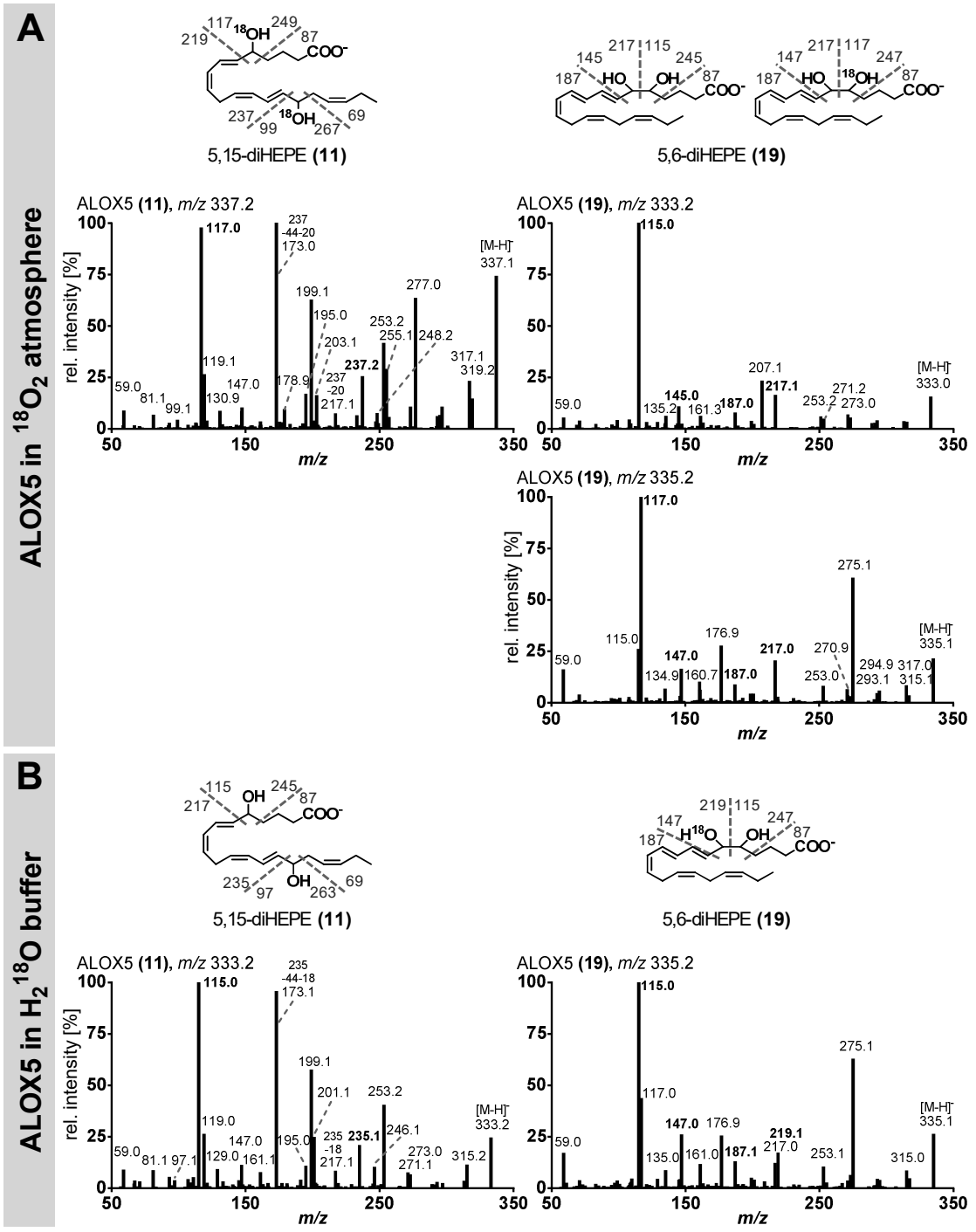

Fig. 5.8: Continued. Formation of double oxygenated products during EPA incubation with recombinant human ALOX5 (10 µM EPA, 15 min, RT) in (**A**) $^{18}O_2$ atmosphere or (**B**) in $H_2{}^{18}O$ buffer.

For ALOX15 we observed the most complex pattern of reaction products, which may result from its catalytic multiplicity: i) ALOX15 exhibits a pronounced double oxygenase activity since it is capable of converting its major reaction product of ARA oxygenation [15-H(p)ETE] to the double oxygenation products 8,15- and 5,15-diH(p)ETE [6, 11]. ii) Similar to ALOX5 this enzyme exhibits a leukotriene synthase activity and thus, 14,15-LTA_4 hydrolysis products are formed [6]. iii) ALOX15 does also exhibit a pronounced lipohydroperoxidase (hydroperoxide isomerase) activity and this activity is responsible for the formation of the epoxy-hydroxy derivatives. The two dominant products, compound 3 and 4 (Fig. 5.2), which were tentatively identified as 8,15-diHEPE isomers on the basis of their fragmentation patterns, are likely to be formed via a similar mechanism as the 5,12-diHEPE isomers formed by ALOX5 (LTA_5 hydrolysis). Incubation under $^{18}O_2$ atmosphere (Fig. 5.9 A) suggested the presence of one ^{18}OH-group (*m/z* 335.2 → 208.1), which is not located at C8 (*m/z* 335.2 → 155.0) but at C15 (*m/z* 335.2 → 179.1). When the incubation was carried out in $H_2{}^{18}O$ buffer (Fig. 5.9 B) an ^{18}OH-group was identified at C8 (*m/z* 335.2 → 157.0). In contrast, the third 8,15-diHEPE isomer (compound 6) apparently originated from double lipoxygenation since incubations in $H_2{}^{18}O$ buffer indicate the insertion of two ^{16}O-atoms from the atmosphere for compound 6 (appendix, Fig. 8.12). The fragmentation patterns of compounds 3 and 4 on the one hand and of compound 6 on the other do not overlap completely (appendix, Fig. 8.9), which might be caused by different double bond configurations as a result of the formation routes. For another dominant product (compound 14) the fragmentation patterns suggested the structure of 14,15-diHEPE. This compound is formed via the double oxygenation pathway since two ^{18}OH-groups were incorporated when the reaction was carried out under $^{18}O_2$ atmosphere (*m/z* 337.2 → 267.1). In contrast, two ^{16}OH-groups were incorporated when the reaction was performed in $H_2{}^{18}O$ buffer (*m/z* 333.2 → 263.3) (Fig. 5.9). The lipohydroperoxidase activity of ALOX15 is responsible for the formation of the epoxy-hydroxy compounds 17 and 20. The isomerization of hydroperoxy fatty acids to hydroxy-epoxy compounds was firstly described for the soybean LOX-1 leading to the formation of 11-hydroxy-12(13)-epoxy derivatives from 13-hydroperoxy octadecadienoic acid

(13-HpODE) [37]. These compounds are formed via an intra-molecular rearrangement of the hydroperoxy oxygen atoms of ARA derived 12-HpETE and EPA-derived 12-HpEPE and were termed hepoxilin A3/B3 and hepoxilin A4/B4, respectively [33, 38, 39]. Indeed, incubations in $^{18}O_2$ gas indicate that compound 20 is formed via this reaction mechanism from 12-HpEPE (Fig. 5.9). Hepoxilins are bioactive compounds as reviewed by Pace-Asciak [39] and for example involved in inflammatory processes, e.g. by affecting the chemotaxis of neutrophils. Moreover, first reports of EPA derived hepoxilin A4 and B4 indicated similar biological potency compared to ARA derived compounds [33]. In addition to two 10-OH-11(12)-EpETE isomers (compounds 20, 21), two 13-OH-14(15)-EpETE isomers (compounds 17, 18) were formed by ALOX15 and ALOX15B, which were also detected in incubations of porcine leukocytes with EPA [40] and might exert similar biological activities.

In the consecutive incubations with ALOX5 the clearly dominating products were compound 11 (for ALOX15 and ALOX15B) and compound 12 (for ALOX12). Both compounds might represent the double lipoxygenation products 5(*S*),15(*S*)-diHEPE (compound 11) and 5(*S*),12(*S*)-diHEPE (compound 12) formed by consecutive single oxygenation of the same molecule by the two ALOX isoforms. The consecutive action of two enzymes is of particular importance during the formation of SPMs, which may be formed via transcellular biosynthesis by 12- or 15-lipoxygenating ALOX and ALOX5 expressing cells [41]. In fact, highest levels of EPA derived LXA_5 were detected in combined incubation of ALOX15B with ALOX5 among several 5,6,15- and 5,14,15-triHEPE isomers as well as other triple oxygenated compounds derived from EPA (Fig. 5.1 C, appendix Fig. 8.10). In order to mimic such transcellular biosynthetic mechanisms, we incubated the 12- and 15-lipoxygenating enzymes and ALOX5 in a consecutive manner. Additionally, simultaneous and inverse-order incubations were performed for the ALOX5/ALOX12 and ALOX5/ALOX15B combinations to explore whether the order of the oxygenation reaction impacts the product profile. Although the principle patterns of oxygenation products were very similar in the different incubation samples, we found that the relative shares of oxygenation products depended on the order of enzyme addition.

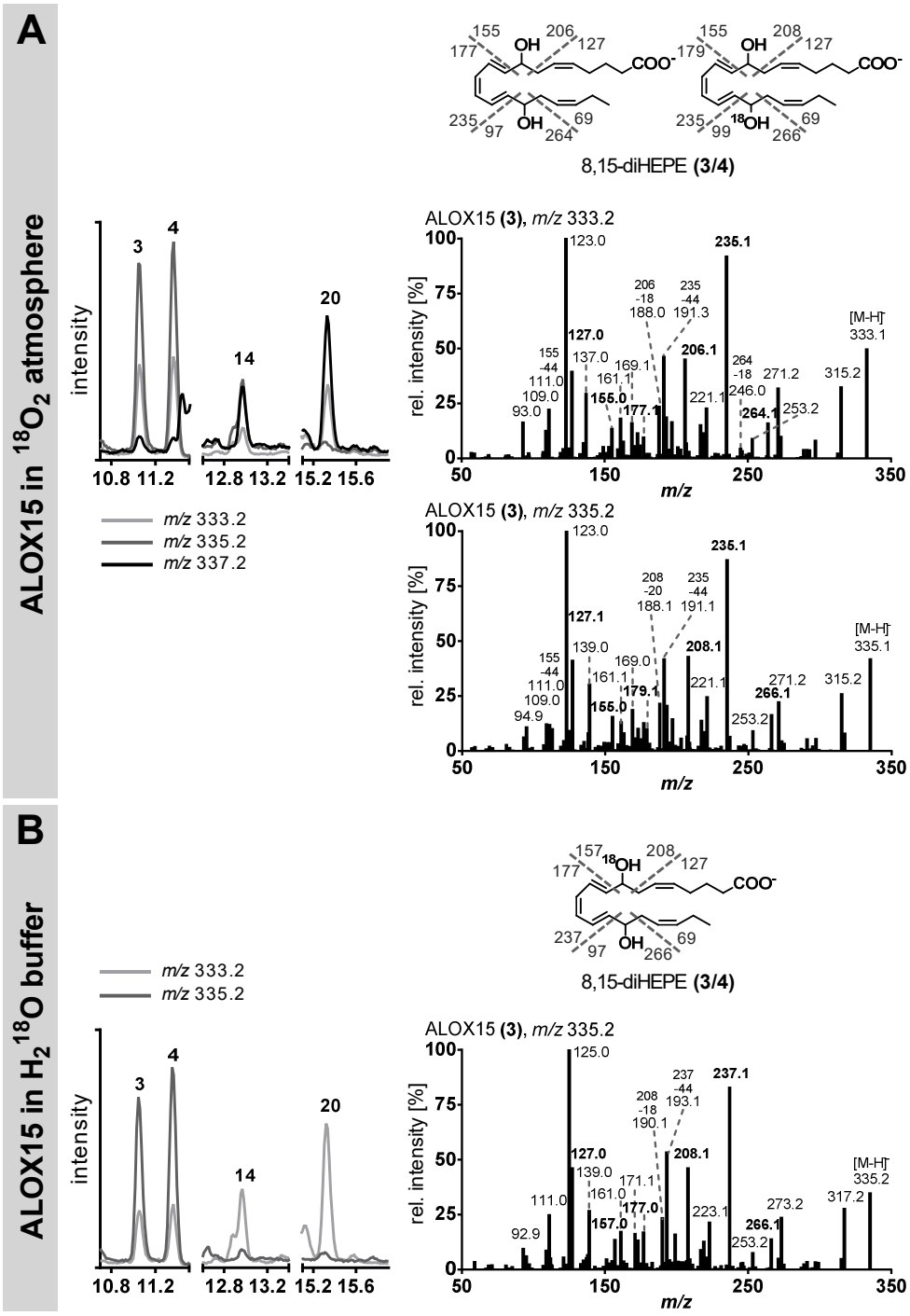

Fig. 5.9: Formation of double oxygenated products during EPA incubation with recombinant human ALOX15 (10 µM EPA, 15 min, RT) in (**A**) $^{18}O_2$ atmosphere or (**B**) in $H_2{}^{18}O$ buffer. Shown are total ion chromatograms of product ion scans (55–340 Da, *m/z* 333.2, 335.2 and 337.2; CE ramp –18 to –26 V) as well as collision induced dissociation product ion spectra of exemplary products (as indicated in Fig. 5.2). Suggested stuctures and fragmentation sites are given considering incorporation of ^{18}O- and/or ^{16}O-atoms. Note that only one of several possible double bond configurations is shown.

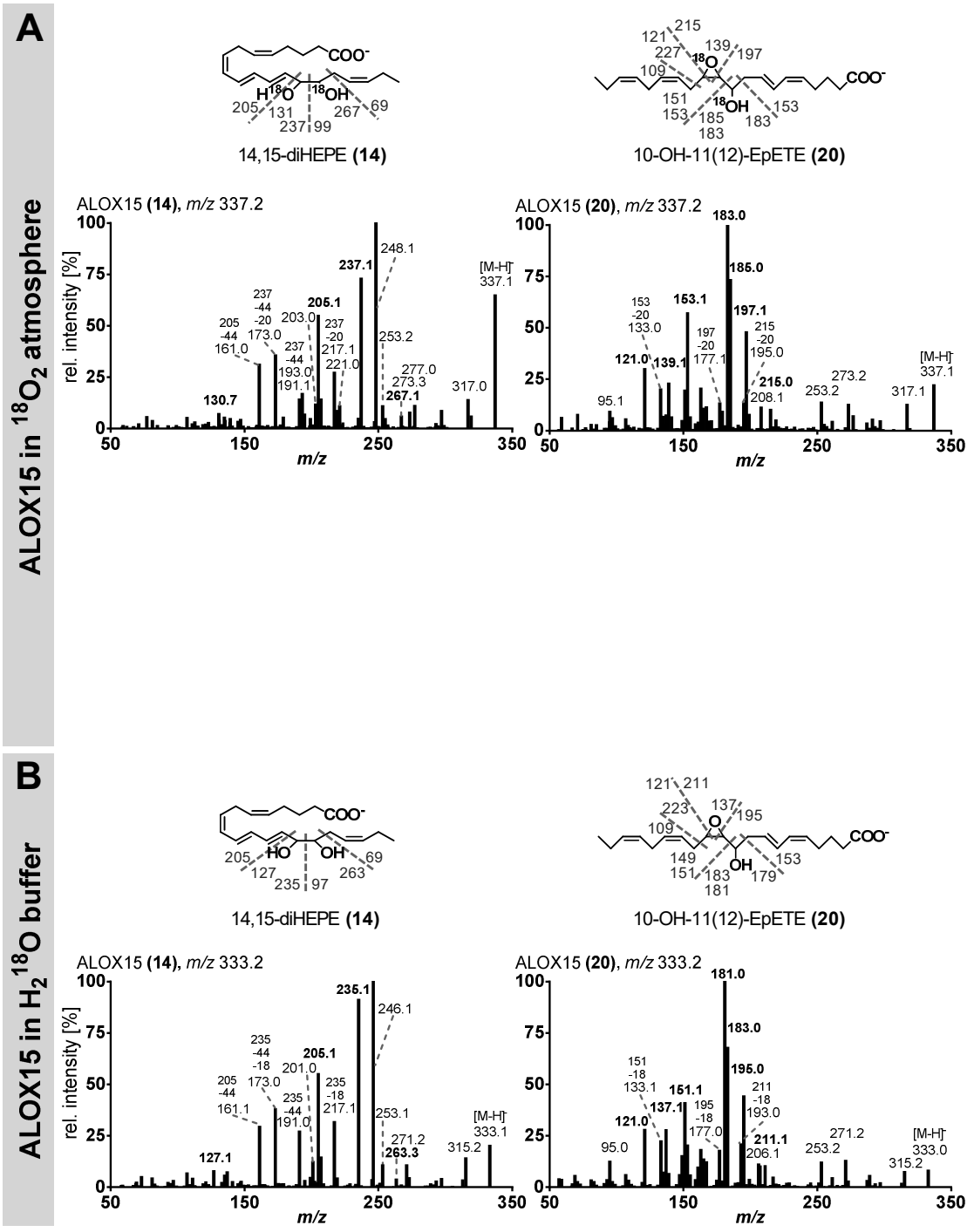

Fig. 5.9: Continued. Formation of double oxygenated products during EPA incubation with recombinant human ALOX15 (10 µM EPA, 15 min, RT) in (**A**) $^{18}O_2$ atmosphere or (**B**) in $H_2{}^{18}O$ buffer.

18-HEPE is only formed in minor amounts by human ALOX isoforms

18-HEPE is an important substrate for the biosynthesis of the E-series resolvins but the *in vivo* source of this compound is still unclear. 18-HEPE derived dihydroxy fatty acids were detected in human plasma with and without dietary EPA supplementation [42]. However, the formation of SPMs, especially triple oxygenated EPA derivatives such as RvE1, is usually low in healthy subjects [43, 44]. Since human ALOX15 is capable of catalyzing hydrogen abstraction from C10 and C13 of EPA [23] there was the possibility that this enzyme can also catalyze C16 hydrogen abstraction and thus, the formation of 18-HEPE. When we incubated human ALOX15 with EPA we found the formation of small amounts of 18-HEPE. This compound, which clearly exceeded the levels in no-enzyme control incubations (Fig. 5.4), only contributed about 1% to the sum of the mono-oxygenation products and analysis of its chirality indicated a preponderance of the 18(*S*)-enantiomer. However, the degree of chirality (*S/R*-ratio of 2.5:1) was lower than that of the major EPA oxygenation products (15(*S*)-HEPE/15(*R*)-HEPE > 10:1, data not shown). Taken together these data indicate that 18-HEPE can be formed from EPA by ALOX15 catalysis. However, this reaction is not very efficient and the stereochemistry is not tightly controlled by the enzyme.

18(R,S)-HEPE is a substrate for human ALOX isoforms

When human ALOX5 oxygenated racemic 18-HEPE a number of di- and trihydroxylated EPA derivatives including RvE2 [5(*S*),18(*R*)-diHEPE] were formed (Fig. 5.6–7). RvE2 formation by ALOX5 is rather straight forward since it simply requires C5 oxygenation of 18-HEPE [45]. In addition, similar amounts of other 5,18- and 8,18-diHEPE isomers were formed and these data indicate a low reaction specificity of the enzyme with this substrate. It should be noted that the substrate concentration (here 10 µM) might affect product formation and lower *in vivo* substrate concentrations might lead to different product patterns/product ratios. Previous studies have implicated ALOX15 in the biosynthesis of RvE3 [17(*R*),18(*R*/*S*)-diHEPE] [21, 46]. Under our experimental conditions we did not detect significant amounts of this metabolite (Fig. 5.6 A). These data do not

necessarily mean that 17,18-diHEPE derivatives are not formed by this enzyme but when compared with ALOX15B much smaller amounts were detected. In fact, among the enzymes tested ALOX15B exhibited the highest RvE3 synthesizing capacity. Interestingly, in the combined ALOX15B+ALOX5 incubations RvE3 formation was completely abolished and a product pattern similar to the single ALOX5 incubation was observed. The most plausible explanation for this finding is that ALOX5 further oxygenates the RvE3 isomers leading to the formation of trihydroxylated EPA derivatives. In fact, significant amounts of such trihydroxy EPA derivatives were detected in the ALOX15B+ALOX5 incubation (Fig. 5.6 B). Similar to ALOX15 human ALOX12 did not exhibit a major RvE3 synthesizing capacity. For this enzyme, as expected, 12,18-diHEPE isomers were identified as major 18(*R*,*S*)-HEPE oxygenation products (Fig. 5.6–7). In the ALOX12+ALOX5 incubations a mixture of the reaction products identified for the single enzyme incubations was observed. Similar 18-HEPE derived dihydroxylated compounds were formed during human as well as murine leukocyte incubations and therefore attributed to the action of leukocyte 12/15-LOX [21]. Moreover, several 11,18- and two 17,18-diHEPE isomers were also formed *in vitro* by incubation of soybean LOX-1 with 18-HEPE [21]. Interestingly, under our experimental conditions, product patterns indicated ALOX5, ALOX12 and ALOX15B with the highest capability for 18-HEPE oxygenation rather than ALOX15. Furthermore, we observed distinct product profiles with 5,18- and 8,18-diHEPE isomers formed by ALOX5, 12,18-diHEPE by ALOX12 and 17,18-diHEPE by ALOX15B. This might have, on the one hand, implications for the *in vivo* synthesis of EPA derived double or triple oxygenated lipid mediators and the cell types capable of synthesizing these compounds. On the other hand, some of these compounds might exert biological activity, e.g. during inflammation and resolution. Isobe *et al.* demonstrated that administration of different 11,18-diHEPE isomers (which were not prominent in our incubations) had only little effect on PMNL infiltration in a murine model of zymosan-induced peritonitis [21]. However, other dihydroxylated EPA derivatives might be more active, for example, 8,18- and 12,18-diHEPE, which were also detected in human plasma and increased upon dietary EPA intake [42].

Trihydroxylated EPA derivatives were mainly detected in the incubations involving ALOX5. When ALOX5 was used as sole catalyst three major trihydroxylated EPA derivatives (compounds e, f, h) were observed. Resolvin E1 was only detected in trace amounts, which is consistent with findings by Tjonahen *et al.* using also recombinant ALOX5 [45] and can be explained by the requirement of enzymatic hydrolysis of the 5,6-epoxy-18-hydroxy intermediate to form the specific stereochemistry of RvE1, hence the involvement of LTA_4 hydrolase [47]. According to our mass spectral data, compounds e and f are 5,12,18-triHEPE derivatives (RvE1 isomers, e.g. 6-*trans*-5,12,18-triHEPE) [47]. The formation of 5,12,18-triHEPE most likely involves the formation of a 5,6-epoxide intermediate from 18-HEPE and its subsequent hydrolysis. It is also possible that the formation route involves C12 oxygenation and such catalytic activity has not been described for ALOX5 before. C12 oxygenation requires C10 hydrogen abstraction and [+2] radical rearrangement. ALOX5 is capable of catalyzing C10 hydrogen abstraction. For [+2] radical rearrangement an inverse substrate alignment of the 5,18-diHEPE would be required. Compound h, which is the third dominant trihydroxylated EPA derivative formed by ALOX5 (Fig. 5.6 B) was tentatively identified as 5,6,18-triHEPE on the basis of its fragmentation pattern (Fig. 5.7). Although we did not carry out more detailed mechanistic experiments, the biosynthetic route for this product likely involves the formation of 5,6-epoxy-18-hydroxy EPA (leukotriene synthase activity of ALOX5). The 5,6-epoxy-18-hydroxy intermediate then undergoes epoxide ring opening (hydrolysis) yielding the 5,6,18-triHEPE [47]. When ALOX15 was used as sole catalyst or when this enzyme was combined with ALOX5 no significant amounts of tri-OH EPA derivatives were observed. The molecular basis for this unexpected outcome has not been explored but two mechanistic scenarios might be discussed: 18-HEPE was almost completely recovered in the sole ALOX15 incubation and should have been available as substrate for ALOX5 (Fig. 5.5 A). However, ALOX15 might interact with either 18-HEPE or ALOX5. If ALOX15 binds 18-HEPE non-covalently without its conversion to reaction products, it might not be available as substrate for ALOX5. Another scenario is the inhibition of ALOX5 by the presence of ALOX15 in the incubation sample. If this would be

correct a physical interaction between ALOX15 and ALOX5 may take place in the incubation sample. Such an ALOX15-ALOX5 interaction has not been reported before but since the two enzymes form dimers [48, 49] mixed dimer formation might be possible. More detailed experiments are needed to test such inhibitory mixed dimer formation. Similar to ALOX15, sole incubation of 18(*R*,*S*)-HEPE with ALOX15B and ALOX12 did not lead to the formation of major triple oxygenated EPA derivatives (Fig. 5.6 B). However, in the combined ALOX15B+ALOX5 incubations two additional triple oxygenated EPA derivatives (compounds g and i) were detected. On the basis of their fragmentation patterns (Fig. 5.7) for both compounds the structure 5,17,18-triHEPE was suggested. Here again, we did not look in more detail into the mechanism of biosynthesis of these two compounds but the following scenario is highly probable: 18(*R*,*S*)-HEPE is firstly oxygenated by ALOX15B to 17,18-diHEPE (RvE3) and the formation of this compound was actually shown for ALOX15B (Fig. 5.6 A). The reaction intermediate is subsequently oxygenated by ALOX5 at C5 yielding 5,17,18-triHEPE. If this reaction mechanism is true and the stereoselectivity of ALOX5 and ALOX15B catalyzed 18-HEPE oxygenation is the same as for EPA the tentative structure of the two compounds should be 5(*S*),17(*R*),18(*S*)- and 5(*S*),17(*R*),18(*R*)-triHEPE. The formation of these compounds from 18-HEPE (or its precursor EPA) by the consecutive action of human ALOX15B and ALOX5 has not been reported before. Since for RvE3 pro-resolving activities were described, e.g. decrease of chemotactic velocity of murine bone marrow PMNs [21], it might be possible that similar properties are exerted by these specific triHEPE compounds or other analogs.

The herein described lipoxygenase products may be formed *in vivo* by a single cell or via trans-cellular synthesis depending on the ALOX isoforms expressed in different cells. For example, blood platelets contain ALOX12 [50], while leukocytes, such as granulocytes and macrophages express ALOX5 [51]. Interactions between platelets and leukocytes have been described as formation pathway for lipoxins [15]. Consequently, the compounds formed in our ALOX12/ALOX5 combined incubations, e.g. 5,12-diHEPE, are likely products of

this biosynthetic route as well. During the course of acute inflammation and inflammatory resolution, naïve monocytes differentiate to M1 (pro-inflammatory) or M2 (resolutory) macrophages that express different ALOX isoforms. For example, following differentiation of monocytes to M2 macrophages with CSF-1 (for 7 days) and interleukin 4 (for the last 2 days), these cells upregulate both ALOX5 and ALOX15B expression upon acute stimulation (16 h) of toll-like receptor 2 and 4 [52]. Therefore, in response to inflammatory stimuli M2 macrophages could be capable of synthesizing ALOX derived products that were detected in single and combined ALOX15B/ALOX5 incubations in the present study. Hence, the herein described double oxygenated products may be formed in human blood cells from their precursor fatty acid EPA present in membrane phospholipids. In order to substantiate this speculation, we screened plasma samples of Ca^{2+} ionophore stimulated human whole blood from EPA+DHA supplemented healthy humans from a previous study [53]. We detected double oxygenated compounds from EPA based on SRM transitions derived from the obtained fragment spectra in ALOX incubations indicating the formation of e.g. 5,15-diHEPE or 5,12-diHEPE in humans (Fig. 5.10). Further experiments will be required to confirm the identity and formation pattern of these EPA derived compounds in human blood cells and investigate their biological relevance. It should be noted that based on a recent study by Norris *et al*. [54], the product 5(*S*),15(*S*)-diHEPE (suggested structure for compound 11) has been recently termed RvE4, which e.g. enhances macrophage efferocytosis, supporting the potential bioactivity of the ALOX products described herein.

Fig. 5.10 (right, page 153): Double oxygenated ALOX products in (**A**) enzyme incubations with EPA, (**B**) heparin plasma from Ca^{2+} ionophore (50 µM A23187) stimulated whole blood samples and (**C**) EDTA plasma from vehicle (0.1% DMSO) treated whole blood samples, both from subjects supplemented with EPA+DHA [53]. Oxylipins were extracted by SPE after protein precipitation with methanol. Selected reaction monitoring (SRM) transitions (CE –22 V, DP –80 V, CXP –9 V) were derived from fragment ion spectra of double oxygenated products in ALOX incubations with EPA: compound 8 and 9 (5,12-diHEPE) with *m/z* 333.2 → 195.0/151.0, compound 16 (5,6-diHEPE) with *m/z* 333.2 → 115.0/145.0, compound 11 (5,15-diHEPE) with *m/z* 333.2 → 173.0/199.1, compound 14 (14,15-diHEPE) with *m/z* 333.2 → 246.1/205.0, compound 12 (5,12-diHEPE) with *m/z* 333.2 → 195.0/151.0 and compound 21 (10-OH-11(12)-EpETE) with *m/z* 333.2 → 181.0/121.1. Human heparin plasma and EDTA plasma samples from six individuals were screened for these products. Two SRM transitions and their area ratio is shown for one representative female subject. Further experiments are needed to confirm the *in vivo* formation of these products in human blood.

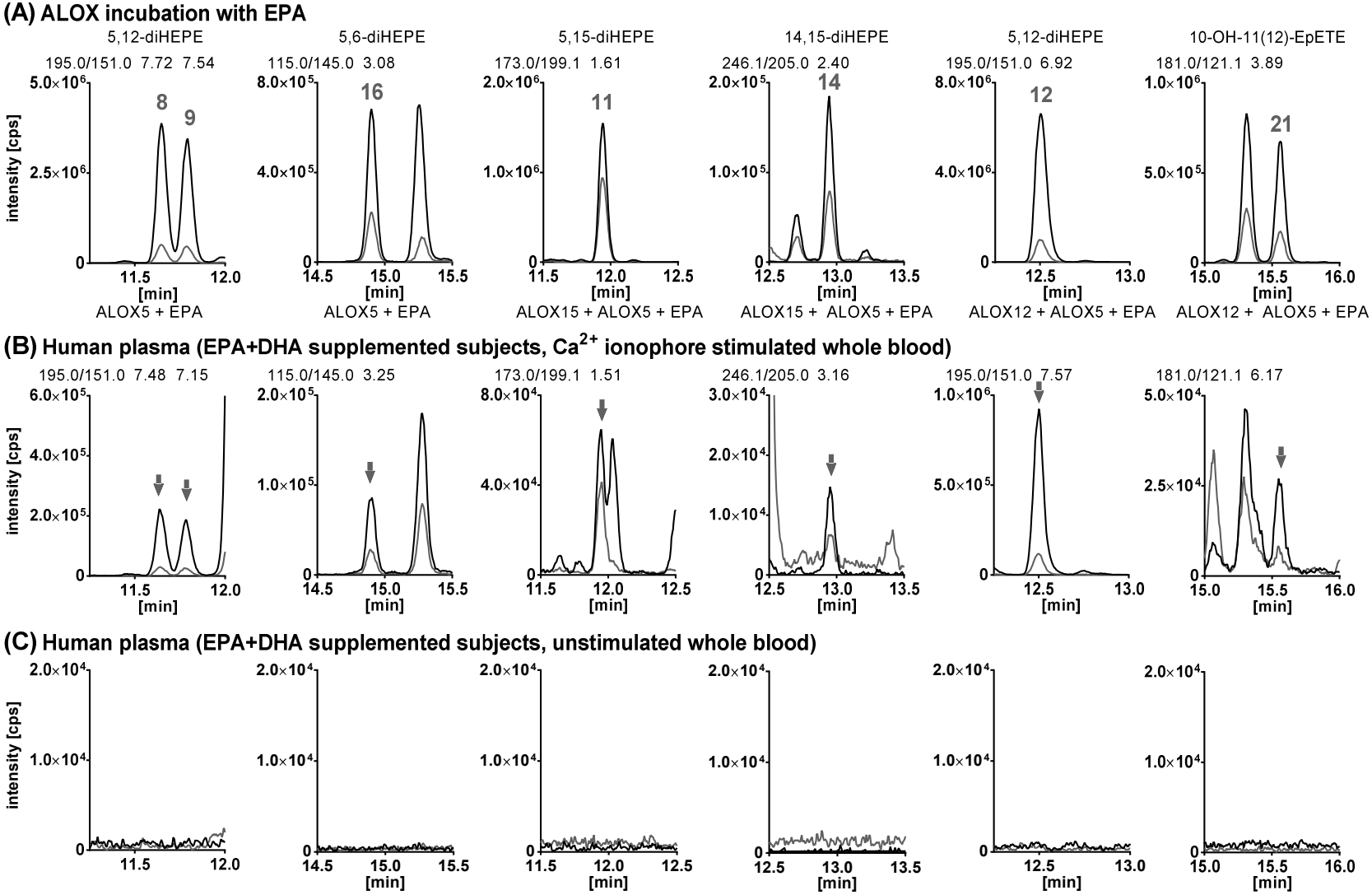
(A) ALOX incubation with EPA
5,12-diHEPE
195.0/151.0 7.72 7.54
8
9
ALOX5 + EPA
5,6-diHEPE
115.0/145.0 3.08
16
ALOX5 + EPA
5,15-diHEPE
173.0/199.1 1.61
11
ALOX15 + ALOX5 + EPA
14,15-diHEPE
246.1/205.0 2.40
14
ALOX15 + ALOX5 + EPA
5,12-diHEPE
195.0/151.0 6.92
12
ALOX12 + ALOX5 + EPA
10-OH-11(12)-EpETE
181.0/121.1 3.89
21
ALOX12 + ALOX5 + EPA
intensity [cps]
[min]
(B) Human plasma (EPA+DHA supplemented subjects, Ca2+ ionophore stimulated whole blood)
195.0/151.0 7.48 7.15
115.0/145.0 3.25
173.0/199.1 1.51
246.1/205.0 3.16
195.0/151.0 7.57
181.0/121.1 6.17
(C) Human plasma (EPA+DHA supplemented subjects, unstimulated whole blood)

In conclusion, ALOX5 and ALOX15 form complex product patterns of double oxygenated compounds from EPA via their double lipoxygenase, leukotriene synthase and lipohydroperoxidase activities. Complexity of formed products increases in combined incubations with ALOX5 simulating consecutive or trans-cellular biosynthesis. ALOX5, ALOX12 and ALOX15B effectively oxygenated 18-HEPE to double oxygenated compounds and several distinct triple oxygenated products were formed, mainly by ALOX5. Regarding the established role of structurally similar compounds such as lipoxins and resolvins, the described ALOX derived products from EPA may also show biologically potent effects. The herein presented, detailed analysis of ALOX secondary product patterns provides insight into the capability of each tested ALOX isoform (ALOX5, ALOX15, ALOX12, ALOX15B) to catalyze the formation of potentially bioactive double and triple oxygenated compounds. Further investigations will address their *in vivo* synthesis and biological functions.

5.5 References

1. Kuhn H, Banthiya S, van Leyen K (2015) Mammalian lipoxygenases and their biological relevance. *Biochim Biophys Acta*, 1851(4), 308-330; doi: 10.1016/j.bbalip.2014.10.002.
2. Bryant RW, Bailey JM, Schewe T, Rapoport SM (1982) Positional specificity of a reticulocyte lipoxygenase. Conversion of arachidonic acid to 15-S-hydroperoxy-eicosatetraenoic acid. *J Biol Chem*, 257(11), 6050-6055.
3. Ivanov I, Kuhn H, Heydeck D (2015) Structural and functional biology of arachidonic acid 15-lipoxygenase-1 (ALOX15). *Gene*, 573(1), 1-32; doi: 10.1016/j.gene.2015.07.073.
4. Shimizu T, Radmark O, Samuelsson B (1984) Enzyme with dual lipoxygenase activities catalyzes leukotriene A4 synthesis from arachidonic acid. *Proc Natl Acad Sci U S A*, 81(3), 689-693; doi: 10.1073/pnas.81.3.689.
5. Ludwig P, Holzhutter HG, Colosimo A, Silvestrini MC, Schewe T, Rapoport SM (1987) A kinetic model for lipoxygenases based on experimental data with the lipoxygenase of reticulocytes. *Eur J Biochem*, 168(2), 325-337; doi: 10.1111/j.1432-1033.1987.tb13424.x.
6. Bryant RW, Schewe T, Rapoport SM, Bailey JM (1985) Leukotriene formation by a purified reticulocyte lipoxygenase enzyme. Conversion of arachidonic acid and 15-hydroperoxyeicosatetraenoic acid to 14, 15-leukotriene A4. *J Biol Chem*, 260(6), 3548-3555.
7. Ivanov I, Heydeck D, Hofheinz K, Roffeis J, O'Donnell VB, Kuhn H, Walther M (2010) Molecular enzymology of lipoxygenases. *Arch Biochem Biophys*, 503(2), 161-174; doi: 10.1016/j.abb.2010.08.016.
8. Bild GS, Ramadoss CS, Lim S, Axelrod B (1977) Double dioxygenation of arachidonic acid by soybean lipoxygenase-1. *Biochem Biophys Res Commun*, 74(3), 949-954; doi: 10.1016/0006-291x(77)91610-2.
9. Van Os CP, Rijke-Schilder GP, Van Halbeek H, Verhagen J, Vliegenthart JF (1981) Double dioxygenation of arachidonic acid by soybean lipoxygenase-1. Kinetics and regio-stereo specificities of the reaction steps. *Biochim Biophys Acta*, 663(1), 177-193; doi: 10.1016/0005-2760(81)90204-6.
10. MacMillan DK, Hill E, Sala A, Sigal E, Shuman T, Henson PM, Murphy RC (1994) Eosinophil 15-lipoxygenase is a leukotriene A4 synthase. *J Biol Chem*, 269(43), 26663-26668.
11. Kuhn H, Wiesner R, Alder L, Fitzsimmons BJ, Rokach J, Brash AR (1987) Formation of lipoxin B by the pure reticulocyte lipoxygenase via sequential oxygenation of the substrate. *Eur J Biochem*, 169(3), 593-601; doi: 10.1111/j.1432-1033.1987.tb13650.x.
12. Kuhn H, Wiesner R, Stender H (1984) The formation of products containing a conjugated tetraenoic system by pure reticulocyte lipoxygenase. *Febs Lett*, 177(2), 255-259; doi: 10.1016/0014-5793(84)81294-6.
13. Serhan CN, Hamberg M, Samuelsson B (1984) Trihydroxytetraenes: a novel series of compounds formed from arachidonic acid in human leukocytes. *Biochem Biophys Res Commun*, 118(3), 943-949; doi: 10.1016/0006-291x(84)91486-4.
14. Serhan CN, Hamberg M, Samuelsson B (1984) Lipoxins: novel series of biologically active compounds formed from arachidonic acid in human leukocytes. *Proc Natl Acad Sci U S A*, 81(17), 5335-5339; doi: 10.1073/pnas.81.17.5335.
15. Serhan CN, Sheppard KA (1990) Lipoxin formation during human neutrophil-platelet interactions. Evidence for the transformation of leukotriene A4 by platelet 12-lipoxygenase in vitro. *J Clin Invest*, 85(3), 772-780; doi: 10.1172/JCI114503.

16. Chavis C, Chanez P, Vachier I, Bousquet J, Michel FB, Godard P (1995) 5-15-diHETE and lipoxins generated by neutrophils from endogenous arachidonic acid as asthma biomarkers. *Biochem Biophys Res Commun*, 207(1), 273-279; doi: 10.1006/bbrc.1995.1183.
17. Ford-Hutchinson AW, Bray MA, Doig MV, Shipley ME, Smith MJ (1980) Leukotriene B, a potent chemokinetic and aggregating substance released from polymorphonuclear leukocytes. *Nature*, 286(5770), 264-265; doi: 10.1038/286264a0.
18. Levine JD, Lam D, Taiwo YO, Donatoni P, Goetzl EJ (1986) Hyperalgesic properties of 15-lipoxygenase products of arachidonic acid. *Proc Natl Acad Sci U S A*, 83(14), 5331-5334; doi: 10.1073/pnas.83.14.5331.
19. Croset M, Lagarde M (1983) Stereospecific inhibition of PGH2-induced platelet aggregation by lipoxygenase products of icosaenoic acids. *Biochem Biophys Res Commun*, 112(3), 878-883; doi: 10.1016/0006-291x(83)91699-6.
20. Schwab JM, Chiang N, Arita M, Serhan CN (2007) Resolvin E1 and protectin D1 activate inflammation-resolution programmes. *Nature*, 447(7146), 869-874; doi: 10.1038/nature05877.
21. Isobe Y, Arita M, Matsueda S, Iwamoto R, Fujihara T, Nakanishi H, Taguchi R, Masuda K, Sasaki K, Urabe D, Inoue M, Arai H (2012) Identification and structure determination of novel anti-inflammatory mediator resolvin E3, 17,18-dihydroxyeicosapentaenoic acid. *J Biol Chem*, 287(13), 10525-10534; doi: 10.1074/jbc.M112.340612.
22. Soberman RJ, Harper TW, Betteridge D, Lewis RA, Austen KF (1985) Characterization and separation of the arachidonic acid 5-lipoxygenase and linoleic acid omega-6 lipoxygenase (arachidonic acid 15-lipoxygenase) of human polymorphonuclear leukocytes. *J Biol Chem*, 260(7), 4508-4515.
23. Kutzner L, Goloshchapova K, Heydeck D, Stehling S, Kuhn H, Schebb NH (2017) Mammalian ALOX15 orthologs exhibit pronounced dual positional specificity with docosahexaenoic acid. *Biochim Biophys Acta*, 1862(7), 666-675; doi: 10.1016/j.bbalip.2017.04.001.
24. Keicher U, Koletzko B, Reinhardt D (1995) Omega-3 fatty acids suppress the enhanced production of 5-lipoxygenase products from polymorph neutrophil granulocytes in cystic fibrosis. *Eur J Clin Invest*, 25(12), 915-919; doi: 10.1111/j.1365-2362.1995.tb01967.x.
25. Wong PY, Hughes R, Lam B (1985) Lipoxene: a new group of trihydroxy pentaenes of eicosapentaenoic acid derived from porcine leukocytes. *Biochem Biophys Res Commun*, 126(2), 763-772; doi: 10.1016/0006-291x(85)90250-5.
26. Kozlov N, Humeniuk L, Ufer C, Ivanov I, Golovanov A, Stehling S, Heydeck D, Kuhn H (2019) Functional characterization of novel ALOX15 orthologs representing key steps in mammalian evolution supports the Evolutionary Hypothesis of reaction specificity. *Biochim Biophys Acta*, 1864(3), 372-385; doi: 10.1016/j.bbalip.2018.12.016.
27. Kutzner L, Rund KM, Ostermann AI, Hartung NM, Galano JM, Balas L, Durand T, Balzer MS, David S, Schebb NH (2019) Development of an optimized LC-MS method for the detection of specialized pro-resolving mediators in biological samples. *Front Pharmacol*, 10, 169; doi: 10.3389/fphar.2019.00169.
28. Rund KM, Ostermann AI, Kutzner L, Galano JM, Oger C, Vigor C, Wecklein S, Seiwert N, Durand T, Schebb NH (2018) Development of an LC-ESI(-)-MS/MS method for the simultaneous quantification of 35 isoprostanes and isofurans derived from the major n3- and n6-PUFAs. *Anal Chim Acta*, 1037, 63-74; doi: 10.1016/j.aca.2017.11.002.
29. Murphy RC, Barkley RM, Zemski Berry K, Hankin J, Harrison K, Johnson C, Krank J, McAnoy A, Uhlson C, Zarini S (2005) Electrospray ionization and tandem mass spectrometry of eicosanoids. *Anal Biochem*, 346(1), 1-42; doi: 10.1016/j.ab.2005.04.042.

30. Blum M, Dogan I, Karber M, Rothe M, Schunck WH (2019) Chiral lipidomics of monoepoxy and monohydroxy metabolites derived from long-chain polyunsaturated fatty acids. *J Lipid Res*, 60(1), 135-148; doi: 10.1194/jlr.M089755.
31. Rouzer CA, Matsumoto T, Samuelsson B (1986) Single protein from human leukocytes possesses 5-lipoxygenase and leukotriene A4 synthase activities. *Proc Natl Acad Sci U S A*, 83(4), 857-861; doi: 10.1073/pnas.83.4.857.
32. Brash AR, Boeglin WE, Chang MS (1997) Discovery of a second 15S-lipoxygenase in humans. *Proc Natl Acad Sci U S A*, 94(12), 6148-6152; doi: 10.1073/pnas.94.12.6148.
33. Pace-Asciak CR (1986) Formation of hepoxilin A4, B4 and the corresponding trioxilins from 12(S)-hydroperoxy-5,8,10,14,17-icosapentaenoic acid. *Prostaglandins Leukot Med*, 22(1), 1-9; doi: 10.1016/0262-1746(86)90017-x.
34. Heidel JR, Taylor SM, Laegreid WW, Silflow RM, Liggitt HD, Leid RW (1989) In vivo chemotaxis of bovine neutrophils induced by 5-lipoxygenase metabolites of arachidonic and eicosapentaenoic acid. *Am J Pathol*, 134(3), 671-676.
35. Lam BK, Wong PY (1988) Biosynthesis and biological activities of lipoxin A5 and B5 from eicosapentaenoic acid. *Adv Exp Med Biol*, 229, 51-59; doi: 10.1007/978-1-4757-0937-7_5.
36. Oh SF, Dona M, Fredman G, Krishnamoorthy S, Irimia D, Serhan CN (2012) Resolvin E2 formation and impact in inflammation resolution. *J Immunol*, 188(9), 4527-4534; doi: 10.4049/jimmunol.1103652.
37. Garssen GJ, Veldink GA, Vliegenthart JF, Boldingh J (1976) The formation of threo-11-hydroxy-trans-12: 13-epoxy-9-cis-octadecenoic acid by enzymic isomerisation of 13-L-hydroperoxy-9-cis, 11-transoctadecadienoic acid by soybean lipoxygenase-1. *Eur J Biochem*, 62(1), 33-36; doi: 10.1111/j.1432-1033.1976.tb10094.x.
38. Pace-Asciak CR (1984) Arachidonic acid epoxides. Demonstration through [18O]oxygen studies of an intramolecular transfer of the terminal hydroxyl group of (12S)-hydroperoxyeicosa-5,8,10,14-tetraenoic acid to form hydroxyepoxides. *J Biol Chem*, 259(13), 8332-8337.
39. Pace-Asciak CR (2015) Pathophysiology of the hepoxilins. *Biochim Biophys Acta*, 1851(4), 383-396; doi: 10.1016/j.bbalip.2014.09.007.
40. Lam BK, Hirai A, Yoshida S, Tamura Y, Wong PY (1987) Transformation of 15-hydroperoxyeicosapentaenoic acid to lipoxin A5 and B5, mono- and dihydroxyeicosapentaenoic acids by porcine leukocytes. *Biochim Biophys Acta*, 917(3), 398-405; doi: 10.1016/0005-2760(87)90118-4.
41. Serhan CN (2005) Lipoxins and aspirin-triggered 15-epi-lipoxins are the first lipid mediators of endogenous anti-inflammation and resolution. *Prostaglandins Leukot Essent Fatty Acids*, 73(3-4), 141-162; doi: 10.1016/j.plefa.2005.05.002.
42. Endo J, Sano M, Isobe Y, Fukuda K, Kang JX, Arai H, Arita M (2014) 18-HEPE, an n-3 fatty acid metabolite released by macrophages, prevents pressure overload-induced maladaptive cardiac remodeling. *J Exp Med*, 211(8), 1673-1687; doi: 10.1084/jem.20132011.
43. Skarke C, Alamuddin N, Lawson JA, Li X, Ferguson JF, Reilly MP, FitzGerald GA (2015) Bioactive products formed in humans from fish oils. *J Lipid Res*, 56(9), 1808-1820; doi: 10.1194/jlr.M060392.
44. Barden AE, Mas E, Croft KD, Phillips M, Mori TA (2015) Specialized proresolving lipid mediators in humans with the metabolic syndrome after n-3 fatty acids and aspirin. *Am J Clin Nutr*, 102(6), 1357-1364; doi: 10.3945/ajcn.115.116384.
45. Tjonahen E, Oh SF, Siegelman J, Elangovan S, Percarpio KB, Hong S, Arita M, Serhan CN (2006) Resolvin E2: identification and anti-inflammatory actions: pivotal role of

human 5-lipoxygenase in resolvin E series biosynthesis. *Chem Biol*, 13(11), 1193-1202; doi: 10.1016/j.chembiol.2006.09.011.

46. Isobe Y, Arita M, Iwamoto R, Urabe D, Todoroki H, Masuda K, Inoue M, Arai H (2013) Stereochemical assignment and anti-inflammatory properties of the omega-3 lipid mediator resolvin E3. *J Biochem*, 153(4), 355-360; doi: 10.1093/jb/mvs151.
47. Oh SF, Pillai PS, Recchiuti A, Yang R, Serhan CN (2011) Pro-resolving actions and stereoselective biosynthesis of 18S E-series resolvins in human leukocytes and murine inflammation. *J Clin Invest*, 121(2), 569-581; doi: 10.1172/JCI42545.
48. Hafner AK, Cernescu M, Hofmann B, Ermisch M, Hornig M, Metzner J, Schneider G, Brutschy B, Steinhilber D (2011) Dimerization of human 5-lipoxygenase. *Biol Chem*, 392(12), 1097-1111; doi: 10.1515/BC.2011.200.
49. Ivanov I, Shang W, Toledo L, Masgrau L, Svergun DI, Stehling S, Gomez H, Di Venere A, Mei G, Lluch JM, Skrzypczak-Jankun E, Gonzalez-Lafont A, Kuhn H (2012) Ligand-induced formation of transient dimers of mammalian 12/15-lipoxygenase: a key to allosteric behavior of this class of enzymes? *Proteins*, 80(3), 703-712; doi: 10.1002/prot.23227.
50. Hamberg M, Samuelsson B (1974) Prostaglandin endoperoxides. Novel transformations of arachidonic acid in human platelets. *Proc Natl Acad Sci U S A*, 71(9), 3400-3404; doi: 10.1073/pnas.71.9.3400.
51. Hafner AK, Kahnt AS, Steinhilber D (2019) Beyond leukotriene formation-The noncanonical functions of 5-lipoxygenase. *Prostaglandins Other Lipid Mediat*, 142, 24-32; doi: 10.1016/j.prostaglandins.2019.03.003.
52. Ebert R, Cumbana R, Lehmann C, Kutzner L, Toewe A, Ferreiros N, Parnham MJ, Schebb NH, Steinhilber D, Kahnt AS (2020) Long-term stimulation of toll-like receptor-2 and -4 upregulates 5-LO and 15-LO-2 expression thereby inducing a lipid mediator shift in human monocyte-derived macrophages. *Biochim Biophys Acta*, 1865(9), 158702; doi: 10.1016/j.bbalip.2020.158702.
53. Fischer R, Konkel A, Mehling H, Blossey K, Gapelyuk A, Wessel N, von Schacky C, Dechend R, Muller DN, Rothe M, Luft FC, Weylandt K, Schunck WH (2014) Dietary omega-3 fatty acids modulate the eicosanoid profile in man primarily via the CYP-epoxygenase pathway. *J Lipid Res*, 55(6), 1150-1164; doi: 10.1194/jlr.M047357.
54. Norris PC, Libreros S, Serhan CN (2019) Resolution metabolomes activated by hypoxic environment. *Sci Adv*, 5(10), eaax4895; doi: 10.1126/sciadv.aax4895.

Chapter 6

Concluding remarks and future perspectives

Within this thesis, the enzymatic and *in vivo* formation of n3-PUFA derived lipid mediators have been investigated with particular emphasis on the biosynthesis of mono- and multiple hydroxylated fatty acids formed by the catalytic activity of lipoxygenase enzymes. Endogenous levels of long-chain n3-PUFA, particularly EPA, are generally low in subjects on a Western diet. Due to beneficial health effects associated with the consumption of these fatty acids, dietary recommendations and interventions are the method of choice to improve the n3-PUFA status. In a murine model, it was shown that both n3-PUFA blood and tissue levels as well as tissue free oxylipin levels can be efficiently increased by a supplementation with EPA or DHA (*chapter 2*). Combining this supplementation with a lower dietary n6-PUFA (LA) intake markedly increased the bioavailability of EPA and decreased the portion of n6 in HUFA. Given present advices on n3-PUFA intake (EPA+DHA) including at least 1 g per day for individuals with coronary heart disease [1], 2–4 g per day to lower blood levels of triglycerides in individuals with hypertriglyceridaemia [1] or ≥ 3 g per day to lower systolic blood pressure in individuals with untreated hypertension [2], a more efficient uptake as well as lower levels of (competing) n6-PUFA could help to evoke the desired effects at lower doses. This is of high importance with respect to sustainability taking the limited sources of marine n3-PUFA and the growing world population into account. It should be noted that in the used diets ALA was kept very low due to the more efficient desaturation and elongation of n3-PUFA in mice compared to men [3]. This results in an extremely high n6/n3-PUFA ratio in the unsupplemented control groups. During the course of this thesis it was possible to demonstrate in a collaborative project that dietary ALA can slightly increase

blood cell (and likely also tissue) EPA levels in humans [4]. Moreover, while sole elevation of ALA led to decreasing DHA levels, combining ALA supplementation with lowering dietary n6-PUFA (LA), DHA levels remained constant and EPA levels increased more rapidly [5]. These findings indicate that both the bioavailability of dietary n3-PUFA and the ALA-EPA-DHA turnover is affected by the dietary n6-PUFA intake. Therefore, it would be interesting to investigate if combining n3-PUFA supplementation with n6-PUFA reduction also enhances the effect of EPA+DHA, e.g. in modifying risk factors related to cardiovascular diseases such as lowering blood pressure and plasma triglyceride concentrations or regulating blood coagulation [6].

In mouse liver tissue, a modulation of the endogenous oxylipin profile upon n3-PUFA feeding was particularly evident for products of the CYP-pathway. Moreover, in n3-PUFA-fed groups, hydroxy fatty acids formed from EPA and DHA constitute a major portion of ALOX derived oxylipins comprising 5- as well as 12- and 15-lipoxygenation products. Despite significant elevation of SPM precursors such as 18-HEPE and 17-HDHA in the EPA and/or DHA supplemented groups, SPMs were generally very low or below the limit of quantification. However, detectable levels of e.g. RvE2 (5(*S*),18(*R*)-diHEPE) in animals with highest 18-HEPE levels indicate that elevated SPM pathway markers correlate with an increased capacity for SPM formation in the mouse. It remains to be explored if a diet that combines n3-PUFA supplementation with low n6-PUFA helps to attenuate inflammation and facilitate resolution *in vivo*, for example in LPS-induced sepsis or zymosan-induced peritonitis models, and if these effects are mediated by increased SPM production. In humans, the situation is likely more complex due to different reaction specificities of ALOX isoforms with different PUFA. During this thesis it was revealed, that while mouse and human ALOX15 orthologs have a similar reaction specificity with EPA, it is completely different with ARA and DHA (*chapter 3*). Humans and higher primates express 15-lipoxygenating ALOX15 orthologs, whereas lower mammals, such as mice or rats express a 12-lipoxygenating ALOX15. This alteration of the ALOX15 specificity has been implicated in an evolutionary concept to improve the

biosynthesis of lipoxins as pro-resolving mediators [7]. Moreover, the pronounced dual reaction specificity of the human ALOX15 described in this thesis, which was particularly evident for DHA, might be another mechanism to increase SPM biosynthesis. ALOX15 effectively catalyzes hydrogen abstraction from the n8- and n11-bisallylic methylene and thereby gives rise to more complex product patterns of (multiple) hydroxylated fatty acid derivatives.

The correlation between n3-PUFA supplementation and the elevation of n3-PUFA derived oxylipins, such as hydroxy- and epoxy-PUFA is well documented in both animals [8, 9] and humans [10, 11] and was also shown within this thesis (*chapter 2*). Detection of endogenous levels of SPMs and their elevation upon n3-PUFA supplementation however is challenging and findings are not always consistent [12]. Formation pathways involve two or more enzymatic conversion steps catalyzed by enzymes that may be expressed in the same cell or different cell types. For example, interaction between 5- and 15-lipoxygenase pathways in human leukocytes during lipoxin formation have been described [13]. Additionally, double lipoxygenation products are formed at lower rates compared to mono-oxygenated products as shown for soybean LOX-1 [14] and this may also contribute to low *in vivo* levels of multiple hydroxylated SPMs. Moreover, their local action and distinct time course of formation need to be considered when analyzing biological samples to ensure meaningful results. In various disease models, SPMs have been shown to be active at pico- to nanomolar levels [15] underscoring the requirement for powerful analytical methods and instrumentation to enable sensitive and selective detection and quantification (*chapter 4*). Optimization of instrumental and electronic parameters is crucial for SPM detection. However, within this thesis it could be demonstrated that parameters suitable for most oxylipins also allow sensitive detection of SPMs with lower limits of quantification ranging between 0.4–4 pg on column. Using selected reaction monitoring (SRM) with collision induced fragmentation, the selection of characteristic fragment ions and optimization of the applied collision energy is highly relevant in order to achieve best selectivity and sensitivity. At least two fragments that are not formed by the unspecific loss of water and/or

carbon dioxide should be chosen to avoid erroneous identification/quantification due to isobaric interferences. For example, RvE2 (5(*S*),18(*R*)-diHEPE), which was detected in mouse liver (*chapter 2*) shows good agreement (± 30%) regarding the ratio of different SRM transitions when compared to the authentic standard. However, ALOX15 derived products, e.g. 8,15-diHEPE, which were characterized in *chapter 5*, might be mistaken for RvE2 due to same molecular mass, overlapping retention times and fragmentation patterns stressing the importance of carefully chosen specific transitions. In addition, method characterization according to internationally accepted guidelines is highly relevant to obtain comparable and reproducible results. With respect to the low endogenous levels of SPMs also pre-analytical sample handling and stability should be examined as source of variability. Finally, conducting inter-laboratory comparisons focusing on SPMs and SPM precursors seem indispensable to obtain harmonized methods and comparable results.

Despite elevation of SPMs alongside with other oxylipins in clinical samples of severe septic shock or peritonitis (*chapter 4*), more detailed examinations are required in order to explore how SPM formation may correlate with the disease severity or outcome. In order to gain a deeper understanding of SPM formation during the onset and resolution of inflammation, investigating the participating immune cells, the enzymes expressed in these cells, their interaction with other cell types and the stimuli triggering the formation and release of specific lipid mediators is crucial. During the course of this thesis, the method developed in *chapter 4* was applied to characterize the lipid mediator profile formed by monocyte-derived macrophages upon pathogen stimulation [16]. Macrophages can differentiate to M1 or M2 macrophages and this polarization can switch during the course of inflammation changing from acute inflammation to inflammatory resolution, which is associated with increased SPM formation. Moreover, macrophages co-express different ALOX isoforms and might therefore be capable of synthesizing multiple hydroxylated PUFA derivatives within a single cell or via trans-cellular interactions. In contrast to differentiated M1 macrophages (CSF-2/INFγ) expressing high levels of ALOX5 and FLAP, elevated expression

of ALOX15 was determined in differentiated M2 macrophages (CSF-1/IL-4). Upon persistent stimulation with bacterial LPS, M2 macrophages also expressed higher levels of ALOX5 and ALOX15B. In both, stimulated M2 macrophages as well as in M1/M2 co-incubations additional treatment with Ca^{2+} ionophore and ARA+EPA+DHA supplementation led to elevated levels of SPMs, being most evident for 15-/5-lipoxygenation products, e.g. RvD5. Of note, detected SPM levels were minimal compared to the amount of mono-hydroxylated PUFA, leukotrienes and prostanoids. Detailed investigations how these very low amounts of SPMs alongside much higher levels of other bioactive oxylipins affect the course and outcome of inflammation *in vivo* are needed in the future.

Moreover, since stimulated M2 macrophages expressed all three investigated ALOX isoforms (ALOX5, ALOX15, ALOX15B) it remains to be elucidated, which enzymes are mainly involved in SPM biosynthesis [16]. For example, formation of EPA derived E-series resolvins requires 18-HEPE as precursor, which was present in all macrophage incubations and for this oxylipin different formation routes have been described including both enzymatic synthesis by acetylated COX-2 [17] or microbial CYP isoforms [18] as well as autoxidation [19]. While only trace amounts of 18-HEPE were detected in ALOX15 incubations, several ALOX isoforms were capable of 18-HEPE oxygenation (*chapter 5*). Particularly ALOX15B could thereby be implicated in the formation of RvE3. Taking together these findings with upregulated ALOX15B expression in stimulated M2 macrophages, this ALOX isoform may play a role in SPM biosynthesis in macrophages, which warrants further investigation. Despite 18-HEPE being an important SPM precursor, 5-HEPE and 15-HEPE were the dominating oxygenation products of EPA in stimulated M1 and M2 macrophages, respectively. Since on the one hand some ALOX isoforms exhibit multiple catalytic activities and on the other hand ALOX enzymes are capable of accepting their primary oxygenation products (mono-hydro(pero)xy fatty acids) as substrate for secondary oxygenation, these enzymes give rise to a multitude of further oxygenation products as shown for EPA in *chapter 5*. Particularly, for ALOX5 and ALOX15 as well as for the consecutive action of two ALOX isoforms, double

oxygenated products constitute a significant share of the total ALOX products. Despite previously described formation pathways, little is known on the biological role of these lipoxygenase derived products e.g. in the regulation of inflammation and resolution and in the activation of immune cells. Thus, investigating the formation of these compounds in both cellular and *in vivo* systems and to determine their bioactivity would be highly interesting with respect to their role in inflammatory conditions. For example, in leukotriene synthesis an additional enzyme, i.e. the leukotriene A_4 hydrolase, is required to generate the specific stereo-chemistry of potent LTB_4, while unspecific hydrolysis products such as 6-*trans*-LTB_4 are less active [20]. Similar formation pathways have been implicated for resolvins, e.g. RvE1 [21]. Therefore, in a cellular system specific structures of the broad spectrum of secondary ALOX products might be formed. In order to determine their exact stereochemistry and differentiate between similar structures of different biosynthetic routes, more comprehensive structural analyses and if necessary chiral LC analysis will be required stressing the relevance of powerful analytical tools in the research of lipid mediator formation.

The field of SPMs is still growing with new mediators or mediator classes being identified. Concerted action of different enzymes that may exhibit multiple catalytic activities underscores the broad spectrum of possible products. This thesis contributes to a better understanding of the role of lipoxygenase enzymes in the biosynthesis of potent lipid mediators being capable of i) effectively oxygenating n6- and n3-PUFA of different chain length (*chapter 3*) and ii) producing a complex mixture of secondary products (*chapter 5*), whose biological activity is yet not completely elucidated.

6.1 References

1. Lichtenstein AH, Appel LJ, Brands M, Carnethon M, Daniels S, Franch HA, Franklin B, Kris-Etherton P, Harris WS, Howard B, Karanja N, Lefevre M, Rudel L, Sacks F, Van Horn L, Winston M, Wylie-Rosett J (2006) Summary of American Heart Association diet and lifestyle recommendations revision 2006. *Arterioscl Throm Vas*, 26(10), 2186-2191; doi: 10.1161/01.ATV.0000238352.25222.5e.
2. EFSA Panel on Dietetic Products, Nutrition and Allergies (2009) Scientific Opinion on the substantiation of health claims related to EPA, DHA, DPA and maintenance of normal blood pressure (ID 502), maintenance of normal HDL-cholesterol concentrations (ID 515), maintenance of normal (fasting) blood concentrations of triglycerides (ID 517), maintenance of normal LDL-cholesterol concentrations (ID 528, 698) and maintenance of joints (ID 503, 505, 507, 511, 518, 524, 526, 535, 537) pursuant to Article 13(1) of Regulation (EC) No 1924/2006. *EFSA Journal*, 7(10), 1263; doi: 10.2903/j.efsa.2009.1263.
3. Anderson BM, Ma DW (2009) Are all n-3 polyunsaturated fatty acids created equal? *Lipids Health Dis*, 8, 33; doi: 10.1186/1476-511X-8-33.
4. Greupner T, Kutzner L, Nolte F, Strangmann A, Kohrs H, Hahn A, Schebb NH, Schuchardt JP (2018) Effects of a 12-week high-alpha-linolenic acid intervention on EPA and DHA concentrations in red blood cells and plasma oxylipin pattern in subjects with a low EPA and DHA status. *Food Funct*, 9(3), 1587-1600; doi: 10.1039/c7fo01809f.
5. Greupner T, Kutzner L, Pagenkopf S, Kohrs H, Hahn A, Schebb NH, Schuchardt JP (2018) Effects of a low and a high dietary LA/ALA ratio on long-chain PUFA concentrations in red blood cells. *Food Funct*, 9(9), 4742-4754; doi: 10.1039/c8fo00735g.
6. Calder PC (2012) Mechanisms of action of (n-3) fatty acids. *J Nutr*, 142(3), 592S-599S; doi: 10.3945/jn.111.155259.
7. Adel S, Karst F, Gonzalez-Lafont A, Pekarova M, Saura P, Masgrau L, Lluch JM, Stehling S, Horn T, Kuhn H, Heydeck D (2016) Evolutionary alteration of ALOX15 specificity optimizes the biosynthesis of antiinflammatory and proresolving lipoxins. *Proc Natl Acad Sci U S A*, 113(30), E4266-4275; doi: 10.1073/pnas.1604029113.
8. Ostermann AI, Waindok P, Schmidt MJ, Chiu CY, Smyl C, Rohwer N, Weylandt KH, Schebb NH (2017) Modulation of the endogenous omega-3 fatty acid and oxylipin profile in vivo-A comparison of the fat-1 transgenic mouse with C57BL/6 wildtype mice on an omega-3 fatty acid enriched diet. *PLoS One*, 12(9), e0184470; doi: 10.1371/journal.pone.0184470.
9. Leng S, Winter T, Aukema HM (2018) Dietary ALA, EPA and DHA have distinct effects on oxylipin profiles in female and male rat kidney, liver and serum. *J Nutr Biochem*, 57, 228-237; doi: 10.1016/j.jnutbio.2018.04.002.
10. Schuchardt JP, Ostermann AI, Stork L, Fritzsch S, Kohrs H, Greupner T, Hahn A, Schebb NH (2017) Effect of DHA supplementation on oxylipin levels in plasma and immune cell stimulated blood. *Prostaglandins Leukot Essent Fatty Acids*, 121, 76-87; doi: 10.1016/j.plefa.2017.06.007.
11. Ostermann AI, West AL, Schoenfeld K, Browning LM, Walker CG, Jebb SA, Calder PC, Schebb NH (2019) Plasma oxylipins respond in a linear dose-response manner with increased intake of EPA and DHA: results from a randomized controlled trial in healthy humans. *Am J Clin Nutr*, 109(5), 1251-1263; doi: 10.1093/ajcn/nqz016.
12. Murphy RC (2015) Specialized pro-resolving mediators: do they circulate in plasma? *J Lipid Res*, 56(9), 1641-1642; doi: 10.1194/jlr.C062356.

13. Serhan CN, Hamberg M, Samuelsson B (1984) Lipoxins: novel series of biologically active compounds formed from arachidonic acid in human leukocytes. *Proc Natl Acad Sci U S A*, 81(17), 5335-5339; doi: 10.1073/pnas.81.17.5335.
14. Bild GS, Ramadoss CS, Lim S, Axelrod B (1977) Double dioxygenation of arachidonic acid by soybean lipoxygenase-1. *Biochem Biophys Res Commun*, 74(3), 949-954; doi: 10.1016/0006-291x(77)91610-2.
15. Serhan CN, Petasis NA (2011) Resolvins and protectins in inflammation resolution. *Chem Rev*, 111(10), 5922-5943; doi: 10.1021/cr100396c.
16. Ebert R, Cumbana R, Lehmann C, Kutzner L, Toewe A, Ferreiros N, Parnham MJ, Schebb NH, Steinhilber D, Kahnt AS (2020) Long-term stimulation of toll-like receptor-2 and -4 upregulates 5-LO and 15-LO-2 expression thereby inducing a lipid mediator shift in human monocyte-derived macrophages. *Biochim Biophys Acta*, 1865(9), 158702; doi: 10.1016/j.bbalip.2020.158702.
17. Serhan CN, Clish CB, Brannon J, Colgan SP, Chiang N, Gronert K (2000) Novel functional sets of lipid-derived mediators with antiinflammatory actions generated from omega-3 fatty acids via cyclooxygenase 2-nonsteroidal antiinflammatory drugs and transcellular processing. *J Exp Med*, 192(8), 1197-1204; doi: 10.1084/jem.192.8.1197.
18. Arita M, Clish CB, Serhan CN (2005) The contributions of aspirin and microbial oxygenase to the biosynthesis of anti-inflammatory resolvins: Novel oxygenase products from omega-3 polyunsaturated fatty acids. *Biochem Biophys Res Commun*, 338(1), 149-157; doi: 10.1016/j.bbrc.2005.07.181.
19. Ostermann AI, Willenberg I, Weylandt KH, Schebb NH (2015) Development of an online-SPE-LC-MS/MS method for 26 hydroxylated polyunsaturated fatty acids as rapid targeted metabolomics approach for the LOX, CYP, and autoxidation pathways of the arachidonic acid cascade. *Chromatographia*, 78(5-6), 415-428; doi: 10.1007/s10337-014-2768-8.
20. Fretland DJ, Widomski DL, Anglin CP, Walsh RE, Levin S, Gaginella TS (1991) 6-trans-leukotriene B4 is a neutrophil chemotaxin in the guinea pig dermis. *J Leukoc Biol*, 49(3), 283-288; doi: 10.1002/jlb.49.3.283.
21. Oh SF, Pillai PS, Recchiuti A, Yang R, Serhan CN (2011) Pro-resolving actions and stereoselective biosynthesis of 18S E-series resolvins in human leukocytes and murine inflammation. *J Clin Invest*, 121(2), 569-581; doi: 10.1172/JCI42545.

Summary

Polyunsaturated fatty acids (PUFA) play an important role in (patho-)physiology and particularly n3-PUFA are associated with beneficial effects on human health. However, an increased consumption of n6-PUFA in industrialized countries in the last century likely led to decreased endogenous levels of EPA and DHA. Several health claims exist for the intake of these long-chain n3-PUFA, for example in the context of cardiovascular and inflammatory conditions. Their biological effects are believed to be at least in part mediated by the enzymatically formed oxidized lipid mediators, i.e. eicosanoids and other oxylipins. Particularly high potency has been attributed to a class of multiple hydroxylated PUFA, the so-called specialized pro-resolving lipid mediators (SPMs). These bioactive compounds are synthesized from EPA and DHA comprising lipoxins, resolvins, maresins and protectins, but also lipoxins formed from the n6-PUFA arachidonic acid (ARA) are involved in the resolution of inflammation. Lipoxygenases (LOX/ALOX) are crucial in catalyzing the enzymatic formation of hydroxylated fatty acids and therefore play an essential role in SPM biosynthesis.

In the first part of this thesis, it was investigated how the modulation of the endogenous blood and tissue n3-PUFA status and tissue free oxylipin pattern upon n3-PUFA feeding is affected by the dietary n6-PUFA background in mice (*chapter 2*). Based on comprehensive analysis of the fatty acid profile in murine liver and blood as well as the free oxylipin pattern in liver tissue it was found that: i) A pronounced decrease of dietary n6-PUFA (linoleic acid) and concomitant increase of dietary monounsaturated fatty acids (oleic acid) did not affect blood and tissue ARA or n3-PUFA levels or the tissue free oxylipins derived from these PUFA. ii) Upon EPA or DHA feeding EPA was more efficiently increased in blood and tissue as were its tissue free oxylipins when dietary LA was low, while DHA

levels were unaffected by the n6-PUFA content of the diet. iii) ARA levels were decreased by n3-PUFA feeding and this was more pronounced when combined with an n6-PUFA-low background diet. iv) Blood cell EPA+DHA was more efficiently increased when n3-PUFA were combined with low n6-PUFA and the reduction of the n6-highly unsaturated fatty acids was more evident. The positive effects of n3-PUFA can be caused by both, their competition with and consequent reduction of n6-PUFA/n6-PUFA derived oxylipins as well as an increase in e.g. less pro-inflammatory, anti-inflammatory or pro-resolving oxylipins. Therefore, a dietary intervention similar to the one used in *chapter 2* may be a promising strategy enhancing n3-PUFA mediated effects.

The LOX branch of the ARA cascade plays a crucial role in the synthesis of both pro- and anti-inflammatory lipid mediators. The second part of this thesis is focused on the catalytic activity and product specificity of human and other mammalian LOX isoforms and the instrumental analysis of their product profiles. Similar to *chapter 2*, rodents such as rats and mice are commonly applied as models in e.g. nutritional or clinical studies. However, drawing conclusions from these studies on humans is limited due to species related differences. With respect to LOX enzymes, the product specificity of the ALOX15 showed distinct differences between various species exhibiting either a 12- (e.g. mouse) or a 15- (e.g. human) lipoxygenation activity (*chapter 3*). Moreover, while the ALOX15 products formed from ARA are well characterized, predicting products or product ratios for other PUFA is hardly possible. Distinct differences could be shown and particularly the dual reaction specificity of human ALOX15 is clearly more pronounced for DHA compared to ARA. This was also evident for other higher mammals, such as chimpanzee or orangutan. Moreover, most ALOX orthologs preferred the n3-PUFA EPA and DHA (with a higher degree of unsaturation) over the n6-PUFA ARA. Both findings are of particular importance for the biosynthesis of SPMs, which – in most cases – involves a 12- or 15-lipoxygenation.

For the sensitive and selective detection of SPMs state-of-the-art RP-LC-MS/MS systems are commonly applied. However, detection and quantification of these

potent lipid mediators is challenging due to their low concentrations in biological samples. The impact of both instrumental and electronic parameters of the used AB Sciex 6500 QTRAP on the sensitivity for SPM detection in selected reaction monitoring mode was assessed in *chapter 4*. It was found that most source parameters had no striking influence on SPM detection, while the choice of specific transitions and individual optimization of collision energy is crucial. In order to ensure selective detection, at least two “backbone” fragment ions formed e.g. in a cleavage of the carbon-carbon bond in α-position to the hydroxy group, should be monitored. A quantitative method for a set of 18 SPMs including ARA derived lipoxins, EPA derived lipoxins and resolvins as well as DHA derived resolvins, maresins and protectins was developed and integrated into an existing multi-analyte targeted metabolomics platform covering a total of 175 enzymatically and autoxidatively formed oxylipins. SPMs could be measured with lower limits of quantification ranging from 0.2–2 nM (0.02–0.2 nM in plasma), corresponding to 0.4–4 pg on column, which was in a similar concentration range compared to structurally different oxylipins formed via other enzymatic pathways. Moreover, the used sample preparation strategy (including protein precipitation and solid phase extraction) allowed good accuracy and precision for SPMs extracted from biological samples, high recovery rates of deuterated internal standards as well as an effective matrix reduction.

Endogenous levels of SPMs are generally low, while their mono-hydroxylated precursor fatty acids and primary LOX products are frequently detected in biological samples. The catalytic activities of LOX enzymes, which play a central role in SPM biosynthesis, also give rise to a multitude of secondary products. In order to get a deeper insight into the formation of SPMs and other multiple hydroxylated fatty acids, the product profiles of different LOX isoforms were investigated with particular emphasis on double and triple oxygenated compounds (*chapter 5*). Recombinant human LOX isoforms, i.e. two 15-lipoxygenating ALOX isoforms ALOX15 (dual positional specificity) and ALOX15B (singular positional specificity) as well as the 12-lipoxygenating ALOX isoform ALOX12 (singular positional specificity) were incubated with EPA. In

addition, product formation of human ALOX5 was assessed alone and in consecutive incubations with the 12- and 15-LOX isoforms since most SPMs are formed via an interaction of these pathways. 18-HEPE, an E-series resolvin precursor and pathway marker was not formed by the ALOX isoforms in considerable amounts. Consequently, E-series resolvins could not be synthesized from EPA by ALOX isoforms alone. Instead, several other double oxygenated compounds were formed especially in ALOX15 and ALOX5 incubations via different formation routes, which were supported by incubations using heavy oxygen isotopes ($^{18}O_2$ gas, $H_2{}^{18}O$ buffer). Products comprised compounds formed via double lipoxygenation, hydrolysis of epoxide (leukotriene) intermediates as well as hydroxy-epoxy compounds (hepoxilins). When pre-formed 18-HEPE was used as substrate, it was readily accepted by most ALOX isoforms and formation of E-series resolvins was observed particularly for ALOX5 and ALOX15B. Moreover, several other distinct double and triple oxygenated products were formed from 18-HEPE. Elucidating the *in vivo* formation of these ALOX derived products, e.g. during inflammatory processes as well as their potential biological activity may be highly relevant in the context of inflammation resolution and should be addressed in future studies.

Appendix

Chapter 2

Tab. 8.1: Composition of feed/feeding oil. Composition of the experimental diets and fatty acid profile of the oils (as %FA of total FA) used for production of the diets. Shown are specifications by the manufacturer (sniff Spezialitäten GmbH) for the diets and own analysis of the feeding oils [mean ± deviation from the mean (n = 2)].

Feed composition	**c/n6-high**	**EPA/n6-high**	**DHA/n6-high**	**c/n6-low**	**EPA/n6-low**	**DHA/n6-low**
Crude protein [%]		17.6			17.6	
Crude fat [%]		10.1			10.1	
Crude fiber [%]		5.0			5.0	
Crude ash [%]		5.3			5.3	
Starch [%]		31.4			31.4	
Sugar [%]		11.0			11.0	
Vitamin A [IU·kg^{-1}]		15000			15000	
Vitamin D3 [IU·kg^{-1}]		1500			1500	
Vitamin E [mg·kg^{-1}]		150			150	
Vitamin K3 [mg·kg^{-1}]		20			20	
Vitamin C [mg·kg^{-1}]		30			30	
Copper [mg·kg^{-1}]		14			14	
Energy [MJ]		16.5			16.5	
Feeding oil [%FA of total FA]	**c/n6-high**	**EPA/n6-high**	**DHA/n6-high**	**c/n6-low**	**EPA/n6-low**	**DHA/n6-low**
C14:0	0.08 ± 0.08	0.10 ± 0.01	<0.05	<LLOQ	<LLOQ	<LLOQ
C15:0	<0.05	<0.05	<LLOQ	<LLOQ	<LLOQ	<LLOQ
C16:0	6.59 ± 0.02	6.17 ± 0.05	6.11 ± 0.03	4.00 ± 0.01	3.738 ± 0.008	3.708 ± 0.003
C17:0	<0.05	0.060 ± 0.001	<0.05	<0.05	<0.05	<0.05
C18:0	3.376 ± 0.007	3.130 ± 0.003	3.13 ± 0.01	2.913 ± 0.001	2.714 ± 0.005	2.706 ± 0.006
C20:0	0.24 ± 0.01	0.227 ± 0.007	0.224 ± 0.003	0.276 ± 0.003	0.261 ± 0.001	0.255 ± 0.001
C22:0	0.84 ± 0.07	1.03 ± 0.01	0.76 ± 0.04	0.84 ± 0.02	0.94 ± 0.01	0.8029 ± 0.0001
C24:0	0.236 ± 0.007	0.23 ± 0.01	0.17 ± 0.01	0.30 ± 0.02	0.260 ± 0.003	0.21 ± 0.01
C16:1n7	0.07 ± 0.01	0.065 ± 0.003	0.052 ± 0.004	<0.05	<0.05	<0.05
C18:1n9	27.14 ± 0.06	25.417 ± 0.002	25.21 ± 0.02	79.97 ± 0.05	75.14 ± 0.02	74.32 ± 0.05
C18:1n7	0.910 ± 0.004	0.82 ± 0.02	0.866 ± 0.007	1.250 ± 0.002	1.21 ± 0.02	1.25 ± 0.02
C20:1n9	0.178 ± 0.006	0.16 ± 0.02	0.154 ± 0.003	0.265 ± 0.007	0.251 ± 0.002	0.258 ± 0.001
C22:1n9	<LLOQ	<0.05	<0.05	<0.05	<0.05	<0.05
C24:1n9	<LLOQ	<LLOQ	0.12 ± 0.02	<LLOQ	<LLOQ	0.116 ± 0.006
C18:3n3	0.080 ± 0.002	0.065 ± 0.003	0.065 ± 0.008	0.167 ± 0.001	0.155 ± 0.001	0.161 ± 0.004
C18:4n3	<LLOQ	0.067 ± 0.004	<LLOQ	<LLOQ	0.052 ± 0.004	<LLOQ
C20:4n3	<LLOQ	0.131 ± 0.002	<LLOQ	<LLOQ	0.129 ± 0.007	<0.05
C20:5n3	<LLOQ	5.735 ± 0.005	0.80 ± 0.02	<LLOQ	5.46 ± 0.02	0.751 ± 0.003
C22:5n3	0.15 ± 0.15	<LLOQ	0.712 ± 0.006	<LLOQ	<LLOQ	0.666 ± 0.005
C22:6n3	<LLOQ	<LLOQ	5.72 ± 0.04	<LLOQ	<LLOQ	5.42 ± 0.03
C18:2n6	60.0 ± 0.3	56.278 ± 0.001	55.79 ± 0.09	9.92 ± 0.01	9.335 ± 0.004	9.2178 ± 0.0002
C20:4n6	<LLOQ	0.264 ± 0.005	<0.05	<LLOQ	0.241 ± 0.005	<0.05
SFA	11.4 ± 0.2	10.97 ± 0.03	10.45 ± 0.02	8.36 ± 0.05	7.95 ± 0.02	7.72 ± 0.01
MUFA	28.30 ± 0.05	26.49 ± 0.04	26.42 ± 0.02	81.55 ± 0.05	76.676 ± 0.003	76.01 ± 0.03
PUFA	60.3 ± 0.1	62.541 ± 0.001	63.133 ± 0.005	10.083 ± 0.008	15.37 ± 0.02	16.28 ± 0.04
n3-PUFA	0.23 ± 0.15	5.998 ± 0.003	7.30 ± 0.08	0.167 ± 0.001	5.79 ± 0.02	7.03 ± 0.03
n6-PUFA	60.0 ± 0.3	56.543 ± 0.004	55.84 ± 0.08	9.92 ± 0.01	9.575 ± 0.009	9.247 ± 0.009
n6/n3-PUFA ratio	260 : 1	9.4 : 1	7.7 : 1	59 : 1	1.7 : 1	1.3 : 1

Tab. 8.2: Primer sequences for qPCR. Oligonucleotide primer sequences, product sizes and primer concentrations for quantitative real-time PCR; bp: base pairs, conc: concentration.

Primer	Sequence	Manufacturer	Size [bp]	Conc. [µM]	Annealing Temp. (time), (cycle no.)
Acaca	5'-CTGGTGAAGCTGGACCTAGA-'3 5'-ACTTTATTTCCCCCAAAACG-3'	Biomol Hamburg, Germany	242	0.1	58 °C (45 s), (50x)
Acadvl	5'-TATCTCTGCCCAGCGACTTT-3' 5'-TGGGTATGGGAACACCTGAT-3'	Biomol Hamburg, Germany	175	0.1	58 °C (45 s), (45x)
Acox1	5'-AGACAGAGATGGGTCATGGA-3' 5'-ACAAAGGCATGTAACCCGTA-3'	Biomol Hamburg, Germany	205	0.2	62.8 °C (45 s), (45x)
B2M	5'-GGCCTGTATGCTATCCAGAA-3' 5'-GAAAGACCAGTCCTTGCTGA-3'	Biomol Hamburg, Germany	198	0.4	58 °C (45 s), (45x)
Cpt1a	5'-TCGACTCACCTTTCCTGAAG-3' 5'-GAAACACCATAGCCGTCATC-3'	Biomol Hamburg, Germany	163	0.2	58 °C (30 s), (45x)
Cpt2	5'-TCCTCGATCAAGATGGGAAC-3' 5'-GATCCTTCATCGGGAAGTCA-3'	Biomol Hamburg, Germany	237	0.1	56 °C (30 s), (45x)
Decr1	5'-ACCGTGGTCTTCCACTTGTC-3' 5'-TGCCCCTTTTTGTTTTTCAC-3'	Biomol Hamburg, Germany	248	0.1	58 °C (45 s), (45x)
Decr2	5'-GCCAGTTCGAAATTAAAGCA-3' 5'-GAATGTCATCCAGCTTCCAC-3'	Biomol Hamburg, Germany	153	0.2	56 °C (30 s), (45x)
Eci1	5'-GGATCAGGTACACAGCAAGG-3' 5'-TGTAGGGACTTCTGGATGGA-3'	Biomol Hamburg, Germany	186	0.2	53 °C (30 s), (40x)
Eci2	5'-CTGTACAAGCAGGCCACAGA-3' 5'-GGCTTTCTCATCAGCTCCAC-3'	Biomol Hamburg, Germany	248	0.4	58 °C (30 s), (50x)
Ehhadh	5'-TTGGCTCCCTATTACAACCA-3' 5'-GTACCTGGTATTGCCCCTCT-3'	Biomol Hamburg, Germany	222	0.2	58 °C (30 s), (45x)
Elovl2	5'-GCCAGTGAGAGGCGTTTAAG-3' 5'-TTTCGTAGCTCTGCATGGTG-3'	Biomol Hamburg, Germany	220	0.4	58 °C (30 s), (50x)
Elovl5	5'-CCCCCGAGATACAAGAGTCA-3' 5'-TGTATTTGCCTTCCCACACA-3'	Biomol Hamburg, Germany	227	0.1	58 °C (45 s), (45x)
Fads1	5'-AAGCACATGCCATACAACCA-3' 5'-CAGCGGCATGTAAGTGAAGA-3'	Biomol Hamburg, Germany	177	0.2	58 °C (30 s), (45x)
Fads2	5'-AAAGAGCCTGCATGTGTTTG-3' 5'-GATGCCGTAGAAAGGGATGT-3'	Biomol Hamburg, Germany	250	0.1	58 °C (45 s), (45x)
Hadha	5'-GTGTTTGAGGACCTCGGTGT-3' 5'-CGTTGTGTCCTTGGAGGTTT-3'	Biomol Hamburg, Germany	225	0.2	62.8 °C (45 s), (45x)
Hadhb	5'-GAGCTGTTCTTCCCAACTGC-3' 5'-ACCCCGAAAGTGCAGCTCTA-3'	Biomol Hamburg, Germany	182	0.2	62.8 °C (45 s), (45x)
Hsd17B4	5'-AAGCCCTGAAGCCAGAGTAT-3' 5'-AATAGGCCACCATTTTCCTC-3'	Biomol Hamburg, Germany	79	0.2	62.8 °C (45 s), (45x)
PGK1	5'-GCAGATTGTTTGGAATGGTC-3' 5'-TGCTCACATGGCTGACTTTA-3'	Biomol Hamburg, Germany	185	0.4	58 °C (45 s), (45x)

Tab. 8.3: Feed consumption. Mean feed consumption across the whole feeding period and feed consumed on day one after diet change. Displayed are mean ± SEM. A t-test was performed to determine statistical significance with **** $p < 0.0001$.

Group	Feed consumed 4 weeks	Feed consumed day 1	t-Test
c/n6-high	25.1 ± 2.0	35	
EPA/n6-high	28.2 ± 1.7	36	
DHA/n6-high	25.5 ± 1.1	30	
c/n6-low	27.3 ± 1.7	33	
EPA/n6-low	26.1 ± 1.7	36	
DHA/n6-low	26.1 ± 1.5	34	
Mean	26.4 ± 0.5	34 ± 0.9	****

Tab. 8.4: Body weight. Mean mice's body weight before and after the feeding period of 28 days. Displayed are mean ± SEM. A t-test was performed to determine statistical significance with ** $p < 0.01$, *** $p < 0.001$, **** $p < 0.0001$.

Group	Body weight before feeding [g]	Body weight after feeding [g]	t-Test
c/n6-high	27.0 ± 0.5	30.9 ± 0.7	****
EPA/n6-high	27.5 ± 0.4	30.9 ± 1.1	**
DHA/n6-high	26.8 ± 0.8	32.2 ± 1.2	***
c/n6-low	27.4 ± 0.4	33.0 ± 0.8	***
EPA/n6-low	27.2 ± 0.4	32.5 ± 1.2	***
DHA/n6-low	26.8 ± 0.6	32.2 ± 0.6	****
Mean	27.1 ± 0.1	32.0 ± 0.4	****

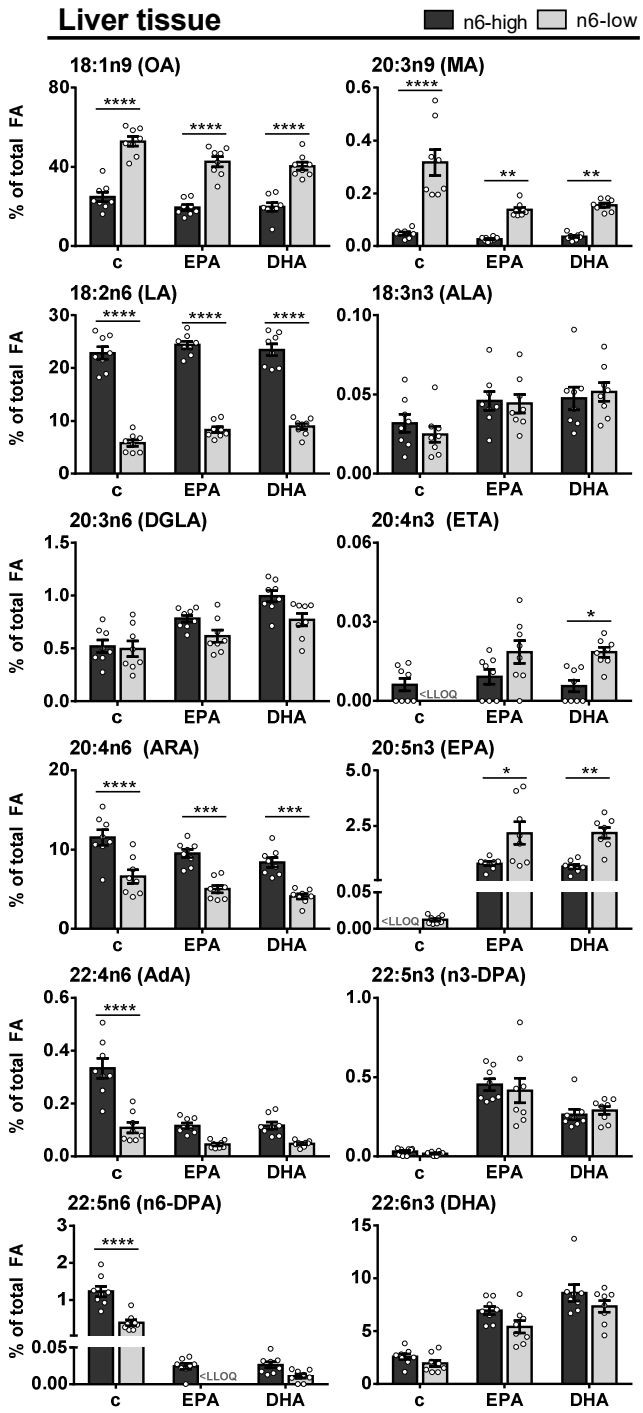

Fig. 8.1: Relative fatty acid concentrations (%FA of total FA) of n9-MUFA and -PUFA as well as n3- and n6-PUFA in liver tissue, blood cells and blood plasma of NMRI mice after 28 days of feeding an n6-PUFA-rich diet (dark grey) or an n6-PUFA-low diet (light grey) without (c) or with n3-PUFA supplementation (EPA, DHA). Shown are mean ± SEM as well as individual values (n = 8). If > 50% of the samples within one group were < LLOQ (lower limit of quantification), no mean was calculated and "< LLOQ" is indicated. Statistically significant differences (* $p < 0.05$; ** $p < 0.01$; *** $p < 0.001$; **** $p < 0.0001$) were determined by two-way ANOVA with Tukey's post-test and are indicated for n6-high vs. n6-low groups (results for comparisons of all groups are summarized in the appendix, Tab. 8.8).

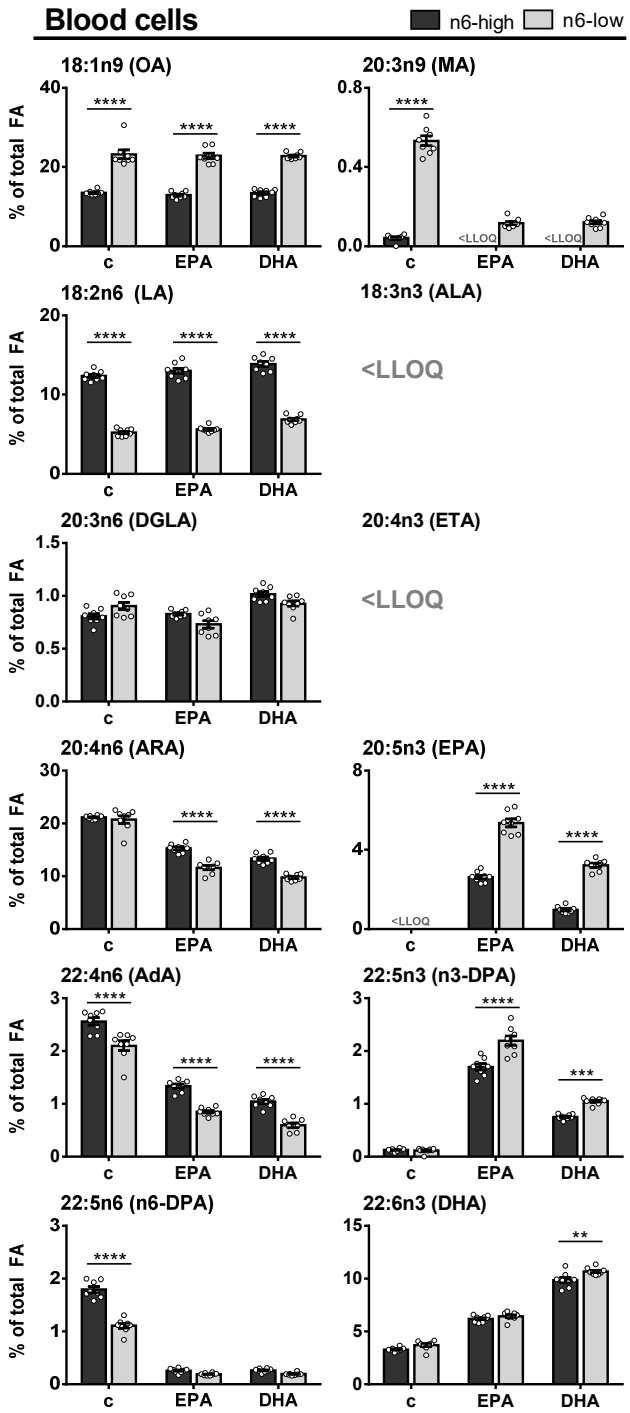

Fig. 8.1: Continued. Relative fatty acid concentrations (%FA of total FA) of n9-MUFA and -PUFA as well as n3- and n6-PUFA in liver tissue, blood cells and blood plasma.

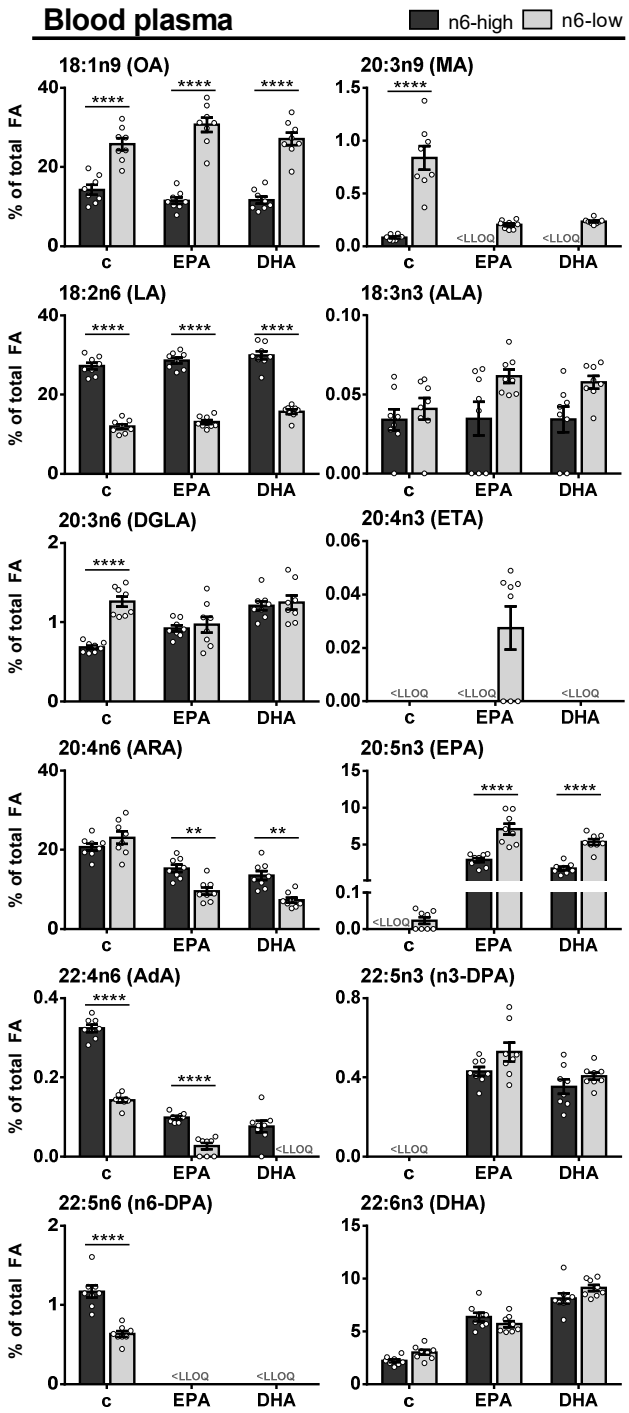

Fig. 8.1: Continued. Relative fatty acid concentrations (%FA of total FA) of n9-MUFA and -PUFA as well as n3- and n6-PUFA in liver tissue, blood cells and blood plasma.

Tab. 8.5: Fatty acid profile in mouse tissue and blood. Concentrations of individual FA and total FA in g/kg wet liver tissue (**A-1**), as well as relative FA profile (%FA of total FA) in liver tissue (**A-2**), blood cells (**B**) and blood plasma (**C**) of NMRI mice after 28 days of feeding an n6-PUFA-rich diet (n6-high) or an n6-PUFA-low diet (n6-low) without (c) or with n3-PUFA supplementation (EPA, DHA). Shown are mean ± SEM (n = 8).[a)]

(A-1) Liver tissue

g FA/kg wet tissue	c/n6-high	EPA/n6-high	DHA/n6-high	c/n6-low	EPA/n6-low	DHA/n6-low
C10:0	<LLOQ	<LLOQ	<LLOQ	<LLOQ	<LLOQ	<LLOQ
C11:0	<LLOQ	<LLOQ	<LLOQ	<LLOQ	<LLOQ	<LLOQ
C12:0	0.005 ± 0.001	0.005 ± 0.000	0.005 ± 0.000	0.012 ± 0.002	0.008 ± 0.001	0.008 ± 0.001
C13:0	<LLOQ	<LLOQ	<LLOQ	<LLOQ	<LLOQ	<LLOQ
C14:0	0.185 ± 0.042	0.139 ± 0.019	0.145 ± 0.021	0.355 ± 0.065	0.257 ± 0.040	0.225 ± 0.031
C14:1n5	0.006 ± 0.001	0.004 ± 0.001	0.005 ± 0.001	0.014 ± 0.002	0.009 ± 0.002	0.009 ± 0.001
C15:0	0.035 ± 0.003	0.032 ± 0.002	0.034 ± 0.003	0.045 ± 0.005	0.043 ± 0.004	0.038 ± 0.003
C15:1n5	<LLOQ	<LLOQ	<LLOQ	<LLOQ	<LLOQ	<LLOQ
C16:0	11.979 ± 1.521	11.471 ± 0.725	11.977 ± 0.561	17.252 ± 2.305	15.434 ± 1.823	14.415 ± 1.187
C16:1n7	1.088 ± 0.230	0.816 ± 0.100	0.720 ± 0.075	2.257 ± 0.408	1.531 ± 0.290	1.329 ± 0.139
C17:0	0.081 ± 0.005	0.071 ± 0.003	0.076 ± 0.004	0.088 ± 0.010	0.080 ± 0.007	0.073 ± 0.005
C17:1n7	<LLOQ	<LLOQ	<LLOQ	<LLOQ	<LLOQ	<LLOQ
C18:0	5.727 ± 0.236	6.084 ± 0.233	6.023 ± 0.171	5.558 ± 0.530	5.659 ± 0.367	5.709 ± 0.372
C18:1n9	15.884 ± 3.540	10.957 ± 1.366	11.325 ± 1.445	53.189 ± 9.758	33.003 ± 5.620	28.362 ± 4.212
C18:1n7	1.457 ± 0.228	1.009 ± 0.121	1.016 ± 0.102	2.971 ± 0.496	1.733 ± 0.256	1.466 ± 0.105
C18:2n6	13.411 ± 1.097	13.348 ± 0.822	13.144 ± 1.054	5.173 ± 0.584	5.981 ± 0.694	5.936 ± 0.371
C18:3n6	0.262 ± 0.039	0.164 ± 0.021	0.139 ± 0.019	0.101 ± 0.016	0.062 ± 0.014	0.047 ± 0.008
C19:0	0.017 ± 0.002	0.018 ± 0.001	0.023 ± 0.002	0.012 ± 0.001	0.014 ± 0.001	0.012 ± 0.001
C18:3n3	0.018 ± 0.003	0.025 ± 0.003	0.027 ± 0.005	0.022 ± 0.004	0.035 ± 0.008	0.034 ± 0.003
C18:4n3	<LLOQ	<LLOQ	<LLOQ	<LLOQ	<LLOQ	<LLOQ
C20:0	0.029 ± 0.001	0.029 ± 0.001	0.027 ± 0.002	0.027 ± 0.002	0.027 ± 0.001	0.026 ± 0.001
C20:1n9	0.178 ± 0.021	0.137 ± 0.014	0.154 ± 0.022	0.575 ± 0.097	0.347 ± 0.050	0.304 ± 0.035
C20:2n6	0.146 ± 0.020	0.148 ± 0.011	0.163 ± 0.013	0.042 ± 0.004	0.049 ± 0.004	0.054 ± 0.002
C20:3n9	0.029 ± 0.005	0.015 ± 0.002	0.020 ± 0.003	0.272 ± 0.031	0.098 ± 0.009	0.104 ± 0.006
C20:3n6	0.291 ± 0.018	0.423 ± 0.016	0.549 ± 0.034	0.413 ± 0.027	0.428 ± 0.034	0.506 ± 0.026
C21:0	<LLOQ	<LLOQ	<LLOQ	<LLOQ	<LLOQ	<LLOQ
C20:4n6	6.477 ± 0.160	5.101 ± 0.159	4.584 ± 0.250	5.590 ± 0.272	3.459 ± 0.258	2.683 ± 0.156
C20:3n3	<LLOQ	<LLOQ	<LLOQ	<LLOQ	<LLOQ	<LLOQ
C20:4n3	0.004 ± 0.001	0.005 ± 0.001	0.004 ± 0.001	<LLOQ	0.012 ± 0.002	0.012 ± 0.001
C20:5n3	<LLOQ	0.431 ± 0.048	0.358 ± 0.050	0.010 ± 0.001	1.326 ± 0.188	1.431 ± 0.138
C22:0	0.122 ± 0.005	0.132 ± 0.004	0.116 ± 0.003	0.128 ± 0.007	0.119 ± 0.003	0.120 ± 0.003
C22:1n9	0.017 ± 0.001	0.017 ± 0.003	0.015 ± 0.002	0.028 ± 0.005	0.027 ± 0.003	0.030 ± 0.005
C22:2n6	<LLOQ	<LLOQ	<LLOQ	<LLOQ	<LLOQ	<LLOQ
C22:4n6	0.185 ± 0.007	0.062 ± 0.004	0.063 ± 0.007	0.088 ± 0.005	0.030 ± 0.001	0.031 ± 0.001
C22:5n6	0.687 ± 0.032	0.014 ± 0.002	0.014 ± 0.002	0.313 ± 0.015	<LLOQ	0.008 ± 0.002
C22:5n3	0.016 ± 0.004	0.243 ± 0.016	0.142 ± 0.011	0.016 ± 0.004	0.264 ± 0.020	0.188 ± 0.008
C24:0	0.097 ± 0.005	0.097 ± 0.004	0.076 ± 0.003	0.091 ± 0.003	0.078 ± 0.003	0.083 ± 0.003
C22:6n3	1.427 ± 0.063	3.731 ± 0.100	4.669 ± 0.198	1.622 ± 0.120	3.662 ± 0.197	4.790 ± 0.159
C24:1n9	0.103 ± 0.004	0.114 ± 0.003	0.159 ± 0.006	0.128 ± 0.008	0.148 ± 0.011	0.170 ± 0.006
Total FA	59.965 ± 6.622	54.841 ± 3.194	55.770 ± 2.900	96.394 ± 14.250	73.924 ± 9.217	68.201 ± 6.177
SFA	18.277 ± 1.783	18.078 ± 0.883	18.501 ± 0.591	23.568 ± 2.903	21.719 ± 2.205	20.709 ± 1.509
MUFA	18.734 ± 4.008	13.053 ± 1.588	13.392 ± 1.619	59.162 ± 10.722	36.798 ± 6.200	31.668 ± 4.469
PUFA	22.954 ± 1.101	23.710 ± 0.999	23.877 ± 1.228	13.664 ± 0.974	15.407 ± 0.998	15.824 ± 0.532
n3-PUFA	1.466 ± 0.066	4.435 ± 0.123	5.200 ± 0.194	1.673 ± 0.126	5.298 ± 0.207	6.456 ± 0.217
n6-PUFA	21.459 ± 1.111	19.260 ± 0.930	18.657 ± 1.187	11.719 ± 0.872	10.011 ± 0.979	9.265 ± 0.538
n9-PUFA	0.029 ± 0.005	0.015 ± 0.002	0.020 ± 0.003	0.272 ± 0.031	0.098 ± 0.009	0.104 ± 0.006
%EPA+DHA	2.573 ± 0.273	7.751 ± 0.434	9.265 ± 0.804	1.959 ± 0.312	7.575 ± 1.027	9.521 ± 0.720
%n3 in HUFA	15.874 ± 0.726	43.990 ± 0.584	49.829 ± 1.144	19.679 ± 0.825	56.897 ± 2.185	65.829 ± 1.526
%n6 in HUFA	83.806 ± 0.701	55.860 ± 0.590	49.975 ± 1.133	76.997 ± 0.476	42.049 ± 2.120	33.108 ± 1.509
D5D-index	22.704 ± 1.145	12.105 ± 0.245	8.422 ± 0.351	13.890 ± 1.054	8.134 ± 0.220	5.311 ± 0.157
D6D-index	0.019 ± 0.002	0.012 ± 0.001	0.010 ± 0.001	0.019 ± 0.002	0.010 ± 0.001	0.008 ± 0.001
Elongase index	0.029 ± 0.001	0.012 ± 0.001	0.014 ± 0.001	0.016 ± 0.001	0.009 ± 0.000	0.012 ± 0.001

[a)] Individual FA that were < LLOQ in all feeding groups were not taken into account for calculation of the sum of total FA and "< LLOQ" is displayed. For FA that were < LLOQ in > 50% of the samples within a feeding group, for the whole group the LLOQ (0.0017 g/kg) was used for calculation of total FA and n3-PUFA status (i.e. %EPA+DHA, %n3 in HUFA, %n6 in HUFA); for FA that were < LLOQ in ≤ 50% within a feeding group for these FA 1/2 LLOQ was used for calculation of mean ± SEM, total FA and n3-PUFA status. For calculation of relative FA distribution only areas of FA > LLOQ were taken into account, FA < LLOQ were set to zero; if > 50% of the samples withis a group were < LLOQ, the whole group was set to zero.

Tab. 8.5: Continued. Fatty acid profile in mouse tissue and blood.

(A-2) Liver tissue

% of total FA	c/n6-high	EPA/n6-high	DHA/n6-high	c/n6-low	EPA/n6-low	DHA/n6-low
C10:0	<LLOQ	<LLOQ	<LLOQ	<LLOQ	<LLOQ	<LLOQ
C11:0	<LLOQ	<LLOQ	<LLOQ	<LLOQ	<LLOQ	<LLOQ
C12:0	0.009 ± 0.000	0.009 ± 0.000	0.009 ± 0.001	0.012 ± 0.001	0.010 ± 0.001	0.011 ± 0.001
C13:0	<LLOQ	<LLOQ	<LLOQ	<LLOQ	<LLOQ	<LLOQ
C14:0	0.289 ± 0.030	0.246 ± 0.021	0.255 ± 0.031	0.357 ± 0.026	0.340 ± 0.026	0.324 ± 0.019
C14:1n5	0.010 ± 0.001	0.007 ± 0.001	0.008 ± 0.001	0.015 ± 0.001	0.011 ± 0.001	0.013 ± 0.001
C15:0	0.059 ± 0.002	0.058 ± 0.002	0.060 ± 0.003	0.049 ± 0.003	0.060 ± 0.003	0.056 ± 0.002
C15:1n5	<LLOQ	<LLOQ	<LLOQ	<LLOQ	<LLOQ	<LLOQ
C16:0	19.821 ± 0.418	20.901 ± 0.388	21.560 ± 0.390	18.173 ± 0.404	21.037 ± 0.507	21.233 ± 0.237
C16:1n7	1.713 ± 0.142	1.456 ± 0.114	1.266 ± 0.089	2.252 ± 0.149	1.968 ± 0.175	1.944 ± 0.101
C17:0	0.140 ± 0.007	0.131 ± 0.005	0.136 ± 0.004	0.096 ± 0.007	0.114 ± 0.007	0.109 ± 0.003
C17:1n7	<LLOQ	<LLOQ	<LLOQ	<LLOQ	<LLOQ	<LLOQ
C18:0	9.960 ± 0.556	11.255 ± 0.498	11.030 ± 0.710	6.149 ± 0.428	8.137 ± 0.595	8.541 ± 0.495
C18:1n9	24.819 ± 2.380	19.482 ± 1.414	19.759 ± 2.069	52.901 ± 2.424	42.630 ± 2.530	40.422 ± 2.013
C18:1n7	2.370 ± 0.130	1.808 ± 0.127	1.797 ± 0.118	3.049 ± 0.173	2.298 ± 0.124	2.181 ± 0.096
C18:2n6	22.844 ± 1.165	24.371 ± 0.705	23.429 ± 1.119	5.787 ± 0.620	8.300 ± 0.544	8.936 ± 0.556
C18:3n6	0.432 ± 0.037	0.298 ± 0.032	0.244 ± 0.026	0.108 ± 0.014	0.080 ± 0.011	0.070 ± 0.009
C19:0	0.031 ± 0.005	0.032 ± 0.002	0.041 ± 0.005	0.015 ± 0.004	0.021 ± 0.004	0.018 ± 0.002
C18:3n3	0.032 ± 0.006	0.046 ± 0.006	0.047 ± 0.007	0.025 ± 0.005	0.044 ± 0.006	0.052 ± 0.006
C18:4n3	<LLOQ	<LLOQ	<LLOQ	<LLOQ	<LLOQ	<LLOQ
C20:0	0.051 ± 0.004	0.054 ± 0.002	0.049 ± 0.003	0.032 ± 0.004	0.040 ± 0.004	0.040 ± 0.003
C20:1n9	0.298 ± 0.022	0.246 ± 0.013	0.269 ± 0.031	0.605 ± 0.056	0.463 ± 0.023	0.445 ± 0.033
C20:2n6	0.263 ± 0.045	0.274 ± 0.018	0.294 ± 0.021	0.051 ± 0.010	0.071 ± 0.007	0.083 ± 0.006
C20:3n9	0.048 ± 0.006	0.027 ± 0.003	0.037 ± 0.005	0.317 ± 0.050	0.137 ± 0.009	0.155 ± 0.008
C20:3n6	0.520 ± 0.058	0.782 ± 0.033	0.994 ± 0.054	0.496 ± 0.074	0.616 ± 0.057	0.771 ± 0.059
C21:0	<LLOQ	<LLOQ	<LLOQ	<LLOQ	<LLOQ	<LLOQ
C20:4n6	11.513 ± 0.983	9.492 ± 0.525	8.367 ± 0.594	6.584 ± 0.834	5.006 ± 0.470	4.092 ± 0.322
C20:3n3	<LLOQ	<LLOQ	<LLOQ	<LLOQ	<LLOQ	<LLOQ
C20:4n3	0.006 ± 0.002	0.009 ± 0.003	0.006 ± 0.002	<LLOQ	0.019 ± 0.004	0.018 ± 0.002
C20:5n3	<LLOQ	0.797 ± 0.090	0.655 ± 0.095	0.012 ± 0.002	2.174 ± 0.503	2.185 ± 0.240
C22:0	0.218 ± 0.021	0.246 ± 0.013	0.212 ± 0.013	0.150 ± 0.019	0.179 ± 0.023	0.183 ± 0.012
C22:1n9	0.030 ± 0.003	0.031 ± 0.005	0.027 ± 0.003	0.035 ± 0.009	0.040 ± 0.006	0.043 ± 0.007
C22:2n6	<LLOQ	<LLOQ	<LLOQ	<LLOQ	<LLOQ	<LLOQ
C22:4n6	0.334 ± 0.037	0.116 ± 0.010	0.116 ± 0.014	0.108 ± 0.020	0.044 ± 0.005	0.048 ± 0.004
C22:5n6	1.233 ± 0.142	0.024 ± 0.004	0.026 ± 0.004	0.391 ± 0.077	<LLOQ	0.011 ± 0.003
C22:5n3	0.030 ± 0.008	0.453 ± 0.037	0.264 ± 0.034	0.017 ± 0.004	0.416 ± 0.078	0.290 ± 0.026
C24:0	0.172 ± 0.016	0.181 ± 0.012	0.141 ± 0.013	0.110 ± 0.016	0.121 ± 0.019	0.128 ± 0.011
C22:6n3	2.570 ± 0.273	6.954 ± 0.395	8.610 ± 0.779	1.947 ± 0.311	5.402 ± 0.582	7.336 ± 0.558
C24:1n9	0.185 ± 0.018	0.213 ± 0.016	0.292 ± 0.024	0.157 ± 0.027	0.220 ± 0.027	0.260 ± 0.020
SFA	30.751 ± 0.621	33.113 ± 0.487	33.493 ± 0.938	25.144 ± 0.801	30.060 ± 0.899	30.645 ± 0.568
MUFA	29.424 ± 2.598	23.244 ± 1.612	23.418 ± 2.231	59.012 ± 2.583	47.632 ± 2.717	45.308 ± 2.014
PUFA	39.825 ± 2.222	43.643 ± 1.324	43.089 ± 1.590	15.843 ± 1.875	22.308 ± 1.948	24.047 ± 1.489
n3-PUFA	2.638 ± 0.281	8.259 ± 0.466	9.582 ± 0.836	2.000 ± 0.316	8.054 ± 1.106	9.881 ± 0.749
n6-PUFA	37.139 ± 1.975	35.357 ± 0.995	33.471 ± 1.209	13.526 ± 1.542	14.117 ± 1.042	14.011 ± 0.930
n9-PUFA	0.048 ± 0.006	0.027 ± 0.003	0.037 ± 0.005	0.317 ± 0.050	0.137 ± 0.009	0.155 ± 0.008
%EPA+DHA	2.570 ± 0.273	7.751 ± 0.434	9.265 ± 0.804	1.959 ± 0.312	7.575 ± 1.027	9.521 ± 0.720
%n3 in HUFA	15.857 ± 0.726	43.991 ± 0.585	49.829 ± 1.144	19.677 ± 0.825	56.908 ± 2.186	65.831 ± 1.526
%n6 in HUFA	83.824 ± 0.702	55.859 ± 0.590	49.975 ± 1.133	76.999 ± 0.476	42.038 ± 2.120	33.107 ± 1.509
D5D index	22.704 ± 1.145	12.105 ± 0.245	8.422 ± 0.351	13.890 ± 1.054	8.134 ± 0.220	5.311 ± 0.157
D6D index	0.019 ± 0.002	0.012 ± 0.001	0.010 ± 0.001	0.019 ± 0.002	0.010 ± 0.001	0.008 ± 0.001
Elongase index	0.029 ± 0.001	0.012 ± 0.001	0.014 ± 0.001	0.016 ± 0.001	0.009 ± 0.000	0.012 ± 0.001

Tab. 8.5: Continued. Fatty acid profile in mouse tissue and blood.

(B) Blood cells

% of total FA	c/n6-high	EPA/n6-high	DHA/n6-high	c/n6-low	EPA/n6-low	DHA/n6-low
C10:0	<LLOQ	<LLOQ	<LLOQ	<LLOQ	<LLOQ	<LLOQ
C11:0	<LLOQ	<LLOQ	<LLOQ	<LLOQ	<LLOQ	<LLOQ
C12:0	<LLOQ	<LLOQ	<LLOQ	<LLOQ	<LLOQ	<LLOQ
C13:0	<LLOQ	<LLOQ	<LLOQ	<LLOQ	<LLOQ	<LLOQ
C14:0	0.158 ± 0.011	0.166 ± 0.019	0.183 ± 0.023	0.195 ± 0.041	0.232 ± 0.025	0.190 ± 0.018
C14:1n5	<LLOQ	<LLOQ	<LLOQ	<LLOQ	<LLOQ	<LLOQ
C15:0	0.077 ± 0.003	0.075 ± 0.002	0.085 ± 0.005	0.073 ± 0.006	0.101 ± 0.008	0.084 ± 0.005
C15:1n5	<LLOQ	<LLOQ	<LLOQ	<LLOQ	<LLOQ	<LLOQ
C16:0	24.386 ± 0.247	26.008 ± 0.209	26.107 ± 0.238	23.244 ± 0.338	25.605 ± 0.295	25.568 ± 0.261
C16:1n7	0.522 ± 0.046	0.524 ± 0.056	0.484 ± 0.053	0.658 ± 0.175	0.606 ± 0.070	0.559 ± 0.071
C17:0	0.219 ± 0.009	0.209 ± 0.004	0.212 ± 0.005	0.173 ± 0.008	0.192 ± 0.009	0.189 ± 0.006
C17:1n7	<LLOQ	<LLOQ	<LLOQ	<LLOQ	<LLOQ	<LLOQ
C18:0	13.096 ± 0.149	13.227 ± 0.165	12.475 ± 0.202	11.253 ± 0.353	11.024 ± 0.193	10.904 ± 0.180
C18:1n9	13.484 ± 0.209	12.882 ± 0.288	13.436 ± 0.336	23.158 ± 1.100	22.797 ± 0.684	22.754 ± 0.281
C18:1n7	1.512 ± 0.039	1.285 ± 0.042	1.312 ± 0.038	1.817 ± 0.050	1.403 ± 0.056	1.343 ± 0.039
C18:2n6	12.350 ± 0.217	12.991 ± 0.346	13.857 ± 0.317	5.210 ± 0.166	5.600 ± 0.132	6.859 ± 0.177
C18:3n6	0.082 ± 0.011	0.053 ± 0.004	0.041 ± 0.006	0.025 ± 0.007	0.018 ± 0.006	0.011 ± 0.004
C19:0	0.079 ± 0.004	0.069 ± 0.003	0.086 ± 0.005	0.055 ± 0.005	0.068 ± 0.004	0.053 ± 0.005
C18:3n3	<LLOQ	<LLOQ	<LLOQ	<LLOQ	<LLOQ	<LLOQ
C18:4n3	<LLOQ	<LLOQ	<LLOQ	<LLOQ	<LLOQ	<LLOQ
C20:0	0.207 ± 0.008	0.210 ± 0.010	0.211 ± 0.012	0.193 ± 0.010	0.215 ± 0.008	0.204 ± 0.006
C20:1n9	0.281 ± 0.007	0.246 ± 0.008	0.265 ± 0.009	0.469 ± 0.021	0.380 ± 0.012	0.364 ± 0.015
C20:2n6	0.267 ± 0.015	0.254 ± 0.007	0.258 ± 0.008	0.116 ± 0.008	0.119 ± 0.006	0.134 ± 0.004
C20:3n9	0.041 ± 0.006	<LLOQ	<LLOQ	0.531 ± 0.025	0.116 ± 0.008	0.121 ± 0.009
C20:3n6	0.805 ± 0.025	0.828 ± 0.012	1.015 ± 0.024	0.903 ± 0.035	0.728 ± 0.034	0.926 ± 0.024
C21:0	<LLOQ	<LLOQ	<LLOQ	<LLOQ	<LLOQ	<LLOQ
C20:4n6	21.134 ± 0.123	15.268 ± 0.283	13.290 ± 0.328	20.717 ± 0.719	11.602 ± 0.398	9.749 ± 0.211
C20:3n3	<LLOQ	<LLOQ	<LLOQ	<LLOQ	<LLOQ	<LLOQ
C20:4n3	<LLOQ	<LLOQ	<LLOQ	<LLOQ	<LLOQ	<LLOQ
C20:5n3	<LLOQ	2.626 ± 0.095	0.967 ± 0.063	<LLOQ	5.353 ± 0.199	3.223 ± 0.101
C22:0	0.765 ± 0.023	0.747 ± 0.028	0.766 ± 0.022	0.722 ± 0.028	0.760 ± 0.023	0.733 ± 0.012
C22:1n9	0.103 ± 0.019	0.160 ± 0.037	0.269 ± 0.083	0.181 ± 0.023	0.173 ± 0.035	0.221 ± 0.025
C22:2n6	<LLOQ	<LLOQ	<LLOQ	<LLOQ	<LLOQ	<LLOQ
C22:4n6	2.560 ± 0.069	1.333 ± 0.039	1.042 ± 0.039	2.098 ± 0.094	0.849 ± 0.026	0.592 ± 0.041
C22:5n6	1.792 ± 0.057	0.255 ± 0.016	0.261 ± 0.013	1.105 ± 0.046	0.188 ± 0.009	0.192 ± 0.009
C22:5n3	0.125 ± 0.010	1.697 ± 0.060	0.753 ± 0.018	0.113 ± 0.017	2.195 ± 0.091	1.050 ± 0.021
C24:0	1.659 ± 0.051	1.709 ± 0.062	1.670 ± 0.053	1.413 ± 0.032	1.491 ± 0.044	1.527 ± 0.037
C22:6n3	3.284 ± 0.070	6.190 ± 0.112	9.855 ± 0.257	3.692 ± 0.156	6.430 ± 0.142	10.674 ± 0.125
C24:1n9	1.013 ± 0.029	0.988 ± 0.033	1.101 ± 0.035	1.885 ± 0.087	1.753 ± 0.048	1.777 ± 0.045
SFA	40.645 ± 0.198	42.420 ± 0.136	41.795 ± 0.261	37.321 ± 0.392	39.689 ± 0.178	39.451 ± 0.180
MUFA	16.915 ± 0.246	16.084 ± 0.337	16.866 ± 0.394	28.168 ± 1.280	27.112 ± 0.747	27.019 ± 0.379
PUFA	42.440 ± 0.187	41.496 ± 0.280	41.339 ± 0.306	34.511 ± 0.973	33.199 ± 0.650	33.530 ± 0.282
n3-PUFA	3.409 ± 0.076	10.514 ± 0.206	11.575 ± 0.284	3.806 ± 0.158	13.978 ± 0.304	14.947 ± 0.188
n6-PUFA	38.990 ± 0.215	30.982 ± 0.283	29.764 ± 0.124	30.174 ± 0.829	19.105 ± 0.520	18.462 ± 0.280
n9-PUFA	0.041 ± 0.006	<LLOQ	<LLOQ	0.531 ± 0.025	0.116 ± 0.008	0.121 ± 0.009
%EPA+DHA	3.284 ± 0.070	8.817 ± 0.170	10.823 ± 0.279	3.692 ± 0.156	11.783 ± 0.266	13.897 ± 0.190
%n3 in HUFA	11.467 ± 0.273	37.302 ± 0.700	42.589 ± 0.703	13.039 ± 0.254	50.951 ± 0.883	56.370 ± 0.742
%n6 in HUFA	88.395 ± 0.272	62.698 ± 0.700	57.411 ± 0.703	85.128 ± 0.183	48.626 ± 0.869	43.174 ± 0.730

Tab. 8.5: Continued. Fatty acid profile in mouse tissue and blood.

(C) Blood plasma

% of total FA	c/n6-high	EPA/n6-high	DHA/n6-high	c/n6-low	EPA/n6-low	DHA/n6-low
C10:0	<LLOQ	<LLOQ	<LLOQ	<LLOQ	<LLOQ	<LLOQ
C11:0	<LLOQ	<LLOQ	<LLOQ	<LLOQ	<LLOQ	<LLOQ
C12:0	<LLOQ	<LLOQ	<LLOQ	<LLOQ	<LLOQ	<LLOQ
C13:0	<LLOQ	<LLOQ	<LLOQ	<LLOQ	<LLOQ	<LLOQ
C14:0	0.262 ± 0.018	0.300 ± 0.013	0.280 ± 0.021	0.267 ± 0.019	0.292 ± 0.022	0.301 ± 0.019
C14:1n5	<LLOQ	<LLOQ	<LLOQ	<LLOQ	<LLOQ	<LLOQ
C15:0	0.101 ± 0.008	0.123 ± 0.005	0.126 ± 0.006	0.093 ± 0.006	0.101 ± 0.003	0.100 ± 0.002
C15:1n5	<LLOQ	<LLOQ	<LLOQ	<LLOQ	<LLOQ	<LLOQ
C16:0	16.558 ± 0.487	17.029 ± 0.255	16.832 ± 0.327	15.542 ± 0.504	17.009 ± 0.265	17.712 ± 0.234
C16:1n7	1.042 ± 0.082	1.019 ± 0.087	0.866 ± 0.084	1.307 ± 0.098	1.368 ± 0.092	1.510 ± 0.066
C17:0	0.177 ± 0.010	0.171 ± 0.004	0.173 ± 0.006	0.139 ± 0.007	0.150 ± 0.007	0.140 ± 0.006
C17:1n7	<LLOQ	<LLOQ	<LLOQ	<LLOQ	<LLOQ	<LLOQ
C18:0	11.772 ± 0.330	12.244 ± 0.507	12.129 ± 0.400	12.051 ± 0.654	9.968 ± 0.371	10.451 ± 0.468
C18:1n9	14.230 ± 1.228	11.497 ± 0.852	11.620 ± 0.908	25.758 ± 1.529	30.653 ± 1.832	27.088 ± 1.609
C18:1n7	1.450 ± 0.100	1.082 ± 0.086	1.050 ± 0.059	1.916 ± 0.144	1.528 ± 0.093	1.457 ± 0.060
C18:2n6	27.206 ± 0.846	28.601 ± 0.754	29.883 ± 1.071	11.925 ± 0.605	13.055 ± 0.527	15.696 ± 0.577
C18:3n6	0.316 ± 0.022	0.214 ± 0.013	0.202 ± 0.009	0.163 ± 0.008	0.103 ± 0.013	0.104 ± 0.011
C19:0	0.110 ± 0.012	0.111 ± 0.007	0.134 ± 0.015	0.082 ± 0.009	0.104 ± 0.009	0.088 ± 0.009
C18:3n3	0.034 ± 0.007	0.035 ± 0.011	0.034 ± 0.008	0.041 ± 0.007	0.061 ± 0.004	0.058 ± 0.004
C18:4n3	<LLOQ	<LLOQ	<LLOQ	<LLOQ	<LLOQ	<LLOQ
C20:0	0.127 ± 0.006	0.138 ± 0.008	0.135 ± 0.009	0.104 ± 0.007	0.114 ± 0.006	0.099 ± 0.006
C20:1n9	0.296 ± 0.020	0.255 ± 0.015	0.270 ± 0.011	0.424 ± 0.035	0.428 ± 0.025	0.383 ± 0.026
C20:2n6	0.231 ± 0.027	0.208 ± 0.011	0.212 ± 0.013	0.106 ± 0.010	0.102 ± 0.003	0.124 ± 0.003
C20:3n9	0.082 ± 0.009	<LLOQ	<LLOQ	0.835 ± 0.111	0.203 ± 0.014	0.234 ± 0.009
C20:3n6	0.684 ± 0.023	0.922 ± 0.040	1.208 ± 0.058	1.260 ± 0.065	0.968 ± 0.098	1.249 ± 0.089
C21:0	<LLOQ	<LLOQ	<LLOQ	<LLOQ	<LLOQ	<LLOQ
C20:4n6	20.660 ± 0.901	15.308 ± 0.927	13.490 ± 1.153	23.059 ± 1.556	9.565 ± 0.951	7.242 ± 0.661
C20:3n3	<LLOQ	<LLOQ	<LLOQ	<LLOQ	<LLOQ	<LLOQ
C20:4n3	<LLOQ	<LLOQ	<LLOQ	<LLOQ	0.027 ± 0.008	<LLOQ
C20:5n3	<LLOQ	2.889 ± 0.304	1.749 ± 0.254	0.023 ± 0.009	7.094 ± 0.747	5.351 ± 0.386
C22:0	0.209 ± 0.009	0.241 ± 0.015	0.222 ± 0.013	0.220 ± 0.007	0.196 ± 0.011	0.208 ± 0.016
C22:1n9	0.282 ± 0.091	0.169 ± 0.028	0.250 ± 0.084	0.266 ± 0.079	0.103 ± 0.050	0.191 ± 0.082
C22:2n6	<LLOQ	<LLOQ	<LLOQ	<LLOQ	<LLOQ	<LLOQ
C22:4n6	0.324 ± 0.009	0.098 ± 0.004	0.076 ± 0.015	0.143 ± 0.006	0.026 ± 0.008	<LLOQ
C22:5n6	1.168 ± 0.076	<LLOQ	<LLOQ	0.634 ± 0.037	<LLOQ	<LLOQ
C22:5n3	<LLOQ	0.430 ± 0.022	0.352 ± 0.037	<LLOQ	0.528 ± 0.047	0.406 ± 0.018
C24:0	0.169 ± 0.013	0.190 ± 0.012	0.166 ± 0.015	0.186 ± 0.007	0.140 ± 0.009	0.154 ± 0.012
C22:6n3	2.214 ± 0.146	6.361 ± 0.406	8.129 ± 0.488	2.999 ± 0.230	5.691 ± 0.283	9.111 ± 0.289
C24:1n9	0.294 ± 0.028	0.364 ± 0.027	0.412 ± 0.037	0.456 ± 0.034	0.422 ± 0.051	0.546 ± 0.047
SFA	29.486 ± 0.630	30.548 ± 0.508	30.197 ± 0.354	28.686 ± 0.479	28.073 ± 0.384	29.252 ± 0.422
MUFA	17.595 ± 1.364	14.387 ± 0.979	14.467 ± 0.907	30.128 ± 1.648	34.502 ± 1.890	31.173 ± 1.675
PUFA	52.919 ± 1.013	55.065 ± 0.690	55.336 ± 0.835	41.187 ± 1.326	37.425 ± 1.597	39.574 ± 1.335
n3-PUFA	2.248 ± 0.146	9.714 ± 0.273	10.265 ± 0.495	3.064 ± 0.226	13.403 ± 0.751	14.926 ± 0.453
n6-PUFA	50.589 ± 0.942	45.351 ± 0.661	45.072 ± 0.973	37.288 ± 1.152	23.819 ± 1.519	24.415 ± 1.238
n9-PUFA	0.082 ± 0.009	<LLOQ	<LLOQ	0.835 ± 0.111	0.203 ± 0.014	0.234 ± 0.009
%EPA+DHA	2.214 ± 0.146	9.250 ± 0.284	9.878 ± 0.472	3.023 ± 0.229	12.785 ± 0.702	14.462 ± 0.439
%n3 in HUFA	8.802 ± 0.410	37.500 ± 1.416	41.366 ± 2.237	10.437 ± 0.481	55.667 ± 2.999	63.345 ± 2.073
%n6 in HUFA	90.859 ± 0.393	62.500 ± 1.416	58.634 ± 2.237	86.592 ± 0.255	43.477 ± 2.963	35.660 ± 2.070

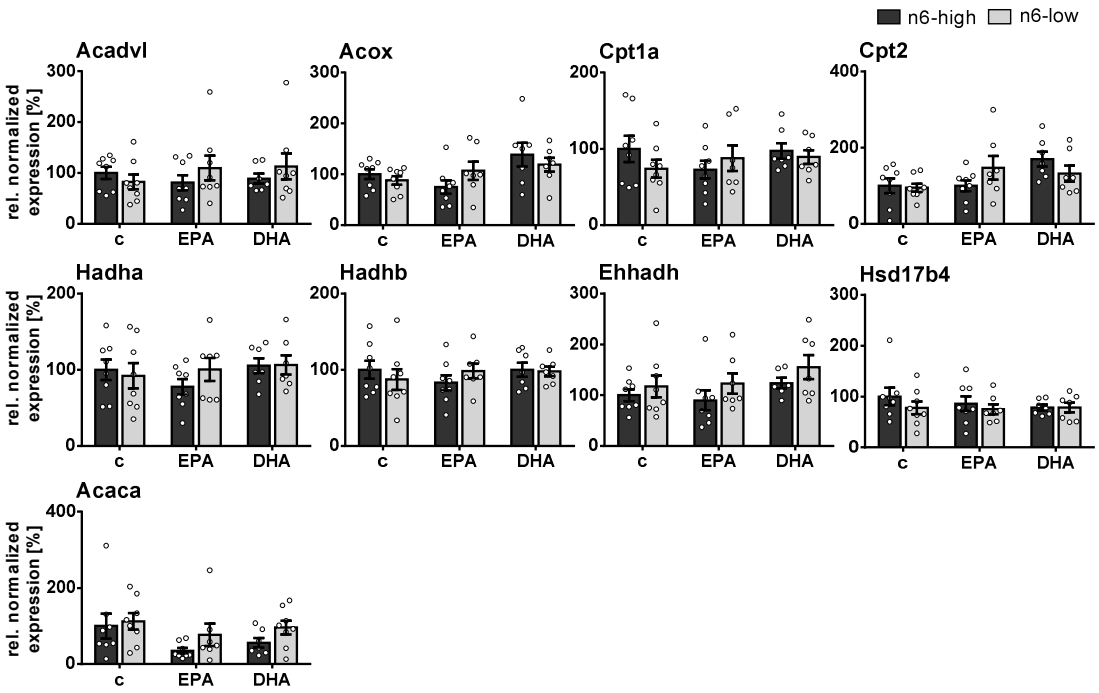

Fig. 8.2: Gene expression of enzymes involved in fatty acid β-oxidation. Normalized gene expression relative to the c/n6-high group of enzymes involved in fatty acid β-oxidation in liver tissue of NMRI mice after 28 days of feeding an n6-PUFA-rich diet (dark grey) or an n6-PUFA-low diet (light grey) without (c) or with n3-PUFA supplementation (EPA, DHA). Shown are mean ± SEM (n = 6–8) as well as individual values for enzymes: very long-chain acyl-CoA dehydrogenase (Acadvl), acyl-CoA oxidase 1 (Acox), carnitine palmitoyltransferase 1a and 2 (Cpt1a, Cpt2), α- and β-subunit of mitochondrial multifunctional protein (Hadha, Hadhb), peroxisomal multifunctional protein (Ehhadh, Hsd17b4) as well as acetyl-CoA carboxylase α (Acaca), which is involved in fatty acid synthesis. Data outliers were removed based on ROUT outlier test (Q = 1%). Statistically significant differences were determined by two-way ANOVA with Tukey's post-test and no significant differences were detected for n6-high vs. n6-low groups (results for comparisons of all groups are summarized in the appendix, Tab. 8.8).

Tab. 8.6: Normalized enzyme expression relative to the c/n6-high group. Gene Expression of enzymes involved in fatty acid β-oxidation, synthesis, elongation and desaturation in liver tissue of NMRI mice after 28 days of feeding an n6-PUFA-rich diet (n6-high) or an n6-PUFA-low diet (n6-low) without (c) or with n3-PUFA supplementation (EPA, DHA). Shown are mean ± SEM (n = 6–8). Outliers were removed according to ROUT outlier test (Q = 1%).

Gene		c/n6-high	EPA/n6-high	DHA/n6-high	c/n6-low	EPA/n6-low	DHA/n6-low
acetyl-CoA carboxylase α	Acaca	100 ± 33	35 ± 7	56 ± 12	112 ± 22	77 ± 30	96 ± 18
acyl-CoA dehydrogenase very long chain	Acadvl	100 ± 12	81 ± 15	89 ± 10	82 ± 15	110 ± 24	113 ± 26
acyl-CoA oxidase 1	Acox1	100 ± 10	75 ± 13	138 ± 23	88 ± 9	107 ± 18	119 ± 14
carnitine palmitoyltransferase 1a	Cpt1a	100 ± 17	73 ± 12	97 ± 10	74 ± 12	88 ± 17	89 ± 9
carnitine palmitoyltransferase 2	Cpt2	100 ± 19	100 ± 14	170 ± 20	95 ± 11	147 ± 31	132 ± 21
mitochondrial multifunctional protein α-subunit	Hadha	100 ± 13	78 ± 10	105 ± 10	92 ± 17	100 ± 15	106 ± 13
mitochondrial multifunctional protein β-subunit	Hadhb	100 ± 12	83 ± 10	100 ± 9	87 ± 14	98 ± 10	98 ± 6
peroxisomal multifunctional protein MFE-1 (L-bifunctional protein, LBP)	Ehhadh	100 ± 11	90 ± 19	124 ± 11	117 ± 22	123 ± 20	155 ± 24
peroxisomal multifunctional protein MFE-2 (D-bifunctional protein, LBP)	Hsd17b4	100 ± 17	86 ± 14	78 ± 6	78 ± 13	75 ± 10	79 ± 10
2,4-dienoyl-CoA reductase 1	Decr1	100 ± 9	128 ± 10	142 ± 23	111 ± 17	121 ± 9	153 ± 20
2,4-dienoyl-CoA reductase 2	Decr2	100 ± 13	85 ± 12	104 ± 6	78 ± 9	90 ± 6	114 ± 10
cis-Δ^3-enoyl-CoA isomerase 1	Eci1	100 ± 10	108 ± 8	134 ± 11	85 ± 6	119 ± 6	139 ± 15
cis-Δ^3-enoyl-CoA isomerase 2	Eci2	100 ± 11	103 ± 11	129 ± 13	97 ± 15	119 ± 8	172 ± 33
fatty acid desaturase 1 (Δ5-desaturase)	Fads1	100 ± 11	64 ± 8	64 ± 8	79 ± 14	74 ± 8	77 ± 9
fatty acid desaturase 2 (Δ6-desaturase)	Fads2	100 ± 13	60 ± 8	89 ± 16	88 ± 19	92 ± 13	113 ± 22
very long chain elongase 2	Elovl2	100 ± 13	71 ± 7	89 ± 8	91 ± 12	97 ± 15	95 ± 9
very long chain elongase 5	Elovl5	100 ± 12	63 ± 8	71 ± 7	89 ± 15	71 ± 6	76 ± 14

Tab. 8.7 (right, page 183): Oxylipin concentrations in mouse liver tissue. Concentrations of oxylipins [nmol/kg wet tissue] in liver tissue of NMRI mice after 28 days of feeding an n6-PUFA-rich diet (n6-high) or an n6-PUFA-low diet (n6-low) without (c) or with n3-PUFA supplementation (EPA, DHA). Shown are mean ± SEM (n = 8). For oxylipins that were < LLOQ in > 50% of the samples within a feeding group, mean value was set to LLOQ; for oxylipins that were < LLOQ in ≤ 50% within a feeding group 1/2 LLOQ was used for calculation of mean ± SEM.
[1)] analyte not quantified in liver tissue due to matrix interference

Tab. 8.7: Continued. Oxylipin concentrations in mouse liver tissue.

	nmol/kg wet tissue	c/n6-high	EPA/n6-high	DHA/n6-high	c/n6-low	EPA/n6-low	DHA/n6-low
Prostanoids and isoprostanoids							
ARA	PGB_2	<0.40	<0.40	<0.40	<0.40	<0.40	<0.40
	PGD_2	2.77 ± 0.78	1.47 ± 0.31	<1.00	5.61 ± 2.26	<1.00	<1.00
	PGE_2	0.83 ± 0.37	0.49 ± 0.19	<0.25	1.57 ± 0.96	<0.25	<0.25
	13,14-dihydro-15-keto-tetranor-PGE_2	<0.25	<0.25	<0.25	<0.25	<0.25	<0.25
	20-OH-PGE_2	<0.25	<0.25	<0.25	<0.25	<0.25	<0.25
	6-keto-$PGF_{1\alpha}$	16.30 ± 4.35	15.87 ± 5.79	8.66 ± 2.81	30.14 ± 10.36	14.57 ± 5.47	<1.81
	$PGF_{2\alpha}$ [1)]	-	-	-	-	-	-
	11b-$PGF_{2\alpha}$	<0.50	<0.50	<0.50	<0.50	<0.50	<0.50
	13,14-dihydro-15-keto-$PGF_{2\alpha}$	2.46 ± 0.67	1.93 ± 0.32	1.49 ± 0.36	4.88 ± 1.27	2.40 ± 0.42	1.78 ± 0.26
	PGJ_2	<1.60	<1.60	<1.60	<1.60	<1.60	<1.60
	15-deoxy-PGJ_2	<0.50	<0.50	<0.50	<0.50	<0.50	<0.50
	D-12-PGJ_2	<1.00	<1.00	<1.00	<1.00	<1.00	<1.00
	TXB_2	1.86 ± 0.39	<1.25	<1.25	3.18 ± 1.20	1.37 ± 0.34	<1.25
	2,3-dinor-TXB_2	1.01 ± 0.19	0.94 ± 0.18	<1.00	2.25 ± 0.74	1.14 ± 0.16	<1.00
	11-dehydro-TXB_2	<0.50	<0.50	<0.50	<0.50	<0.50	<0.50
	12-HHTrE	12.13 ± 4.03	4.10 ± 0.97	2.86 ± 0.68	27.73 ± 18.75	3.83 ± 0.94	1.70 ± 0.20
	15(*S*)-F_{2t}-IsoP (8i-$PGF_{2\alpha}$)	<1.00	<1.00	<1.00	<1.00	<1.00	<1.00
	5(*R*,*S*)-F_{2t}-IsoP	<0.50	<0.50	<0.50	0.96 ± 0.13	<0.50	<0.50
EPA	PGD_3	<1.00	<1.00	<1.00	<1.00	<1.00	<1.00
	PGE_3	<0.30	<0.30	<0.30	<0.30	<0.30	<0.30
	D17-6-keto-$PGF_{1\alpha}$	<1.00	<1.00	<1.00	<1.00	<1.00	<1.00
	TXB_3	<0.25	<0.25	<0.25	<0.25	<0.25	<0.25
	11-dehydro-TXB_3	<1.00	<1.00	<1.00	<1.00	<1.00	<1.00
DGLA	PGD_1	<0.50	<0.50	<0.50	<0.50	<0.50	<0.50
	PGE_1	<0.33	<0.33	<0.33	<0.33	<0.33	<0.33
	13,14-dihydro-15-keto-PGE_1	<0.50	<0.50	<0.50	<0.50	<0.50	<0.50
	$PGF_{1\alpha}$	0.69 ± 0.23	<0.25	<0.25	<0.25	<0.25	<0.25
	15-keto-$PGF_{1\alpha}$	<0.25	<0.25	<0.25	<0.25	<0.25	<0.25
	TXB_1	<0.50	<0.50	<0.50	<0.50	<0.50	<0.50
	2,3-dinor-TXB_1	<5.01	<5.01	<5.01	<5.01	<5.01	<5.01
AdA	dihomo-$PGF_{2\alpha}$	<0.10	<0.10	<0.10	<0.10	<0.10	<0.10

Tab. 8.7: Continued. Oxylipin concentrations in mouse liver tissue.

	nmol/kg wet tissue	c/n6-high	EPA/n6-high	DHA/n6-high	c/n6-low	EPA/n6-low	DHA/n6-low
Multiple hydroxylated FA							
ARA	LTB_4	<0.25	<0.25	<0.25	<0.25	<0.25	<0.25
	6-trans-LTB_4	<0.50	<0.50	<0.50	<0.50	<0.50	<0.50
	20-COOH-LTB_4	<1.00	<1.00	<1.00	<1.00	<1.00	<1.00
	20-OH-LTB_4	<0.25	<0.25	<0.25	<0.25	<0.25	<0.25
	5(*S*),6(*R*),15(*S*)-LXA_4	<0.25	<0.25	<0.25	<0.25	<0.25	<0.25
	5(*S*),6(*R*),15(*R*) LXA_4	<0.25	<0.25	<0.25	<0.25	<0.25	<0.25
	5(*S*),6(*S*),15(*S*)-LXA_4	<0.25	<0.25	<0.25	<0.25	<0.25	<0.25
	LXB_4	<1.00	<1.00	<1.00	<1.00	<1.00	<1.00
	8,15-DiHETE	1.70 ± 0.47	<0.80	<0.80	2.36 ± 0.88	<0.80	<0.80
	5,15-DiHETE	0.44 ± 0.16	<0.25	<0.25	0.49 ± 0.17	<0.25	<0.25
EPA	LTB_5	<0.10	<0.10	<0.10	<0.10	<0.10	<0.10
	LXA_5	<1.00	<1.00	<1.00	<1.00	<1.00	<1.00
	RvE1	<0.50	<0.50	<0.50	<0.50	<0.50	<0.50
	18(*R*)-RvE2 (333 → 253)	<2.00	<2.00	<2.00	<2.00	5.11 ± 1.99	<2.00
	18(*R*)-RvE2 (333 → 199)	<2.00	<2.00	<2.00	<2.00	5.08 ± 1.61	<2.00
	18(*R*)-RvE2 (333 → 159)	<2.00	<2.00	<2.00	<2.00	5.80 ± 2.25	<2.00
	18(*S*)-RvE3	<1.00	<1.00	<1.00	<1.00	<1.00	<1.00
	18(*R*)-RvE3	<0.50	<0.50	<0.50	<0.50	<0.50	<0.50
DHA	RvD1	<0.25	<0.25	<0.25	<0.25	<0.25	<0.25
	17(*R*)-RvD1	<0.75	<0.75	<0.75	<0.75	<0.75	<0.75
	RvD2	<0.75	<0.75	<0.75	<0.75	<0.75	<0.75
	RvD3	<0.38	<0.38	<0.38	<0.38	<0.38	<0.38
	RvD5	<0.75	<0.75	<0.75	<0.75	<0.75	<0.75
	MaR1	<2.00	<2.00	<2.00	<2.00	<2.00	<2.00
	7(*S*)-MaR1	<0.50	<0.50	<0.50	<0.50	<0.50	<0.50
	PDX (359 → 153)	<0.25	0.89 ± 0.50	1.19 ± 0.31	0.54 ± 0.19	1.29 ± 0.38	1.09 ± 0.18
	PDX (359 → 206)	<0.25	0.91 ± 0.48	1.19 ± 0.31	0.48 ± 0.19	1.37 ± 0.44	1.07 ± 0.17
n3-DPA	7(*S*),17(*S*)-DiHDPA	<0.75	<0.75	<0.75	<0.75	<0.75	<0.75
DGLA	LTB_3	<0.50	<0.50	<0.50	<0.50	<0.50	<0.50

Tab. 8.7: Continued. Oxylipin concentrations in mouse liver tissue.

	nmol/kg wet tissue	c/n6-high	EPA/n6-high	DHA/n6-high	c/n6-low	EPA/n6-low	DHA/n6-low
Hydroxy FA							
ARA	5-HETE	25.04 ± 4.59	20.35 ± 6.83	12.91 ± 1.64	22.76 ± 6.25	12.53 ± 2.10	6.53 ± 0.61
	8-HETE	47.64 ± 10.72	35.72 ± 11.22	26.86 ± 4.80	40.92 ± 13.06	23.61 ± 4.86	12.13 ± 1.38
	9-HETE	14.58 ± 3.35	11.54 ± 4.11	7.19 ± 0.88	13.48 ± 3.69	7.57 ± 1.30	3.91 ± 0.35
	11-HETE	31.39 ± 5.99	21.14 ± 5.63	16.30 ± 1.92	34.40 ± 10.18	15.35 ± 1.85	9.51 ± 1.17
	12-HETE	109.27 ± 25.48	121.86 ± 65.20	51.79 ± 12.46	146.24 ± 46.52	54.21 ± 13.06	30.06 ± 6.24
	15-HETE	71.22 ± 13.95	51.24 ± 17.48	38.36 ± 4.47	94.93 ± 26.81	37.12 ± 5.00	26.28 ± 4.87
	19-HETE	9.97 ± 1.18	8.12 ± 1.21	<10.01	11.18 ± 2.21	<10.01	<10.01
	20-HETE	2.11 ± 0.65	1.42 ± 0.36	<1.00	3.21 ± 0.69	1.78 ± 0.29	<1.00
EPA	5-HEPE	<0.50	20.40 ± 4.26	10.66 ± 1.57	0.63 ± 0.14	39.86 ± 8.26	15.49 ± 1.31
	8-HEPE	<0.63	47.61 ± 11.16	27.23 ± 6.61	<0.63	115.95 ± 34.44	34.83 ± 3.24
	9-HEPE	<0.50	21.38 ± 5.06	10.01 ± 1.98	<0.50	45.38 ± 10.71	14.28 ± 1.17
	11-HEPE	<0.50	31.63 ± 6.40	16.92 ± 3.41	0.78 ± 0.21	71.89 ± 17.13	26.32 ± 2.00
	12-HEPE	<0.63	57.58 ± 13.60	28.85 ± 5.54	2.33 ± 0.62	145.32 ± 36.23	52.06 ± 5.52
	15-HEPE	<1.25	37.20 ± 10.37	17.25 ± 3.27	<1.25	81.09 ± 21.44	30.84 ± 2.76
	18-HEPE	<1.00	36.08 ± 7.64	19.23 ± 3.04	1.10 ± 0.19	87.75 ± 18.87	46.69 ± 9.17
	19-HEPE	<0.71	13.01 ± 1.40	10.95 ± 0.77	<0.71	34.09 ± 5.36	25.65 ± 2.22
	20-HEPE	8.54 ± 0.52	37.08 ± 4.40	22.55 ± 1.79	9.23 ± 1.65	59.38 ± 12.02	30.17 ± 1.61
DHA	4-HDHA	6.53 ± 1.64	25.66 ± 8.67	35.91 ± 4.88	10.32 ± 2.09	31.84 ± 4.14	36.37 ± 1.97
	7-HDHA	3.79 ± 1.23	13.18 ± 3.86	24.10 ± 3.42	5.76 ± 1.31	20.60 ± 3.73	23.50 ± 1.47
	8-HDHA	10.18 ± 2.58	40.94 ± 12.70	61.14 ± 6.89	17.42 ± 3.52	56.17 ± 6.66	67.34 ± 3.12
	10-HDHA	20.02 ± 8.02	57.53 ± 16.36	118.06 ± 23.09	25.88 ± 7.28	100.82 ± 25.01	99.14 ± 7.27
	11-HDHA	5.93 ± 1.81	20.16 ± 5.94	36.87 ± 5.85	9.76 ± 2.50	32.90 ± 6.40	34.82 ± 1.94
	13-HDHA	12.20 ± 3.48	37.22 ± 9.51	67.34 ± 10.31	20.30 ± 5.38	56.71 ± 9.53	65.28 ± 3.49
	14-HDHA	30.25 ± 10.06	102.16 ± 37.35	149.34 ± 27.16	58.82 ± 18.20	134.87 ± 30.05	150.64 ± 14.79
	16-HDHA	11.41 ± 2.55	33.22 ± 7.27	56.08 ± 5.84	20.16 ± 4.62	49.37 ± 6.08	61.83 ± 4.09
	17-HDHA	29.57 ± 8.51	96.90 ± 27.15	171.46 ± 26.78	56.34 ± 14.90	143.13 ± 26.43	165.70 ± 6.59
	20-HDHA	14.49 ± 3.49	47.69 ± 10.65	76.84 ± 8.76	24.68 ± 5.50	67.78 ± 9.12	81.72 ± 3.07
	21-HDHA	23.13 ± 2.38	77.83 ± 7.15	90.90 ± 6.34	32.39 ± 5.46	105.53 ± 7.08	123.21 ± 8.84
	22-HDHA	3.08 ± 0.79	7.68 ± 1.03	29.69 ± 2.51	4.04 ± 0.82	14.59 ± 1.72	34.53 ± 6.00
ALA	9-HOTrE	1.00 ± 0.26	1.14 ± 0.27	1.18 ± 0.20	1.01 ± 0.25	1.91 ± 0.43	1.28 ± 0.15
	13-HOTrE	2.34 ± 0.60	2.34 ± 0.63	2.06 ± 0.53	4.71 ± 1.40	3.10 ± 0.65	3.21 ± 0.99
LA	9-HODE	233.55 ± 51.33	215.65 ± 56.29	168.11 ± 13.57	107.62 ± 23.79	116.71 ± 16.79	97.63 ± 15.20
	13-HODE	313.25 ± 66.75	417.35 ± 207.65	205.99 ± 21.79	218.50 ± 58.34	168.19 ± 35.23	183.96 ± 52.01
DGLA	5(*S*)-HETrE	0.50 ± 0.10	<0.20	<0.20	2.23 ± 0.42	0.72 ± 0.06	0.38 ± 0.05
	15(*S*)-HETrE	13.53 ± 2.10	11.42 ± 2.58	11.04 ± 1.03	21.33 ± 5.00	11.79 ± 1.27	12.77 ± 2.46

Tab. 8.7: Continued. Oxylipin concentrations in mouse liver tissue.

	nmol/kg wet tissue	c/n6-high	EPA/n6-high	DHA/n6-high	c/n6-low	EPA/n6-low	DHA/n6-low
Epoxy FA							
ARA	5(6)-EpETrE	23.60 ± 2.82	14.40 ± 1.80	10.84 ± 1.14	21.99 ± 4.52	11.24 ± 0.96	6.39 ± 0.71
	8(9)-EpETrE	3.30 ± 0.41	2.21 ± 0.45	1.63 ± 0.16	3.64 ± 0.56	1.80 ± 0.15	<1.00
	11(12)-EpETrE	2.80 ± 0.26	2.03 ± 0.29	1.32 ± 0.14	2.67 ± 0.50	1.36 ± 0.07	0.84 ± 0.07
	14(15)-EpETrE	4.72 ± 0.36	3.19 ± 0.38	2.45 ± 0.21	4.40 ± 0.72	2.17 ± 0.14	1.42 ± 0.12
EPA	8(9)-EpETE	<1.00	1.53 ± 0.20	<1.00	<1.00	3.47 ± 0.56	1.70 ± 0.10
	11(12)-EpETE	<0.50	1.81 ± 0.23	0.84 ± 0.06	<0.50	3.96 ± 0.60	1.76 ± 0.16
	14(15)-EpETE	<0.50	2.60 ± 0.26	1.31 ± 0.08	<0.50	5.11 ± 0.78	2.54 ± 0.14
	17(18)-EpETE	<1.00	7.90 ± 0.98	4.56 ± 0.39	<1.00	18.72 ± 2.36	9.27 ± 0.78
DHA	10(11)-EpDPE	0.79 ± 0.14	2.82 ± 0.35	4.62 ± 0.22	1.50 ± 0.20	4.23 ± 0.36	5.76 ± 0.24
	13(14)-EpDPE	0.63 ± 0.10	2.17 ± 0.27	3.24 ± 0.22	1.05 ± 0.13	3.06 ± 0.28	4.21 ± 0.22
	16(17)-EpDPE	0.69 ± 0.12	2.61 ± 0.26	3.99 ± 0.28	1.26 ± 0.14	3.33 ± 0.24	4.79 ± 0.21
	19(20)-EpDPE	4.95 ± 0.59	17.37 ± 1.97	25.64 ± 2.07	8.57 ± 0.67	21.65 ± 1.38	28.26 ± 2.05
ALA	9(10)-EpODE	<0.40	<0.40	<0.40	<0.40	<0.40	<0.40
	12(13)-EpODE	<0.50	<0.50	<0.50	<0.50	<0.50	<0.50
	15(16)-EpODE	0.72 ± 0.12	0.88 ± 0.12	1.04 ± 0.29	0.87 ± 0.17	1.34 ± 0.12	1.20 ± 0.16
LA	9(10)-EpOME	18.57 ± 2.20	20.12 ± 3.12	16.08 ± 1.20	7.43 ± 0.90	8.92 ± 0.60	8.60 ± 0.66
	12(13)-EpOME	22.61 ± 2.46	23.68 ± 3.37	18.54 ± 1.37	8.97 ± 1.19	10.29 ± 0.74	9.64 ± 0.72
OA	9(10)-Ep-stearic acid	111.19 ± 7.01	111.07 ± 9.35	97.89 ± 7.77	139.07 ± 11.18	135.44 ± 9.97	126.47 ± 8.93
Dihydroxy FA							
ARA	5,6-DiHETrE	1.45 ± 0.19	0.91 ± 0.18	0.65 ± 0.11	1.59 ± 0.31	0.74 ± 0.06	<0.50
	8,9-DiHETrE	9.53 ± 0.90	6.30 ± 0.70	5.31 ± 0.67	8.74 ± 1.41	5.22 ± 0.45	3.67 ± 0.43
	11,12-DiHETrE	19.85 ± 1.51	13.18 ± 1.26	11.96 ± 1.23	16.87 ± 2.21	9.88 ± 0.90	7.25 ± 0.66
	14,15-DiHETrE	59.03 ± 3.90	43.11 ± 3.76	37.25 ± 3.70	50.12 ± 5.40	30.61 ± 2.21	22.35 ± 1.76
EPA	8,9-DiHETE	<0.50	3.10 ± 0.33	2.74 ± 0.20	0.56 ± 0.10	9.25 ± 1.36	6.82 ± 0.57
	11,12-DiHETE	0.85 ± 0.10	4.23 ± 0.32	4.16 ± 0.27	0.96 ± 0.15	10.17 ± 1.29	8.59 ± 0.58
	14,15-DiHETE	2.40 ± 0.32	15.18 ± 1.74	14.01 ± 0.80	2.73 ± 0.47	36.59 ± 4.72	29.12 ± 1.83
	17,18-DiHETE	7.10 ± 0.89	30.95 ± 2.45	34.47 ± 2.21	7.41 ± 1.17	65.82 ± 6.20	68.46 ± 5.44
DHA	4,5-DiHDPE	2.24 ± 0.51	5.21 ± 1.08	8.23 ± 0.96	6.64 ± 1.67	11.67 ± 1.64	18.51 ± 3.83
	7,8-DiHDPE	1.22 ± 0.19	2.82 ± 0.35	3.48 ± 0.31	2.10 ± 0.37	4.23 ± 0.35	5.50 ± 0.36
	10,11-DiHDPE	4.72 ± 0.47	10.56 ± 1.05	12.89 ± 1.53	7.46 ± 1.30	14.30 ± 0.93	17.77 ± 1.14
	13,14-DiHDPE	6.58 ± 0.60	16.79 ± 1.79	19.22 ± 1.90	9.01 ± 1.26	21.03 ± 1.79	25.98 ± 1.83
	16,17-DiHDPE	18.06 ± 1.75	49.18 ± 4.11	53.71 ± 3.83	22.09 ± 2.27	62.26 ± 5.72	72.47 ± 5.10
	19,20-DiHDPE	49.40 ± 4.43	137.24 ± 10.55	153.98 ± 10.12	63.24 ± 9.94	184.82 ± 16.04	222.54 ± 14.61
ALA	9,10-DiHODE	0.23 ± 0.04	0.21 ± 0.03	0.22 ± 0.04	0.19 ± 0.04	0.31 ± 0.02	0.30 ± 0.02
	12,13-DiHODE	<1.00	<1.00	<1.00	<1.00	<1.00	<1.00
	15,16-DiHODE	1.04 ± 0.18	1.26 ± 0.25	0.96 ± 0.15	1.20 ± 0.20	2.17 ± 0.22	1.82 ± 0.16
LA	9,10-DiHOME	34.78 ± 4.18	26.27 ± 2.23	23.55 ± 2.55	11.66 ± 1.39	14.74 ± 0.78	13.97 ± 1.64
	12,13-DiHOME	89.25 ± 9.38	80.64 ± 8.27	58.64 ± 5.08	29.70 ± 3.90	37.20 ± 1.40	37.44 ± 3.40
OA	9,10-DiH-stearic acid	17.31 ± 4.10	10.22 ± 0.74	17.09 ± 4.09	18.77 ± 2.34	15.64 ± 1.99	20.13 ± 4.50

Tab. 8.7: Continued. Oxylipin concentrations in mouse liver tissue.

	nmol/kg wet tissue	c/n6-high	EPA/n6-high	DHA/n6-high	c/n6-low	EPA/n6-low	DHA/n6-low
Miscellaneous							
ARA	11,12,15-TriHETrE[1)]	-	-	-	-	-	-
	5-oxo-ETE	<2.00	<2.00	<2.00	<2.00	<2.00	<2.00
	15-oxo-ETE	2.17 ± 0.41	2.67 ± 1.33	1.48 ± 0.21	2.50 ± 0.62	1.50 ± 0.23	0.75 ± 0.14
	THF-diol	<0.25	<0.25	<0.25	<0.25	<0.25	<0.25
EPA	12-OH-17(18)-EpETE	<0.50	<0.50	<0.50	<0.50	<0.50	<0.50
LA	13-oxo-ODE	<1.00	<1.00	<1.00	<1.00	<1.00	<1.00
	9-oxo-ODE	14.66 ± 2.06	23.54 ± 9.68	18.64 ± 3.84	7.06 ± 0.79	9.20 ± 1.00	8.05 ± 0.85

Tab. 8.8 (right, page 189): Results for two-way ANOVA with Tukey's post-test for multiple comparisons. Shown are significant differences and multiplicity adjusted p-values (ns $p > 0.05$; * $p < 0.05$; ** $p < 0.01$; *** $p < 0.001$; **** $p < 0.0001$) for group comparisons. Two-way ANOVA was performed with GraphPad Prism Software [factor 1: background diet (n6-high, n6-low); factor 2: n3-PUFA feeding (c, EPA, DHA)] and Tukey's post-test to corret for multiple comparisons (each mean with every other mean). If one group was < LLOQ, only 4 groups were analyzed with two-way ANOVA and (if applicable) additional analyses were performed with one-way ANOVA or a t-Test. Statistical analysis was carried out for a subset of FA in liver (**A-1**, **A-2**), blood cells (**B**), blood plasma (**C**), for qPCR analysis (**D**) and a subset of oxylipins in liver (**E**).
[a)] One-way ANOVA with Tukey's-post test for comparison of three groups with the same background diet.
[b)] t-Test for comparison of two groups.

Tab. 8.8: Continued. Results for two-way ANOVA with Tukey's post-test for multiple comparisons.

(A-1) ANOVA of liver tissue FA concentrations (g/kg liver tissue)

FA	Tukey's multiple comparisons test	c:n6-high vs. EPA:n6-high	c:n6-high vs. DHA:n6-high	EPA:n6-high vs. DHA:n6-high	c:n6-low vs. EPA:n6-low	c:n6-low vs. DHA:n6-low	EPA:n6-low vs. DHA:n6-low	c:n6-high vs. c:n6-low	EPA:n6-high vs. EPA:n6-low	DHA:n6-high vs. DHA:n6-low	EPA:n6-high vs. DHA:n6-low	EPA:n6-low vs. DHA:n6-high
C18:1n9	Summary	ns	ns	ns	ns	*	ns	***	*	ns	ns	ns
	Adjusted P Value	0.9840	0.9887	> 0.9999	0.0854	0.0179	0.9878	0.0001	0.0472	0.2069	0.1882	0.0533
C20:3n9	Summary	ns	ns	ns	****	****	ns	****	**	**	***	**
	Adjusted P Value	0.9791	0.9978	0.9998	< 0.0001	< 0.0001	0.9997	< 0.0001	0.0013	0.0012	0.0005	0.0029
C18:2n6	Summary	ns	ns	ns	ns	ns	ns	****	****	****	****	****
	Adjusted P Value	> 0.9999	0.9999	> 0.9999	0.9803	0.9848	> 0.9999	< 0.0001	< 0.0001	< 0.0001	< 0.0001	< 0.0001
C18:3n6	Summary	*	**	ns	ns	ns	ns	****	*	*	**	ns
	Adjusted P Value	0.0305	0.0031	0.9595	0.7916	0.4964	0.9965	< 0.0001	0.0203	0.0491	0.0053	0.1447
C20:2n6	Summary	ns	ns	ns	ns	ns	ns	****	****	****	****	****
	Adjusted P Value	> 0.9999	0.8999	0.9420	0.9961	0.9631	0.9995	< 0.0001	< 0.0001	< 0.0001	< 0.0001	< 0.0001
C20:3n6	Summary	*	****	*	ns	ns	ns	*	ns	ns	ns	*
	Adjusted P Value	0.0127	< 0.0001	0.0186	0.9986	0.1550	0.3191	0.0253	> 0.9999	0.8528	0.2527	0.0267
C20:4n6	Summary	***	****	ns	****	****	ns	ns	****	****	****	**
	Adjusted P Value	0.0007	< 0.0001	0.5412	< 0.0001	< 0.0001	0.1338	0.0593	< 0.0001	< 0.0001	< 0.0001	0.0077
C22:4n6	Summary	****	****	ns	****	****	ns	****	***	***	***	***
	Adjusted P Value	< 0.0001	< 0.0001	> 0.9999	< 0.0001	< 0.0001	> 0.9999	< 0.0001	0.0005	0.0004	0.0008	0.0002
C22:5n6	Summary	**** a)	****	ns a)	-	****	-	****	-	ns	-	-
	Adjusted P Value	< 0.0001	< 0.0001	> 0.9999	-	< 0.0001	-	< 0.0001	-	0.9943	-	-
C18:3n3	Summary	ns	ns	ns	ns	ns	ns	ns	ns	ns	ns	ns
	Adjusted P Value	0.9281	0.8252	0.9998	0.5240	0.5738	> 0.9999	0.9911	0.7523	0.9093	0.7953	0.8801
C20:4n3	Summary	ns a)	ns a)	ns	-	-	ns	-	*	**	**	**
	Adjusted P Value	0.6152	0.9902	0.8907	-	-	0.9976	-	0.0116	0.0011	0.0072	0.0019
C20:5n3	Summary	-	-	ns	**** a)	**** a)	ns	-	****	****	****	****
	Adjusted P Value	-	-	0.9742	< 0.0001	< 0.0001	0.9276	-	< 0.0001	< 0.0001	< 0.0001	< 0.0001
C22:5n3	Summary	****	****	****	****	****	***	ns	ns	ns	*	****
	Adjusted P Value	< 0.0001	< 0.0001	< 0.0001	< 0.0001	< 0.0001	0.0009	> 0.9999	0.8217	0.0919	0.0285	< 0.0001
C22:6n3	Summary	****	****	***	****	****	****	ns	ns	ns	***	***
	Adjusted P Value	< 0.0001	< 0.0001	0.0008	< 0.0001	< 0.0001	< 0.0001	0.9354	0.9994	0.9920	0.0001	0.0003
total FA	Summary	ns	ns	ns	ns	ns	ns	*	ns	ns	ns	ns
	Adjusted P Value	0.9975	0.999	> 0.9999	0.3738	0.1543	0.9958	0.0293	0.5543	0.8818	0.8466	0.6063
SFA	Summary	ns	ns	ns	ns	ns	ns	ns	ns	ns	ns	ns
	Adjusted P Value	> 0.9999	> 0.9999	> 0.9999	0.9786	0.8742	0.9987	0.3297	0.7180	0.9543	0.9078	0.8095
MUFA	Summary	ns	ns	ns	ns	*	ns	***	ns	ns	ns	ns
	Adjusted P Value	0.9803	0.9850	> 0.9999	0.0813	0.0168	0.9875	0.0001	0.0546	0.2294	0.2124	0.0604
n3-PUFA	Summary	****	****	*	****	****	***	ns	**	****	****	ns
	Adjusted P Value	< 0.0001	< 0.0001	0.0236	< 0.0001	< 0.0001	0.0002	0.9478	0.0076	< 0.0001	< 0.0001	0.9982
n6-PUFA	Summary	ns	ns	ns	ns	ns	ns	****	****	****	****	****
	Adjusted P Value	0.5893	0.3240	0.9976	0.8045	0.4706	0.9936	< 0.0001	< 0.0001	< 0.0001	< 0.0001	< 0.0001
n9-PUFA	Summary	ns	ns	ns	****	****	ns	****	**	**	***	**
	Adjusted P Value	0.9791	0.9978	0.9998	< 0.0001	< 0.0001	0.9997	< 0.0001	0.0013	0.0012	0.0005	0.0029
%EPA+DHA	Summary	****	****	ns	****	****	ns	ns	ns	ns	ns	ns
	Adjusted P Value	< 0.0001	< 0.0001	0.5826	< 0.0001	< 0.0001	0.3080	0.9851	> 0.9999	0.9998	0.4117	0.4631
%n3 HUFA	Summary	****	****	*	****	****	***	ns	****	****	****	**
	Adjusted P Value	< 0.0001	< 0.0001	0.0290	< 0.0001	< 0.0001	0.0002	0.3130	< 0.0001	< 0.0001	< 0.0001	0.0046
%n6 HUFA	Summary	****	****	*	****	****	****	**	****	****	****	***
	Adjusted P Value	< 0.0001	< 0.0001	0.0186	< 0.0001	< 0.0001	< 0.0001	0.0043	< 0.0001	< 0.0001	< 0.0001	0.0006

Tab. 8.8: Continued. Results for two-way ANOVA with Tukey's post-test for multiple comparisons.

(A-2) ANOVA of liver tissue FA profile (% of total FA)

FA	Tukey's multiple comparisons test	c:n6-high vs. EPA:n6-high	c:n6-high vs. DHA:n6-high	EPA:n6-high vs. DHA:n6-high	c:n6-low vs. EPA:n6-low	c:n6-low vs. DHA:n6-low	EPA:n6-low vs. DHA:n6-low	c:n6-high vs. c:n6-low	EPA:n6-high vs. EPA:n6-low	DHA:n6-high vs. DHA:n6-low	EPA:n6-high vs. DHA:n6-low	EPA:n6-low vs. DHA:n6-high
C18:1n9	Summary	ns	ns	ns	*	**	ns	****	****	****	****	****
	Adjusted P Value	0.5152	0.5724	> 0.9999	0.0201	0.0027	0.9785	< 0.0001	< 0.0001	< 0.0001	< 0.0001	< 0.0001
C20:3n9	Summary	ns	ns	ns	****	****	ns	****	**	**	**	*
	Adjusted P Value	0.9809	0.9989	0.9995	< 0.0001	< 0.0001	0.9901	< 0.0001	0.0075	0.0033	0.0013	0.0181
C18:2n6	Summary	ns	ns	ns	ns	ns	ns	****	****	****	****	****
	Adjusted P Value	0.7798	0.9959	0.9649	0.2821	0.0976	0.9939	< 0.0001	< 0.0001	< 0.0001	< 0.0001	< 0.0001
C18:3n6	Summary	**	****	ns	ns	ns	ns	****	****	***	****	***
	Adjusted P Value	0.004	< 0.0001	0.6076	0.9595	0.8636	0.9996	< 0.0001	< 0.0001	0.0001	< 0.0001	0.0003
C20:2n6	Summary	ns	ns	ns	ns	ns	ns	****	****	****	****	****
	Adjusted P Value	0.9995	0.9232	0.9861	0.9878	0.9093	0.9988	< 0.0001	< 0.0001	< 0.0001	< 0.0001	< 0.0001
C20:3n6	Summary	*	****	ns	ns	*	ns	ns	ns	ns	ns	***
	Adjusted P Value	0.0276	< 0.0001	0.1158	0.6781	0.0179	0.4106	0.9997	0.3371	0.0868	> 0.9999	0.0004
C20:4n6	Summary	ns	*	ns	ns	ns	ns	****	***	***	****	*
	Adjusted P Value	0.2759	0.0189	0.8316	0.5453	0.1032	0.9222	< 0.0001	0.0003	0.0006	< 0.0001	0.0101
C22:4n6	Summary	****	****	ns	ns	ns	ns	****	ns	ns	ns	ns
	Adjusted P Value	< 0.0001	< 0.0001	> 0.9999	0.1694	0.2163	> 0.9999	< 0.0001	0.0966	0.1199	0.1271	0.0908
C22:5n6	Summary	**** a)	****	ns a)	-	*	-	****	-	ns	-	-
	Adjusted P Value	< 0.0001	< 0.0001	0.9998	-	0.0123	-	< 0.0001	-	0.9991	-	-
C18:3n3	Summary	ns	ns	ns	ns	*	ns	ns	ns	ns	ns	ns
	Adjusted P Value	0.5518	0.4380	> 0.9999	0.2113	0.0294	0.9481	0.9575	> 0.9999	0.9962	0.9837	0.9987
C20:4n3	Summary	ns a)	ns a)	ns	-	-	ns	-	ns	*	ns	*
	Adjusted P Value	0.6682	0.9884	0.8288	-	-	> 0.9999	-	0.1334	0.0225	0.1404	0.0211
C20:5n3	Summary	-	-	ns	*** a)	*** a)	ns	-	*	**	**	**
	Adjusted P Value	-	-	0.9849	0.0003	0.0003	> 0.9999	-	0.0104	0.0040	0.0097	0.0043
C22:5n3	Summary	****	**	*	****	***	ns	ns	ns	ns	ns	ns
	Adjusted P Value	< 0.0001	0.0019	0.0184	< 0.0001	0.0002	0.2403	> 0.9999	0.9852	0.9968	0.0605	0.0930
C22:6n3	Summary	****	****	ns	***	****	ns	ns	ns	ns	ns	***
	Adjusted P Value	< 0.0001	< 0.0001	0.2261	0.0003	< 0.0001	0.1052	0.9543	0.2895	0.5066	0.9948	0.0009
SFA	Summary	ns	ns	ns	***	****	ns	****	ns	ns	ns	*
	Adjusted P Value	0.2329	0.1137	0.9991	0.0004	< 0.0001	0.9930	< 0.0001	0.0581	0.0913	0.1933	0.0235
MUFA	Summary	ns	ns	ns	*	**	ns	****	****	****	****	****
	Adjusted P Value	0.4283	0.4603	> 0.9999	0.0148	0.0020	0.9801	< 0.0001	< 0.0001	< 0.0001	< 0.0001	< 0.0001
n3-PUFA	Summary	****	****	ns	****	****	ns	ns	ns	ns	ns	ns
	Adjusted P Value	< 0.0001	< 0.0001	0.7559	< 0.0001	< 0.0001	0.4375	0.9862	> 0.9999	0.9996	0.5682	0.6290
n6-PUFA	Summary	ns	ns	ns	ns	ns	ns	****	****	****	****	****
	Adjusted P Value	0.9324	0.3908	0.9155	0.9996	0.9998	> 0.9999	< 0.0001	< 0.0001	< 0.0001	< 0.0001	< 0.0001
n9-PUFA	Summary	ns	ns	ns	****	****	ns	****	**	**	**	*
	Adjusted P Value	0.9809	0.9989	0.9995	< 0.0001	< 0.0001	0.9901	< 0.0001	0.0075	0.0033	0.0013	0.0181
%EPA+DHA	Summary	****	****	ns	****	****	ns	ns	ns	ns	ns	ns
	Adjusted P Value	< 0.0001	< 0.0001	0.5826	< 0.0001	< 0.0001	0.3082	0.9854	> 0.9999	0.9998	0.4117	0.4632
%n3 HUFA	Summary	****	****	*	****	****	***	ns	****	****	****	**
	Adjusted P Value	< 0.0001	< 0.0001	0.0291	< 0.0001	< 0.0001	0.0002	0.3089	< 0.0001	< 0.0001	< 0.0001	0.0045
%n6 HUFA	Summary	****	****	*	****	****	***	**	****	****	****	***
	Adjusted P Value	< 0.0001	< 0.0001	0.0187	< 0.0001	< 0.0001	0.0001	0.0042	< 0.0001	< 0.0001	< 0.0001	0.0006

Tab. 8.8: Continued. Results for two-way ANOVA with Tukey's post-test for multiple comparisons.

(B) ANOVA of blood cell FA profile (% of total FA)

FA	Tukey's multiple comparisons test	c:n6-high vs. EPA:n6-high	c:n6-high vs. DHA:n6-high	EPA:n6-high vs. DHA:n6-high	c:n6-low vs. EPA:n6-low	c:n6-low vs. DHA:n6-low	EPA:n6-low vs. DHA:n6-low	c:n6-high vs. c:n6-low	EPA:n6-high vs. EPA:n6-low	DHA:n6-high vs. DHA:n6-low	EPA:n6-high vs. DHA:n6-low	EPA:n6-low vs. DHA:n6-high
C18:1n9	Summary	ns	ns	ns	ns	ns	ns	****	****	****	****	****
	Adjusted P Value	0.9759	> 0.9999	0.9834	0.9977	0.9961	> 0.9999	< 0.0001	< 0.0001	< 0.0001	< 0.0001	< 0.0001
C20:3n9	Summary	-	-	-	**** a)	**** a)	ns a)	**** b)	-	-	-	-
	Adjusted P Value	-	-	-	< 0.0001	< 0.0001	0.9742	< 0.0001	-	-	-	-
C18:2n6	Summary	ns	***	ns	ns	***	**	****	****	****	****	****
	Adjusted P Value	0.4213	0.0008	0.1302	0.8568	0.0002	0.0072	< 0.0001	< 0.0001	< 0.0001	< 0.0001	< 0.0001
C18:3n6	Summary	*	**	ns	ns	ns	ns	****	*	*	**	ns
	Adjusted P Value	0.0409	0.0012	0.8062	0.9846	0.7154	0.9739	< 0.0001	0.0104	0.0391	0.0012	0.2037
C20:2n6	Summary	ns	ns	ns	ns	ns	ns	****	****	****	****	****
	Adjusted P Value	0.8866	0.9754	0.9994	0.9997	0.6629	0.8280	< 0.0001	< 0.0001	< 0.0001	< 0.0001	< 0.0001
C20:3n6	Summary	ns	****	***	***	ns	****	ns	ns	ns	ns	****
	Adjusted P Value	0.9890	< 0.0001	0.0002	0.0005	0.9906	< 0.0001	0.1180	0.1117	0.1936	0.1231	< 0.0001
C20:4n6	Summary	****	****	*	****	****	*	ns	****	****	****	*
	Adjusted P Value	< 0.0001	< 0.0001	0.0111	< 0.0001	< 0.0001	0.0203	0.9740	< 0.0001	< 0.0001	< 0.0001	0.0435
C22:4n6	Summary	****	****	**	****	****	*	****	****	****	****	ns
	Adjusted P Value	< 0.0001	< 0.0001	0.0083	< 0.0001	< 0.0001	0.0276	< 0.0001	< 0.0001	< 0.0001	< 0.0001	0.1709
C22:5n6	Summary	****	****	ns	****	****	ns	****	ns	ns	ns	ns
	Adjusted P Value	< 0.0001	< 0.0001	> 0.9999	< 0.0001	< 0.0001	> 0.9999	< 0.0001	0.6630	0.6221	0.7076	0.5758
C20:5n3	Summary	-	-	****	-	-	****	-	****	****	*	****
	Adjusted P Value	-	-	< 0.0001	-	-	< 0.0001	-	< 0.0001	< 0.0001	0.0111	< 0.0001
C22:5n3	Summary	****	****	****	****	****	****	ns	****	***	****	****
	Adjusted P Value	< 0.0001	< 0.0001	< 0.0001	< 0.0001	< 0.0001	< 0.0001	> 0.9999	< 0.0001	0.0007	< 0.0001	< 0.0001
C22:6n3	Summary	****	****	****	****	****	****	ns	ns	**	****	****
	Adjusted P Value	< 0.0001	< 0.0001	< 0.0001	< 0.0001	< 0.0001	< 0.0001	0.4365	0.8805	0.0067	< 0.0001	< 0.0001
SFA	Summary	****	*	ns	****	****	ns	****	****	****	****	****
	Adjusted P Value	< 0.0001	0.0175	0.4492	< 0.0001	< 0.0001	0.9806	< 0.0001	< 0.0001	< 0.0001	< 0.0001	< 0.0001
MUFA	Summary	ns	ns	ns	ns	ns	ns	****	****	****	****	****
	Adjusted P Value	0.9493	> 0.9999	0.9606	0.8709	0.8257	> 0.9999	< 0.0001	< 0.0001	< 0.0001	< 0.0001	< 0.0001
n3-PUFA	Summary	****	****	*	****	****	*	ns	****	****	****	****
	Adjusted P Value	< 0.0001	< 0.0001	0.0146	< 0.0001	< 0.0001	0.0322	0.7861	< 0.0001	< 0.0001	< 0.0001	< 0.0001
n6-PUFA	Summary	****	****	ns	****	****	ns	****	****	****	****	****
	Adjusted P Value	< 0.0001	< 0.0001	0.3905	< 0.0001	< 0.0001	0.9066	< 0.0001	< 0.0001	< 0.0001	< 0.0001	< 0.0001
n9-PUFA	Summary	-	-	-	**** a)	**** a)	ns a)	**** b)	-	-	-	-
	Adjusted P Value	-	-	-	< 0.0001	< 0.0001	0.9742	< 0.0001	-	-	-	-
%EPA+DHA	Summary	****	****	****	****	****	****	ns	****	****	****	*
	Adjusted P Value	< 0.0001	< 0.0001	< 0.0001	< 0.0001	< 0.0001	< 0.0001	0.7060	< 0.0001	< 0.0001	< 0.0001	0.0185
%n3 HUFA	Summary	****	****	****	****	****	****	ns	****	****	****	****
	Adjusted P Value	< 0.0001	< 0.0001	< 0.0001	< 0.0001	< 0.0001	< 0.0001	0.5161	< 0.0001	< 0.0001	< 0.0001	< 0.0001
%n6 HUFA	Summary	****	****	****	****	****	****	**	****	****	****	****
	Adjusted P Value	< 0.0001	< 0.0001	< 0.0001	< 0.0001	< 0.0001	< 0.0001	0.0084	< 0.0001	< 0.0001	< 0.0001	< 0.0001

Tab. 8.8: Continued. Results for two-way ANOVA with Tukey's post-test for multiple comparisons.

(C) ANOVA of blood plasma FA profile (% of total FA)

FA	Tukey's multiple comparisons test	c:n6-high vs. EPA:n6-high	c:n6-high vs. DHA:n6-high	EPA:n6-high vs. DHA:n6-high	c:n6-low vs. EPA:n6-low	c:n6-low vs. DHA:n6-low	EPA:n6-low vs. DHA:n6-low	c:n6-high vs. c:n6-low	EPA:n6-high vs. EPA:n6-low	DHA:n6-high vs. DHA:n6-low	EPA:n6-high vs. DHA:n6-low	EPA:n6-low vs. DHA:n6-high
C18:1n9	Summary	ns	ns	ns	ns	ns	ns	****	****	****	****	****
	Adjusted P Value	0.7236	0.7600	> 0.9999	0.1422	0.9828	0.4561	< 0.0001	< 0.0001	< 0.0001	< 0.0001	< 0.0001
C20:3n9	Summary	-	-	-	**** a)	**** a)	ns a)	**** b)	-	-	-	-
	Adjusted P Value	-	-	-	< 0.0001	< 0.0001	0.9417	< 0.0001	-	-	-	-
C18:2n6	Summary	ns	ns	ns	ns	*	ns	****	****	****	****	****
	Adjusted P Value	0.7789	0.1439	0.8328	0.8941	0.0120	0.1539	< 0.0001	< 0.0001	< 0.0001	< 0.0001	< 0.0001
C18:3n6	Summary	****	****	ns	*	*	ns	****	****	***	****	****
	Adjusted P Value	< 0.0001	< 0.0001	0.9900	0.0379	0.0431	> 0.9999	< 0.0001	< 0.0001	0.0001	< 0.0001	< 0.0001
C20:2n6	Summary	ns	ns	ns	ns	ns	ns	****	****	***	**	****
	Adjusted P Value	0.8334	0.9150	> 0.9999	> 0.9999	0.9330	0.8646	< 0.0001	< 0.0001	0.0006	0.0011	< 0.0001
C20:3n6	Summary	ns	****	*	*	ns	ns	****	ns	ns	*	ns
	Adjusted P Value	0.1480	< 0.0001	0.0475	0.0416	> 0.9999	0.0548	< 0.0001	0.9964	0.9981	0.0159	0.1415
C20:4n6	Summary	*	***	ns	****	****	ns	ns	**	**	****	ns
	Adjusted P Value	0.0112	0.0003	0.8293	< 0.0001	< 0.0001	0.637	0.6046	0.0054	0.0020	< 0.0001	0.1162
C22:4n6	Summary	****	**** a)	ns a)	****	-	-	****	****	-	-	-
	Adjusted P Value	< 0.0001	< 0.0001	0.2910	< 0.0001	-	-	< 0.0001	< 0.0001	-	-	-
C22:5n6	Summary	-	-	-	-	-	-	**** b)	-	-	-	-
	Adjusted P Value	-	-	-	-	-	-	< 0.0001	-	-	-	-
C18:3n3	Summary	ns	ns	ns	ns	ns	ns	ns	ns	ns	ns	ns
	Adjusted P Value	> 0.9999	> 0.9999	> 0.9999	0.3388	0.5598	0.9990	0.9818	0.1040	0.1993	0.2186	0.0932
C20:5n3	Summary	-	-	ns	**** a)	**** a)	ns	-	****	****	**	****
	Adjusted P Value	-	-	0.3260	< 0.0001	< 0.0001	0.0592	-	< 0.0001	< 0.0001	0.0043	< 0.0001
C22:5n3	Summary	-	-	ns	-	-	ns	-	ns	ns	ns	**
	Adjusted P Value	-	-	0.3746	-	-	0.0659	-	0.1800	0.6754	0.9561	0.0045
C22:6n3	Summary	****	****	**	****	****	****	ns	ns	ns	****	****
	Adjusted P Value	< 0.0001	< 0.0001	0.0054	< 0.0001	< 0.0001	< 0.0001	0.5405	0.6969	0.2942	< 0.0001	< 0.0001
SFA	Summary	ns	ns	ns	ns	ns	ns	ns	**	ns	ns	*
	Adjusted P Value	0.6076	0.8921	0.9947	0.9398	0.9561	0.4971	0.8348	0.0074	0.7179	0.3918	0.0307
MUFA	Summary	ns	ns	ns	ns	ns	ns	****	****	****	****	****
	Adjusted P Value	0.6302	0.6548	> 0.9999	0.2955	0.9956	0.5932	< 0.0001	< 0.0001	< 0.0001	< 0.0001	< 0.0001
n3-PUFA	Summary	****	****	ns	****	****	ns	ns	****	****	****	***
	Adjusted P Value	< 0.0001	< 0.0001	0.9481	< 0.0001	< 0.0001	0.1632	0.7773	< 0.0001	< 0.0001	< 0.0001	0.0001
n6-PUFA	Summary	*	*	ns	****	****	ns	****	****	****	****	****
	Adjusted P Value	0.0211	0.0132	> 0.9999	< 0.0001	< 0.0001	0.9989	< 0.0001	< 0.0001	< 0.0001	< 0.0001	< 0.0001
n9-PUFA	Summary	-	-	-	**** a)	**** a)	ns a)	**** b)	-	-	-	-
	Adjusted P Value	-	-	-	< 0.0001	< 0.0001	0.9417	< 0.0001	-	-	-	-
%EPA+DHA	Summary	****	****	ns	****	****	ns	ns	****	****	****	***
	Adjusted P Value	< 0.0001	< 0.0001	0.8961	< 0.0001	< 0.0001	0.0743	0.7511	< 0.0001	< 0.0001	< 0.0001	0.0002
%n3 HUFA	Summary	****	****	ns	****	****	ns	ns	****	****	****	****
	Adjusted P Value	< 0.0001	< 0.0001	0.6835	< 0.0001	< 0.0001	0.0580	0.9887	< 0.0001	< 0.0001	< 0.0001	< 0.0001
%n6 HUFA	Summary	****	****	ns	****	****	*	ns	****	****	****	****
	Adjusted P Value	< 0.0001	< 0.0001	0.6745	< 0.0001	< 0.0001	0.0476	0.5771	< 0.0001	< 0.0001	< 0.0001	< 0.0001

Tab. 8.8: Continued. Results for two-way ANOVA with Tukey's post-test for multiple comparisons.

(D) ANOVA of liver tissue qPCR data (rel. normalized expression)

Enzyme/ enzyme index	Tukey's multiple comparisons test	c:n6-high vs. EPA:n6-high	c:n6-high vs. DHA:n6-high	EPA:n6-high vs. DHA:n6-high	c:n6-low vs. EPA:n6-low	c:n6-low vs. DHA:n6-low	EPA:n6-low vs. DHA:n6-low	c:n6-high vs. c:n6-low	EPA:n6-high vs. EPA:n6-low	DHA:n6-high vs. DHA:n6-low	EPA:n6-high vs. DHA:n6-low	EPA:n6-low vs. DHA:n6-high
Decr1	Summary	ns	ns	ns	ns	ns	ns	ns	ns	ns	ns	ns
	Adjusted P Value	0.7877	0.4127	0.9894	0.9977	0.4231	0.6986	0.9956	0.9993	0.9963	0.8767	0.9288
Decr2	Summary	ns	ns	ns	ns	ns	ns	ns	ns	ns	ns	ns
	Adjusted P Value	0.8853	0.9998	0.7709	0.9581	0.1405	0.5807	0.6035	0.9994	0.9827	0.3449	0.9302
Eci1	Summary	ns	ns	ns	ns	**	ns	ns	ns	ns	ns	ns
	Adjusted P Value	0.9905	0.1802	0.4459	0.1568	0.0052	0.7260	0.8691	0.9536	0.9993	0.2170	0.9154
Eci2	Summary	ns	ns	ns	ns	*	ns	ns	ns	ns	ns	ns
	Adjusted P Value	> 0.9999	0.8619	0.9041	0.9455	0.0385	0.3081	> 0.9999	0.9856	0.5247	0.0693	0.9991
Fads1	Summary	ns	ns	ns	ns	ns	ns	ns	ns	ns	ns	ns
	Adjusted P Value	0.1340	0.1436	> 0.9999	0.9995	> 0.9999	> 0.9999	0.6691	0.9816	0.9464	0.9519	0.9779
Fads2	Summary	ns	ns	ns	ns	ns	ns	ns	ns	ns	ns	ns
	Adjusted P Value	0.4708	0.9958	0.8106	> 0.9999	0.8649	0.9351	0.9945	0.7303	0.8862	0.1772	> 0.9999
Elovl2	Summary	ns	ns	ns	ns	ns	ns	ns	ns	ns	ns	ns
	Adjusted P Value	0.4137	0.9807	0.8614	0.9994	0.9999	> 0.9999	0.9919	0.5914	0.9989	0.6477	0.9971
Elovl5	Summary	ns	ns	ns	ns	ns	ns	ns	ns	ns	ns	ns
	Adjusted P Value	0.1746	0.4043	0.9961	0.8533	0.9466	0.9998	0.9795	0.9939	0.9995	0.9638	> 0.9999
Acaca	Summary	ns	ns	ns	ns	ns	ns	ns	ns	ns	ns	ns
	Adjusted P Value	0.3029	0.7349	0.9860	0.8733	0.9949	0.9900	0.9986	0.7776	0.8024	0.3694	0.9874
Acadvl	Summary	ns	ns	ns	ns	ns	ns	ns	ns	ns	ns	ns
	Adjusted P Value	0.9747	0.9982	0.9996	0.8855	0.8277	> 0.9999	0.9808	0.8670	0.9406	0.8050	0.9681
Acox	Summary	ns	ns	*	ns	ns	ns	ns	ns	ns	ns	ns
	Adjusted P Value	0.8104	0.4633	0.0462	0.9420	0.6836	0.9938	0.9903	0.6452	0.9436	0.3099	0.6983
Cpt1a	Summary	ns	ns	ns	ns	ns	ns	ns	ns	ns	ns	ns
	Adjusted P Value	0.6677	> 0.9999	0.7834	0.9755	0.9614	> 0.9999	0.7026	0.9667	0.9984	0.9495	0.9963
Cpt2	Summary	ns	ns	ns	ns	ns	ns	ns	ns	ns	ns	ns
	Adjusted P Value	> 0.9999	0.1484	0.1513	0.4249	0.7563	0.9950	> 0.9999	0.5521	0.7794	0.8605	0.9684
Hadha	Summary	ns	ns	ns	ns	ns	ns	ns	ns	ns	ns	ns
	Adjusted P Value	0.8227	0.9997	0.6823	0.9975	0.9730	0.9997	0.9978	0.8302	> 0.9999	0.6571	0.9998
Hadhb	Summary	ns	ns	ns	ns	ns	ns	ns	ns	ns	ns	ns
	Adjusted P Value	0.8520	> 0.9999	0.8665	0.9755	0.9810	> 0.9999	0.9499	0.9098	> 0.9999	0.9233	> 0.9999
Ehhadh	Summary	ns	ns	ns	ns	ns	ns	ns	ns	ns	ns	ns
	Adjusted P Value	0.9986	0.9504	0.8127	> 0.9999	0.6948	0.8358	0.9834	0.8052	0.8731	0.1515	> 0.9999
Hsd17b4	Summary	ns	ns	ns	ns	ns	ns	ns	ns	ns	ns	ns
	Adjusted P Value	0.9614	0.8309	0.9984	> 0.9999	> 0.9999	> 0.9999	0.7934	0.9907	> 0.9999	0.9985	> 0.9999
D6D index	Summary	**	****	ns	****	****	ns	ns	ns	ns	ns	ns
	Adjusted P Value	0.0022	< 0.0001	0.8779	< 0.0001	< 0.0001	0.8560	> 0.9999	0.6763	0.6443	0.1108	0.9989
D5D index	Summary	****	****	**	****	****	*	****	**	*	****	ns
	Adjusted P Value	< 0.0001	< 0.0001	0.0043	< 0.0001	< 0.0001	0.0496	< 0.0001	0.0018	0.0231	< 0.0001	0.9996
Elongase index	Summary	****	****	ns	****	**	ns	****	*	ns	ns	***
	Adjusted P Value	< 0.0001	< 0.0001	0.7140	< 0.0001	0.0087	0.0949	< 0.0001	0.0456	0.5158	0.9995	0.0008

Tab. 8.8: Continued. Results for two-way ANOVA with Tukey's post-test for multiple comparisons.

(E) ANOVA of liver tissue oxylipin concentrations (nmol/kg liver tissue)

Oxylipin	Tukey's multiple comparisons test	c:n6-high vs. EPA:n6-high	c:n6-high vs. DHA:n6-high	EPA:n6-high vs. DHA:n6-high	c:n6-low vs. EPA:n6-low	c:n6-low vs. DHA:n6-low	EPA:n6-low vs. DHA:n6-low	c:n6-high vs. c:n6-low	EPA:n6-high vs. EPA:n6-low	DHA:n6-high vs. DHA:n6-low	EPA:n6-high vs. DHA:n6-low	EPA:n6-low vs. DHA:n6-high
5-HETE	Summary	ns	ns	ns	ns	ns	ns	ns	ns	ns	ns	ns
	Adjusted P Value	0.9726	0.3788	0.8319	0.5661	0.1125	0.9244	0.9990	0.8007	0.9039	0.2423	> 0.9999
5-HEPE	Summary	-	-	ns	**** a)	ns a)	**	-	*	ns	ns	***
	Adjusted P Value	-	-	0.4810	< 0.0001	0.0991	0.0060	-	0.0349	0.8892	0.8840	0.0009
4-HDHA	Summary	ns	***	ns	*	**	ns	ns	ns	ns	ns	ns
	Adjusted P Value	0.0558	0.0007	0.6192	0.0223	0.0032	0.9813	0.9916	0.9310	> 0.9999	0.5735	0.9885
7-HDHA	Summary	ns	****	ns	**	***	ns	ns	ns	ns	ns	ns
	Adjusted P Value	0.1797	< 0.0001	0.0786	0.0059	0.0006	0.9756	0.9958	0.4182	> 0.9999	0.1107	0.9455
12-HETE	Summary	ns	ns	ns	ns	ns	ns	ns	ns	ns	ns	ns
	Adjusted P Value	0.9998	0.8552	0.7220	0.4466	0.2034	0.9964	0.9752	0.7502	0.9978	0.4493	> 0.9999
12-HEPE	Summary	-	-	ns	*** a)	ns a)	*	-	*	ns	ns	**
	Adjusted P Value	-	-	0.7339	0.0003	0.2431	0.0120	-	0.0194	0.8391	0.9972	0.0014
14-HDHA	Summary	ns	*	ns	ns	ns	ns	ns	ns	ns	ns	ns
	Adjusted P Value	0.3320	0.0175	0.7580	0.2735	0.1150	0.9975	0.9631	0.9356	> 0.9999	0.7367	0.9984
15-HETE	Summary	ns	ns	ns	ns	*	ns	ns	ns	ns	ns	ns
	Adjusted P Value	0.9266	0.6121	0.9888	0.0790	0.0219	0.9949	0.8599	0.9831	0.9917	0.8322	> 0.9999
15-HEPE	Summary	-	-	ns	-	-	*	-	ns	ns	ns	**
	Adjusted P Value	-	-	0.6529	-	-	0.0314	-	0.0714	0.8566	0.9821	0.0045
17-HDHA	Summary	ns	***	ns	*	**	ns	ns	ns	ns	ns	ns
	Adjusted P Value	0.2025	0.0002	0.1229	0.0469	0.0058	0.9688	0.9366	0.6002	> 0.9999	0.1838	0.9207
18-HEPE	Summary	-	-	ns	*** a)	* a)	ns	-	*	ns	ns	**
	Adjusted P Value	-	-	0.7172	0.0001	0.0373	0.0696	-	0.0153	0.3309	0.9092	0.0010
PDX	Summary	-	-	ns	ns a)	ns a)	ns	-	ns	ns	ns	ns
(*m/z* 359 → 153)	Adjusted P Value	-	-	0.9348	0.1408	0.3254	0.9811	-	0.8660	0.9973	0.9789	0.9977
PDX	Summary	-	-	ns	ns a)	ns a)	ns	-	ns	ns	ns	ns
(*m/z* 359 → 206)	Adjusted P Value	-	-	0.9539	0.1032	0.3478	0.9377	-	0.8182	0.9960	0.9908	0.9843
14(15)-EpETrE	Summary	ns	**	ns	**	****	ns	ns	ns	ns	*	ns
	Adjusted P Value	0.069	0.0017	0.7436	0.0021	< 0.0001	0.7369	0.9906	0.4177	0.4109	0.0238	0.9948
17(18)-EpETE	Summary	-	-	ns	-	-	***	-	****	ns	ns	****
	Adjusted P Value	-	-	0.3208	-	-	0.0002	-	< 0.0001	0.0890	0.8903	< 0.0001
19(20)-EpDPE	Summary	****	****	**	****	****	ns	ns	ns	ns	***	ns
	Adjusted P Value	< 0.0001	< 0.0001	0.0078	< 0.0001	< 0.0001	0.0540	0.5918	0.4110	0.8487	0.0002	0.4866
14,15-DiHETrE	Summary	*	**	ns	**	****	ns	ns	ns	ns	**	ns
	Adjusted P Value	0.0398	0.0017	0.8647	0.0062	< 0.0001	0.6040	0.5246	0.1735	0.0637	0.0031	0.7916
17,18-DiHETE	Summary	***	****	ns	****	****	ns	ns	****	****	****	****
	Adjusted P Value	0.0005	< 0.0001	0.9834	< 0.0001	< 0.0001	0.9956	> 0.9999	< 0.0001	< 0.0001	< 0.0001	< 0.0001
19,20-DiHDPE	Summary	****	****	ns	****	****	ns	ns	ns	**	****	ns
	Adjusted P Value	< 0.0001	< 0.0001	0.9073	< 0.0001	< 0.0001	0.2145	0.9569	0.0600	0.0018	< 0.0001	0.4250
20-HETE	Summary	ns	-	-	ns	-	-	ns	ns	-	-	-
	Adjusted P Value	0.7945	-	-	0.2366	-	-	0.4592	0.9650	-	-	-
20-HEPE	Summary	**	ns	ns	****	ns	**	ns	ns	ns	ns	***
	Adjusted P Value	0.0064	0.4485	0.4067	< 0.0001	0.0844	0.0050	> 0.9999	0.0559	0.9135	0.9415	0.0002
22-HDHA	Summary	ns	****	****	ns	****	***	ns	ns	ns	****	**
	Adjusted P Value	0.8556	< 0.0001	< 0.0001	0.1076	< 0.0001	0.0001	0.9999	0.5168	0.8264	< 0.0001	0.0060

Chapter 4

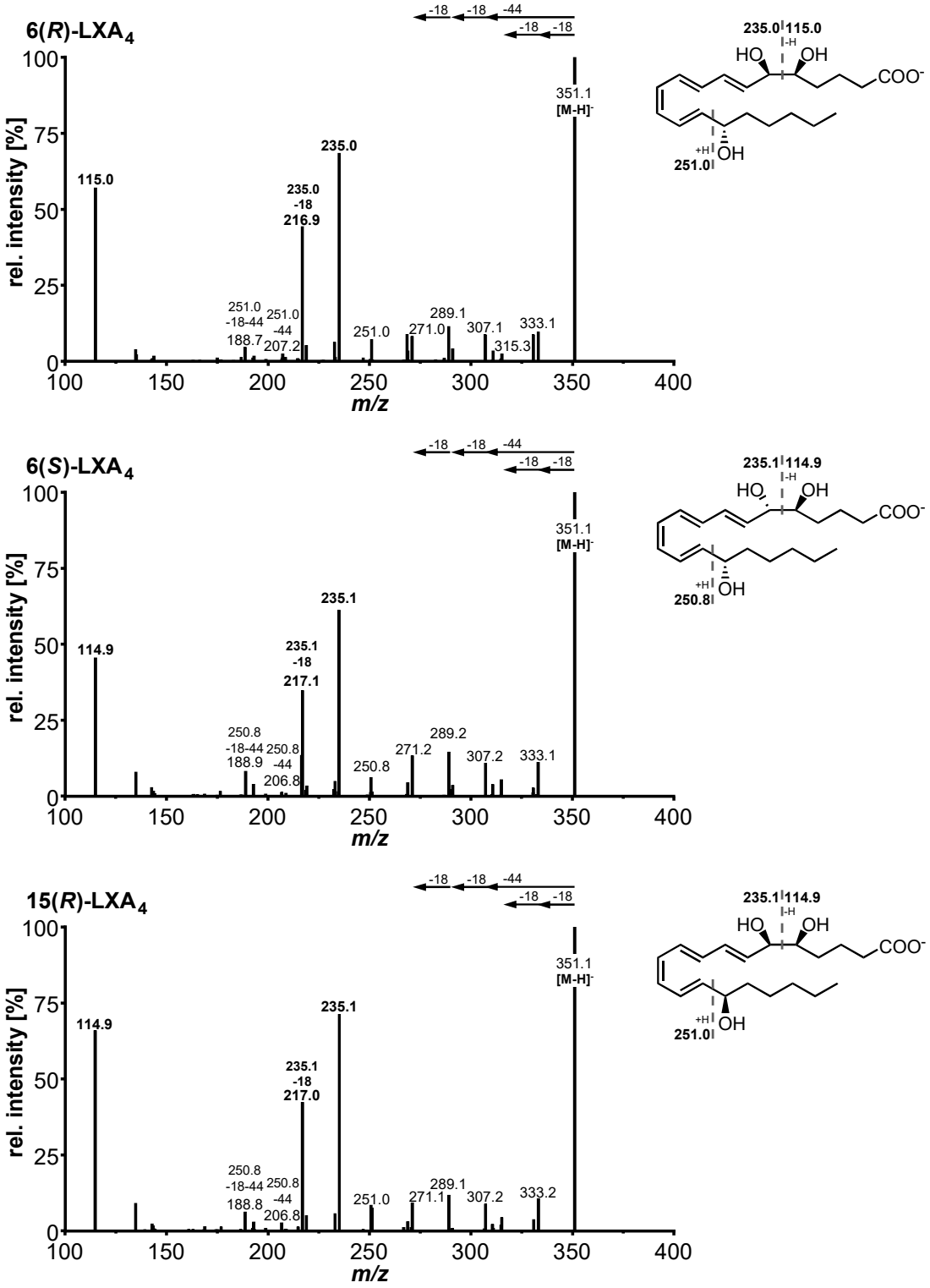

Fig. 8.3: Product ion spectra of ARA, EPA and DHA derived SPMs. The fragment ion spectra were aquired via collision induced dissociation applying a ramped collision energy (CE) from –16 to –22 V. Molecular structure and suggested sites of fragmentation are indicated.

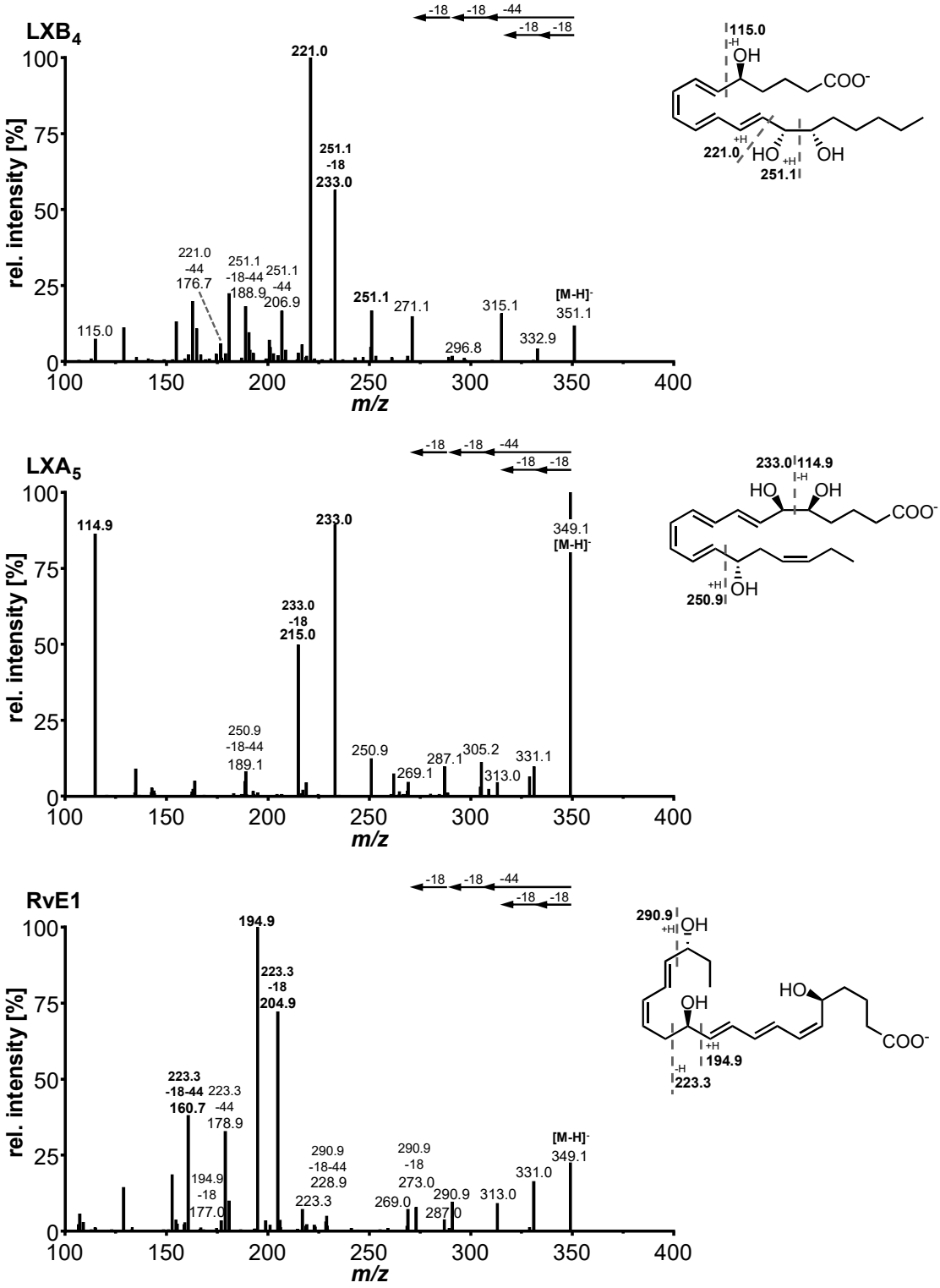

Fig. 8.3: Continued. Product ion spectra of ARA, EPA and DHA derived SPMs.

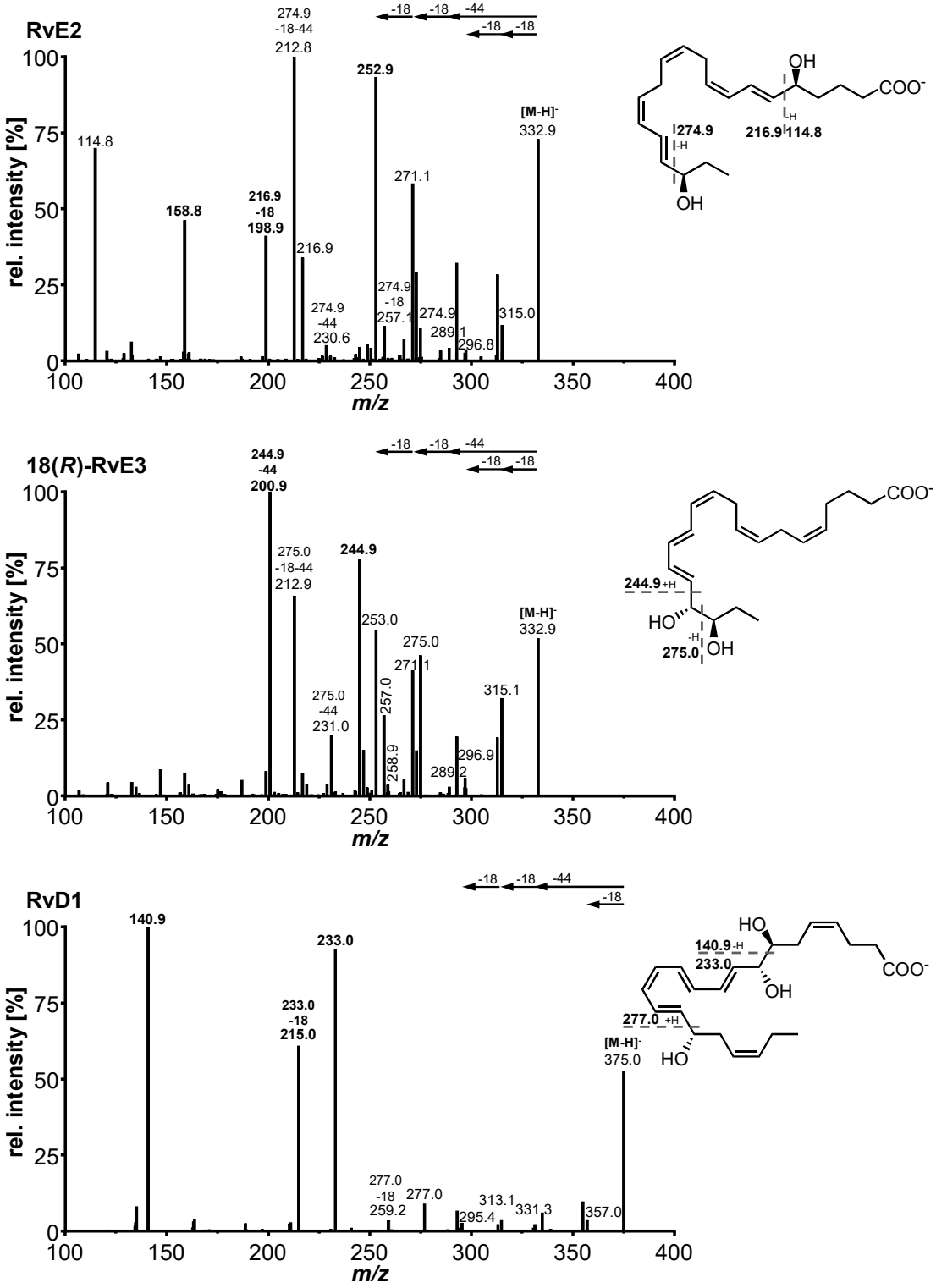

Fig. 8.3: Continued. Product ion spectra of ARA, EPA and DHA derived SPMs.

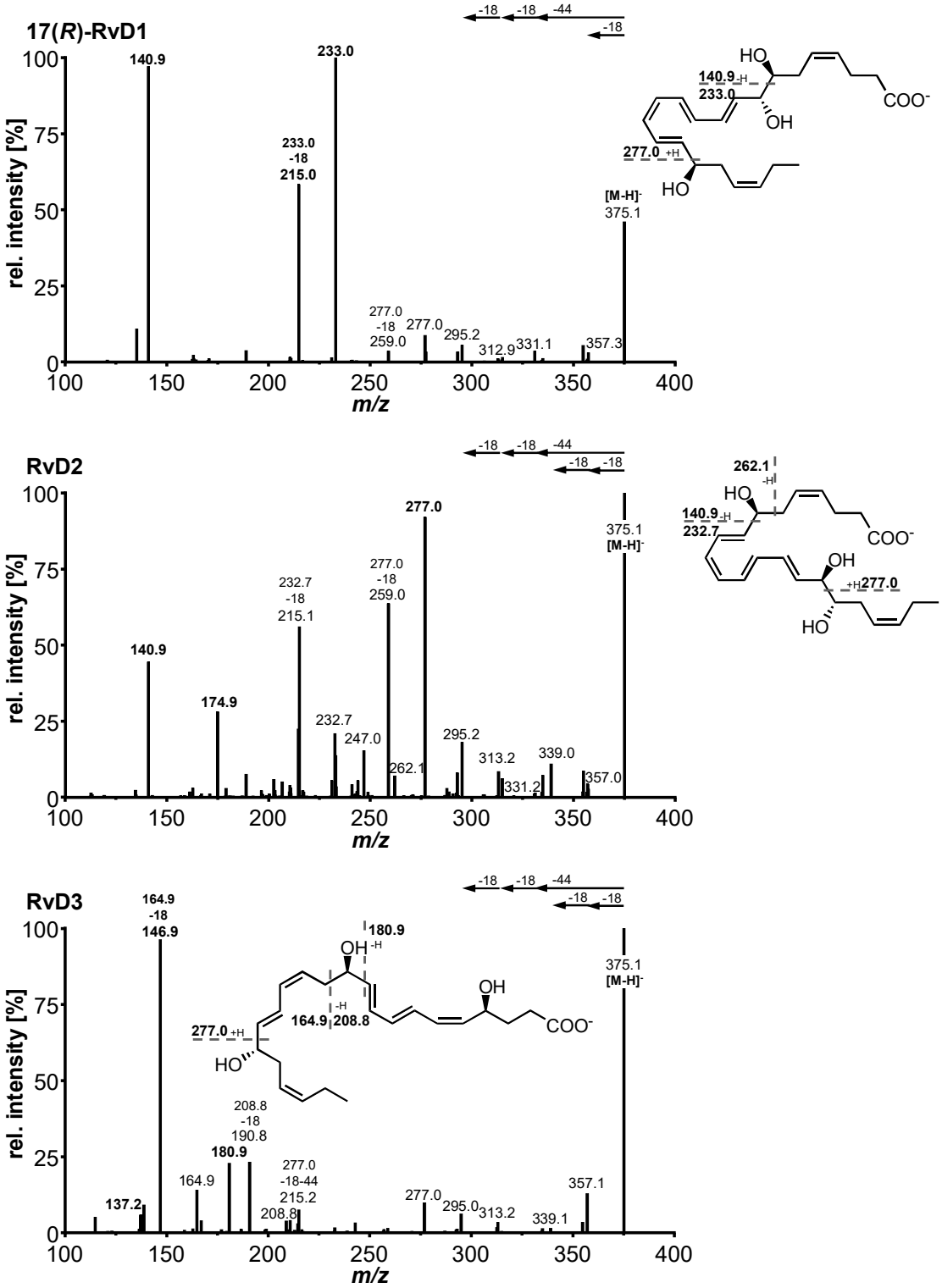

Fig. 8.3: Continued. Product ion spectra of ARA, EPA and DHA derived SPMs.

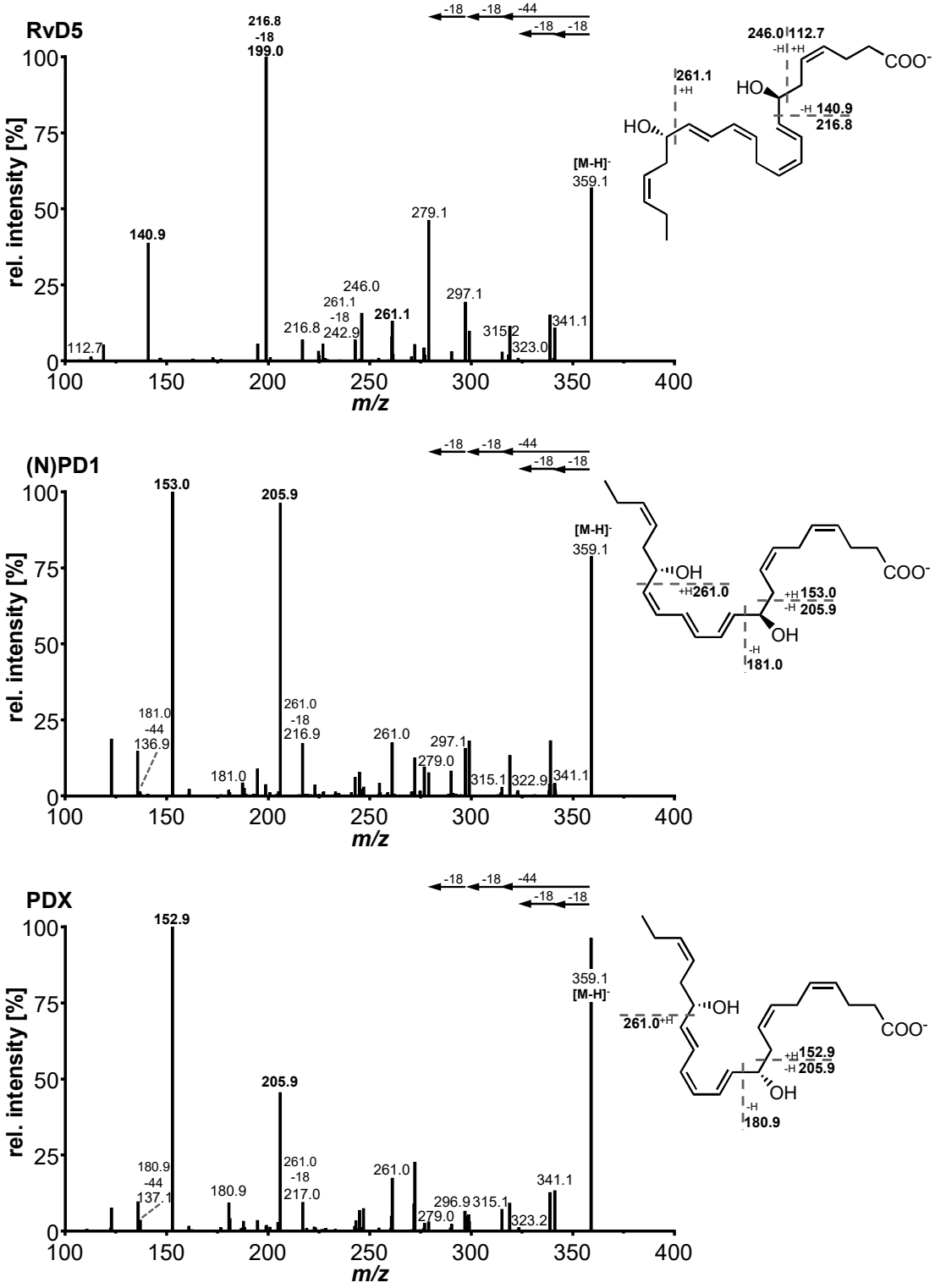

Fig. 8.3: Continued. Product ion spectra of ARA, EPA and DHA derived SPMs.

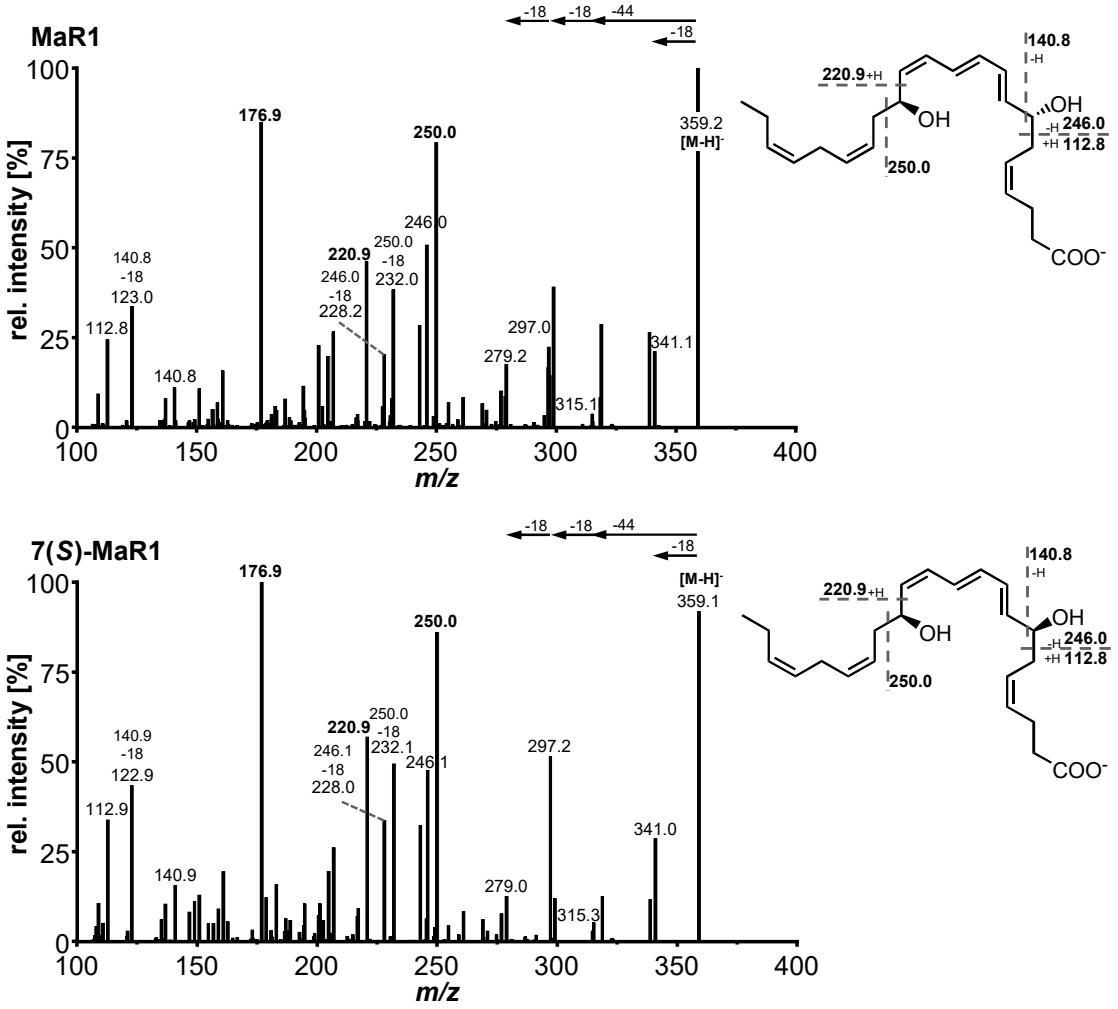

Fig. 8.3: Continued. Product ion spectra of ARA, EPA and DHA derived SPMs.

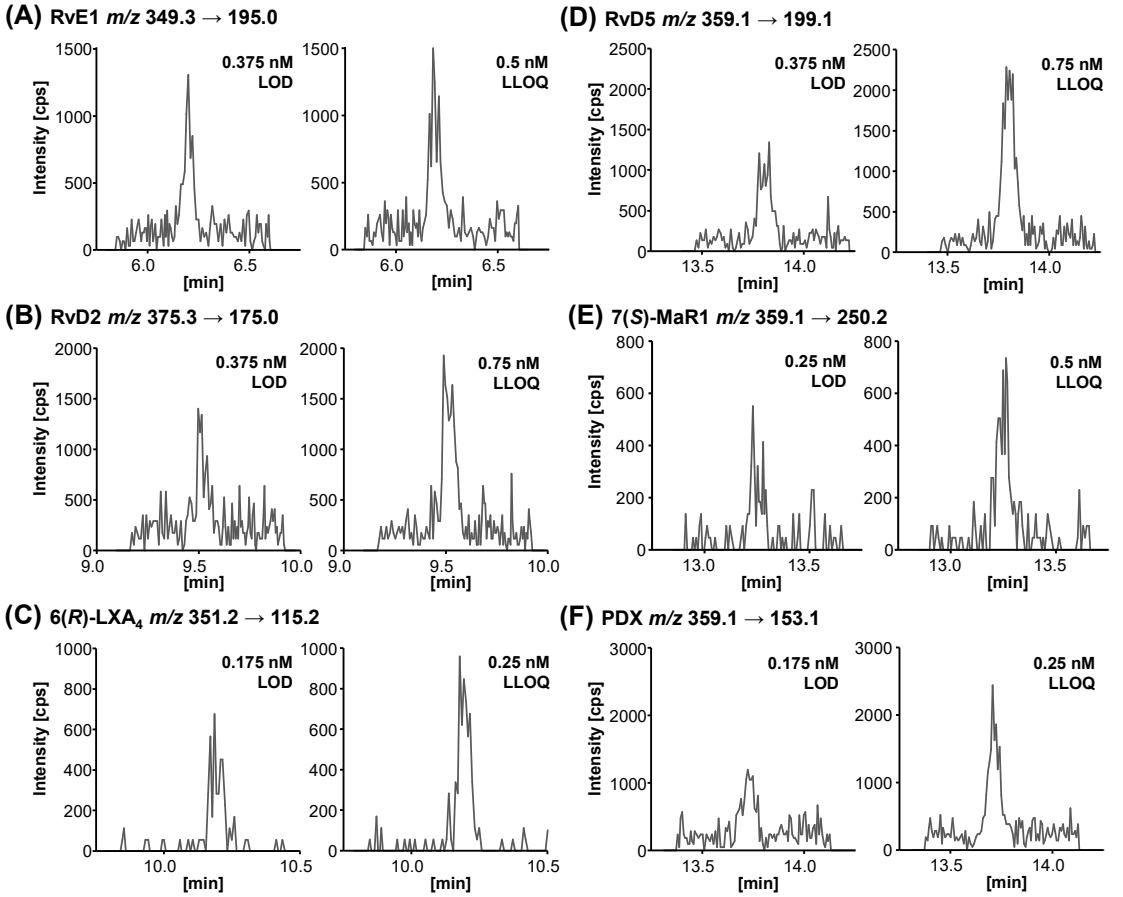

Fig. 8.4: Chromatographic peaks for the concentrations representing the lower limits of detection (LOD) and quantification (LLOQ) for structurally representative SPMs for 5 µL injection volume. (**A**) EPA derived trihydroxy-FA RvE1, (**B**) DHA derived trihydroxy-FA RvD2, (**C**) ARA derived trihydroxy-FA 6(*R*)-LXA_4, (**D**) DHA derived dihydroxy-FA RvD5, (**E**) DHA derived dihydroxy-FA 7(*S*)-MaR1 and (**F**) DHA derived protectin PDX.

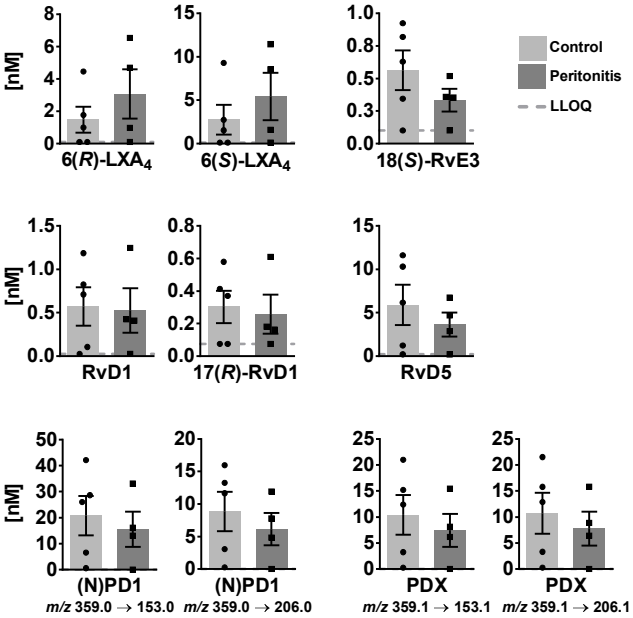

Fig. 8.5: Concentrations of SPMs in serum from patients with end stage renal disease treated with peritoneal dialysis (PD) with (peritonitis, n = 4) or without (control, n = 5) acute inflammation. Shown are concentrations in nM as individual values and mean ± SEM of SPMs derived from ARA, EPA and DHA that were not displayed in Fig. 4.11. For concentrations < LLOQ, the LLOQ is given. The LLOQ is indicated as dotted line. For (N)PD1 and PDX two transitions are displayed. PDX shows good agreement between determined concentrations for both transitions, while for (N)PD1 the transitions lead to different apparent concentrations, probably due to matrix interferences.

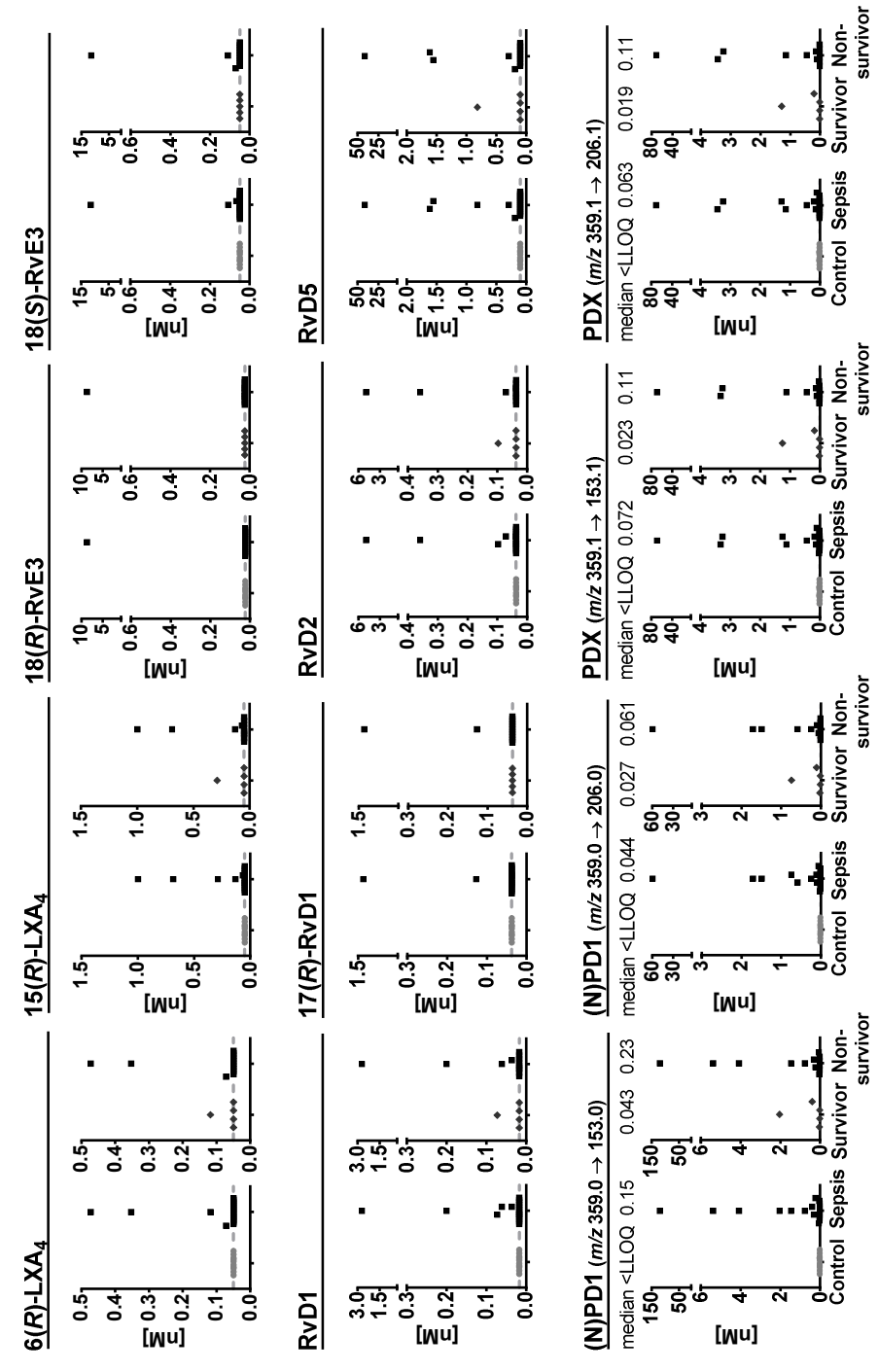

Fig. 8.6: Concentrations of SPMs measured in plasma from patients with (sepsis, n = 18) and without (control, n = 10) septic shock. Patients with septic shock are divided into survivors (> 28 days, n = 5) and non-survivors (n = 13). Shown are concentrations in nM as individual values of SPMs derived from ARA, EPA and DHA that were not displayed in Fig. 4.12. Median is given, if > 50% of the samples are > LLOQ. The LLOQ is indicated as dotted line. For (N)PD1 and PDX two transitions are displayed. PDX shows good agreement between determined concentrations for both transitions, while for (N)PD1 the transitions lead to different apparent concentrations, probably due to matrix interferences.

Chapter 5

No substrate incubations (enzyme only)

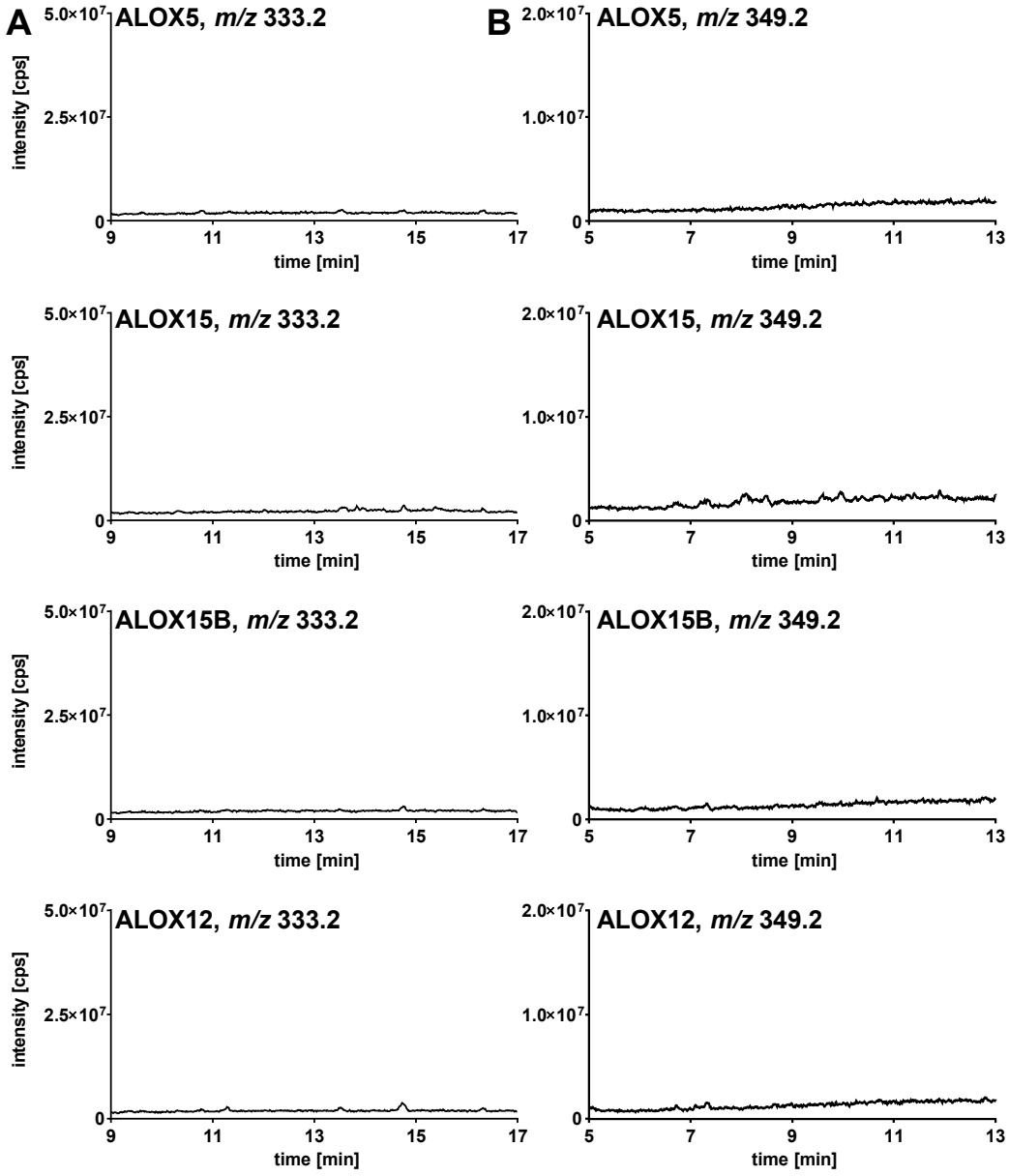

Fig. 8.7: No substrate (enzyme only) control incubations of recombinant human ALOX isoforms ALOX5, ALOX15, ALOX15B and ALOX12 (15 min, RT). Instead of fatty acid substrate solvent only (methanol) was added to the incubation mixture, samples were acidified and extracted twice with ethyl acetate. (**A**) Total ion chromatograms of product ion scans of *m/z* 333.2 (100–350 Da, CE ramp –18 to –26 V), (**B**) total ion chromatograms of product ion scans of *m/z* 349.2 (100–350 Da, CE ramp –18 to –26 V).

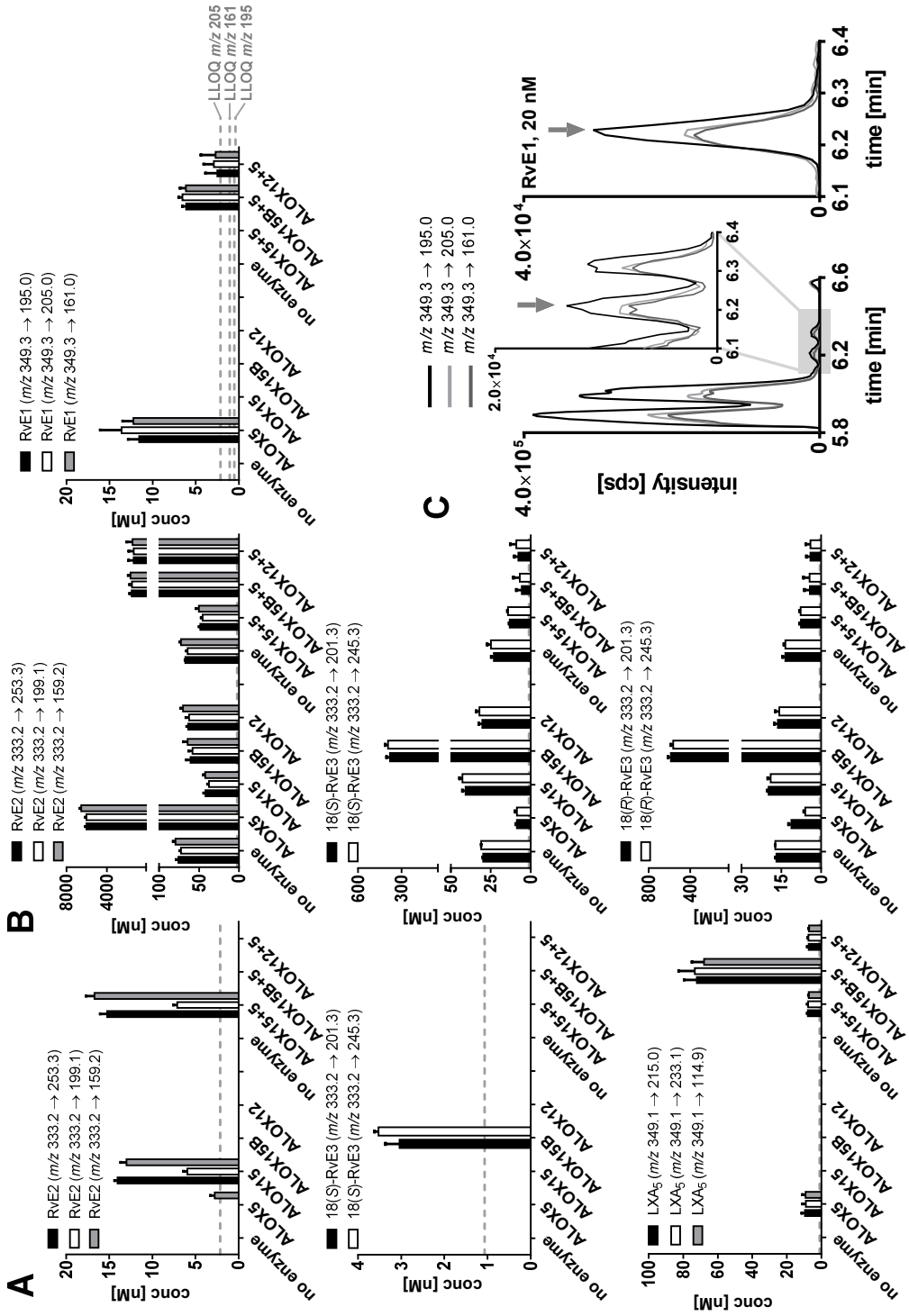

Fig. 8.8: Comparison of apparent concentrations using different SRM transitions for EPA derived di- and trihydroxy fatty acids formed in incubations of (**A**) EPA and (**B**–**C**) 18(*R*,*S*)-HEPE with recombinant human ALOX5, ALOX15, ALOX15B and ALOX12 alone and in combination with ALOX5. Shown are mean ± SD (n = 3). The lower limit of quantification (LLOQ) is indicated as dotted line. (**A**) Incubations of EPA (10 µM, 15 min, RT). (**B**) Incubations of 18(*R*,*S*)-HEPE (10 µM, 15 min, RT). (**C**) SRM transitions of RvE1 for an exemplary sample (ALOX5 incubation with 18(*R*,*S*)-HEPE) compared to RvE1 standard (20 nM).

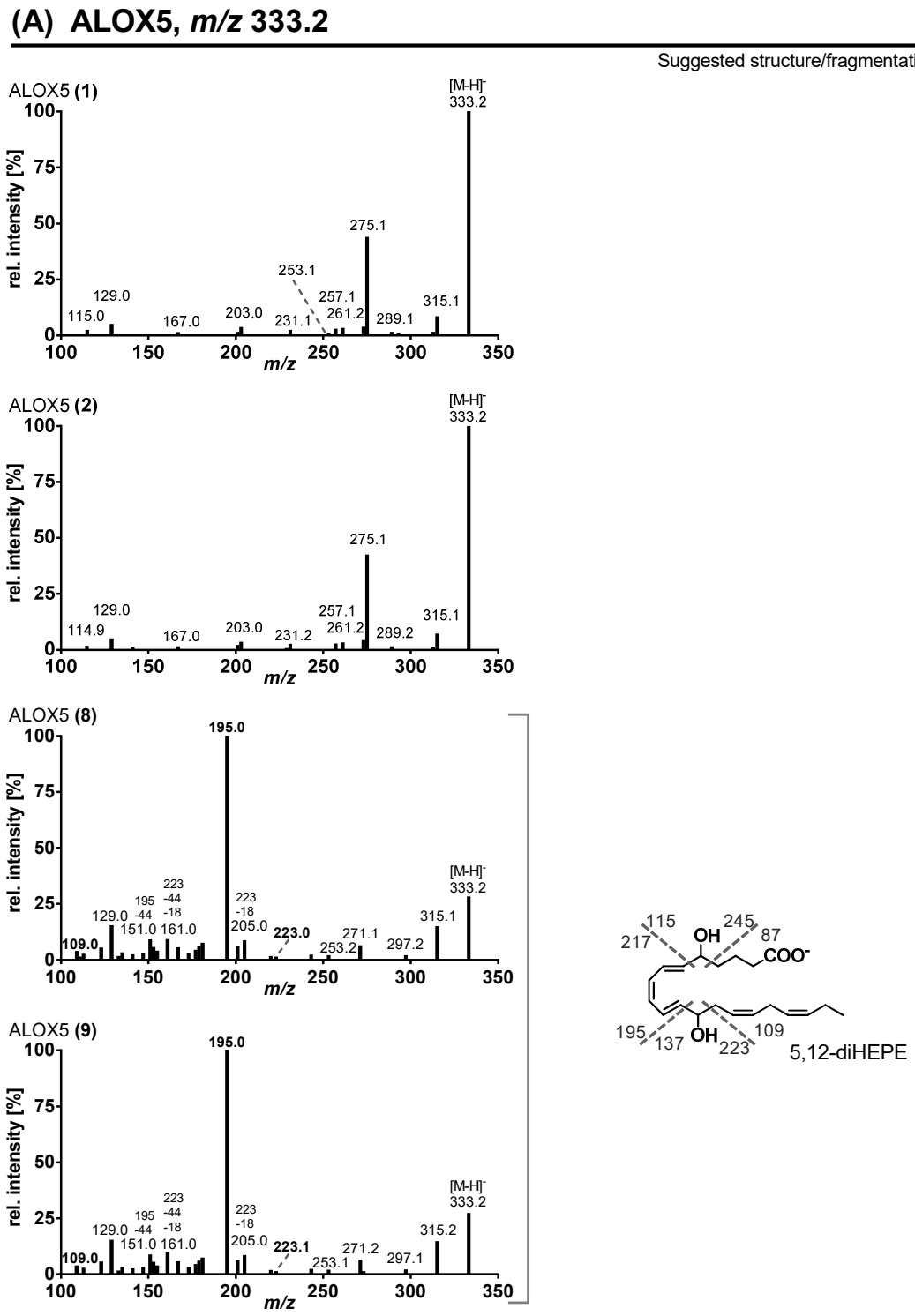

Fig. 8.9: Collision induced dissociation product ion spectra of ALOX products with *m/z* 333.2 formed during EPA incubation with recombinant human ALOX isoforms (10 µM EPA, 15 min, RT). Shown are product ion spectra of *m/z* 333.2 (100–350 Da, CE ramp –18 to –26 V) for products formed by (**A**) ALOX5, (**B**) ALOX15, (**C**) ALOX15B, (**D**) ALOX12 and in combined incubations of (**E**) ALOX15+ALOX5, (**F**) ALOX15B+ALOX5 and (**G**) ALOX12+ALOX5 alongside suggested structures and fragmentation sites. Note that only one of several possible double bond configurations is shown.

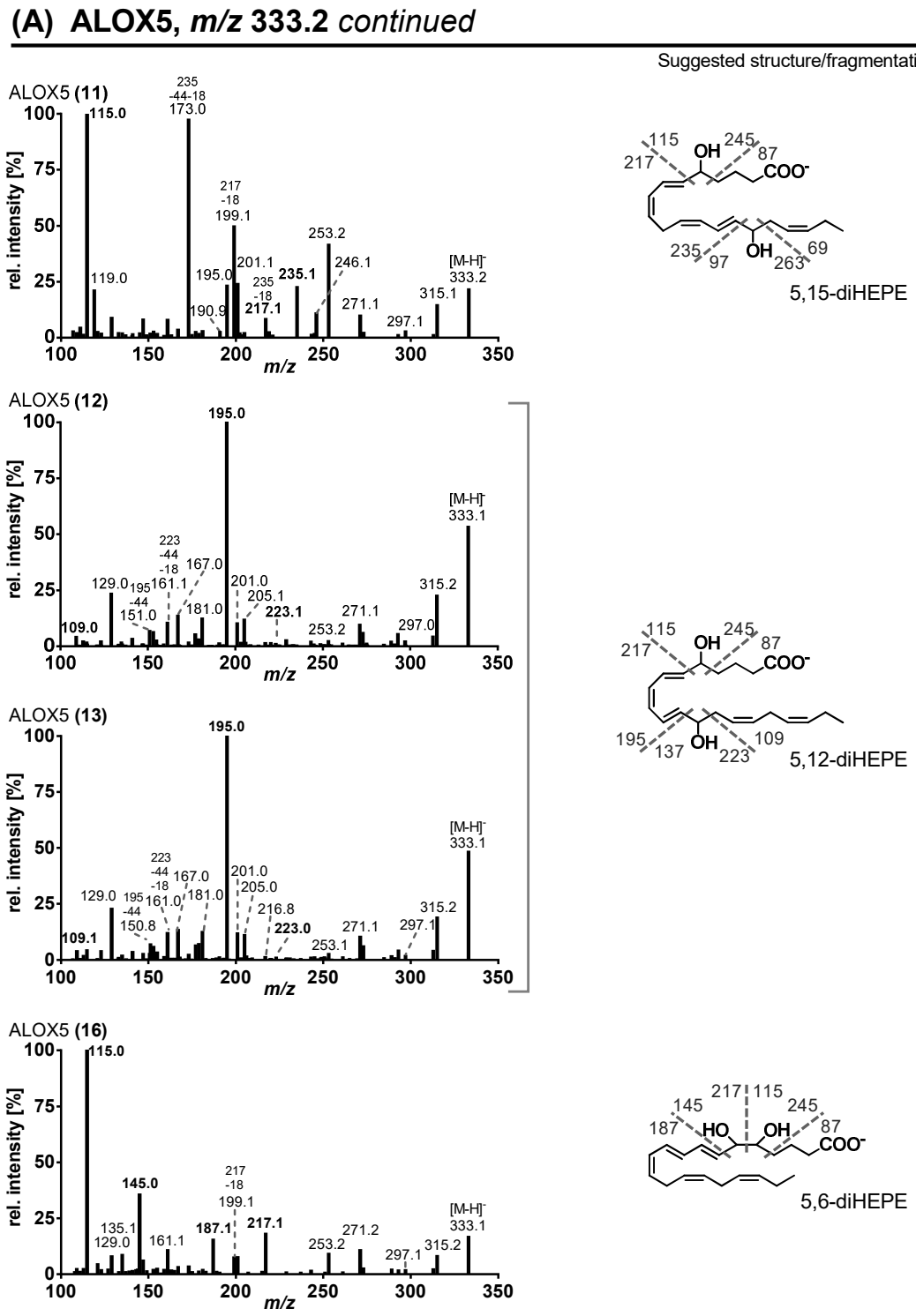

Fig. 8.9: Continued. Collision induced dissociation product ion spectra of ALOX products with *m/z* 333.2 formed during EPA incubation.

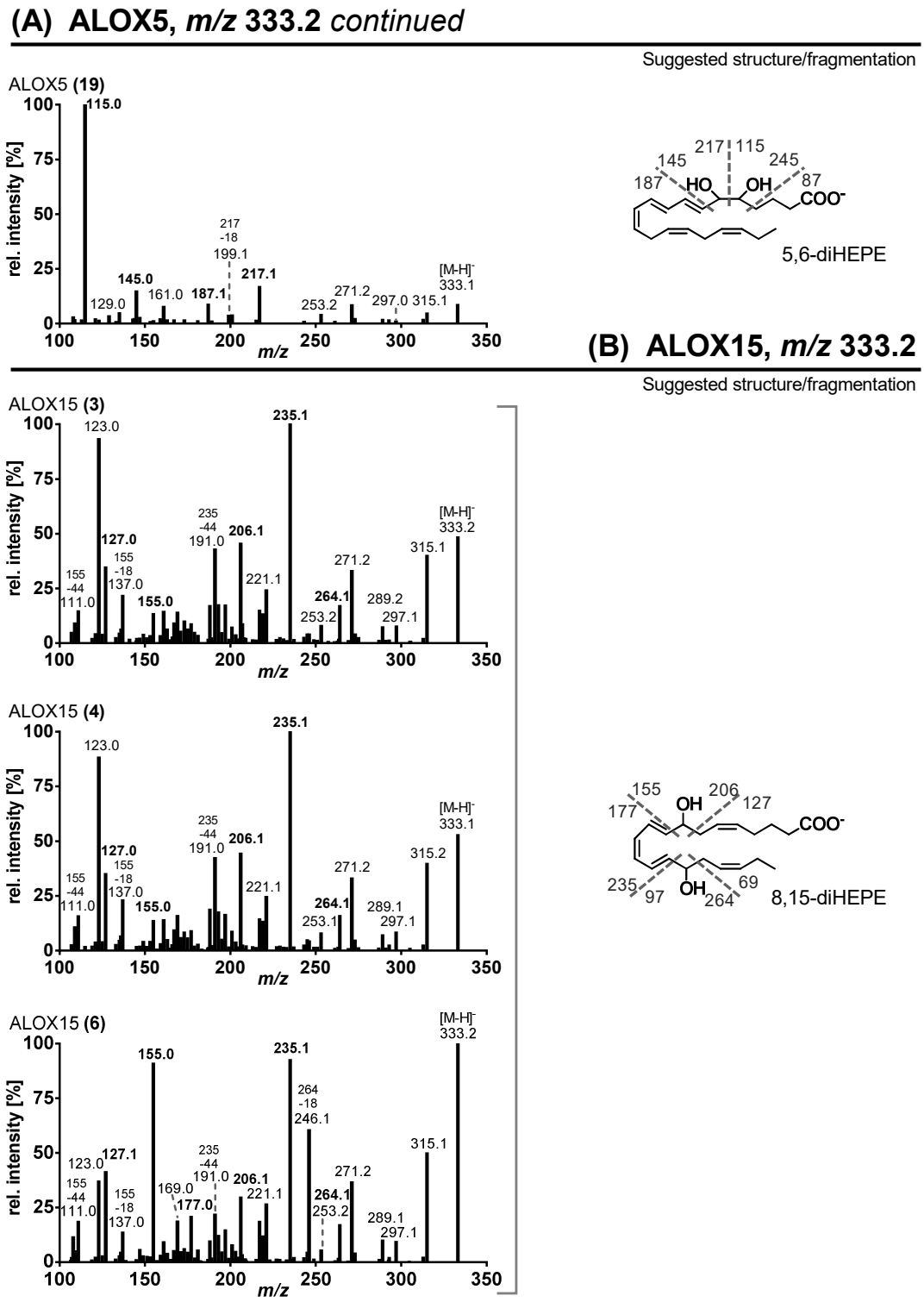

Fig. 8.9: Continued. Collision induced dissociation product ion spectra of ALOX products with *m/z* 333.2 formed during EPA incubation.

(B) ALOX15, *m/z* 333.2 *continued*

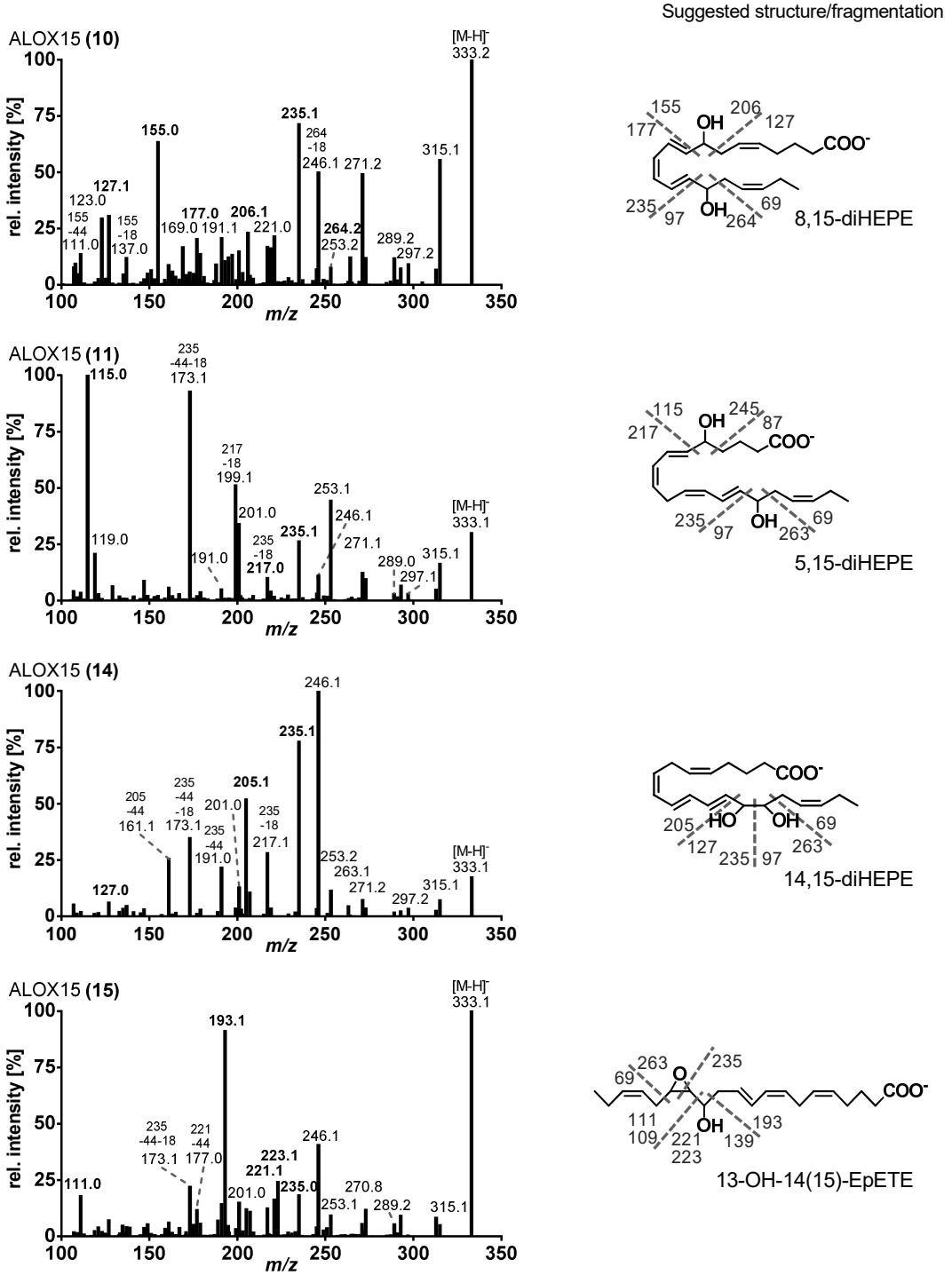

Fig. 8.9: Continued. Collision induced dissociation product ion spectra of ALOX products with *m/z* 333.2 formed during EPA incubation.

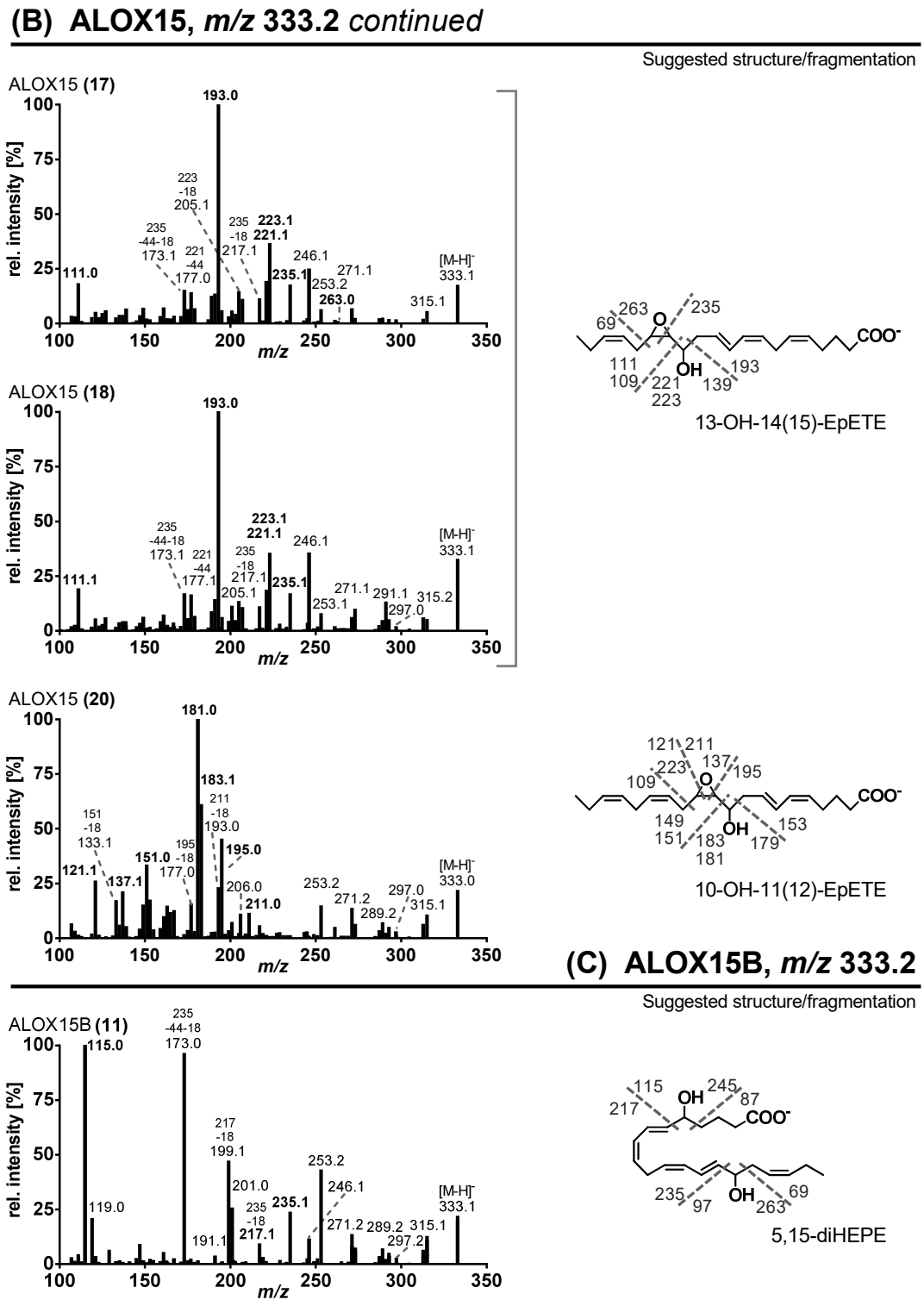

Fig. 8.9: Continued. Collision induced dissociation product ion spectra of ALOX products with *m/z* 333.2 formed during EPA incubation.

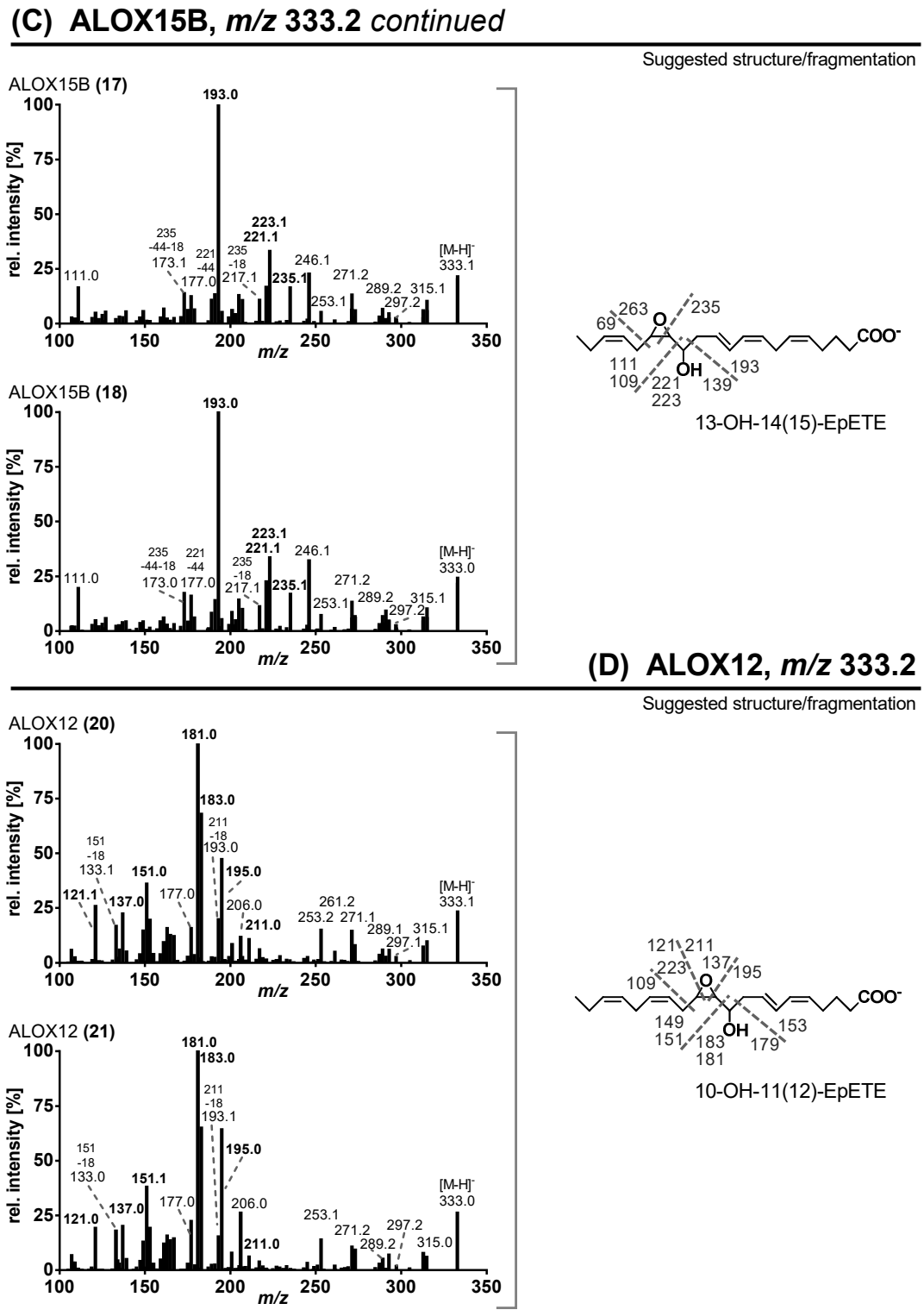

Fig. 8.9: Continued. Collision induced dissociation product ion spectra of ALOX products with *m/z* 333.2 formed during EPA incubation.

(E) ALOX15+ALOX5, *m/z* 333.2

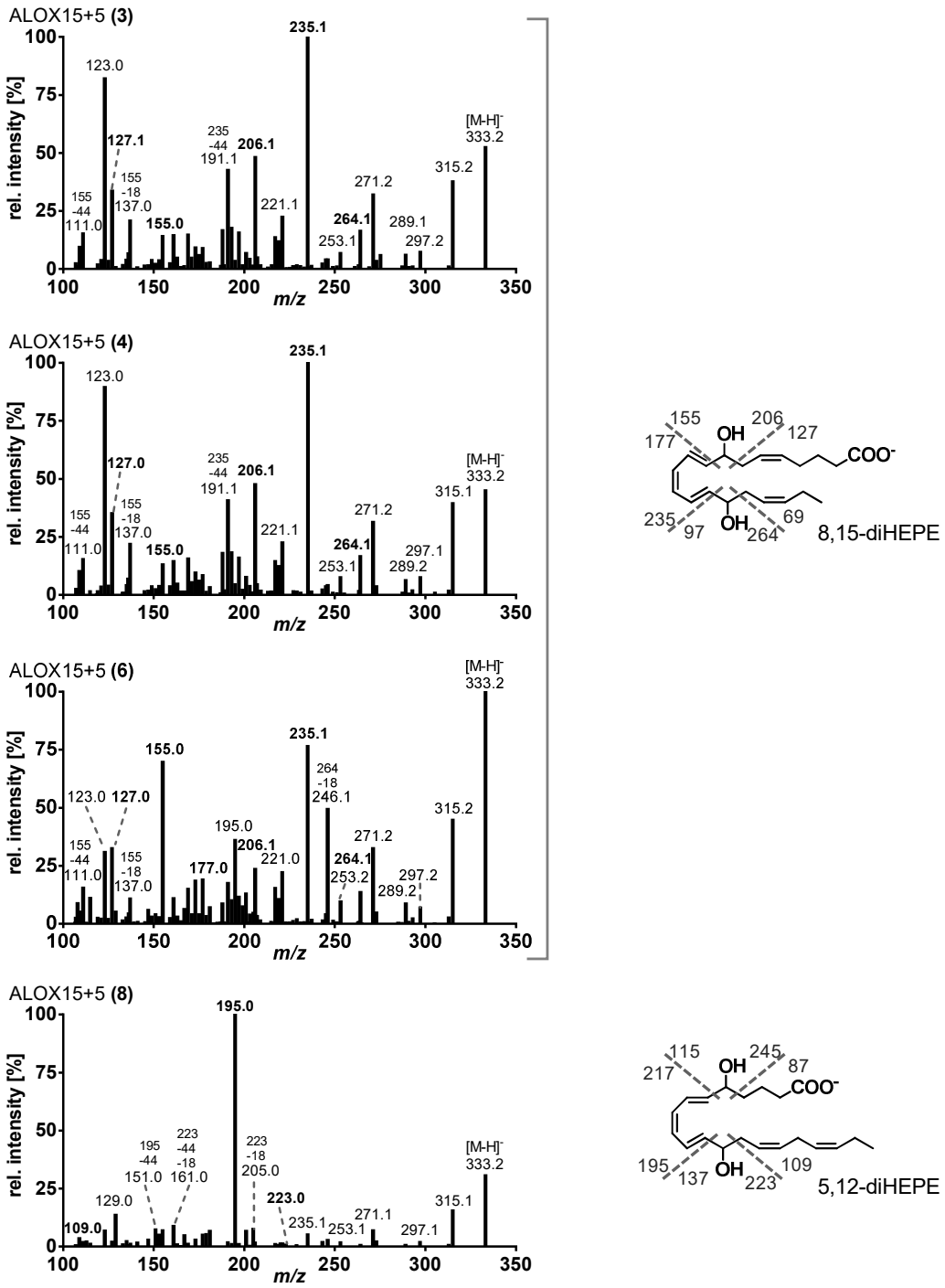

Fig. 8.9: Continued. Collision induced dissociation product ion spectra of ALOX products with *m/z* 333.2 formed during EPA incubation.

(E) ALOX15+ALOX5, *m/z* 333.2 *continued*

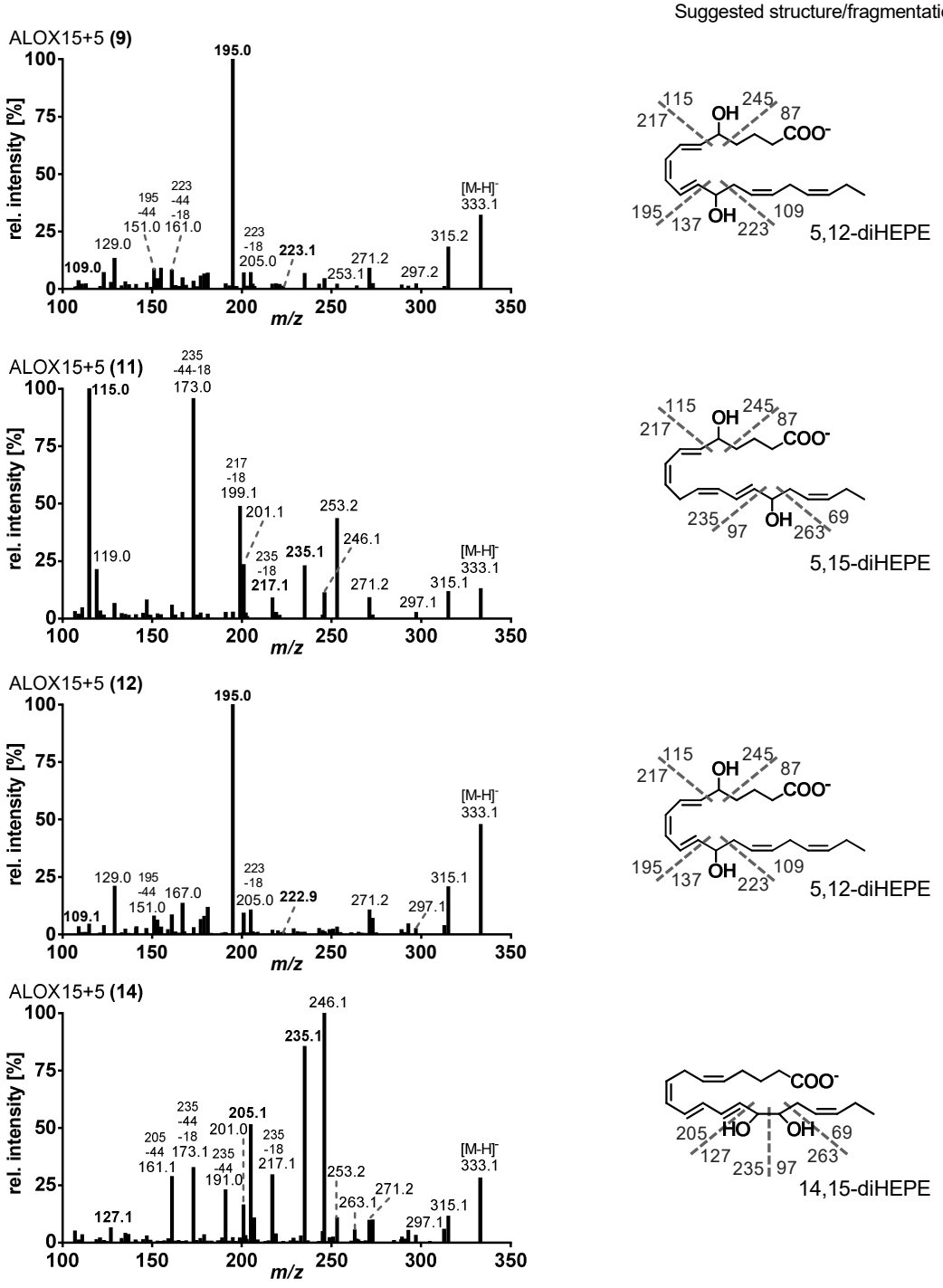

Fig. 8.9: Continued. Collision induced dissociation product ion spectra of ALOX products with *m/z* 333.2 formed during EPA incubation.

(E) ALOX15+ALOX5, *m/z* 333.2 *continued*

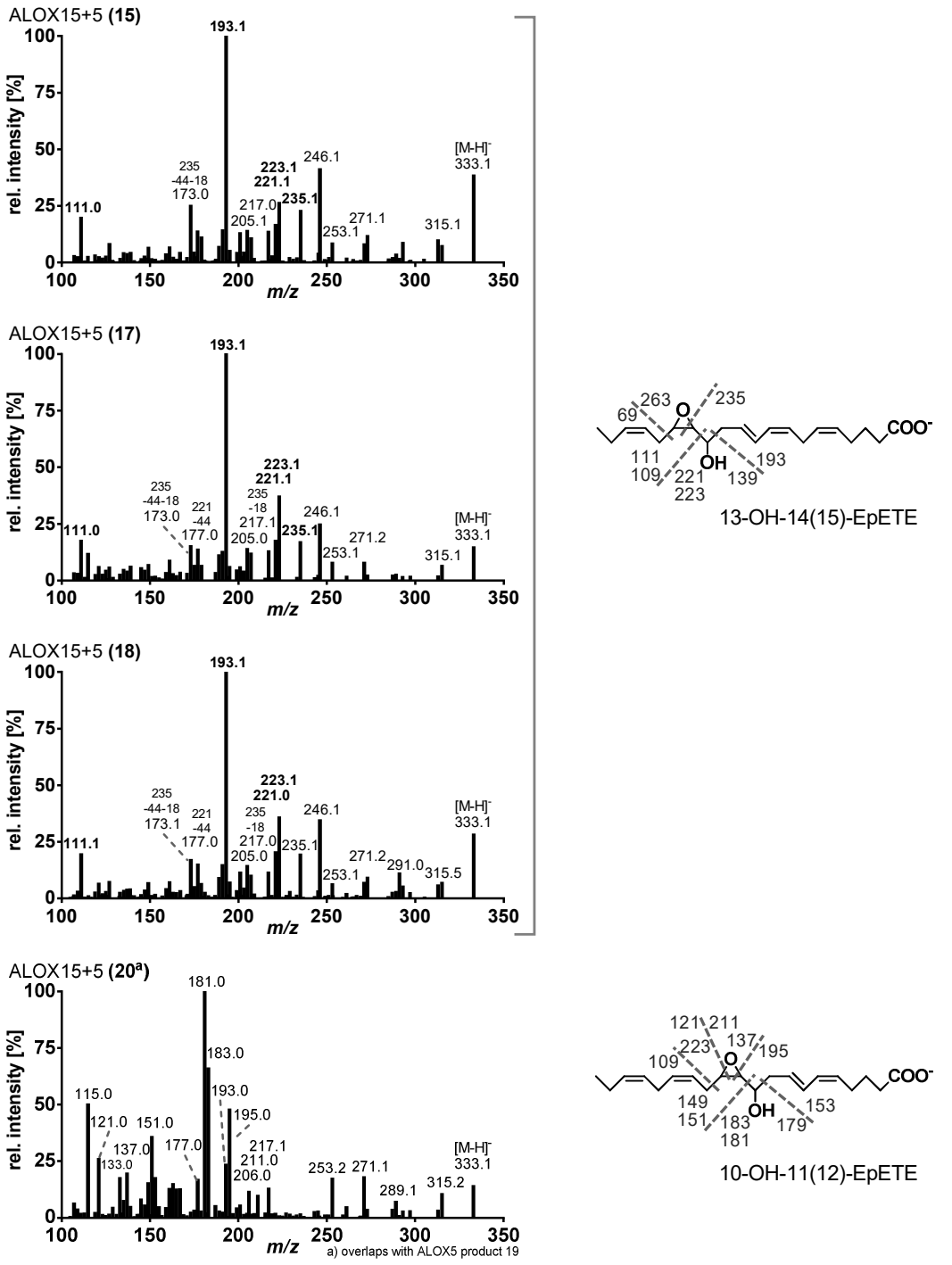

Fig. 8.9: Continued. Collision induced dissociation product ion spectra of ALOX products with *m/z* 333.2 formed during EPA incubation.

(F) ALOX15B+ALOX5, *m/z* 333.2

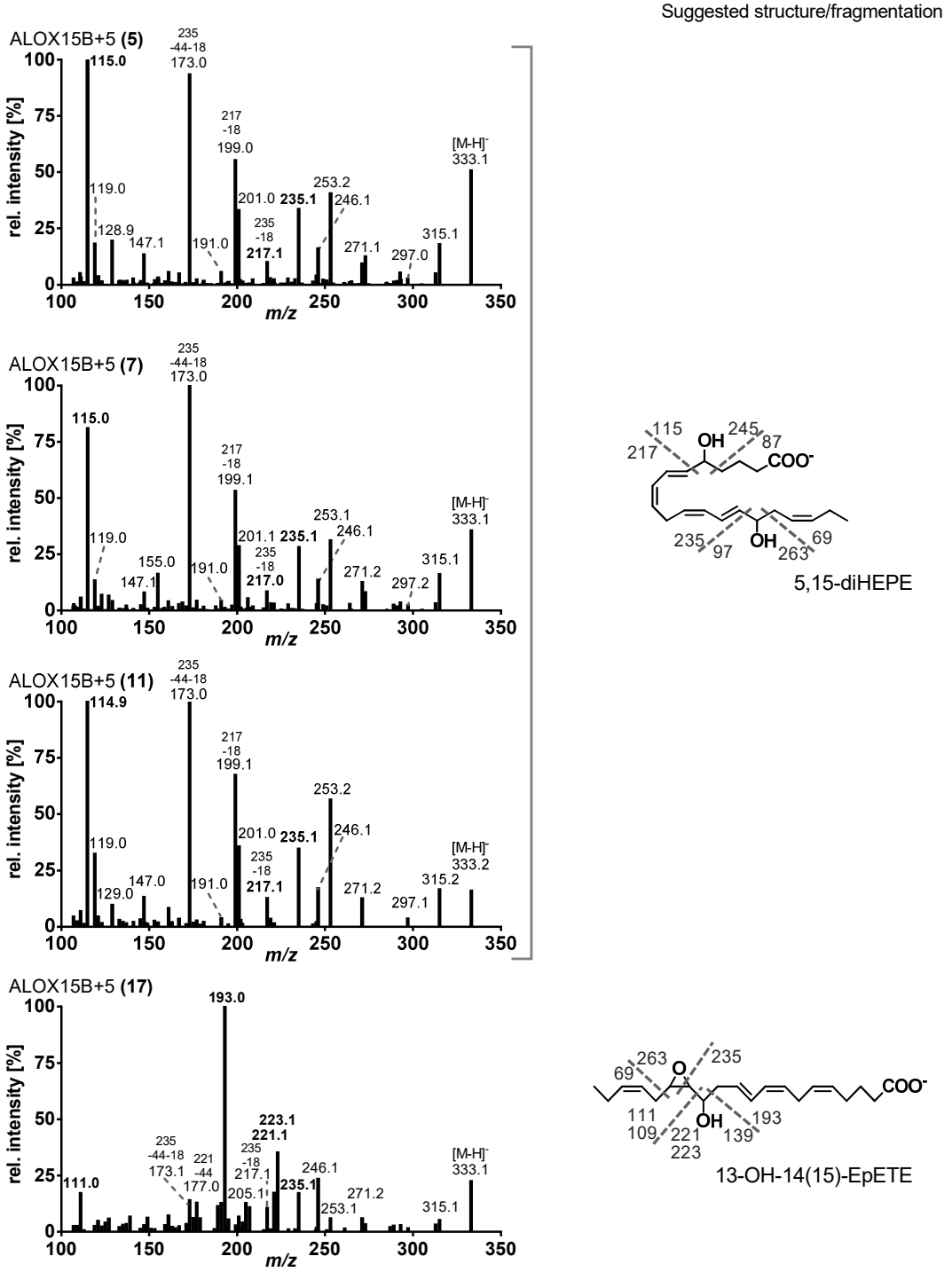

Fig. 8.9: Continued. Collision induced dissociation product ion spectra of ALOX products with *m/z* 333.2 formed during EPA incubation.

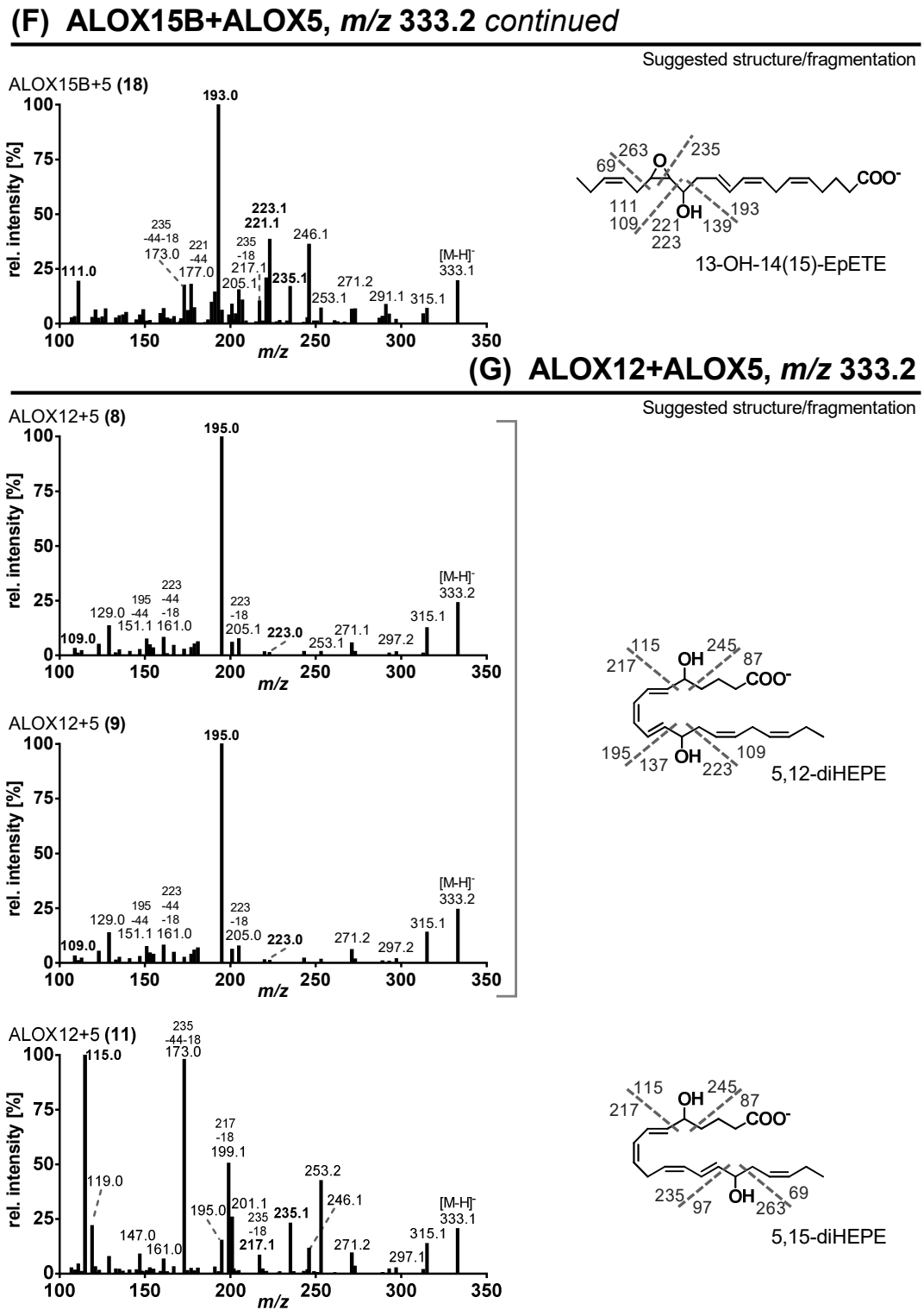

Fig. 8.9: Continued. Collision induced dissociation product ion spectra of ALOX products with *m/z* 333.2 formed during EPA incubation.

(G) ALOX12+ALOX5, *m/z* 333.2 *continued*

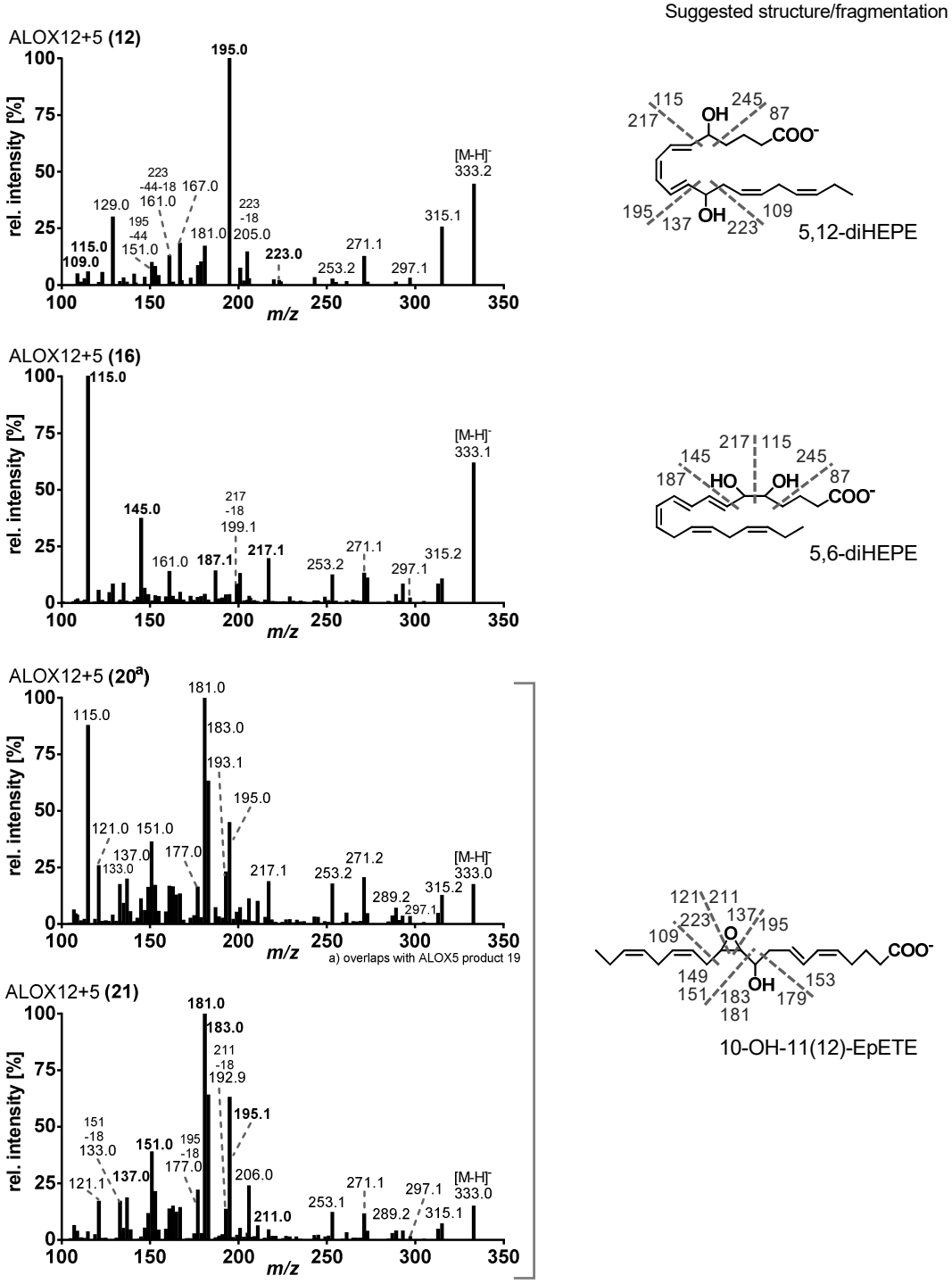

Fig. 8.9: Continued. Collision induced dissociation product ion spectra of ALOX products with *m/z* 333.2 formed during EPA incubation.

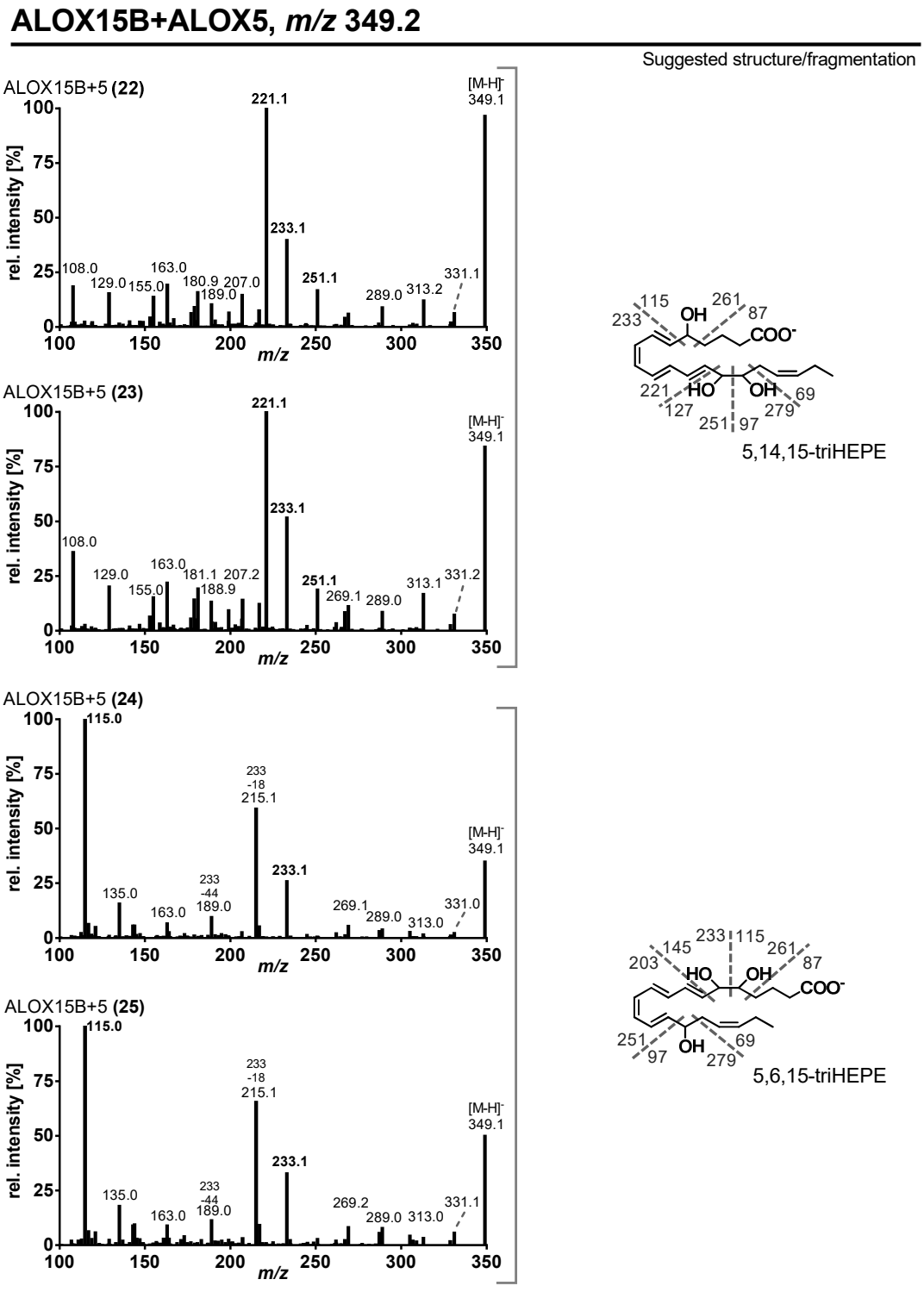

Fig. 8.10: Collision induced dissociation product ion spectra of ALOX products with *m/z* 349.2 formed during EPA incubation with recombinant human ALOX isoforms (10 µM EPA, 15 min, RT). Shown are product ion spectra of *m/z* 349.2 (100–350 Da, CE ramp –18 to –26 V) for products formed during combined incubation of ALOX15B+ALOX5 alongside suggested structures and fragmentation sites. Note that only one of several possible double bond configurations is shown.

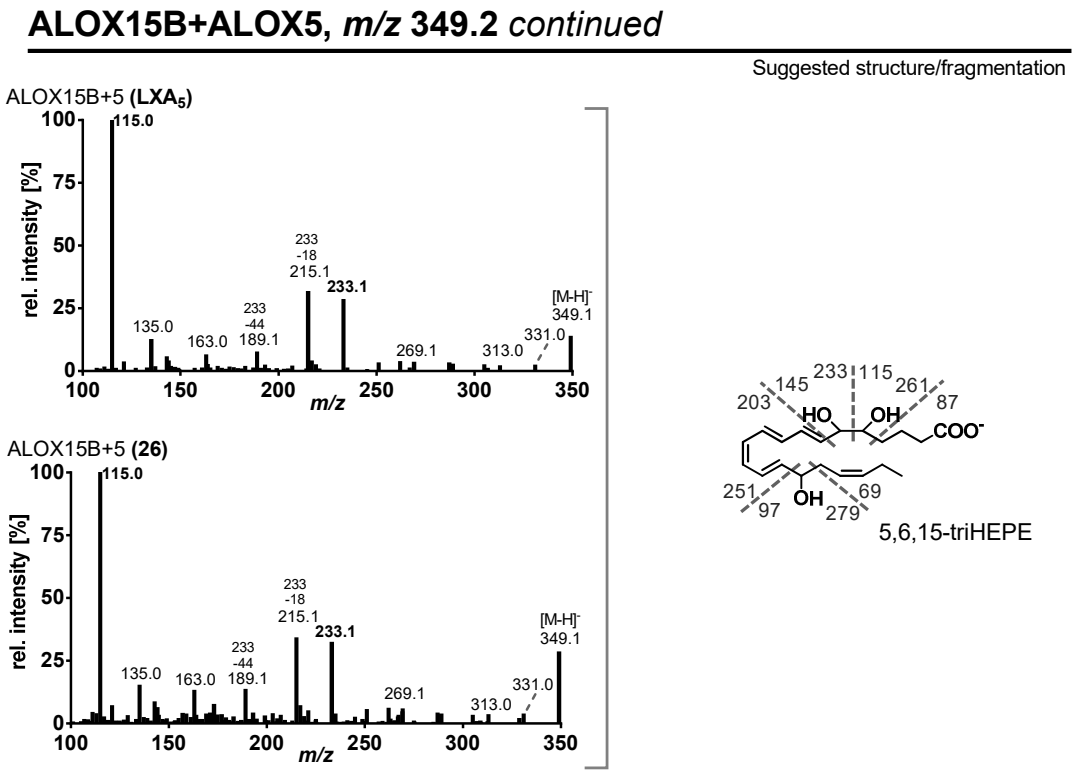

Fig. 8.10: Continued. Collision induced dissociation product ion spectra of ALOX products with *m/z* 349.2 formed during EPA incubation.

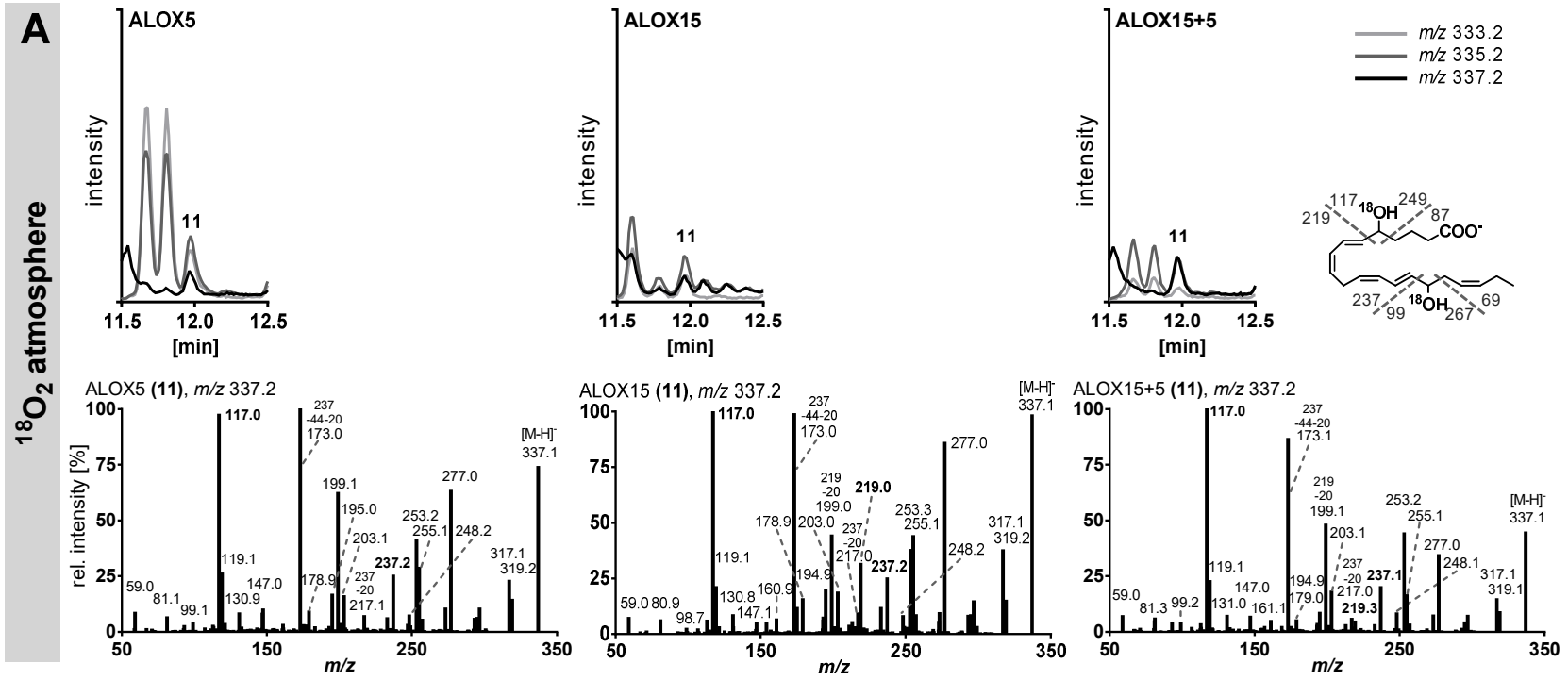

Fig. 8.11: Formation of compound 11 (5,15-diHEPE) during EPA incubation with recombinant human ALOX5 or ALOX15 or ALOX15+ALOX5 consecutively (10 µM EPA, 15 min, RT) (**A**) with $^{18}O_2$ gas or (**B**) in $H_2{}^{18}O$ buffer. Shown are total ion chromatograms of product ion scans (55–340 Da, *m/z* 333.2, 335.2, 337.2; CE ramp –18 to –26 V) as well as collision induced dissociation product ion spectra. Prevailing detection of compound 11 with *m/z* 333.2 in $H_2{}^{18}O$ buffer indicates insertion of two ^{16}O-atoms by the ALOX enzyme instead of formation via hydrolysis of an epoxide intermediate. Consistently, in incubation samples with $^{18}O_2$-gas 5,15-diHEPE with two ^{18}O-atoms (*m/z* 337.2) was detected.

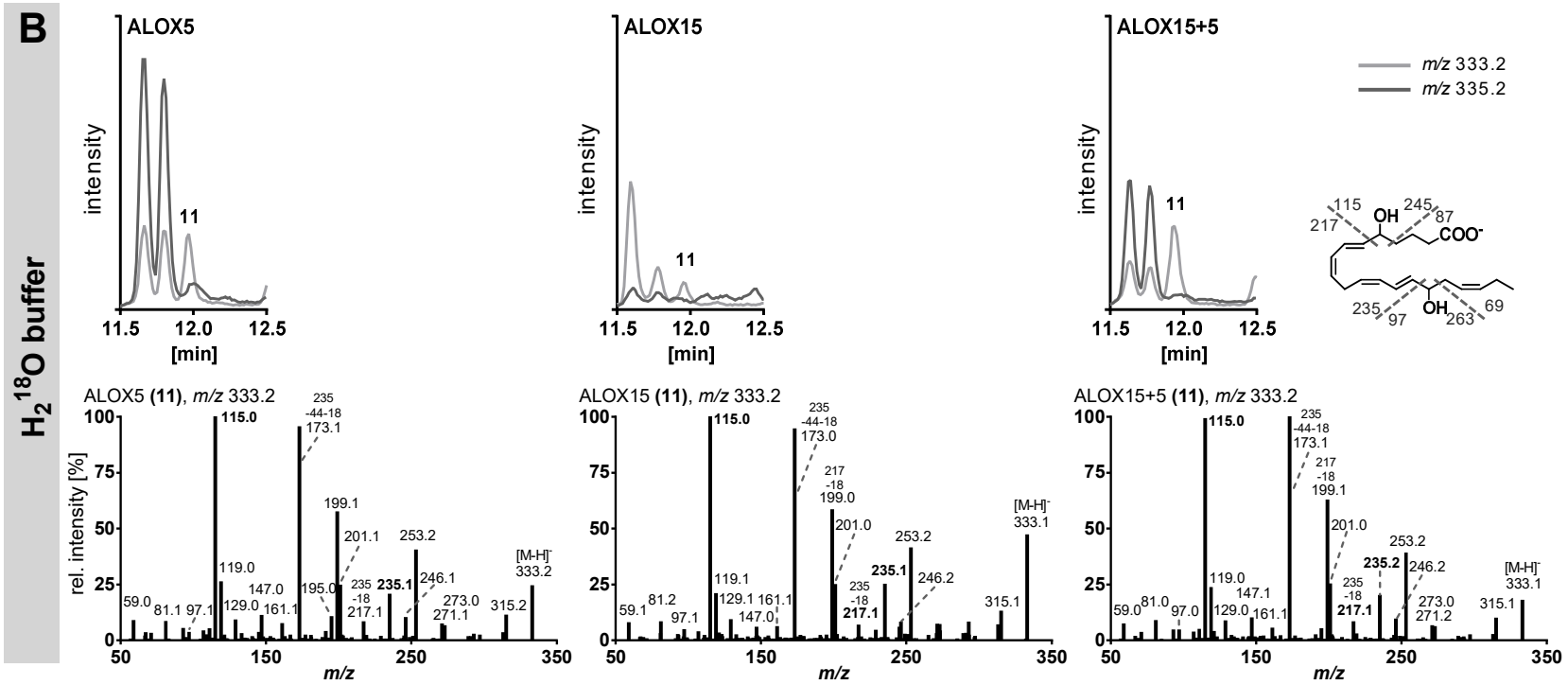

Fig. 8.11: Continued. Formation of compound 11 (5,15-diHEPE) during EPA incubation with recombinant human ALOX5 or ALOX15 or ALOX15+ALOX5 consecutively (10 µM EPA, 15 min, RT) (**A**) with $^{18}O_2$ gas or (**B**) in $H_2{}^{18}O$ buffer.

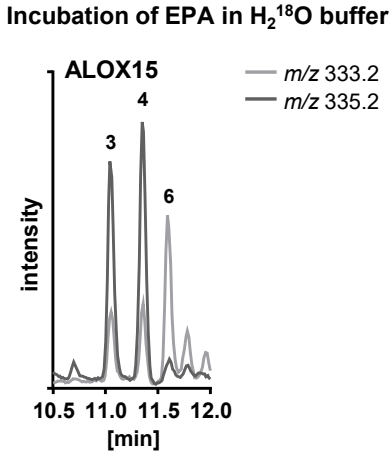

Fig. 8.12: Formation of compounds 3, 4 and 6 (8,15-diHEPE isomers) during EPA incubation with recombinant human ALOX15 (10 µM EPA, 15 min, RT) in $H_2{}^{18}O$ buffer. Shown are total ion chromatograms of product ion scans (55–340 Da, *m/z* 333.2 and 335.2; CE ramp –18 to –26 V). Prevailing detection of compounds 3 and 4 with *m/z* 335.2 in $H_2{}^{18}O$ buffer indicates formation via hydrolysis of an epoxide intermediate, while compound 6 with *m/z* 333.2 indicates insertion of two ^{16}O-atoms by the ALOX enzyme.

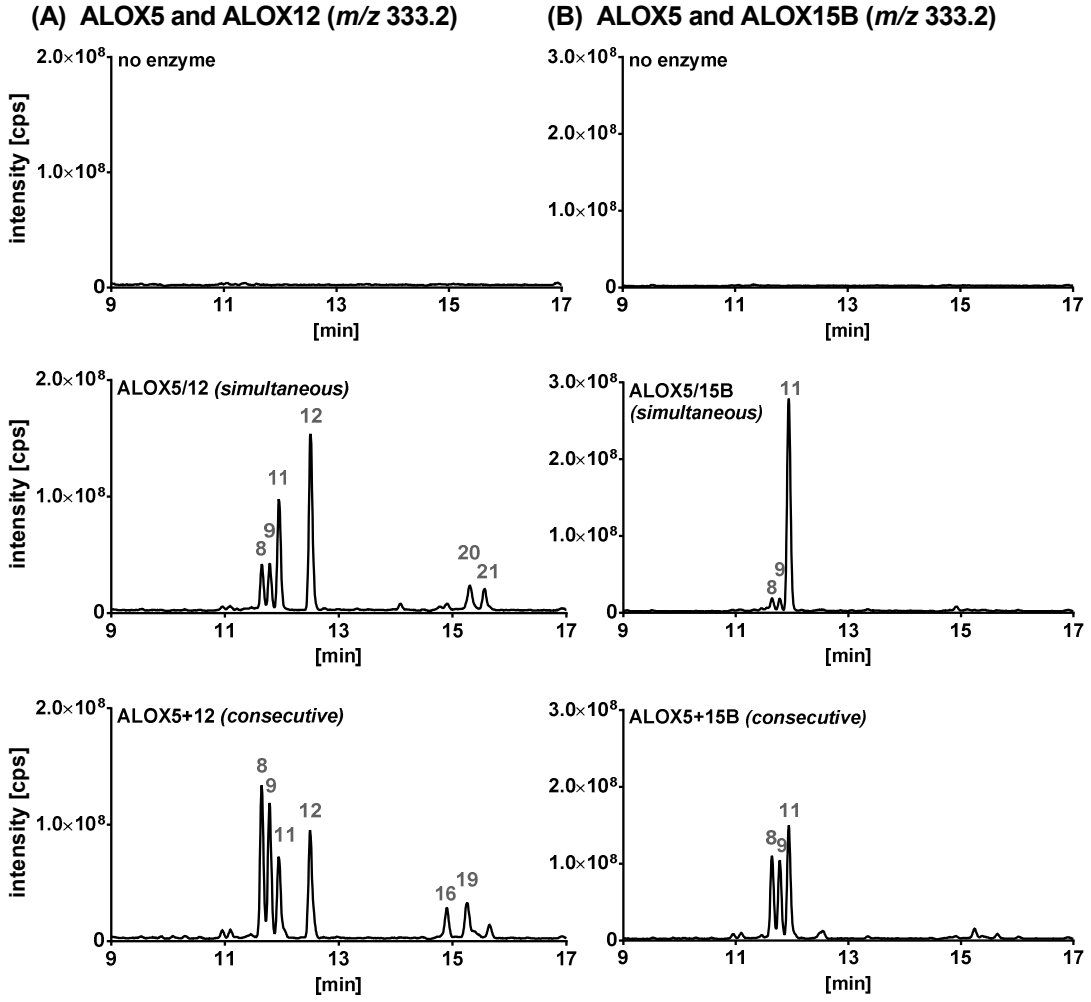

Fig. 8.13: Formation of double oxygenated products from EPA by recombinant human ALOX isoforms. Simultaneous and consecutive incubations were carried out as described (10 µM EPA, 15 min, RT), with the two enzymes added simultaneously or consecutively with ALOX5 added prior ALOX12 or ALOX15B to the incubation mixture. Shown are total ion chromatograms of product ion scans of *m/z* 333.2 (100–350 Da, CE ramp –18 to –26 V). Major double oxygenated products are labeled as indicated in Tab. 5.2.

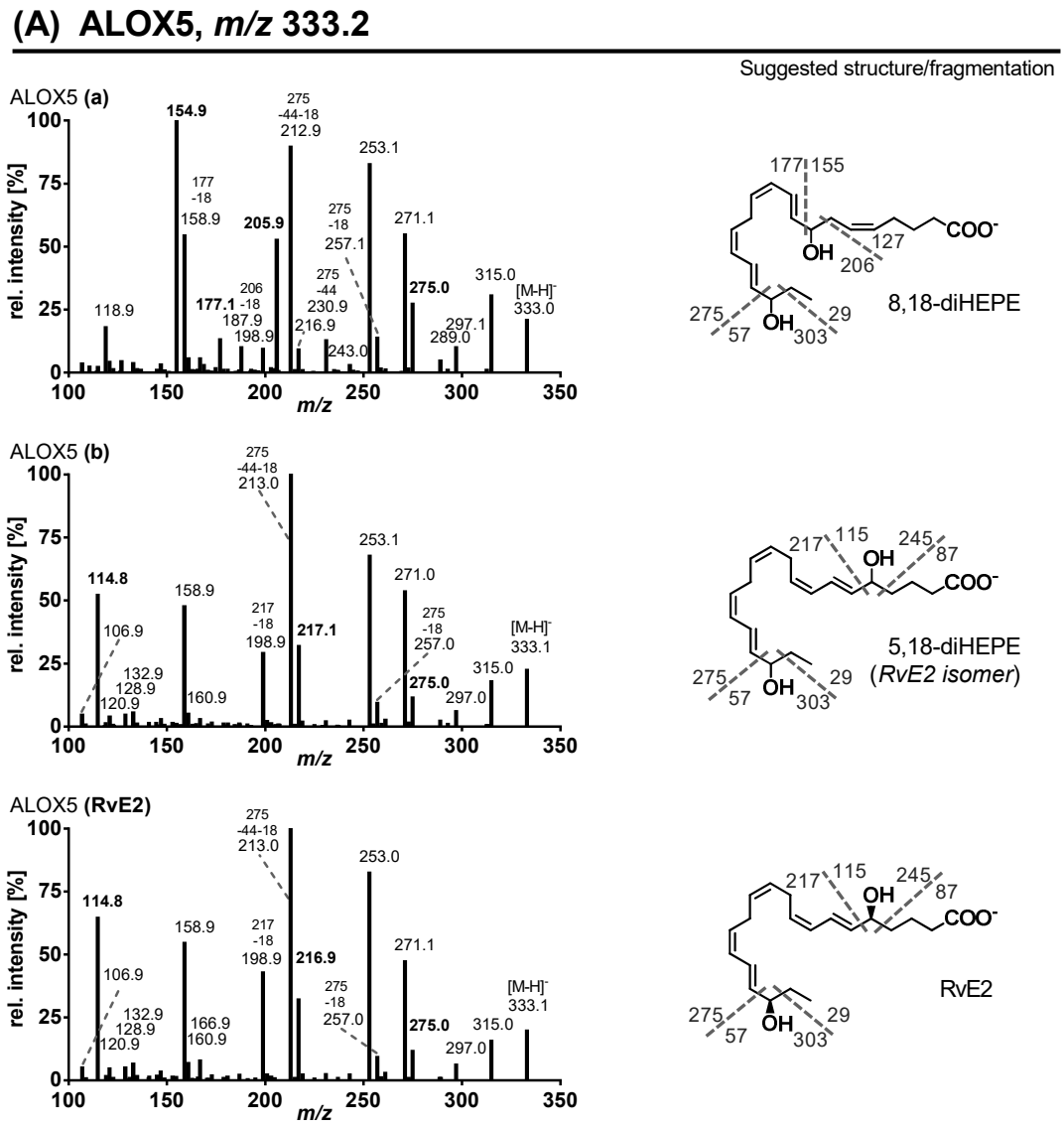

Fig. 8.14: Collision induced dissociation product ion spectra of ALOX products with *m/z* 333.2 formed during 18(*R*,*S*)-HEPE incubation with recombinant human ALOX isoforms (10 µM 18(*R*,*S*)-HEPE, 15 min, RT). Shown are product ion spectra of *m/z* 333.2 (100–340 Da, CE ramp –18 to –26 V) for products formed by (**A**) ALOX5, (**B**) ALOX15B, (**C**) ALOX12 and in combined incubations of (**D**) ALOX15B+ALOX5, (**E**) ALOX12+ALOX5 alongside suggested structures and fragmentation sites. Note that only one of several possible double bond configurations is shown.

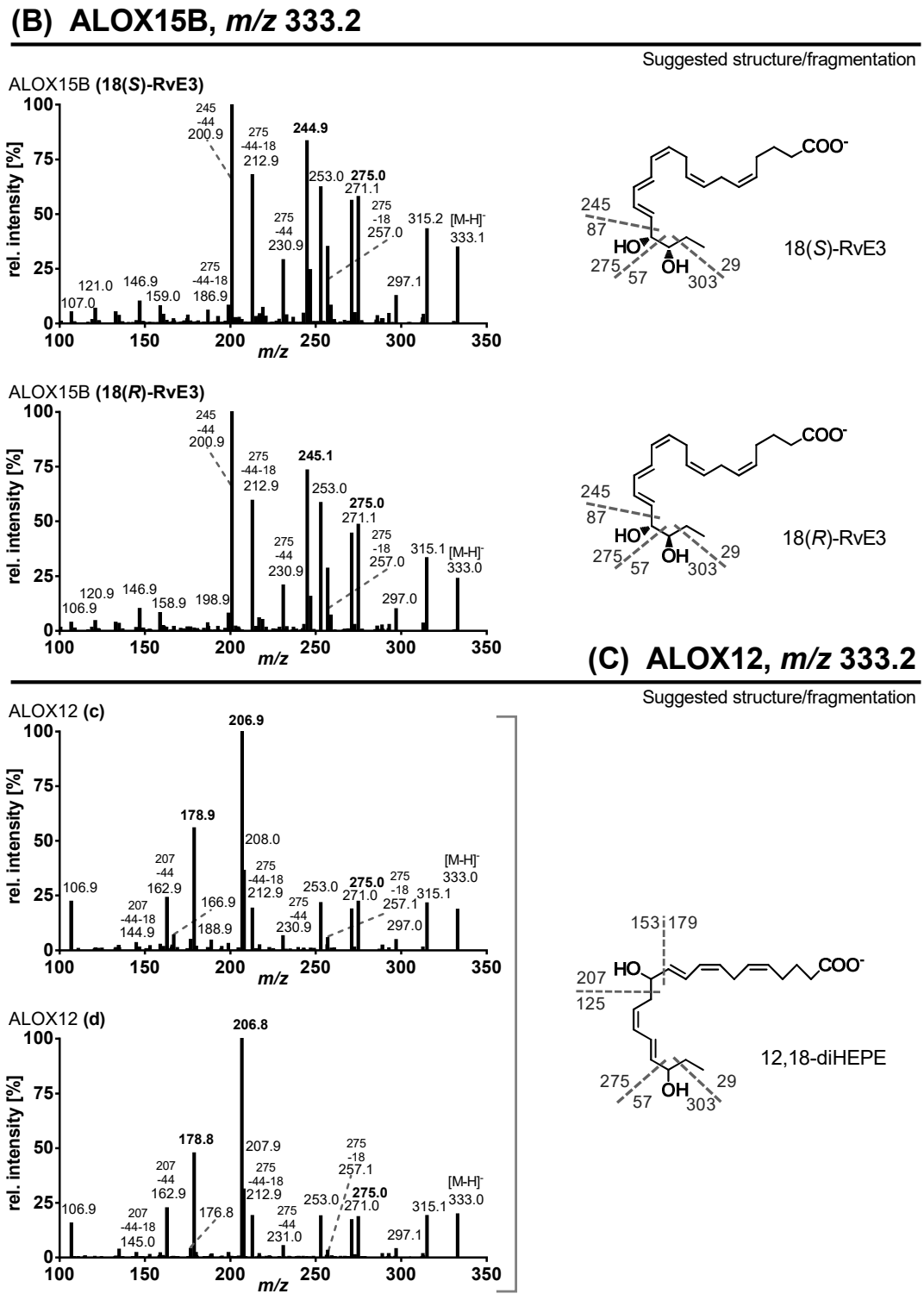

Fig. 8.14: Continued. Collision induced dissociation product ion spectra of ALOX products with *m/z* 333.2 formed during 18(*R*,*S*)-HEPE incubation.

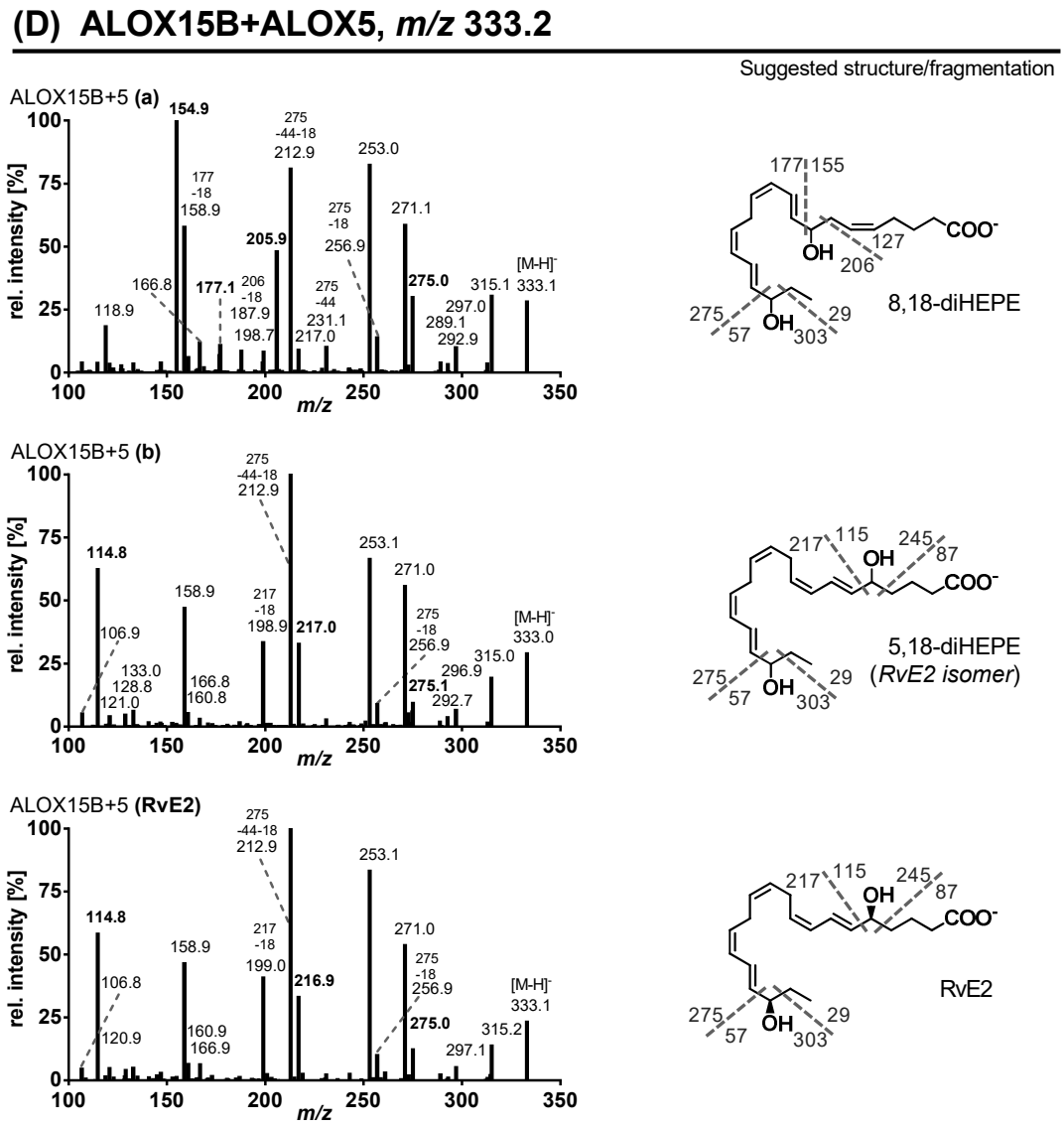

Fig. 8.14: Continued. Collision induced dissociation product ion spectra of ALOX products with *m/z* 333.2 formed during 18(*R*,*S*)-HEPE incubation.

(E) ALOX12+ALOX5, *m/z* 333.2

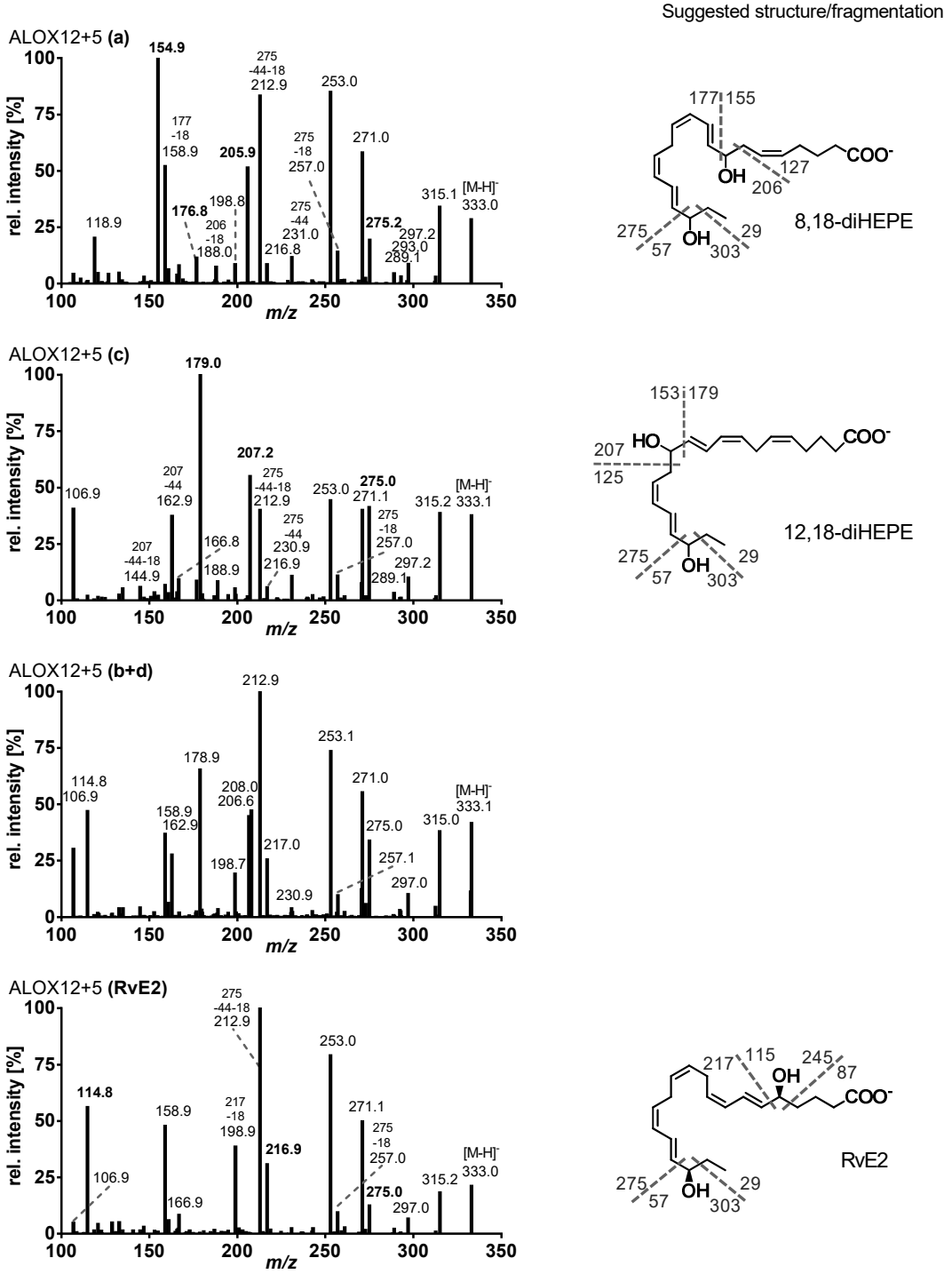

Fig. 8.14: Continued. Collision induced dissociation product ion spectra of ALOX products with *m/z* 333.2 formed during 18(*R*,*S*)-HEPE incubation.

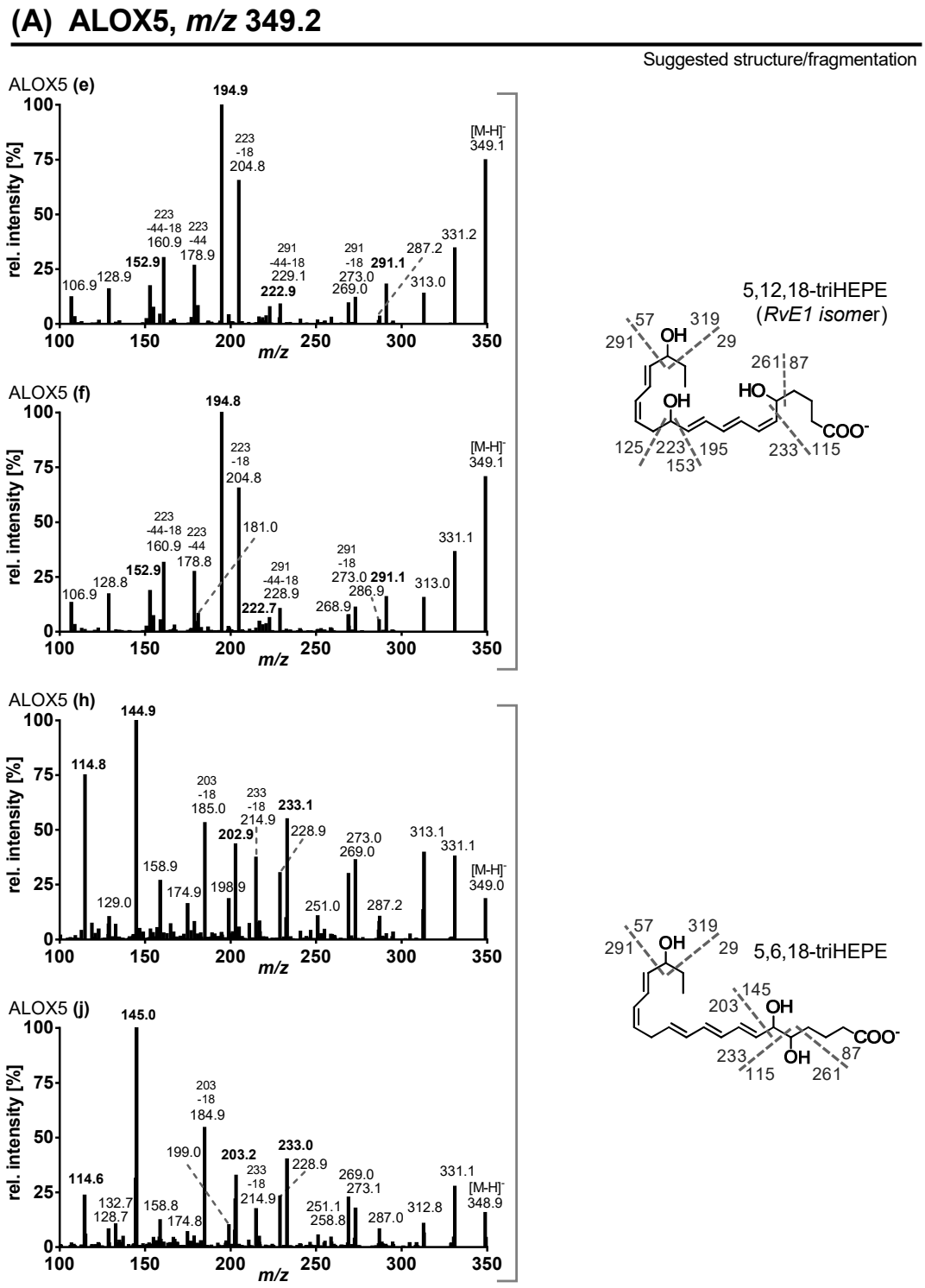

Fig. 8.15: Collision induced dissociation product ion spectra of ALOX products with *m/z* 349.2 formed during 18(*R*,*S*)-HEPE incubation with recombinant human ALOX isoforms (10 µM 18(*R*,*S*)-HEPE, 15 min, RT). Shown are product ion spectra of *m/z* 349.2 (100–350 Da, CE ramp –18 to –26 V) for products formed by (**A**) ALOX5 and in combined incubations of (**B**) ALOX15B+ALOX5 and (**C**) ALOX12+ALOX5 alongside suggested structures and fragmentation sites. Note that only one of several possible double bond configurations is shown.

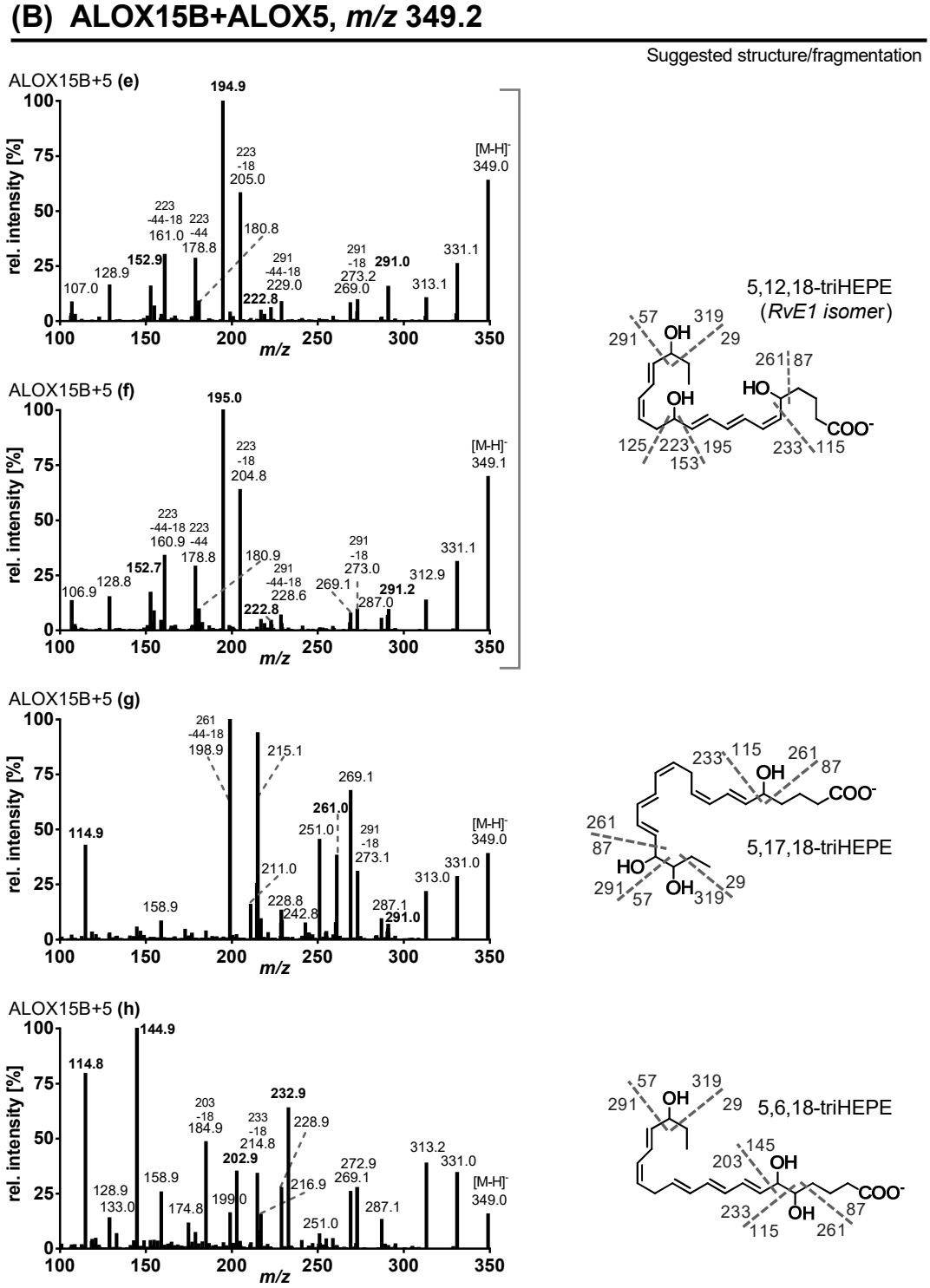

Fig. 8.15: Continued. Collision induced dissociation product ion spectra of ALOX products with *m/z* 349.2 formed during 18(*R*,*S*)-HEPE incubation.

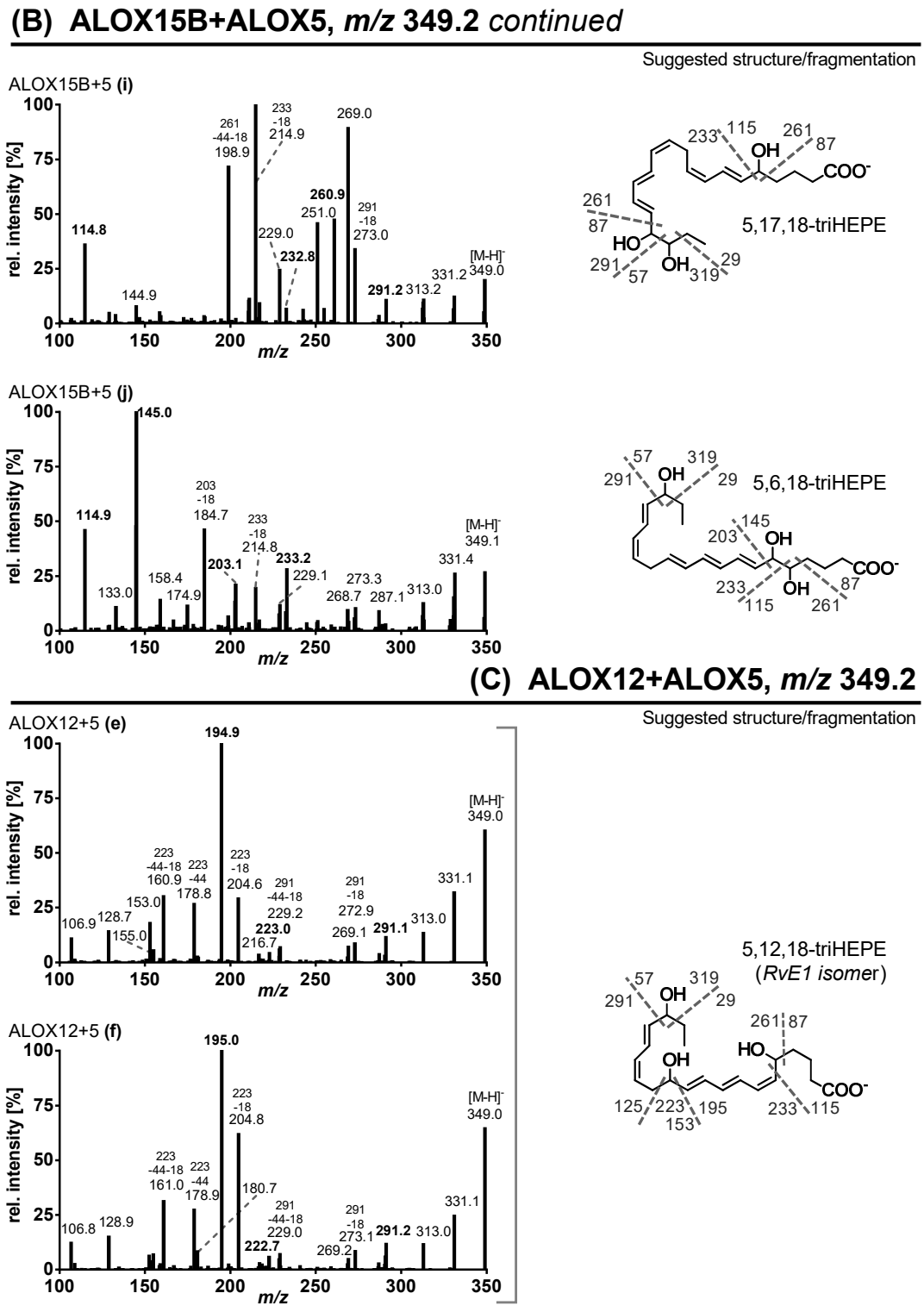

Fig. 8.15: Continued. Collision induced dissociation product ion spectra of ALOX products with *m/z* 349.2 formed during 18(*R*,*S*)-HEPE incubation.

(C) ALOX12+ALOX5, *m/z* 349.2 *continued*

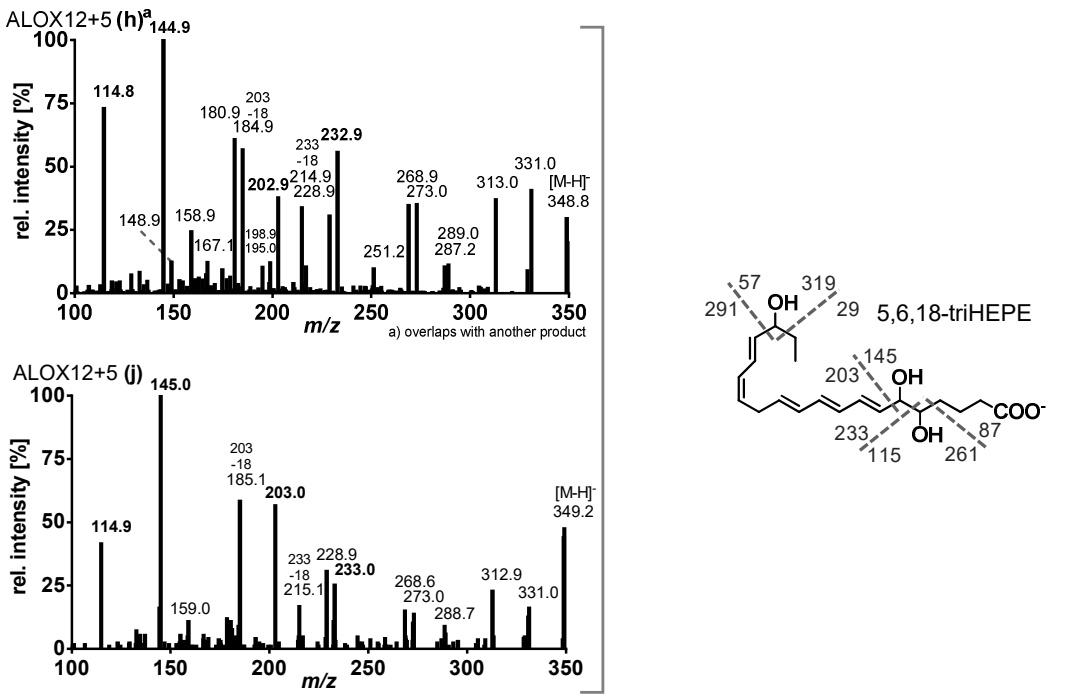

Fig. 8.15: Continued. Collision induced dissociation product ion spectra of ALOX products with *m/z* 349.2 formed during 18(*R*,*S*)-HEPE incubation.

Abbreviations

15(*R*)-LXA$_4$	5*S*,6*R*,15*R*-trihydroxy-7*E*,9*E*,11*Z*,13*E*-eicosatetraenoic acid
17(*R*)-RvD1	7*S*,8*R*,17*R*-trihydroxy-4*Z*,9*E*,11*E*,13*Z*,15*E*,19*Z*-docosahexaenoic acid
18(*R*)-RvE3	17*R*,18*R*-dihydroxy-5*Z*,8*Z*,11*Z*,13*E*,15*E*-eicosapentaenoic acid
18(*S*)-RvE3	17*R*,18*S*-dihydroxy-5*Z*,8*Z*,11*Z*,13*E*,15*E*-eicosapentaenoic acid
6(*R*)-LXA$_4$	5*S*,6*R*,15*S*-trihydroxy-7*E*,9*E*,11*Z*,13*E*-eicosatetraenoic acid
6(*S*)-LXA$_4$	5*S*,6*S*,15*S*-trihydroxy-7*E*,9*E*,11*Z*,13*E*-eicosatetraenoic acid
7(*S*)-MaR1	7*S*,14*S*-dihydroxy-4*Z*,8*E*,10*E*,12*Z*,16*Z*,19*Z*-docosahexaenoic acid
ACN	acetonitrile
AdA	adrenic acid, C22:4n6
ALA	alpha-linolenic acid, C18:3n3
ALOX/LOX	lipoxygenase
ANOVA	analysis of variance
ARA	arachidonic acid, C20:4n6
BC	blood cell(s)
BHT	butylated hydroxytoluene
CAD	collision activated dissociation
CID	collision induced dissociation
CE	collision energy
COX	cyclooxygenase
CXP	collision cell exit potential
CYP	cytochrome P450 monooxygenase
D5D	Δ5-desaturase
D6D	Δ6-desaturase
DGLA	dihomo-gamma linolenic acid, C20:3n6
DHA	docosahexaenoic acid, C22:6n3
diH	dihydroxy
DiOH-FA	dihydroxy fatty acid(s)
DiHDHA	dihydroxy docosahexaenoic acid
DiHDPE	dihydroxy docosapentaenoic acid

DiHEPE	dihydroxy eicosapentaenoic acid
DiHETE	dihydroxy eicosatetraenoic acid
DiHETrE	dihydroxy eicosatrienoic acid
DiHODE	dihydroxy octadecadienoic acid
DiHOME	dihydroxy octadecenoic acid
DP	declustering potential
DPA	docosapentaenoic acid, C22:5n3/C22:5n6
EDTA	ethylenediaminetetraacetic acid
EE	ethyl ester
ELISA	enzyme-linked immunosorbent assay
EP	entrance potential
EPA	eicosapentaenoic acid, C20:5n3
Ep-FA	epoxy fatty acid(s)
EpDPE	epoxy docosapentaenoic acid
EpETE	epoxy eicosatetraenoic acid
EpETrE	epoxy eicosatrienoic acid
EpODE	epoxy octadecadienoic acid
EpOME	epoxy octadecenoic acid
ESI	electrospray ionization
ETA	eicosatetraenoic acid, C20:4n3
FA	fatty acid(s)
FAME	fatty acid methyl ester
FIA	flow injection analysis
FWHM	full width at half maximum
GC-FID	gas chromatography with flame ionization detection
GLA	gamma-linolenic acid, C18:3n6
HDHA	hydroxy docosahexaenoic acid
HEPE	hydroxy eicosapentaenoic acid
HETE	hydroxy eicosatetraenoic acid
HETrE	hydroxy eicosatrienoic acid
HHT/ HHTrE	hydroxy heptadecatrienoic acid
HOAc	acetic acid
HODE	hydroxy octadecadienoic acid
HOTrE	hydroxy octadecatrienoic acid
HpEPE	hydroperoxy eicosapentaenoic acid

HpETE	hydroperoxy eicosatetraenoic acid
HPLC	high performance liquid chromatography
HUFA	highly unsaturated fatty acid(s)
IL	interleukin
IS	internal standard
LA	linoleic acid, C18:2n6
LC-MS/MS	liquid chromatography tandem mass spectrometry
LC-UV	liquid chromatography with ultraviolet detection
LLOQ	lower limit of quantification
LOD	limit of detection
LT	leukotriene
LX	lipoxin(s)
LXA_5	5*S*,6*R*,15*S*-trihydroxy-7*E*,9*E*,11*Z*,13*E*,17*Z*-eicosapentaenoic acid
LXB_4	5*S*,14*R*,15*S*-trihydroxy-6*E*,8*Z*,10*E*,12*E*-eicosatetraenoic acid
m/z	mass to charge ratio
MA	mead acid, C20:3n9
MaR	maresin(s)
MaR1	7*R*,14*S*-dihydroxy-4*Z*,8*E*,10*E*,12*Z*,16*Z*,19*Z*-docosahexaenoic acid
MeOH	methanol
MRM	multiple reaction monitoring
mRNA	messenger ribonucleic acid
MS	mass spectrometry/ mass spectrometric
MTBE	methyl *tert*-butyl ether
MUFA	monounsaturated fatty acid(s)
n3/n6/n9	omega-3/6/9
NMRI	Naval Medical Research Institute
(N)PD1	10*R*,17*S*-dihydroxy-4*Z*,7*Z*,11*E*,13*E*,15*Z*,19*Z*-docosahexaenoic acid
OA	oleic acid, C18:1n9
OH-FA	hydroxy fatty acid(s)
oxo-ETE	oxo eicosatetraenoic acid
oxo-ODE	oxo octadecadienoic acid
PBS	phosphate buffered saline
PD	peritoneal dialysis
PDX	10*S*,17*S*-dihydroxy-4*Z*,7*Z*,11*E*,13*Z*,15*E*,19*Z*-docosahexaenoic acid
PG	prostaglandin(s)

PLA	phospholipase A
PUFA	polyunsaturated fatty acid(s)
qPCR	quantitative polymerase chain reaction
RP	reversed phase
RT	retention time
RT	room temperature
Rv	resolvin(s)
RvD1	7*S*,8*R*,17*S*-trihydroxy-4*Z*,9*E*,11*E*,13*Z*,15*E*,19*Z*-docosahexaenoic acid
RvD2	7*S*,16*R*,17*S*-trihydroxy-4*Z*,8*E*,10*Z*,12*E*,14*E*,19*Z*-docosahexaenoic acid
RvD3	4*S*,11*R*,17*S*-trihydroxy-5*Z*,7*E*,9*E*,13*Z*,15*E*,19*Z*-docosahexaenoic acid
RvD5	7*S*,17*S*-dihydroxy-4*Z*,8*E*,10*Z*,13*Z*,15*E*,19*Z*-docosahexaenoic acid
RvE1	5*S*,12*R*,18*R*-trihydroxy-6*Z*,8*E*,10*E*,14*Z*,16*E*-eicosapentaenoic acid
RvE2	5*S*,18*R*-dihydroxy-6*E*,8*Z*,11*Z*,14*Z*,16*E*-eicosapentaenoic acid
S/N	signal to noise ratio
SD	standard deviation
sEH	soluble epoxide hydrolase
SEM	standard error of the mean
SFA	saturated fatty acid(s)
SIM	selected ion monitoring
SPE	solid phase extraction
SPM	specialized pro-resolving lipid mediator
SRM	selected reaction monitoring
t-AUCB	*trans*-4-[4-(3-adamantan-1-yl-ureido)-cyclohexyloxy]-benzoic acid
TG	triglyceride
TIC	total ion chromatogram
TriHEPE	trihydroxy eicosapentaenoic acid
TriHETE	trihydroxy eicosatetraenoic acid
TX	thromboxane(s)
ULOQ	upper limit of quantification
VLDL	very low density lipoprotein

Acknowledgement

This thesis was carried out from January 2016 to August 2020 at the Institute for Food Toxicology (University of Veterinary Medicine Hannover) and at the Chair of Food Chemistry (University of Wuppertal) in the research group of Prof. Dr. Nils Helge Schebb.

I would like to acknowledge all the people who accompanied me during this time, colleagues and friends, for their help and support and invaluable contributions to the completion of this thesis.

First of all, I would like to thank my supervisor Prof. Dr. Nils Helge Schebb for the opportunity to be part of his group and work in this interesting research field on many different projects for which I could apply instrumental analytical techniques to work on relevant biological questions. I thank him for his scientific advice, motivation and encouragement as well as the opportunity to visit many national and international conferences to present and discuss my results.

I would like to thank Prof. Dr. Hartmut Kühn for being a board member of the PhD committee and particularly for the kind cooperation, his continuous support and advice in all the projects involving lipoxygenases within my thesis and beyond. Moreover, I thank Prof. Kühn's working group (Kateryna Goloshchapova, Dagmar Heydeck, Sabine Stehling and Eugenia Marbach-Breitrück) for the friendly collaboration.

I want to thank Prof. Dr. Gunter P. Eckert and the members of his group for the cooperation in the feeding study in chapter 2. I thank Nicole Franke for her work during the animal experiment and Carsten Esselun for the enzyme expression analyses, his valuable input for the interpretation of the data and writing of the manuscript and for working on the "never-ending story" with me.

I would like to thank the “18-HEPE-Team” including Dr. Michael Rothe and the members of Lipidomix not only for the contributions to the experiments in chapter 5, but also for the cooperation during the work on SPM detection and quantification. I want to thank Dr. Wolf-Hagen Schunck for his kind support, critical questions and valuable input. I thank Dr. Maximilian Blum for his contributions to chapter 5 as well as Prof. Dr. Stefan F. Kirsch and Dr. Martin Jübermann for the organic synthesis of 18-HEPE.

I thank Dr. Michael Balzer and PD Dr. Sascha David for the friendly cooperation and providing the clinical samples for the experiments in chapter 4.

For organic compound synthesis and their contributions to chapter 4, I would like to acknowledge Prof. Dr. Thierry Durand and the members of his group (Jean-Marie Galano, Laurence Balas, Camille Oger, Valerie Bultel and Alexandre Guy).

I thank Kirsten Schönfeld for her valuable contribution to this work during her master thesis.

I thank Prof. Dr. Kietzmann for the opportunity to finish parts of my work at the University of Veterinary Medicine in Hannover and Prof. Dr. Bettina Seeger for the uncomplicated arrangements after moving to Wuppertal.

I would like to thank Prof. Dr. Julia Bornhorst and the AGB (Merle Nicolai and Vivien Michaelis) for always being helpful and supportive and the nice working atmosphere in Wuppertal.

A huge thank you goes to my colleagues from the AG Schebb for all the time we spent working together in these past years:
Katharina Rund for always being ready for a quick question or elaborate discussion, her moral support, critical opinion and good advice on all matters and for always digging out some (expired) chocolate if needed ☺; Nicole Hartung for never giving up her life-coach efforts even for apparently un-coachable people and how she constantly triggered my *Inspirationsakzeptase* expression; Nadja Kampschulte for managing countless technical and practical issues and for

granting access to her coffee, sweets and noodles stores; Malwina Mainka for introducing me to all the tricky details of the OXYdeluxe method and not being bothered by my questions; Elisabeth Koch for all our sometimes challenging but also funny GC sessions and for working together on many projects involving fatty acid analyses (… Fettsäuren können wir! ☺).

Moreover, I want to thank Dieter Riegel for the pleasant working together on food supplements at the very beginning of my PhD project and later on, during practical courses and moving GCs; Claudia Steinhage for organizing unforgettable “Betriebsausflüge” and Sabine Scalet for being patient with me whenever I forgot to fill out another form.

Furthermore, I want to thank my former colleague Annika Ostermann for showing me all tips and tricks regarding the fatty acid and oxylipin analysis during the begin of my master thesis and after that, for being always helpful and supportive and for all the funny moments during work, at conferences and beyond.

I would like to thank all former colleagues from the University of Veterinary Medicine in Hannover for the nice time working there, especially Michael Empl for spaghetti and equipping long working days with the best-ever soundtrack; Tina Kostka and Maren Schenke for organizing enjoyable evenings with Döner, Pizza and games and for Helga ☺.

Mein letzter und zugleich wichtigster Dank gilt meiner Familie, ganz besonders meinen Eltern und Geschwistern sowie Verwandten und Freunden. Danke, dass ihr mir alles ermöglicht habt, mich immer unterstützt und an mich geglaubt habt, auch (und besonders dann) wenn es mir selbst manchmal schwergefallen ist und in jeder Situation ein offenes Ohr und ein motivierendes Wort für mich parat hattet. Habt vielen lieben DANK für alles!

Curriculum Vitae

Der Lebenslauf ist in der Online-Version aus Gründen des Datenschutzes nicht enthalten.

List of Publications

PUBLICATIONS IN PEER-REVIEWED JOURNALS

WITHIN THE SCOPE OF THIS THESIS

L. Kutzner, C. Esselun, N. Franke, K. Schoenfeld, G.P. Eckert, N.H. Schebb (**2020**) Effect of dietary EPA and DHA on murine blood and liver fatty acid profile and liver oxylipin pattern depending on high and low dietary n6-PUFA. *Food Funct*; doi: 10.1039/D0FO01462A.

L. Kutzner, K. Goloshchapova, K.M. Rund, M. Jübermann, M. Blum, M. Rothe, S.F. Kirsch, W.H. Schunck, H. Kühn, N.H. Schebb (**2020**) Human lipoxygenase isoforms form complex patterns of double and triple oxygenated compounds from eicosapentaenoic acid. *Biochim Biophys Acta*, 1865(12), 158806; doi: 10.1016/j.bbalip.2020.158806.

L. Kutzner, K.M. Rund, A.I. Ostermann, N.M. Hartung, J.M. Galano, L. Balas, T. Durand, M.S. Balzer, S. David, N.H. Schebb (**2019**) Development of an optimized LC-MS method for the detection of specialized pro-resolving mediators in biological samples. *Front Pharmacol*, 10, 169; doi: 10.3389/fphar.2019.00169.

L. Kutzner, K. Goloshchapova, D. Heydeck, S. Stehling, H. Kühn, N.H. Schebb (**2017**) Mammalian ALOX15 orthologs exhibit pronounced dual positional specificity with docosahexaenoic acid. *Biochim Biophys Acta*, 1862(7), 666-675; doi: 10.1016/j.bbalip.2017.04.001.

FURTHER PUBLICATIONS

S. Vordenbäumen, A. Sokolowski, L. Kutzner, K.M. Rund, C. Dusing, G. Chehab, J.G. Richter, R. Brinks, M. Schneider, N.H. Schebb (**2020**) Erythrocyte membrane polyunsaturated fatty acid profiles are associated with systemic inflammation and fish consumption in systemic lupus erythematosus: a cross-sectional study. *Lupus*, 29(6), 554-559; doi: 10.1177/0961203320912326.

A.I. Ostermann, E. Koch, K.M. Rund, L. Kutzner, M. Mainka, N.H. Schebb (**2020**) Targeting esterified oxylipins by LC-MS – Effect of sample preparation on oxylipin pattern. *Prostaglandins Other Lipid Mediat*, 146, 106384; doi: 10.1016/j.prostaglandins.2019.106384.

E. Marbach-Breitrück, L. Kutzner, M. Rothe, R. Gurke, Y. Schreiber, P. Reddanna, N.H. Schebb, S. Stehling, L.H. Wieler, D. Heydeck, H. Kühn (**2020**) Functional characterization of knock-in mice expressing a 12/15-lipoxygenating Alox5 mutant instead of the 5-lipoxygenating wild-type enzyme. *Antioxid Redox Sign*, 32(1), 1-17; doi: 10.1089/ars.2019.7751.

E. Koch, M. Mainka, C. Dalle, A.I. Ostermann, K.M. Rund, L. Kutzner, L.F. Froehlich, J. Bertrand-Michel, C. Gladine, N.H. Schebb (**2020**) Stability of oxylipins during plasma generation and long-term storage. *Talanta*, 217, 121074; doi: 10.1016/j.talanta.2020.121074.

R. Ebert, R. Cumbana, C. Lehmann, L. Kutzner, A. Toewe, N. Ferreiros, M.J. Parnham, N.H. Schebb, D. Steinhilber, A.S. Kahnt (**2020**) Long-term stimulation of toll-like receptor-2 and -4 upregulates 5-LO and 15-LO-2 expression thereby inducing a lipid mediator shift in human monocyte-derived macrophages. *Biochim Biophys Acta*, 1865(9), 158702; doi: 10.1016/j.bbalip.2020.158702.

K.H. Weylandt, C. Schmöcker, A.I. Ostermann, L. Kutzner, I. Willenberg, S. Kiesler, E. Steinhagen-Thiessen, N.H. Schebb, U. Kassner (**2019**) Activation of lipid mediator formation due to lipoprotein apheresis. *Nutrients*, 11(2), 363; doi: 10.3390/nu11020363.

T. Greupner, E. Koch, L. Kutzner, A. Hahn, N.H. Schebb, J.P. Schuchardt (**2019**) Single-dose SDA-rich echium oil increases plasma EPA, DPAn3, and DHA concentrations. *Nutrients*, 11(10), 2346; doi: 10.3390/nu11102346.

K.M. Rund, A.I. Ostermann, L. Kutzner, J.M. Galano, C. Oger, C. Vigor, S. Wecklein, N. Seiwert, T. Durand, N.H. Schebb (**2018**) Development of an LC-ESI(-)-MS/MS method for the simultaneous quantification of 35 isoprostanes and isofurans derived from the major n3- and n6-PUFAs. *Anal Chim Acta*, 1037, 63-74; doi: 10.1016/j.aca.2017.11.002.

A.I. Ostermann, T. Greupner, L. Kutzner, Nicole M. Hartung, A. Hahn, J.P. Schuchardt, N.H. Schebb (**2018**) Intra-individual variance of the human plasma oxylipin pattern: low inter-day variability in fasting blood samples versus high variability during the day. *Anal Methods*, 10(40), 4935-4944; doi: 10.1039/C8AY01753K.

T. Greupner, L. Kutzner, S. Pagenkopf, H. Kohrs, A. Hahn, N.H. Schebb, J.P. Schuchardt (**2018**) Effects of a low and a high dietary LA/ALA ratio on long-chain PUFA concentrations in red blood cells. *Food Funct*, 9(9), 4742-4754; doi: 10.1039/c8fo00735g.

T. Greupner*, L. Kutzner*, F. Nolte, A. Strangmann, H. Kohrs, A. Hahn, N.H. Schebb, J.P. Schuchardt (**2018**) Effects of a 12-week high-alpha-linolenic acid intervention on EPA and DHA concentrations in red blood cells and plasma oxylipin pattern in subjects with a low EPA and DHA status. *Food Funct*, 9(3), 1587-1600; doi: 10.1039/c7fo01809f.
*Authors contributed equally to this work.

H. Gottschall, C. Schmöcker, D. Hartmann, N. Rohwer, K. Rund, L. Kutzner, F. Nolte, A.I. Ostermann, N.H. Schebb, K.H. Weylandt (**2018**) Aspirin alone and combined with a statin suppresses eicosanoid formation in human colon tissue. *J Lipid Res*, 59(5), 864-871; doi: 10.1194/jlr.M078725.

A.I. Ostermann, M. Reutzel, N. Hartung, N. Franke, L. Kutzner, K. Schoenfeld, K.H. Weylandt, G.P. Eckert, N.H. Schebb (**2017**) A diet rich in omega-3 fatty acids enhances expression of soluble epoxide hydrolase in murine brain. *Prostaglandins Other Lipid Mediat*, 133, 79-87; doi: 10.1016/j.prostaglandins.2017.06.001.

L. Kutzner*, A.I. Ostermann*, T. Konrad, D. Riegel, S. Hellhake, J.P. Schuchardt, N.H. Schebb (**2017**) Lipid class specific quantitative analysis of n-3 polyunsaturated fatty acids in food supplements. *J Agric Food Chem*, 65(1), 139-147; doi: 10.1021/acs.jafc.6b03745.
*Authors contributed equally to this work.

J.P. Schuchardt, A.I. Ostermann, L. Stork, L. Kutzner, H. Kohrs, T. Greupner, A. Hahn, N.H. Schebb (**2016**) Effects of docosahexaenoic acid supplementation on PUFA levels in red blood cells and plasma. *Prostaglandins Leukot Essent Fatty Acids*, 115, 12-23; doi: 10.1016/j.plefa.2016.10.005.

ORAL PRESENTATIONS

L. Kutzner (**2016**) Determination of the quantitative distribution of fatty acids among different lipid classes in food supplements and plasma samples. 26. Doktorandenseminar des AK Separation Science der GDCh Fachgruppe Analytische Chemie, 10.–12.01.2016, Hohenroda, Germany.

POSTER PRESENTATIONS

C. Schmöcker, N. Rohwer, H. Gottschall, K.M. Rund, L. Kutzner, A.I. Ostermann, D. Hartmann, N.H. Schebb, K.H. Weylandt (**2019**) Aspirin treatment changes oxylipin levels in murine and human colon tissue. United European Gastroenterology (UEG) Week, 19.–23.10.2019, Barcelona, Spain.

L. Kutzner, K.M. Rund, N.H. Schebb (**2019**) Detection of specialized pro-resolving mediators on a QTRAP 6500 system. 8. Berliner LC-MS/MS Sciex Symposium, 02.04.2019, Berlin, Germany.

L. Kutzner, K.M. Rund, M.S. Balzer, S. David, N.H. Schebb (**2019**) LC-MS based analysis of specialized pro-resolving mediators in biological samples – method optimization and application. Arbeitstagung 2019 des Regionalverbandes NRW der Lebensmittelchemischen Gesellschaft, 06.03.2019, Wuppertal, Germany.

L. Kutzner, A.I. Ostermann, M.S. Balzer, S. David, N.H. Schebb (**2018**) Optimized quantification of specialized pro-resolving mediators in biological samples by means of LC-MS. 7th European Workshop on Lipid Mediators, 12.–14.09.2018, Brussels, Belgium.

C. Schmöcker, H. Gottschall, C.D. Hartmann, N. Rohwer, K.M. Rund, L. Kutzner, F. Nolte, A.I. Ostermann, N.H. Schebb, K.H. Weylandt (**2018**) Oxylipin formation in human colon tissue. 7th European Workshop on Lipid Mediators, 12.–14.09.2018, Brussels, Belgium.

T. Greupner, L. Kutzner, F. Nolte, H. Kohrs, A. Hahn, N.H. Schebb, J.P. Schuchardt (**2018**) A high-ALA diet does not increase ΣEPA+DHA in red blood cells. 13th Congress of the International Society for the Study of Fatty Acids and Lipids, 27.–31.05.2018, Las Vegas, USA.

T. Greupner, L. Kutzner, H. Kohrs, S. Pagenkopf, T. Konrad, A. Hahn, N.H. Schebb, J.P. Schuchardt (**2018**) Effects of a high and a low dietary LA/ALA ratio on fatty acid concentrations in red blood cells. 13th Congress of the International Society for the Study of Fatty Acids and Lipids, 27.–31.05.2018, Las Vegas, USA.

L. Kutzner, R.A. Colas, A.I. Ostermann, M. Rothe, K.H. Weylandt, J. Dalli, N.H. Schebb (**2018**) Optimized LC-MS based analysis of specialized pro-resolving mediators in biological samples – an interlaboratory comparison exercise. 17th Winter Eicosanoid Conference, 11.–13.03.2018, Baltimore, USA.

C. Schmöcker, H. Gottschall, N. Rohwer, K.M. Rund, L. Kutzner, A.I. Ostermann, N.H. Schebb, K.H. Weylandt (**2018**) Oxylipins in human colon mucosa, adenoma and carcinoma tissues. 17th International Winter Eicosanoid Conference, 11.–13.03.2018, Baltimore, USA.

L. Kutzner, D. Heydeck, N.H. Schebb, H. Kühn (**2016**) Reaction specificity of 12- and 15-lipoxygenating ALOX15 orthologs with different polyunsaturated fatty acids. 6th European Workshop on Lipid Mediators, 27.–30.09.2016, Frankfurt am Main, Germany.

S. Hellhake, L. Kutzner, A.I. Ostermann, D. Riegel, J.P. Schuchardt, N.H. Schebb (**2016**) Quantitative fatty acid profile of lipid classes in food supplements. 45. Deutscher Lebensmittelchemikertag, 12.–14.09.2016, Freising-Weihenstephan, Germany.

H. Gottschall, C. Schmöcker, D. Hartmann, K.M. Rund, L. Kutzner, F. Nolte, N.H Schebb, K.H. Weylandt (**2016**) Quantitative profiling of 15-lipoxygenase lipid metabolites in human colon tissue reveals distinct lipidomic profiles for human colon carcinoma and adenoma tissue. Wissenschaftliches Symposium der Gastroenterologischen Abteilungen der Charité – Universitätsmedizin Berlin, 15.–16.07.2016, Potsdam, Germany.

C. Claßen, K.M. Rund, L. Kutzner, V. Beumler, A.I. Ostermann, K.H. Weylandt, N.H. Schebb (**2016**) Modulation of the fatty acid- and oxylipin-pattern by an EPA/DHA-rich

diet and its effects on DSS-induced acute colitis in Sprague-Dawley rats. Arbeitstagung des Regionalverbandes NRW der Lebensmittelchemischen Gesellschaft der GDCh, 9.03.2016, Möchengladbach, Germany.

A. Riegelmeyer, S. Hellhake, M. Krohn, L. Kutzner, N.H. Schebb (**2016**) Size-exclusion chromatography based separation of plasma lipoproteins and analysis of the fatty acid composition of VLDL, HDL and LDL fractions. Arbeitstagung des Regionalverbandes NRW der Lebensmittelchemischen Gesellschaft der GDCh, 9.03.2016, Möchengladbach, Germany.

L. Kutzner, A.I. Ostermann, T. Konrad, D. Riegel, S. Hellhake, J.P. Schuchardt, N.H. Schebb (**2016**) Determination of the quantitative distribution of fatty acids among different lipid classes in food supplements and plasma samples. 53. Wissenschaftlicher Kongress der Deutschen Gesellschaft für Ernährung, 02.–04.03.2016, Fulda, Germany.

L. Kutzner, A.I. Ostermann, T. Konrad, D. Riegel, J.P. Schuchardt, N.H. Schebb (**2015**) Differentiated analysis of the fatty acid pattern in food supplements. Lipidomics Forum, 15.–17.11.2015, Borstel, Germany.

A.I. Ostermann, L. Kutzner, T. Konrad, D. Riegel, J.P. Schuchardt, N.H. Schebb (**2015**) Specific analysis of the fatty acid pattern in neutral lipids, phospholipids and free fatty acids in food supplements. 14th International Conference on Bioactive Lipids in Cancer, Inflammation, and Related Diseases, 12.–15.07.2015, Budapest, Hungary.